Terms and Conditions of Use of Digitised Theses from Trinity College Library Dublin

Copyright statement

All material supplied by Trinity College Library is protected by copyright (under the Copyright and Related Rights Act, 2000 as amended) and other relevant Intellectual Property Rights. By accessing and using a Digitised Thesis from Trinity College Library you acknowledge that all Intellectual Property Rights in any Works supplied are the sole and exclusive property of the copyright and/or other IPR holder. Specific copyright holders may not be explicitly identified. Use of materials from other sources within a thesis should not be construed as a claim over them.

A non-exclusive, non-transferable licence is hereby granted to those using or reproducing, in whole or in part, the material for valid purposes, providing the copyright owners are acknowledged using the normal conventions. Where specific permission to use material is required, this is identified and such permission must be sought from the copyright holder or agency cited.

Liability statement

By using a Digitised Thesis, I accept that Trinity College Dublin bears no legal responsibility for the accuracy, legality or comprehensiveness of materials contained within the thesis, and that Trinity College Dublin accepts no liability for indirect, consequential, or incidental, damages or losses arising from use of the thesis for whatever reason. Information located in a thesis may be subject to specific use constraints, details of which may not be explicitly described. It is the responsibility of potential and actual users to be aware of such constraints and to abide by them. By making use of material from a digitised thesis, you accept these copyright and disclaimer provisions. Where it is brought to the attention of Trinity College Library that there may be a breach of copyright or other restraint, it is the policy to withdraw or take down access to a thesis while the issue is being resolved.

Access Agreement

By using a Digitised Thesis from Trinity College Library you are bound by the following Terms & Conditions. Please read them carefully.

I have read and I understand the following statement: All material supplied via a Digitised Thesis from Trinity College Library is protected by copyright and other intellectual property rights, and duplication or sale of all or part of any of a thesis is not permitted, except that material may be duplicated by you for your research use or for educational purposes in electronic or print form providing the copyright owners are acknowledged using the normal conventions. You must obtain permission for any other use. Electronic or print copies may not be offered, whether for sale or otherwise to anyone. This copy has been supplied on the understanding that it is copyright material and that no quotation from the thesis may be published without proper acknowledgement.

Molecular characterisation of the *Salmonella*-specific protein PagN

A dissertation presented for the degree of Doctor of Philosophy, in the Faculty of Science, Trinity College Dublin

By

Matthew A. Lambert

2007

Department of Microbiology,
Moyne Institute of Preventive Medicine
Trinity College Dublin

Declaration

I, Matthew Lambert, declare that the work presented herein represents my own work, except where duly acknowledged in text, and has not been previously presented for a higher degree at this or any other university. I agree that the library of Trinity College Dublin may lend or copy this thesis upon request.

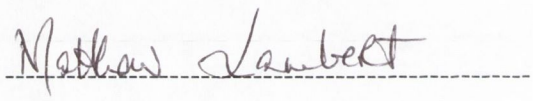

Matthew Lambert

Summary

Salmonella infect a broad spectrum of animals resulting in host responses ranging from severe disease to asymptomatic carriage. Infection of a host gives rise to symptoms such as fever or self-limiting gastroenteritis. Illness due to *Salmonella* infection is a serious problem in both developed and developing countries, affecting both humans and animals alike.

Central to the ability of *Salmonella* to cause disease is its capacity to penetrate the intestinal mucosa. Once internalised massive fluid secretion takes place resulting in diarrhoea. The bacteria can cross the basolateral membrane and disseminate around the host body leading to systemic infection. Much work has been carried out investigating the pathogenesis of *Salmonella* and elucidating the steps involved in disease. Many of the virulence determinants have been identified and characterised.

The purpose of this study was to characterise *pagN*, a gene broadly distributed throughout the genus but absent in closely related bacterial species. The distribution of *pagN* along with its chromosomal location and organisation has been established. However, at the protein level the gene-product remains uncharacterised.

Expression of the PhoP-activated gene was found to be induced within both epithelial and macrophage cells. Transcriptional activation was dependent upon a functional PhoP system and occurred as a result of binding of the PhoP response regulator to a putative promoter region, located directly upstream of the open reading frame.

The gene-product, PagN is a 26-kDa protein located in the outer membrane of *Salmonella*. It is predicted to adopt a β-barrel conformation consisting of 8 anti-parallel, amphipathic β-sheets connected by 4 short periplasmic turns and 4 surface-exposed loops.

Over-expression of the PagN protein in an *Escherichia coli* K-12 host conferred the ability to agglutinate erythrocytes and to adhere to and invade human intestinal epithelial cells. PagN-mediated invasion of epithelial cells was found to be dependent upon actin polymerisation. PagN-defective bacteria were less well able to invade epithelial cells. The O antigen component of bacterial lipopolysaccharide was identified as masking PagN/receptor interactions. Interestingly, PagN promoted bacterial invasion of epithelial cells in a manner

which was independent of a functional SPI-1-encoded type III secretion system. The PagN protein also promoted bacterial survival within macrophages.

The mammalian cell surface receptor for PagN was identified as heparinated proteoglycan. This was demonstrated by the ability of heparin to inhibit PagN-promoted invasion of CHO-K1 cells in a dose dependent fashion. Enzymatic removal of glycosaminoglycan proteoglycan moieties also inhibited invasion. Data presented suggests that unidentified serum factors enhance PagN-promoted invasion by interacting with the protein at the bacterial cell surface.

Finally, structural analysis of the protein revealed that all four predicted loops are required for PagN-mediated invasion of epithelial cells. This suggests that these loops have a structural role and may form a binding domain. Selected, conserved residues located within loop 2 were shown to contribute to PagN function.

Taken together the data presented within this thesis demonstrates that PagN is an outer membrane β-barrel protein that functions as an afimbrial adhesin/invasin. The protein promotes invasion of human intestinal epithelial cells and survival within macrophages indicating a role during both the enteric and more systemic stages of *Salmonella* infection.

Acknowledgements

I'd like to say a huge thank you to Dr. Stephen Smith for giving me the opportunity to "investigate" in his lab. over the last few years. You've been a great supervisor and it's been a lot of fun working with you. You've given me great advice over the course of my PhD both scientific and otherwise, and encouraged me throughout. Thanks Stephen.

A special thanks to present and past members of the Smith lab, the trials and tribulations of the world of science wouldn't have been as enjoyable without you guys being around: Vivienne, for keeping me up to speed with everything celebrity, and just having a laugh- I'll miss you. Robert, thanks for all the help throughout, especially in the first couple of months: you made it a lot easier. And thanks for the invasion assay diagram!! Gwen, for reminding me of the wonder that is The Hoff. Aileen, for having great fun the first six months of my PhD. To Mike and Mary, honourary Smith lab. members: Mike thanks for the entertaining stories, and insights into the world of medicine! Mary, thanks for restoring my faith in medicine after Mike's insights!!!

To my friends in The Moyne, thanks for great nights out and loads of laughs. To Fiona, Eithne, Brian and Marie: there are too many memories to start listing, and too many nights out to remember, or not remember!! In you, I've made great friends. To Tadhg, thanks for all the help and laughs- pure witchcraft!

To my family, H & B, what can I say: you're the best. Your support throughout my PhD and especially while writing up have helped so much. It's been a long road and I couldn't have done it without you two. To David, who has the patience of a saint, thanks for all the help. It was invaluble. To Mark, for trying to keep me somewhat fit throughout my PhD and my write-up, thanks! I promise we'll go back climbing now, but not outdoors!

And finally to Susan, what can I say, the thought of square tables and chandeliers has kept me going for the last while! Thanks for helping me forget about the stresses of science. You're always there for me and make me smile instantly. Your constant love and support has meant the most to me. Thanks. x

Table of Contents

List of Abbreviations

Abbreviation	Full name
DMEM	Dulbecco's modified Eagle's medium
DMF	dimethylformamide
DMSO	N,N-dimethylsulphoxide
DTT	dithiothreitol
EDTA	Ethylenediaminetetraacetic acid
FITC	Fluorescein-5-isothiocyanate
IPTG	isopropylthiogalactoside
OD	Optical density
PBS	phosphate-buffered saline
PIPES	Piperazine-1,4-bis(2-ethansulfonic acid)
PVDF	Polyvinylidene difluoride
SDS-PAGE	Sodium dodecylsulphate-polyacrylamide gel electrophoresis
TBE	Tris-borate-EDTA buffer
X-Gal	5-bromo-4-chloro-3-indoyl-β-D-galactoside

List of Figures

List of Tables

Chapter 1

General Introducation

1.1 *Salmonella*, an introduction

The species *Salmonella*, a close relative of *Escherichia coli*, are motile, gram-negative, rod-shaped intracellular pathogens belonging to the *Enterobacteriaceae* family. First described by Eberth in 1880 and cultured in 1884 by Gaffky (53), strains were differentiated based on their reaction to sera, each new serotype corresponding to a new species. Now, it is generally accepted that the genus *Salmonella* be divided into two species, *Salmonella bongori* (previously subspecies V) and *Salmonella enterica* (formerly named *choleraesuis*). The *enterica* species can be further divided into 6 subspecies comprised of numerous serovars.

The species *S. bongori* is considered to be phylogenetically older than *S. enterica* and only very rarely associated with human disease (179), while *S. enterica* are capable of infecting a range of animal hosts including poultry, cattle, pigs, mice and humans (308). *Salmonella enterica* serovar Typhimurium (hereafter referred to as *S.* Typhimurium) is a facultative anaerobe and is distinguishable from other enteric bacteria on the basis of its biochemical properties. Unlike *E. coli* or *Shigella*, *S.* Typhimurium can utilise citrate as a carbon source, is unable to metabolise lactose, is urease negative and is unable to produce indole from tryptophan (374).

Salmonella are of importance not only as an ongoing concern in world-wide public health services, but they also serve as a paradigm for the study of the mechanisms of bacterial pathogenesis. In the last decade, the genomes of both *S.* Typhimurium strain LT2 and *S.* Typhi strain CT18 have been sequenced (264, 315). Indeed at present the Sanger Institute has completed sequencing the genome of *S. bongori* 12419 ATCC 4397 as well as several other S. *enterica* serovars. The publication of such genomes will supply us with unparalleled information for further study.

1.1.1 Salmonellosis

Salmonella enterica serovars are a significant cause of morbidity and mortality worldwide. Salmonellosis is a major public health burden representing a sizeable cost to society in both developing and developed nations. The principal diseases associated with *Salmonella* infection are typhoid fever and gastroenteritis. The exclusively human

typhoidal *Salmonella* serovars *S.* Typhi and *S.* Paratyphi cause systemic illness that leads to an estimated 20 million cases and 200,000 deaths world-wide each year (76). Although very few countries collate data on economic cost of the disease, the World Health Organisation reports that in America, approximately 1.4 million non-typhoidal *Salmonella* infections occur annually, with costs ranging from $40 to $4.6 million representing uncomplicated cases to cases ending in mortality (http://www.who.int/mediacentre/factsheets/fs139/en/).

The clinical manifestations of typhoid include fever, abdominal pain and transient diarrhoea or constipation. Without treatment mortality is 10-15% (308). Non-typhoidal *Salmonella* serovars such as Typhimurium, Enteritidis, Newport and Heidelberg infect a wide range of animal hosts, and typically cause a self-limiting gastroenteritis. Initial symptoms include nausea and vomiting, which are followed by abdominal pain and diarrhoea. The nature and severity of the disease is largely dependent on the *Salmonella* serovar and host species involved (81).

1.2 *Salmonella* pathogenesis

The first step in the disease process is transmission, usually achieved by consumption of contaminated food or water. The route of infection carries the bacteria first to the harsh, acidic conditions of the stomach before entering the small intestine where they bind to epithelial cells lining the intestinal wall. A large inoculum is required to overcome the stomach acidity and to compete with the normal flora of the intestinal tract (386, 392).

Upon attachment, huge host cell cytoskeletal rearrangements occur causing the intestinal epithelium to be thrown into large convoluted membrane folds called ruffles (121). These membrane ruffles engulf the *S.* Typhimurium cells, resulting in the uptake of the invading bacteria into a vesicle/vacuole, referred to as the *Salmonella*-containing vesicle (SCV). Within this pseudo-phagosome, *Salmonella* resist the advances of the host cell's defense systems by arresting and diverting the maturation program of the invasion vacuole thus preventing SCV/lysosome fusion and avoiding death (47). Passage of the bacteria to adjacent epithelial cells and the secretion of effector proteins promotes inflammation, fluid secretion and cytokine release from the host cells, resulting in the gastroenteritis disease associated with *S.* Typhimurium infection of healthy animal hosts (81, 130, 308).

S. Typhimurium is capable of traversing the basolateral membrane of intestinal epithelial cells. Here, bacteria are phagocytosed by macrophage cells. Inactivation of the macrophage function, and eventual *Salmonella*-induced macrophage death, allows persistence of the bacteria and subsequent dissemination from the point of intestinal breach (192, 243). The general aspects of *S.* Typhimurium pathogenesis are highlighted in Fig. 1.1.

1.2.1 Models used for the study of *Salmonella*

As stated, *Salmonella* is a paradigm of enteric bacterial infection. Researchers studying *Salmonella* employ the use of tissue culture and animal models, enabling the dissection of distinct aspects of the virulence process. Animal models are available for the study of both the intestinal and systemic phases of salmonellosis. Cattle are often used to study enteric disease caused by *S.* Typhimurium while the infection of mice serves as a model for systemic disease as it shares many aspects with human typhoid. Infection of chicks is mainly used as a colonisation model as disease symptoms rarely manifest themselves in adult animals.

The supplementation of tissue culture models with animal models is key to understanding salmonellosis. Animal models represent an important area of research as *Salmonella* infection of livestock and chickens, as well as being a significant financial burden, acts as a major reservoir for transmission of bacteria to humans.

1.2.2 Genetic virulence determinants of *Salmonella*

For *Salmonella*, full virulence involves multiple factors. It is thought that approximately 200 genes, corresponding to 4% of the *S.* Typhimurium genome, are required for lethal infection of mice (41). Both temporal and spatial regulation of these genes and the coordinate control of the expression of their protein products are of paramount importance to the survival of *Salmonella* within the host organism. Genes associated with *S.* Typhimurium virulence are scattered throughout the chromosome and are also located on pSLV, the 90-kb *Salmonella* large virulence plasmid. It is established that these virulence

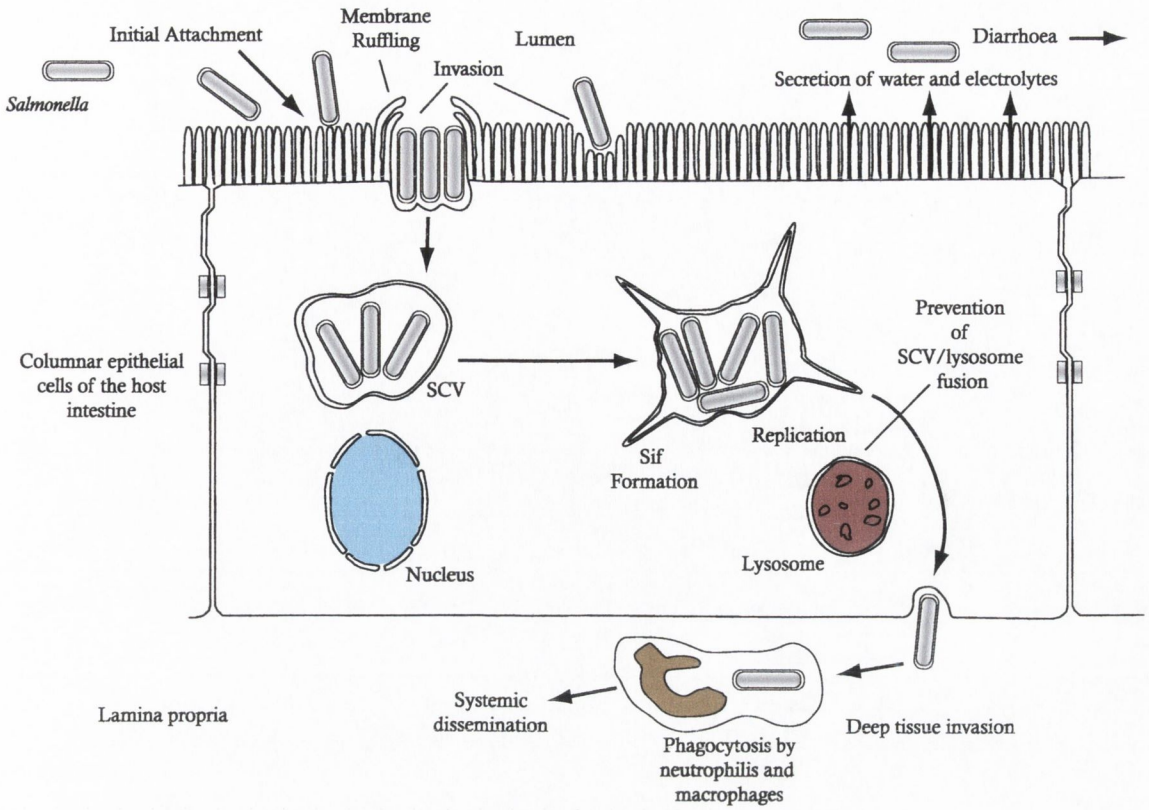

FIG 1.1. Selected events in *Salmonella* pathogenesis. Bacterial cells make initial contact with the epithelium of the host intestine. Delivery of secreted toxins directly into the cytosol of the host causes actin polymerisation resulting in the surface of the mammalian cell being thrown into massive convolutions called ruffles. These ruffles cause endocytosis of the bacteria. The bacteria reside within a *Salmonella*-containing vesicle within the host cell. Normal phagosome maturation is prevented and replication takes place. *Salmonella* have the ability to traverse the basolateral membrane where they are taken up by macrophages. The bacteria avoid cell death and proliferate within the macrophage thus leading to dissemination around the host body.

genes are often grouped in clusters, consisting of a few genes (termed pathogenicity islets) or on large cassettes organised into single genes and poly-cistronic operons (termed pathogenicity islands (PAIs)) (149, 306). Pathogenicity islands typically cluster genes associated with a particular virulence phenotype responsible for establishing specific interactions with the host, whether that be invasion of the epithelium or intracellular survival. *Salmonella* PAIs (SPIs) generally have a lower G+C content (37-47%) than the rest of the chromosomal DNA (52%) and are often located in regions containing tRNA genes (257). These features suggest that SPIs, as with all PAIs, are generally acquired through horizontal gene transfer from phages, transposons, or other sources during the course of a bacterium's evolution. It is the acquisition of these large, virulence islands that is thought to be responsible for *Salmonella* becoming a pathogen (148). So far, a total of four SPIs, numbered 1-4, have been characterised in detail for *S.* Typhimurium, while a fifth has been characterised for *S.* Dublin. These SPIs are associated with distinct aspects of *Salmonella* pathogenesis and may vary in function between different serovars and within different host organisms. The accepted model regarding *S.* Typhimurium infection of mice, is that SPI-1 is required for invasion of epithelial cells lining the intestine while SPI-2, -3 and -4 are generally associated with systemic growth and survival within the host (257). SPI-5 seems to mediate inflammation and enhance the chloride secretion associated with the diarrhoeal characteristics of salmonellosis. Recently, it has been established that SPI-1 and -2 encode determinants required for the colonisation of cattle. However, disruption of these virulence factors caused only minor defects in chick colonisation (283). In the same study, transposon insertions in SPI-4 compromised *S.* Typhimurium colonisation of cattle, but not chicks indicating that SPIs may be considered host-specific virulence determinants of *S.* Typhimurium.

1.2.2.1 SPI-1

SPI-1, the best characterised of the five SPIs is 43 kb in size, located at centisome 63, and contains at least 35 genes (Fig. 1.1) (257). It is flanked by *fhlA* and *mutS* and has an overall G+C content of 42%. Importantly, SPI-1 forms a distinct, coordinated unit including genes encoding a TTSS (Section 1.3.3), and effector proteins along with their cognate chaperones and regulatory proteins (70). The TTSS of SPI-1 promotes invasion of the epithelial cells of the small intestine (278). Many of the effector proteins necessary for

invasion are encoded by SPI-1, while additional effector proteins are encoded elsewhere on the chromosome. For example, SopB is encoded within SPI-5 at centisome 25 (414) and the gene encoding SopE is located within the integrated P2-like phage SopEΦ at centisome 60 (163).

Injection of the TTSS effector molecules into the host cell promotes cytoskeletal rearrangements resulting in membrane ruffling and traversal of the intestinal epithelium by *S.* Typhimurium (Section 1.3.4). SPI-1-defective *S.* Typhimurium are attenuated for virulence in a mouse model when injected orally but not intraperitoneally (132), suggesting SPI-1 is involved solely with penetration of the epithelium and not in the later, systemic stages *S.* Typhimurium infection. However, it has been demonstrated that SPI-1-encoded genes are required for long-term systemic virulence in mice (230), thus expanding our current understanding of the role of SPI-1. Paradoxically, a Δ*spi-1 S.* Typhimurium mutant is capable of traversing the gastrointestinal tract gaining access to the spleen resulting from uptake by CD18-expressing phagocytes (403). Importantly, del-Potillo *et al.* recently presented work at The Second ASM Conference on *Salmonella* held in Victoria, Canada demonstrating that SPI-1-defective *S.* Typhimurium were capable of invading fibroblasts efficiently. They observed that unlike epithelial cells, fibroblast invasion was independent of Rac-1, Cdc42 and Rho activity representing a novel method of invasion of non-phagocytic cells.

1.2.2.2 SPI-2

SPI-2 is a 40-kb virulence determinant located at centisome 31, inserted adjacent to the $tRNA^{ValV}$ gene on the *S.* Typhimurium chromosome (Fig. 1.2 (A)) (307, 358). After *S.* Typhimurium have become internalised in the intestinal epithelium it utilises SPI-2, with its 42 ORFs, for intracellular replication within host cells, and for persistent, systemic infection (179, 307). SPI-2-defective mutants are severely attenuated in comparison to wild-type *Salmonella*, regardless of whether they are infected orally, intraperitoneally or intravenously (181, 307, 358). Interestingly, it has recently been established that SPI-2 genes are also expressed prior to bacterial penetration of the intestine (44). SPI-2 expression was detectable in bacteria that were resident in the lumen of the ileum suggesting that early SPI-2 expression may be involved in preparing *Salmonella* to resist the antimicrobial environment encountered within host cells (44).

SPI-2 is divided into two distinct regions, one of 25 kb (containing genes important for virulence) (Fig.1.2), and another of 15 kb, each one acquired independently by horizontal gene transfer (180). The 25-kb region, flanked by the $tRNA^{ValV}$ gene at 31 cs and *ssrB*, occurs only in *S. enterica* species while the 15-kb element is present in both *S. enterica* and *S. bongori* species (180). As it is restricted to isolates of *S. enterica*, acquisition of the 25-kb region may represent a more recent genetic event in *Salmonella* evolution. The smaller 15-kb region of SPI-2 is flanked by ORF 242 and *pykF* at 30.5 cs and is not required for virulence (180). The 15-kb region, together with seven ORFs of unknown function, harbours a cluster of *ttr* genes involved in anaerobic tetrathionate reduction.

Most importantly, within the 25-kb region of SPI-2 are genes encoding a TTSS as well as regulatory, chaperone and effector proteins. This TTSS is unique in that it functions to secrete its effector proteins from an intracellular environment (179). The TTSS and related proteins are encoded for by 31 genes organised into four operons termed regulatory, structural I, structural II and effector/chaperone (67, 180, 358). These genes were named to reflect the function of the products they encoded: regulatory proteins were designated *ssr* (secretion system regulator), components of the TTSS were designated *ssa* (secretion system apparatus), while substrate proteins and their cognate chaperones were designated *sse* (secretion system effector), and *ssc* (secretion system chaperone) respectively (182).

Subsequent analysis of SPI-2 genes contradicted initial functional predictions resulting in the re-annotation of several genes. Characterisation of the putative effector protein SseA, revealed that it was in fact a chaperone of the translocon components SseB and SseD (338, 423). Other corrections included the re-naming of SsaB which had been incorrectly described as a component of the TTSS apparatus. It was renamed SpiC upon demonstration that it inhibits phagosome-lysosome fusion and interferes with intracellular trafficking (393).

The function of the SPI-2 encoded TTSS and effector proteins will not be discussed further in this section. A more thorough exploration of their role in *Salmonella* pathogenesis is presented in Section 1.4.

1.2.2.3 SPI-3

SPI-3 is 17-kb element with G+C content of 47.5%, inserted downstream of the *selC* tRNA gene at centisome 82 of the *S.* Typhimurium chromosome (Fig. 1.2), (36, 37). SPI-3

harbours 10 ORFs organised into 6 transcriptional units (36), which include the *mgtCB* operon encoding the macrophage survival protein MgtC and the high-affinity Mg^{2+} transporter MgtB (369). Transcription of the *mgtCB* operon is induced under conditions of low Mg^{2+} by the PhoP/Q two-component signal transduction system (36, 368). None of the other SPI-3 genes are PhoP-regulated nor are they required for survival in macrophage or for invasion of epithelial cells. Of the other ORFs, one, encoding a membrane insertion and secretion protein, MisL exhibits sequence similarity to the AIDA-I adhesin of enteropathogenic *E. coli* (30), while another, encoding MarT (for membrane-associated regulator) displays 43% identity at the C-terminal end to the ToxR transcriptional regulator from *Vibrio cholerae* (277). The function of the remaining ORFs is undefined but as their distribution varies between serovars of *Salmonella* it is postulated they contribute to host specificity or chronic infection (11).

1.2.2.4 SPI-4

SPI-4, located at centisome 92, is a 27-kb genetic element flanked by putative tRNA genes, which contains a previously identified locus required for survival in murine macrophages (Fig. 1.2), (112, 413). Upon publication of the complete genome sequence of *S.* Typhimurium strain LT2, the element, originally thought to encode 18 putative ORFs, forming one operon, was reorganised into six ORFs (numbered STM4257-62) (264). The first conclusive evidence supporting a role for SPI-4 in pathogenesis demonstrated that *S.* Typhimurium, defective in SPI-4, was attenuated in a calf infection model (283). SPI-4 mutants have since been shown to be attenuated relative to wild-type bacteria during systemic infection of mice (230). STM4257-62 have been renamed *siiA-F*, for *Salmonella* intestinal infection (283). Upstream of *siiA* lies an operon polarity suppressor (*ops*) motif, required for transcription elongation under the control of the RfaH protein, and is thought to regulate expression of *siiABCD* acting in conduction with RfaH (283, 289). The products of *siiCD* and *F* form a type I secretion system which secretes a surface-expressed protein (encoded by *siiE*) of ~600 kDa (282). SiiC is predicted to be an outer membrane component linked to the inner membrane by SiiD, while SiiF is predicted to be an ATP-binding cassette localised to the inner membrane (282). The function of the large SiiE protein is unknown at present. The *sii* genes share sequence identity with genes on SPI-9, which also encode a type I secretion system and a large 365-kDa protein (283). This

protein, BapA from *S.* Enteritidis, is involved in biofilm formation, however SiiE does not share this function (227, 282).

1.2.2.5 SPI-5

Located at centisome 25 of the *S.* Typhimurium chromosome, SPI-5 is flanked by *serT* and *copR* with an overall G+C content of 43.6%, and has been characterised in detail in *S.* Dublin (Fig. 1.2), (189, 414). SPI-5, like SPI-1, is involved in traversal of the intestinal epithelium (414). It is not thought to be associated with systemic disease, although two genes, *pipD* encoding a cysteine protease homologue, and *copS,* encoding a histidine kinase, have been recently implicated in systemic infection (230). SPI-5 encodes the SopB effector protein (Section 1.3.4.1 (A)), which is secreted through the SPI-1-encoded TTSS, and thought to be responsible for inducing fluid secretion from host epithelial cells (138).

1.2.2.6 The *Salmonella* virulence plasmid

Pathogenic, non-typhoidal serovars of *Salmonella* carry a large, low copy number virulence plasmid required for systemic disease (155, 336). Depending on the serovar, the size of the virulence plasmid varies between 50-100 kb, and it is estimated to be present at 2.75 copies per cell (65, 264). In the case of *S.* Typhimurium, the virulence plasmid is 90 kb in size and by increasing the growth rate of the bacteria inside host cells, contributes to systemic infection in mice (157). Not withstanding the heterogeous size of virulence plasmids, a region of 7.8 kb is highly conserved throughout. This region encodes five genes *spvRABCD* (designated *Salmonella* plasmid virulence (*spv*) genes) and is sufficient to restore virulence to plasmid-cured bacteria (156).

The *spv* locus consists of a transcriptional regulator *spvR* and four structural genes, *spvABCD.* SpvR is a transcriptional activator of the LysR family, which activates expression from both the P_{spvR} and P_{spvA} promoters. The SpvB protein is a mono(ADP-ribosyl)transferase that modifies actin, destabilising the cytoskeleton of infected cells (234, 388), and appears to be responsible for *spv*-promoted virulence (234). In serovar Dublin, the *spv* genes have been reported to enhance both intestinal and systemic disease, whereas

in other serovars, only systemic aspects of virulence are affected by *spv* (20, 80, 154, 238) . Although the functions of SpvC and SpvD are undefined; SpvC is considered a virulence determinant as it was demonstrated that along with SpvB, it could restore partial virulence to plasmid-cured strains of *S.* Typhimurium (262).

The *spv* genes are induced during the stationary phase of bacterial growth, in mice and macrophages (172, 260, 333). In addition to SpvR, the expression of the *spv* locus is regulated by the stationary phase sigma factor RpoS, the nucleoid-associated proteins H-NS (304), and IHF (261), the leucine-responsive regulatory protein Lrp (261), and the cAMP receptor protein CRP (303).

Loci located outside this conserved region include the plasmid encoded fimbrial operon *pef* (Section 1.3.1), the *rck* operon (Section 1.3.2.1), the conjugal transfer gene *traT* as well as the *rsk* loci, which is thought to play a role in regulation of *S.* Typhimurium virulence (336, 402). The encoded TraT protein resembles the known TraT proteins of the plasmids of the F incompatibility group (382). It has been demonstrated that apart from its functions in prevention of self-mating of cells carrying identical plasmids, a Gly→Arg mutation in one of the two strongly hydrophobic regions of TraT leads to increased hydrophobic permeability of the *S.* Typhimurium outer membrane (382). The *S.* Typhimurium virulence plasmid also harbours the *tlpA* gene encoding a heat inducible α-helical coiled coil protein (218).

Interestingly, it was recently demonstrated that the *rck* operon is up-regulated by SdiA, in an *N*-acyl homoserine lactone-dependent manner in actively migrating swarmer populations of *S.* Typhimurium (211). SdiA is a component of a cell-cell signaling system coupled to swarmer differentiation in *S.* Typhimurium (4). Swarming refers to the tendency of almost all members of the *Salmonella* genus to differentiate and migrate on semisolid surfaces in a coordinated population thought to be relevant to the differentiation state displayed within an animal host (211).

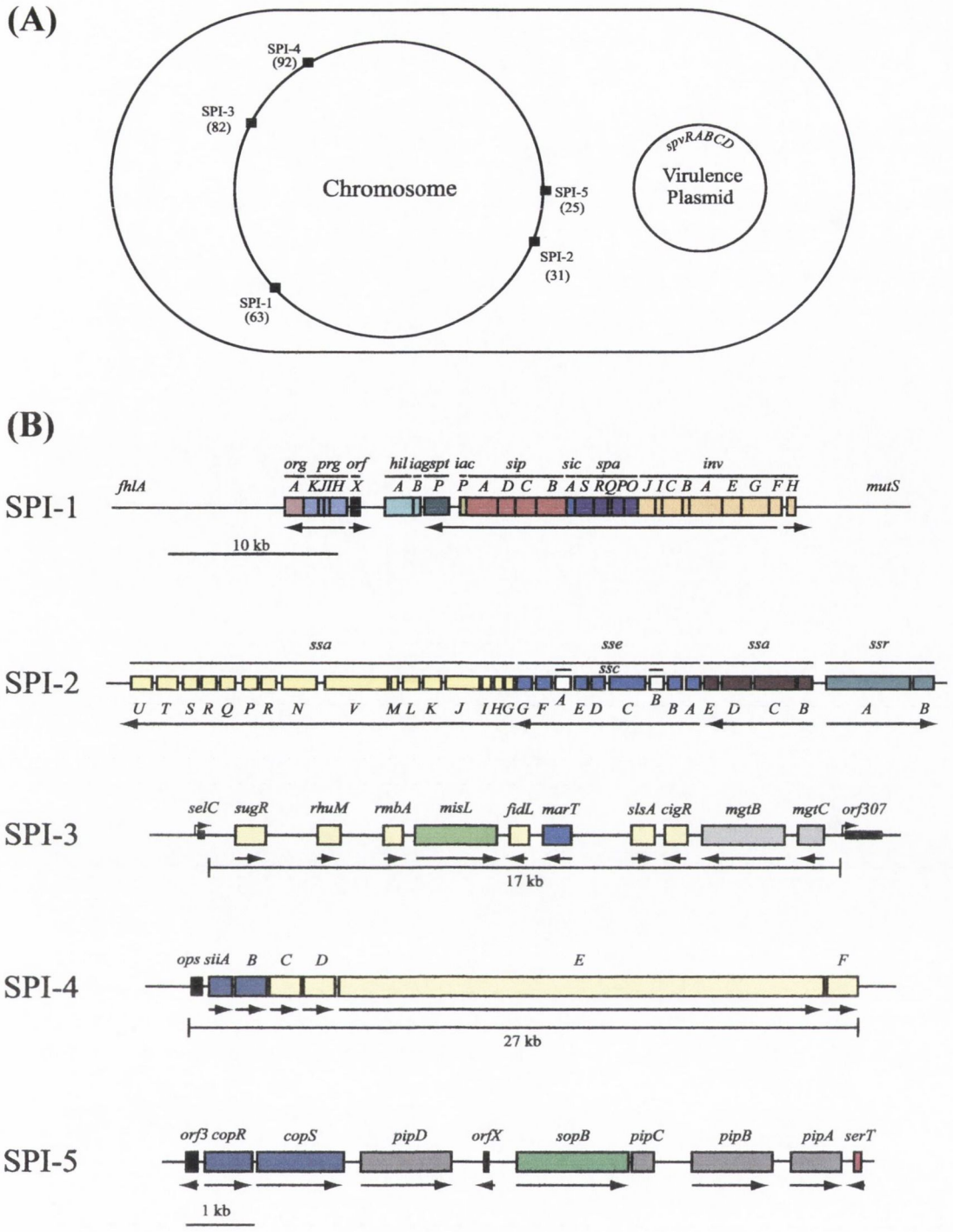

FIG 1.2. The Pathogenicity Islands of *S.* Typhimurium. (A) Schematic representation of the *S.* Typhimurium chromosome. The centisome location of SPIs 1-5 are indicated. **(B) Schematic representation of SPIs 1-5.** Genes are represented by coloured boxes and the transcriptional direction is indicated below each box. Within SPI-1 and SPI-2 genes are grouped by colour according to the predicted or known function of each gene. SPI-2 only shows the 25-kb region which is implicated in intracellular survival (see text). The 15-kb region, absent in *S.* Bongori is not shown. Within SPI-3, SPI-4,and SPI-5 genes of unknown function are coloured yellow, while genes of known function, where possible, are grouped by colour according to their predicted function. Adapted from Marcus, S. L. *et al.* (257), Hensel, M (179), Amavisit, P. *et al.* (11) and Morgan, E. *et al.* (282).

1.3 Intestinal invasion by *Salmonella*

1.3.1 The fimbriae of *Salmonella*

It is thought that fimbrial adhesins facilitate attachment; the first step during the initial colonisation of the intestinal mucosa (23, 25, 26, 246). Since the discovery of fimbriae in 1958 (100), and up until the mid 1990s it was generally accepted that there were 4 kinds of *Salmonella* fimbriae, encoded by four distinct operons. These long, cylindrical projections were categorised as Type I (*fim* operon) (68), Long Polar (*lpf* operon) (22), Plasmid-encoded (*pef* operon) (126), and Thin aggregative (*agf* operon) fimbriae (71). Interestingly, fimbrial expression is phase variable giving rise to mixed populations of bacteria within the same culture, some expressing fimbriae and some not. Phase variable transcriptional regulation has been demonstrated for *lpf* (300), *pef (292)* and *fim* (383).

The blockage of individual fimbrial adhesins does not strongly reduce mouse virulence of *S.* Typhimurium (187), it has therefore been speculated that compensation for a functional defect of an individual fimbrial adhesin is achieved through one of the three other adhesins. This proposition was strengthened in studies in which an *S.* Typhimurium strain, carrying mutations in all four fimbrial operons, had a 26-fold increased oral 50% lethal dose (LD_{50}) for mice (398).

In addition to the four established fimbrial operons, three operons were discovered, these including *stf* (*Salmonella* enterica serovar Typhimurium fimbriae) (104), *bcf* (bovine colonising factor) (390) and *saf* (*Salmonella* atypical fimbrial) (119). However, of the 7 fimbrial operons, only two, *fim* and *agf*, had been shown to mediate the expression of filaments on the surfaces of *S.* Typhimurium cells grown in broth or on agar plates, respectively (100, 151).

Subsequently, the publication of the *S.* Typhimurium strain LT2 genome revealed the presence of a total of 13 operons containing ORFs with similarity to fimbrial gene sequences (264). The 6 addition operons were termed *stb*, *stc*, *std*, *sth*, *sti* and *stj*. Expression analysis of the major fimbrial subunits from 11 of these fimbrial operons demonstrated that only FimA was detectable on the bacterial surfaces after growth of the organism in broth (194). However, the expression of nine of the operons was detected on the bacterial surface of cells recovered from bovine ligated ileal loops, suggesting that the majority of *S.* Typhimurium fimbriae, although poorly expressed *in vitro*, are induced in

the host environment (194). Injection of mice with *S.* Typhimurium, resulted in seroconversion to all 11 fimbriae thus confirming their *in vivo* expression (193).

Fimbrial adhesins are thought to mediate attachment to the intestinal surface. In support of this, it has been established that fimbriae promote attachment of *S.* Typhimurium to various cell lines *in vitro*. Interestingly, each fimbrial operon seems only to be required for attachment to and invasion of an individual cell line (24). Thus fimbriae may allow *S.* Typhimurium to distinguish between different cell types. A model has been suggested in which the expression of individual fimbriae determines the target cell type for entry, while TTSSs supply a general invading capability (195). It has also been suggested that fimbriae form the basis of host specificity; this is based on the identification of the *bcf* operon, required by *S.* Typhimurium for colonisation of bovine, but not murine Peyer's patches (390).

An attractive model applied to fimbriae encompasses aspects of function (attachment) as well as regulation (phase variation). It is thought that fimbrial phase variation is employed by *Salmonella* as a means of evading cross-immunity between serovars provoked by shared fimbrial antigens (195). Bacteria evading the immune system by switching off expression of certain fimbriae must therefore express others in order to establish infection. It is imagined that the degree of functional redundancy displayed by fimbriae makes this a possibility (195). This model provides an attractive explanation as to why *Salmonella* genomes contain large numbers of phase variable, fimbrial operons which display partial functional redundancy.

1.3.2 Afimbrial adhesins of *Salmonella*

In addition to the many fimbrial operons harboured by *S.* Typhimurium, this intracellular pathogen is known to utilise outer membrane proteins, which provide specialised functions enabling the bacteria to enter into and survive within the host environment. Some of these proteins are involved in the more progressive, systemic aspects of infection, while many are thought to be involved in the initial attachment to the intestinal epithelium. For instance, PagC is known to mediate survival of *S.* Typhimurium in macrophages (327). As PagC is not an adhesin, it will not be discussed further. The main, established afimbrial adhesins of *S.* Typhimurium will be discussed in the following sections.

1.3.2.1 Rck

As discussed in Section 1.2.2.6, the *S.* Typhimurium virulence plasmid encodes the gene for Rck. Rck is a member of a family of related 17- to 19-kDa outer membrane proteins including PagC from *S.* Typhimurium (274), Ail from *Yersinia enterocolitica* (276), OmpX from *E. coli* (267), and Lom (bacteriophage lambda-lysogenic *E. coli*) (19). Structural predictions for Rck indicate that it is a β-barrel protein consisting of 8 anti-parallel β-sheets, giving rise to 4 surface-exposed loops (169). It has been proven that Rck confers high-level serum resistance by interfering with the formation of polymerised C9 tubular membrane attack complexes (170). In addition, expression of the *rck* gene in non-invasive *E. coli* promoted adhesion to and invasion of cultured mammalian cell monolayers (171). Loop-deletion mutagenesis experiments and construction of Rck-PagC hybrid fusion proteins have established that loop 3 of the predicted Rck structure, is required for serum resistance and invasion in *E. coli* (66). The Rck protein is multi-functional, inducing bacterial binding to extracellular matrix (ECM) preparations, and to the ECM component laminin (75).

1.3.2.2 OmpD

The *ompD* gene encodes the most abundant protein in the outer membrane of *S.* Typhimurium, a 34-kDa porin displaying sequence similarity to the major porins OmpC, OmpF, and PhoE as well the NmpC and Lc porins of *E. coli* K-12 (205, 366, 367). OmpD is absent from other gram-negative bacteria, including *E. coli*. The abundance of OmpD in the outer membrane is determined primarily at the transcriptional level, increasing in response to anaerobiosis and decreasing in response to low pH (345).

The virulence functions of OmpD have been the subject of much debate. It was originally reported that *S.* Typhimurium strains harbouring an *ompD* mutation displayed a reduction in virulence for BALB/c mice (92). However conflicting data presented by Meyer, P. *et al.* disputed these findings stating "There is no statistically significant difference in virulence between the *S. typhimurium* wild type strains and their corresponding *ompD* mutants" (270). Subsequently, it has been established that *ompD* mutants display lower levels of macrophage and epithelial cell binding *in vitro*, thus

suggesting that although possibly not involved in the lethality of mice, OmpD is involved in the recognition of *S.* Typhimurium by human macrophages and intestinal epithelial cells (162).

1.3.3 The SPI-1-encoded Type three secretion system of *Salmonella*

Salmonella encode two distinct virulence-associated TTSS involved with different stages of the infection process (191). The SPI-2-encoded TTSS is associated with intracellular survival, whereas the SPI-1 TTSS is required for epithelial cell invasion and enteric pathogenesis (181, 191). These bacterial appendages provide a conduit for the direct transport of effector molecules from the cytoplasm of the bacteria to the host cell. Made up of more than 20 proteins, TTSSs are considered the most complex secretion systems in bacteria. Present in many different gram-negative species, the main components of the apparatus seem to be generally conserved while the arsenal of effector proteins they deliver is specific to each system (136).

Although SPI-1-independent methods of cell invasion exist, the SPI-1-encoded TTSS is generally considered central to entry of the intestinal epithelium. It is composed of a supramolecular structure called the needle complex (NC) which shares sequence homology with proteins of the flagellar export machinery (222). The NC consists of a multi-ring base which anchors the structure to the bacterial envelope, with a filamentous needle-like projection (composed of PrgI) that protrudes ~50 nm from the bacterial surface (Fig. 1.3). The base is formed by InvG, PrgH and PrgK (222), in a ratio of 1:1:1 (259), and features four distinct rings, two associated with the outer membrane (OR1 and OR2) and two contacting the inner membrane (IR1 and IR2) (Fig. 1.3 (A)), (259). The base is traversed by a cylindrical inner rod (PrgJ) connecting the needle to a socket substructure, stabilised by InvJ, at the neck of the inner rings (Fig. 1.3 (B)). The assembly of the apparatus is a multi-step process with the base complex being constructed prior to the addition of the inner rod, socket and needle components (Fig. 1.3 (C)) (223, 259). Once fully assembled, the base substructure (InvG, PrgH and PrgK) begins to function as a secretion apparatus devoted to transport of factors required to assemble the needle and inner rod substructures; on completion of the NC, the specificity of the machine changes and it becomes concerned with the export of effector proteins (69, 223).

The mechanism of substrate-switching, is the subject of much debate, but it is thought to involve a downward movement of a cup-like structure situated at the centre of the cytoplasmic face of the base along with IR2 (Fig. 1.3 (B)), (259). A model for substrate-switching has been proposed involving the completion of the inner rod and the socket-like structure at the basal side of IR1 (258). It is suggested that the socket region serves as a nucleation point for inner rod assembly. Once construction of the inner rod is complete, the needle becomes firmly anchored leading to conformational changes in the cytoplasmic side of the base, giving rise to reprogramming of the apparatus making it competent for effector secretion (258).

The diameter of the needle complex is such that effector proteins, once targeted for secretion, must pass through the needle in an unfolded state. There also seems to be some semblance of a hierarchy regarding the order in which the effectors are secreted (69, 321, 417). It is therefore thought that a complex substrate-recognition system exists involving multiple signals and accessory proteins (372). All known TTSS effector proteins, within the first 20-30 amino acids, possess signal sequences, thought to be involved in their targeting to the secretion apparatus (351, 373). However, upon secretion, these sequences remain unprocessed, and attached to the mature protein. The organisation of these signal peptides seem to be very simple and it has been proposed that the important information held within them is communicated at the mRNA level (12), although the amino acid sequence has been established as important for at least some TTSS effector proteins (245, 341). Although the subject of much debate, the stringency of substrate-specificity within the TTSS seems to be supplied by somewhat generic signal sequences, made specific by the addition of chaperones and accessory proteins. These TTSS-associated chaperones are small, acidic, dimeric proteins, which unlike other chaperones lack ATP-binding or hydrolysing capabilities (111). In general, these chaperones bind a ~15-100 amino acid domain immediately downstream of the effector protein signal sequence (111). The proteins usher the effectors towards the apparatus mouth, priming them for rapid unfolding before secretion, to facilitate their transport through the narrow needle channel (375).

Upon TTSS recognition of the effector/chaperone complex, it must strip the effector protein from the chaperone. Evidence suggests that ATPases, in close proximity to the NC (287), are responsible for disassociation of the effector from the chaperone and subsequent presentation of an unfolded protein to the apparatus for secretion (6).

Finally, the effector proteins must be delivered into the host cell. This is the least understood aspect of type III secretion. A model was proposed in which the needle complex punctured the target cell membrane and injected proteins directly into the host

cytosol (188). This model has since been disproved. It has been established that TTSSs need a set of effectors termed translocators, thought to insert into the target cell's membrane forming a channel through the membrane and a "dock" for the needle to complex with (160, 385). The needles of several TTSSs are thought to interact with this dock via an accessory structure at the tip, consisting of one protein. Examples of this include LcrV from *Yersinia entercolitica* (285) and EspA from *E. coli* (215). However, it is not known how the translocators insert into the target membrane, how docking of the needle takes place and it remains unclear how the effector proteins are ultimately delivered into the host cell.

1.3.4 Bacterial-promoted endocytosis

Entry of *S.* Typhimurium into epithelial cells is accompanied by the formation of large host cell surface membrane ruffles (131, 137). These ruffles are brought about through the actions of effector proteins delivered by the SPI-1 TTSS. Unlike other bacterial toxins that modify target host cell proteins in a non-reversible manner, TTSS effectors seem to act by mimicking the function of host cell proteins (376). These "eukaryotic protein mimics" often seem to be the product of divergent evolution rather than alternate versions of hijacked mammalian genes (136). Indeed many of the bacterial effector proteins do not share any sequence or structural similarity to their eukaryotic counterparts, however they process mammalian cellular targets in a manner that is indistinguishable from that of the interaction of the bona fide eukaryotic protein and the same target (52). A corollary of this theme is that it is extremely difficult to predict the function of most TTSS effector proteins from amino acid sequence analysis. The function of the main TTSS effector proteins including the *Salmonella* outer proteins (Sop) SopE, SopE2, SopB, the secreted protein tyrosine phosphatase SptP, and the *Salmonella* invasion proteins (Sip), SipA and SipC will be discussed below.

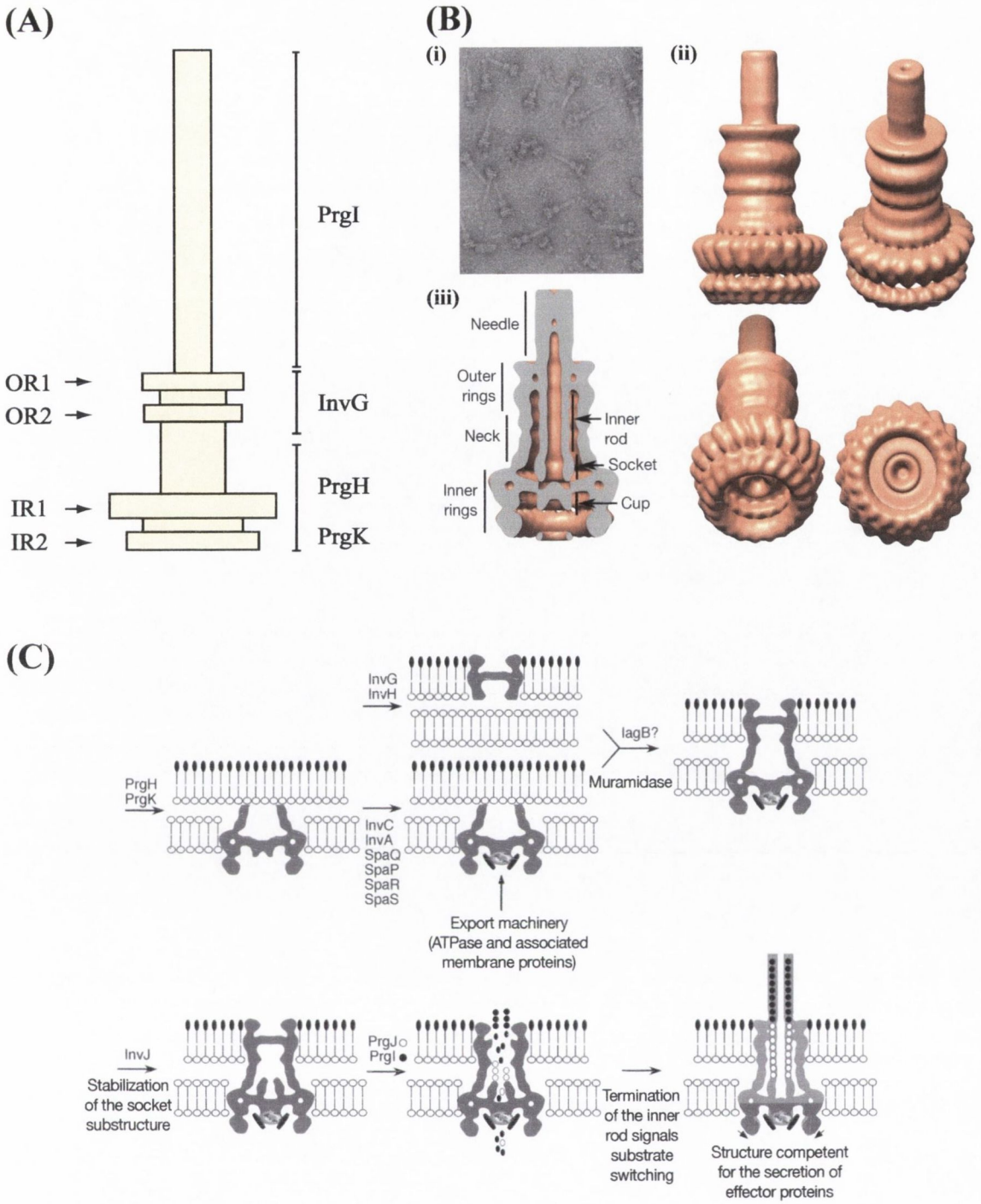

FIG 1.3. The needle complex of *S.* Typhimurium. (A) Structural features of the needle complex. The distinctive substructures are indicated: the ring complexes forming the base and the extracellular needle filament. The proteins making up these components are indicated. **(B) (i)** Electron micrographs of negatively-stained isolated needle complexes. **(ii)** Cross-section of the needle complex indicating the location of its varioud substructures. **(iii)** Surface rendering of the structure of the needle complex. **(C)** Model of the assembly pathway of the needle complex. Assembly occurs in descrete steps. InvC is an ATPase recruited to the TTSS involved in chaperone recogntion. A muramidase (IagB) helps transport the apparatus through the peptidoglycan. InvH chaperones the assembly of InvG to form the outer ring, while InvA, SpaP, SpaQ, SpaR and SpaS are inner membrane proteins that form part of the export apparatus. See text for more details. Panel B and C are taken from Galan, J. E. and H. Wolf-Watz (134).

1.3.4.1 Indirect manipulation of actin cytoskeletal arrangement by *Salmonella*

The effector proteins SopE, SopE2 and SptP are capable of activating (SopE and SopE2) and inactivating (SptP) Cdc42 and Rac-1, members of the Rho-family of low-molecular-weight GTPases. Rho GTPases have two peptide regions, called Switch I and II that undergo conformational changes depending on the nucleotide bound (161). SopE and SopE2 are guanine nucleotide exchange factors that catalyse exchange of GDP to GTP (17). Upon translocation into the host cell SopE binds and activates both Cdc42 and Rac-1. SopE2 has significant activity only towards Cdc42 and not Rac-1 (125). When GTP is bound, Rho GTPases are in an active state with Switch I and II in a conformation such that they can bind signaling molecules. This activation ultimately leads to recruitment of downstream effectors such as N-WASP and WAVE which mediate Arp2/3 complex-dependent actin nucleation (395). Such remodeling of host actin near the cell surface produces the characteristic membrane ruffles that accompany bacterial entry (Fig. 1.4).

1.3.4.1 (A) SopB

SopB, identified independently by two different groups and therefore also termed SigD (*Salmonella* invasion gene D) (138, 189), is also capable of Cdc42 activation, however it is not a nucleotide-exchange factor. It functions by inducing changes in phosphoinositol metabolism through its inositol phosphate phosphatase activity (299).

There is a general requirement for phosphatidylinositol-4,5-bisphosphate [PtdIns(4,5)P_2] depletion at sites of phagocytosis and endocytosis (40, 203). It has been established that SopB is responsible for the elimination of PtdIns(4,5)P_2 at the base of membrane ruffles and for promoting membrane fission to facilitate bacterial entry during *Salmonella* invasion of epithelium (387). Interestingly, it has recently been demonstrated that SopE, SopE2 and SopB, disrupt tight junction structure and function through their Rho GTPase activating capabilities (42). Disruption of tight junctions is likely to contribute to the production of diarrhoea.

1.3.4.1 (B) SptP

The activity of effector proteins delivered by the SPI-1 TTSS is tightly coordinated in a temporal manner (221). This regulation allows for the delivery of proteins with apparently antagonistic functions. StpP is a GTPase activating protein (GAP), which catalyses the loss of the γ-phosphate, during hydrolysis of GTP to GDP thus inactivating the Rho GTPases Cdc42 and Rac-1 (206). This enzymatic activity reverses the cytoskeletal changes induced during internalisation of *Salmonella*, restoring normal actin architecture at the site of bacterial entry (128). To facilitate temporal regulation of actin assembly and disassembly, *Salmonella* exploits the host cell ubiquitin-mediated proteasome degradation pathway. Due to differences in protein stability, determined by the N-terminal secretion and translocation domain found in each protein, SopE is ubiquitinated and rapidly degraded upon entry into host cells, while SptP is much more stable and persists (221). Hence, the longevity of SptP compared with the relatively short-lived SopE ensures that SopE-induced actin rearrangements at the bacterial entry site can be restored to normal.

1.3.4.2 Direct manipulation of actin cytoskeletal architecture

In addition to the indirect reorganisation of actin by the Sops, *Salmonella* secrete effector proteins that can modulate actin dynamics directly. Two important factors involved in such activities are SipC and SipA proteins (also known as *Salmonella* secreted proteins, SspC and SspA). These factors function in a cooperative manner manipulating processes of actin nucleation and polymerisation required for membrane ruffling during bacterial invasion (265, 266). In addition, SipB and SipC associate with lipid bilayers *in vitro* and with the host cell plasma membrane during *Salmonella* infection *in vivo* (168, 350).

1.3.4.2 (A) SipC

SipC is a 42-kDa protein crucial for early bacterial entry of epithelial cells. SipC is essential for the translocation of other effector proteins into the mammalian cytoplasm

(129, 415). It itself is secreted into host cells and becomes inserted in the epithelial plasma membrane (350). The SipC protein is multi-functional with individual functions being ascribed to particular domains of the protein. The protein can be divided into three regions, the N-terminal domain which is involved in F-actin bundling, a C-terminal domain that directly nucleates actin *in vitro* and a middle hydrophobic, transmembrane region that is thought to form an integral part of the translocation apparatus pore (167). It has recently been reported that the C-terminal domain can be further divided into two regions: residues 201-220 are essential for actin nucleation while residues 321-409 are required for effector translocation (60).

1.3.4.2 (B) SipA

The *sipA* gene encodes one of the largest known *Salmonella* secreted proteins (87 kDa). The protein like SopE/E2 and SopB is responsible for tight junction disruption during *Salmonella* infection (42). The activity of SipA is manifold. It enhances SipC-induced actin nucleation and bundling (266), while itself is capable of binding to F-actin (266, 422) and G-actin reducing the minimal concentration for G-actin polymerisation (422). It also complexes with and promotes the actin-bundling activity of host T plastin at the site of bacterial/host contact (421). Furthermore, SipA locally inhibits ADF/cofilin- and gelsolin-directed actin-depolymerisation (79, 265) thus stabilising the activities of other effector proteins. Therefore it can be seen that *Salmonella* secretes effector proteins into the host cell that not only trigger actin polymerisation but also counteract the attempted disassembly of these new structures by the host cell.

1.4 Intracellular survival of *Salmonella*

When foreign bodies, such as bacteria, viruses and protoazoa enter mammalian cells they become encased in a lipid-based phagosome. Immature phagosomes undergo biochemical changes whereby they mature and are directed towards the centriole of the cell. Nucleation at the centriole coincides with lysosome trafficking to the centriole where upon the phagosomes and lysosomes collide, bringing about killing of the intra-phagosome foreign-

bodies (47). *Salmonella* have the ability to prevent this maturation thus avoiding lysosomal killing (47, 407).

Typical phagosomal maturation starts with the acquisition of a small GTPase, Rab5 (334). Rab5 directs the association and/or stimulation of a phoshatidyl-inositol 3-kinase (PI3K), the enzyme responsible for the generation of phoshatidyl-inositol 3-phosphate (PI3P), which is absolutely required for phagosomal maturation (122). This enzyme in turn binds EEA1 (early endosome-associated protein) and Hrs, which are responsible for bridging vesicles (122), and forming multi-vesicle (330) bodies respectively. Hrs also interacts with ubuiquitylated proteins and triggers inner budding of vesicles in a process involving ESCRT (endosomal sorting complex required for transport) complexes (329). Maturation of phagosomes is accompanied by the accumulation of LBPA (lyso-*bis*phosphatidic acid), and lysosomal glycoproteins LAMP-1 and -2 (47). In the final stage of maturation, Rab5 and EEA1 dissociate from the phagosome and are replaced by another GTPase, Rab7 (405), which interacts with RILP (Rab-interacting lysosomal protein) (55). RILP bridges Rab7-containing vesicles with a dynein motor complex that powers the trafficking of phagosomes along microtubules to the centriole (55, 165). This physical translocation facilitates the collision and fusion of phagosomes with lysosomes (165).

The SCV displays many of the markers of phagosome maturation. However, SCVs undergo repeated cycles of PI3P formation and depletion (318). SCVs progress through many of the stages of phagosomal maturation but ultimately do not fuse with the lysosome. At early time points, SCVs contain Rab5 and EEA1 which are subsequently replaced by Rab7 (286, 354). Other markers such as PI3P (354), and LAMP-1/-2 (268) also accumulate at SCVs. Even the RILP protein which facilitates trafficking to the centriole has been found to associate with the SCV within the first hours following invasion (164).

The bacterial factors that block SCV fusion with lysomes, although shown to include SPI-1-encoded effectors (286), mainly include members of PhoP/Q regulon (Section 1.5.1) and components of SPI-2. A role in preventing lysosomal fusion to SCVs has been proposed for the PhoP/Q regulon (140). However, the PhoP/Q system controls the expression of numerous proteins and as such the absence of a functional system is likely to have pleiotropic effects on bacterial virulence. The involvement of PhoP/Q in intra-epithelium survival will not be discussed further in this section. The SpiC SPI-2-encoded TTSS effector protein was reported to be translocated into the cytosol of host cells affecting membrane fusion events (393). Two targets of SpiC, namely TassC (231), and Hook3 (364), are thought to be involved in vesicle fusion. TassC binds to SCVs only in a *spiC*-deficient mutant and is thought to be involved in vesicle transport (231). Hook3 is

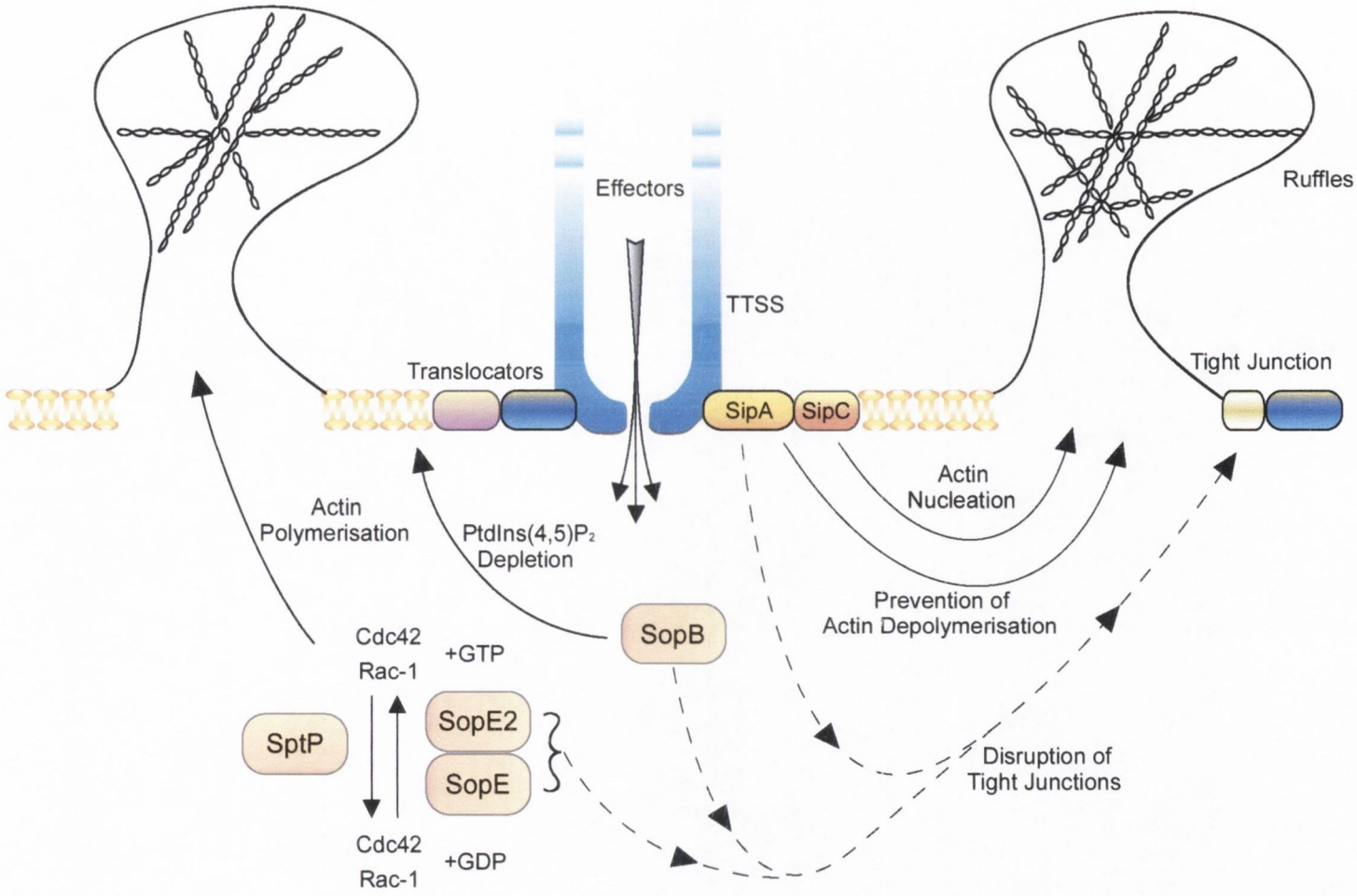

FIG 1.4. Schematic representation of selected SPI-1 TTSS-promoted events during *S.* Typhimurium invasion of epithelial cells. The TTSS makes contact with the translocator "dock". From this position effector proteins are secreted into the host cell. The effector proteins hijack the host cell's actin processing machinery and cause massive nucleation and polymerisation of actin. This process results in membrane ruffles and bacterial internalisation.

related to the *Drosophila* Hook protein required to prevent early fusion of multi-vesicle bodies with the lysosomal compartment (220).

The most dramatic aspect of intra-cellular survival of *S.* Typhimurium is the extensive fusion of endosomal compartments, which form long tubular extensions of the SCV known as *Salmonella*-induced filaments (Sifs), an event that coincides with the initiation of bacterial replication (139). The formation of these filaments requires the delivery of SifA into the host cytosol by the SPI-2-encoded TTSS (46). In a Rab7-dependent manner, Sifs colocalise with and rely upon microtubules for their formation and support (46, 48). Another SPI-2 TTSS effector protein, SseJ, with acyltransferase/lipase activity, is thought to act in concert with SifA, complimenting its activity and modulating the stability of the SCV (339). Sif filaments are enriched in cholesterol and contain both LAMP-1 and processed cathepsin D (48). Other effectors are also thought to be involved in Sif formation, for example, deletion of *sseF* and *sseG* blocks Sif formation at an intermediate stage resulting in "pseudo-Sifs" that lack LAMP-1 (224).

The method of blocking lysosome fusion is not fully understood. However, SifA is thought to block the interaction between Rab7 and RILP thus preventing trafficking of SCVs to the lysosome nucleation site (164). Another consideration comes from reports by Salcedo and Holden, who demonstrated that SCVs become surrounded by membranes of the *trans*-Golgi network at times greater than 4 h post invasion (224). This process required SseG, which was directed to the golgi apparatus and may serve to prevent lysosomal fusion.

1.4.1 Survival within macrophages and dissemination

When *S.* Typhimurium cross the basolateral membrane of intestinal epithelial cells, they are met by neutrophils and macrophages. These professional phagocytes engulf the *Salmonella*, encasing them in a SCV; this time composed of macrophage/neutrophil membrane. It is the ability of *S.* Typhimurium to survive with murine macrophages that leads to bacterial dissemination and systemic infection. *S.* Typhimurium display three main capabilities which enable them to survive within the otherwise harsh intra-macrophage environment. These are the ability to prevent lysosomal fusion at the SCV (47), to avoid killing by products of the macrophage respiratory burst (243), and to cause macrophage programmed cell death (192). Apart from these three aspects of survival, *S.*

Typhimurium has also been shown to promote increased cyclooxygenase 2 expression, resulting in the up-regulation of prostaglandin production in macrophages, thought to facilitate bacterial survival (394).

The factors involved in the interference of phagosomal maturation and trafficking employed by *S.* Typhimurium residing within macrophage cells are thought to be identical to those employed while in epithelial cells. Experiments have established that deletion of the *sifA* gene in *S.* Typhimurium leads to release of bacteria into the cell cytosol of the infected cell (33). However, in the cytosol of macrophages, bacteria die whereas they replicate rapidly in epithelial cells thus indicating the inhospitable conditions present within the intra-macrophage environment (33, 49).

Reactive oxidants are a primary weapon of the macrophage antibacterial arsenal (243). But, by synthesising enzymes and products that counteract them, *Salmonella* reduces the effectiveness of these bactericidal and bacteriostatic free radicals. The macrophage has many enzymes such as the phagocyte NADPH oxidase and xanthine oxidase capable of producing reactive oxygen species that place the bacteria under stress, damaging their DNA (404). *S.* Typhimurium employs enzymes to defend against oxidative stress *in vitro*. Examples of such enymes include the periplasmic superoxidase dismutases, *sodCI* and *sodCII* (86, 109, 110), and glucose 6-phosphate dehydrogenase (251), which is required for NADPH synthesis. The *recA* and *recBC* DNA repair systems play a role in persistence and are required for full virulence (50, 51). A *Salmonella* gene designated *sspJ*, encoding a 392-amino-acid protein has also been established as being involved in protection against oxidative stress (397). *sspJ* mutants are hypersensitive to superoxides *in vitro*, attenuated for virulence in mice and defective for growth in macrophage (397). The mechanism of action of SspJ is however, currently undefined.

Like superoxides, nitric oxide, is also synthesised in macrophage and is a precursor of a range of toxic, reactive nitrogen species (reviewed in (254)). The inducible nitric oxide synthase (iNOS), in response to IFNγ and bacterial LPS, is responsible for converting L-arginine to NO (101). iNOS can also react with NO to generate peroxynitrite. *In vitro*, a peroxynitrite ($ONOO^-$) donor is bacteriocidal, and the nitrate derivative, S-nitrosoglutathione is bacteriostatic towards *S.* Typhimurium (85, 87). It is established that the SPI-2-encoded TTSS plays a role in limiting the bacteriostatic effects mediated by iNOS (57). Indeed SPI-2 has been implicated in mechanisms of protection from both phagosomal oxidases and iNOS-dependent processes (57, 404). Although it seems likely, it is unresolved whether the method of SPI-2-mediated protection from phagocyte oxidases and iNOS is independent.

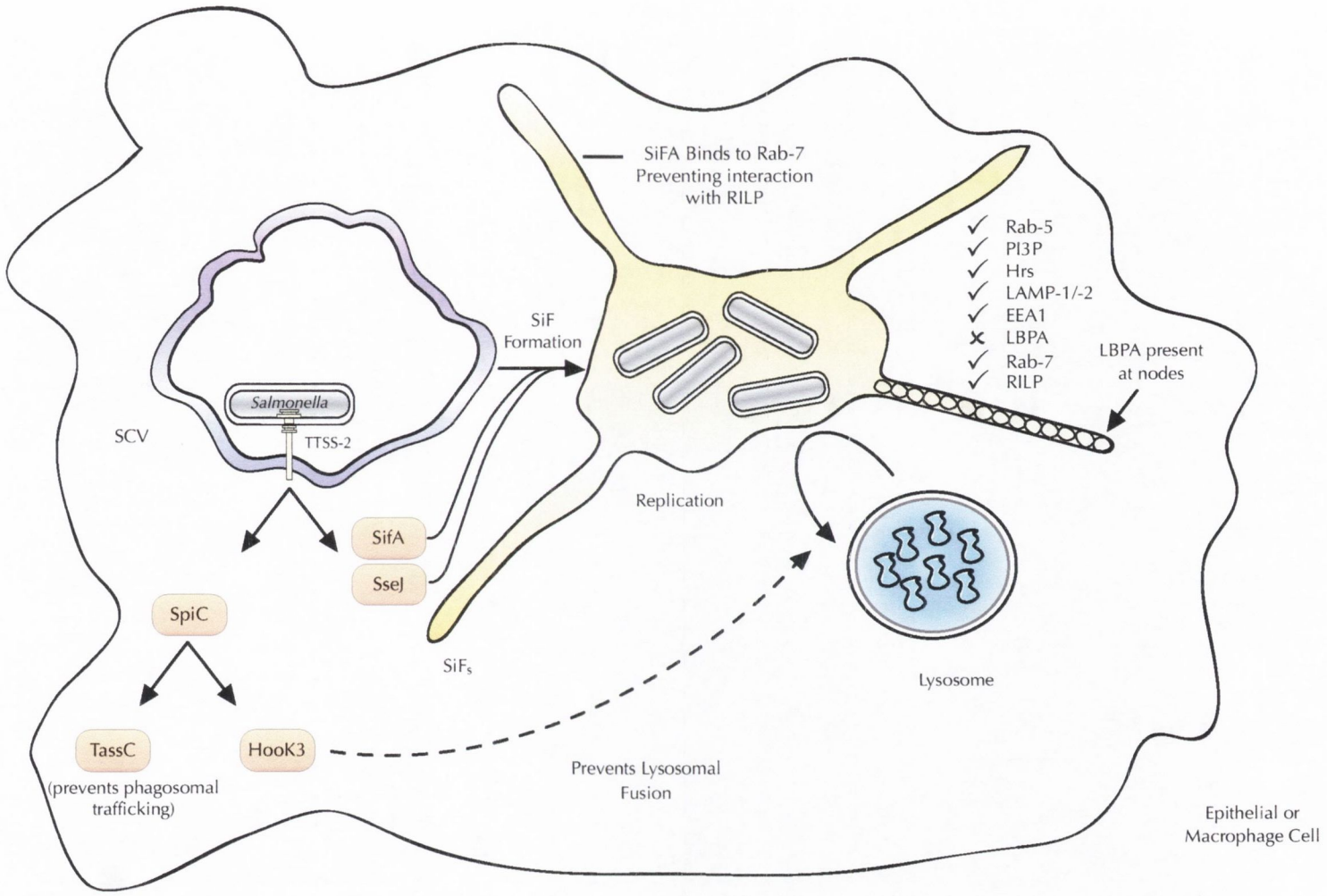

FIG 1.5. Schematic representation of how *Salmonella* redirects phagosomal maturation within macrophage and epithelial cells. From an intra-SCV location *S.* Typhimurium secretes effector proteins into the host cell cytosol using the SPI-2-encoded TTSS. These effector proteins interfere with normal maturation of the phagosome and subsequent lysosomal fusion.

The final defense mechanism employed by *S.* Typhimurium to thwart the harmful advances of macrophage is the ability to induce macrophage cell death. The mechanism of *Salmonella*-induced macrophage cell death has been the subject of some confusion and debate. Both the time taken to cause cell death as well as the type of cell death undergone by macrophages has been debated. Some groups have reported rapid macrophage cell death upon infection (43, 63, 280), while others disagree, demonstrating a requirement for a much longer time period (153, 242). *S.* Typhimurium causes death of macrophage in a process that does not fit any conventional categorisation. The macrophage cell appears to exhibit both the typical signs of apoptosis (chromatin fragmentation, caspase-3 activation, membrane blebbing (63, 202, 280)), and necrosis (lack of caspase-3 activity and loss of membrane integrity (43, 63, 408)). Indeed, it has been specifically noted that populations of macrophages undergoing cell death are highly heterogenous, displaying significantly different features (63).

Oddly, *S.* Typhimurium-induced macrophage death is dependent on both the SPI-1 and SPI-2 encoded TTSSs. This is slightly counterintuitive as SPI-1-located genes are likely to be down-regulated (Sections 1.2.2.1 and 1.5.1) in an intra-macrophage environment. *In vitro*, the proportion of macrophages carrying markers for a necrotic-type of cell death as apposed to an apoptotic one is favoured by conditions in which SPI-1 TTSS expression is promoted and the multiplicity of infection is high (63). However, it has been reported that *in vivo*, only one or two bacterial cells are internalised per macrophage (359), suggesting that promotion of the necrotic-type of cell death may be an artifact of the experimental conditions and may not represent the situation within a live host.

The SPI-1-encoded TTSS is shown to promoting rapid (within ~45 min of infection) macrophage cell death in a manner independent of cytoskeletal disruption (63). Macrophage programmed cell death, a process incorporating aspects of both necrosis and apoptosis, is brought about by *S.* Typhimurium through the activity of TTSS effector proteins. The effector protein SipB interacts with caspase-1, causing the release of IL-1β and IL-18, which in turn promotes rapid programmed cell death (184). Interestingly in macrophage cells deficient in caspase-1 production, rapid cell death does not occur and takes as long as 3 h (183). This caspase-1 independent programmed cell death is also dependent upon SipB (183). The effector is thought to bring about cell death as a consequence of its ability to induce autophagy by damaging macrophage mitochondria (183).

In the absence of a functional SPI-1, *S.* Typhimurium is still capable of promoting caspase-1-dependent macrophage killing; it employs the SPI-2 and *spv* loci to accomplish

this in a process that takes up to 24 h (45, 279, 399). This delayed form of *Salmonella*-induced cell death also requires the protein kinase PKR and activation of Toll-like receptor 4 on macrophages by bacterial LPS (190). Normally complex signal transduction pathways balance pro- and anti-apoptotic regulation. While NF-κB and p38 mitogen-activated protein kinase promote the production of anti-apoptotic factors, PKR is required for the promotion of bacterial-induced apoptosis (192). The SPI-2-encoded TTSS is essential to push this balance in favour of apoptosis. However, the effector proteins involved remain poorly characterised. Interestingly, a deletion in the virulence plasmid gene, *spvB*, abolished the ability of *S.* Typhimurium to induce this delayed-form of macrophage cell death (45). As stated in Section 1.2.2.6, SpvB is an ADP ribosylating toxin which interferes with actin processing. However, it is unknown whether this activity is responsible for the induction of programmed cell death of macrophage.

In a study examining *S.* Dublin infection of the human macrophage-like cell line THP-1, it was revealed that within 5.5 h, 90% of THP-1 cells displayed DNA fragmentation. This process required an intact *phoP* gene and reveals yet another method by which *Salmonella* can destroy normal macrophage function (396).

1.5 Coordinate regulation of virulence in *Salmonella*

To survive each stage of life, *Salmonella* must adapt to a series of ecological niches. Each new environment encountered can be defined in terms of specific parameters including temperature, nutrient availability, osmotic pressure, oxygen status, and pH. To adapt to each of these stresses the bacterium must sense its environment and then communicate this information to the DNA. The cell then modulates its gene expression profiles in a manner that enhances the fitness of the bacterium within that specific environment. This requires the coordinated control of the expression of a large number of genes using complex regulatory networks.

The regulation of gene expression during *Salmonella* pathogenesis has been the subject of much study. Regulatory networks interact and overlap to switch distinct sets of genes on and off in response to the environmental stimuli present. As discussed, *S. enterica* encode two distinct TTSSs, operating at different steps of the infection cycle. The expression of these systems is, not surprisingly, differentially regulated: the expression of the SPI-1 TTSS is stimulated by environmental queues present in the intestinal tract (high

osmolarity, low O_2 levels), whereas the expression of the SPI-2 TTSS is stimulated by conditions present within host cells (low Mg^{2+} concentration and acidic pH) (78).

Expression of SPI-1-encoded genes is controlled by the several regulatory loci both within the PAI and located elsewhere on the chromosome (250). Within SPI-1, four transcriptional regulators, HilD, HilC, HilA and InvF, act in an ordered fashion to coordinately activate expression of the SPI-1 TTSS (15, 102, 347). The *hilC* and *hilD* genes encode HilC and HilD, members of the AraC transcriptional regulators (347). These proteins induce expression of the regulatory gene *hilA* by derepression and/or direct activation of transcription at the *hilA* promoter region (38, 347, 349). HilC and HilD can also activate a subset of SPI-1 genes independently of their positive regulation of *hilA* (5).

The *hilA* gene encodes HilA (15), an OmpR/ToxR-like protein that activates the transcription of *invF*, which encodes InvF, another AraC family member (102). InvF displays an unusual mode action; it has been established as the first transcriptional regulator to require interaction with a TTSS chaperone protein (82). Inactive InvF binds to its target promoter region. Once the TTSS chaperone protein, SicA, is produced, it binds to InvF resulting in transcriptional activation by a mechanism in which SicA is thought to induce conformational changes in InvF, facilitating InvF/RNA polymerase interactions (82).

Components of the SPI-1 regulatory network are also encoded by loci located outside of SPI-1. The products of these genes include the two-component sytems EnvZ/OmpR, PhoP/PhoQ and SirA/BarA, as well as FliZ, a member of the flagellar regulon, HilE, PhoB, CsrA (carbon storage regulatory gene), RtsA (AraC family) and RtsB (103, 142, 229, 249, 250).

A further level of regulation is placed upon SPI-1 gene expression by the nucleoid-associated proteins Fis, H-NS and HU (348). These proteins, through their manipulation of the level of DNA supercoiling, are thought to fine-tune SPI-1 virulence gene expression (133).

1.5.1 The PhoP/Q two-component system

The regulation of components involved in the enteric aspects of *Salmonella* virulence is accomplished by many different factors acting in concert. While this is also true for the systemic aspects of infection, ultimately, the PhoP/Q system is responsible for controlling

expression of genes involved in the more persistent aspects of *Salmonella* pathogenesis (424). As mentioned in Section 1.4, it is established that the PhoP/Q system is absolutely required for intracellular survival within both macrophages and epithelial cells (35, 112, 145). Interestingly the role of PhoP/Q may not be consistent in all cell types. Unexpectedly, this regulatory system was shown to be dispensable for bacterial survival and proliferation within dendritic cells (95, 293). Indeed, inactivation of the PhoP/Q system (which causes survival defects within macrophages and epithelial cells), promotes an increase in the numbers of intracellular *Salmonella* within fibroblasts (54). It has been proposed that PhoP/Q may be involved in restraining the intracellular growth rate within fibroblasts and dendritic cells shortly after traversal of the epithelium. It is here that *Salmonella* retard their growth and establish a persistence niche (389).

The genes *phoP* and *phoQ* form a di-cistronic operon encoding a two-component regulatory system consisting of a membrane-located sensor/kinase/phosphatase domain (PhoQ) and a cytoplasmically located response regulator (PhoP) (146, 274). In response to specific signals PhoQ, the membrane-located sensor, modifies the phosphorylation state of the cytoplasmically-located DNA-binding protein PhoP, increasing its DNA-binding capabilities (56, 58, 281). Three different cues have been proposed to activate the PhoP/Q system inside macrophages: a mild acidic pH (8, 14), antimicrobial peptides (14), and low Mg^{2+} (144). However, the significance of an acidic pH and antimicrobial peptides is currently unclear (147). In the presence of high Mg^{2+} concentrations the system is off, while at lower levels, such as those found within macrophages, the system is switched on and regulates the expression of over 100 genes in *S.* Typhimurium, representing ~3% of the *Salmonella* genome (424). Genes that are activated are referred to as *pags* (PhoP-activated genes) while those that are repressed are called *prgs* (PhoP-repressed genes).

Such is the importance of this regulatory system that inactivation of either the *phoQ* or *phoP* genes results in a 5-fold reduction in *S.* Typhimurium virulence for mice and an inability to survive within phagocytic cells (134, 146, 274). PhoP/Q controls virulence determinants both directly and indirectly by regulating the expression of several transcriptional factors required for *S.* Typhimurium virulence, such as PhoP/Q itself (371), SsrB (35), SlyA (301), PmrA (219), RpoS (391), and HilA (16) (Fig. 1.6).

It is thought that PhoP/Q is responsible for the modulation of gene expression during the transition of *S.* Typhimurium from an invading bacterium to an intracellular one (145). PhoP is known to bind to the *hilA* promoter and repress expression of the SPI-1 activator (16). This repression, coupled with the negative regulation of the TTSS NC components PrgK, PrgH and PrgI results in switching off of the factors involved in cellular invasion.

Surprisingly, a PhoP-activated operon has been identified within SPI-1 (2). This operon, composed of the *orgB* and *orgC* genes, encodes a protein that interacts with the InvC ATPase and a putative effector protein of the TTSS, respectively (2). It was revealed that in contrast to the rest of SPI-1, *orgBC* is expressed during and after *Salmonella* invasion of intestinal cells, suggesting a dual role for the products of this operon (2).

It was recently demonstrated that the function of PhoP/Q, through a positive feedback loop, is to promote a transcriptional surge that jump-starts the intracellular *Salmonella* virulence circuit (363). The *phoPQ* operon contains two promoters, a constitutive promoter that provides basal levels of these proteins, required for responding to environmental stimuli and a second promoter that is activated by PhoP upon PhoQ sensing of low Mg^{2+} concentrations (371). Induction of the PhoP/Q system results in an initial surge of PhoP phosphorylation, the occupancy of target promoters and the subsequent transcription of *pags*. This is followed by a subsidence of transcription and the establishment of steady-state levels (363). This activity was shown to be dependent upon the autoregulation of PhoP, and was essential for *Salmonella* virulence. It is thought that the initial surge in transcription allows for the immediate establishment of a new phenotypic state enabling the bacteria to adapt to the conditions that triggered activation of the system. The post-surge, steady-state levels of gene expression serve to maintain the phenotypic state (363).

Although initially thought not to regulate SPI-2 genes (271), PhoP/Q has been established as controlling SPI-2 gene expression through its influence on the SPI-2-encoded two-component system, SsrA/B (35). PhoP regulates transcription of the response regulator SsrB through a direct binding of the *ssrB* promoter. In the same study, it was demonstrated that PhoP controls the SsrA sensor post-transcriptionally via a 5′ un-translated region in the *ssrA* mRNA (35).

PhoP/Q enforces a further level of influence upon SPI-2 gene expression through its activation of the transcriptional regulator SlyA (301, 361). SlyA is a member of the MarA family of transcriptional factors known to act as activators, repressors, or both. These homodimeric, winged-helix transcriptional factors are thought to control their DNA binding activity by interactions with small molecules within a cleft formed at the junction between the subunits (143). It has recently been established that SlyA induces transcription of the SsrA sensor kinase by binding to the *ssrA* promoter, thus directly regulating SPI-2 gene expression (309). The promotion of *slyA* transcriptional by PhoP also influences the expression of a set of genes located outside SPI-2. Indeed, PhoP and SlyA have been established as exerting a degree of co-regulation on many of these genes.

SlyA-regulated genes such as *pagC*, *pagD*, *ugtL*, *mig-14*, *virK*, *phoN*, *pgtE*, *pipB2*, *sopD2*, *pagJ* and *pagK* are also controlled by the PhoP/Q system (290).

PhoP/Q influences another set of genes also controlled primarily by a two-component system. The PmrA/B two-component system controls resistance to the antimicrobial peptide polymyxin B and is induced by high iron (416). By promoting the transcription of the *pmrD* gene, PhoP/Q has expanded its regulon to include the PmrA/B regulon (219). The PmrD protein activates the PmrA response regulator thus promoting up-regulation of the PmrA/B regulon (219). PmrD controls the activity of the PmrA/B system at a post-transcriptional level (219). Interestingly, the PmrA/B system responds to activation in an identical manner to PhpP/Q, producing an initial surge of gene activation which then subsides into more steady-state levels (363).

The highly influential PhoP/Q two-component system enforces a final level of influence upon systemic virulence through its interaction with the stationary phase sigma factor RpoS. As discussed in Section 1.2.2.6, RpoS is involved in the expression of *spv* genes and is also required to cope with stresses such as nutrient starvation, hyperosmolarity, and heat shock. The level of RpoS within the cell is controlled at the transcriptional and post-transcriptional level (174, 247). Regulated proteolysis is thought to be the critical mechanism that ultimately controls the level of RpoS within a cell (175). It is at this level that PhoP/Q exerts its influence. The MviA protein in *Salmonella* targets RpoS to the ClpXP protease for degradation (27, 353). PhoP counteracts this activity by stabilising the RpoS protein through up-regulation of the *iraP* gene (391). The IraP protein binds to MviA preventing the trafficking of RpoS to the ClpXP protease, thereby promoting the accumulation of the stationary-phase sigma factor (391).

It is evident that the PhoP/Q system is a master regulator of *S.* Typhimurium virulence. The system influences the transcription of genes both directly and indirectly in a complex and highly coordinated gene regulation network. The regulatory network is outlined in Fig. 1.6, and serves to highlight the immense influence that PhoP/Q has upon systemic aspects of *S.* Typhimurium pathogenesis.

1.6 Overview of thesis

The *Salmonella*-specific gene *pagN* has been characterised at the DNA level in the context of the *Salmonella* chromosome. At the protein level, the gene-product PagN is

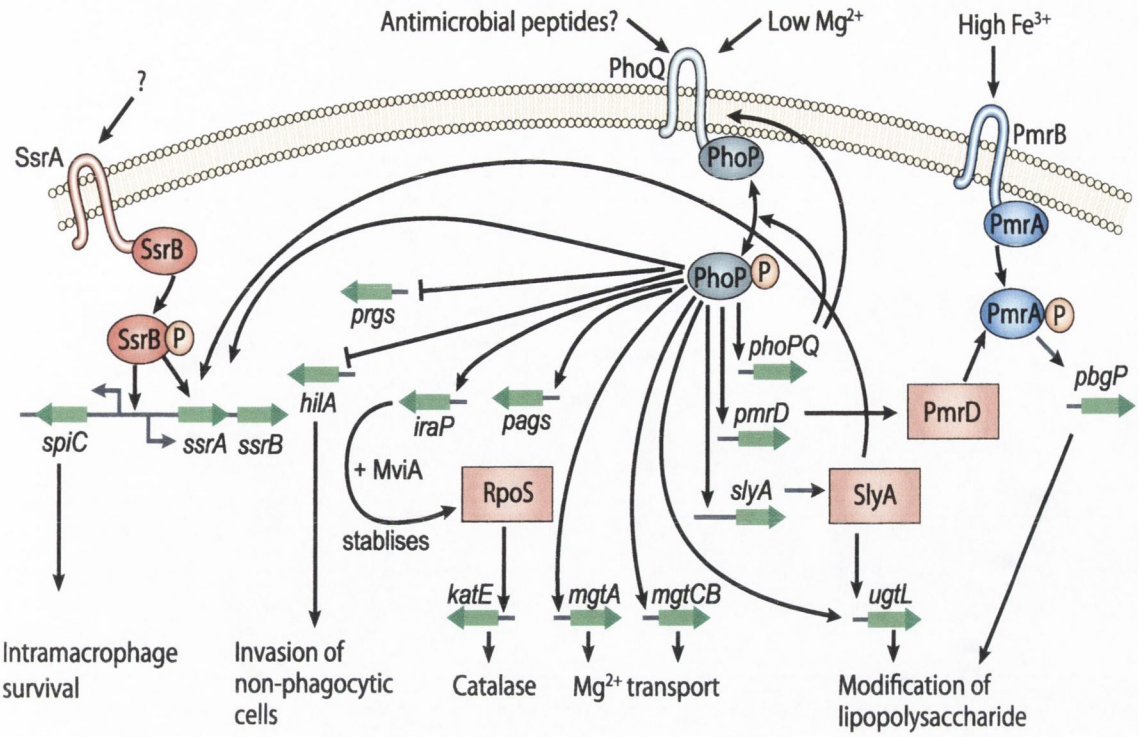

FIG 1.6. The PhoP/Q regulatory network of *S.* Typhimurium. The membrane-located PhoQ sensor domain responds to low levels of Mg^{2+}. The correct signal causes the PhoQ domain to phosphorylate the cytoplasmic response regulator PhoP, thereby activating the protein. Activated PhoP binds to the promoter regions of a large regulon of genes causing up- (*pag*), and down-regulation (*prg*) of the genes. The variety of other regulatory proteins controlled by PhoP is illustrated. Control of these proteins expands the PhoP/Q regulon creating a complex gene regulation network. Adapted from Groisman and Mouslim (145).

completely uncharacterised. The aim of this thesis is to characterise the PagN protein, identifying its sub-cellular location, the conditions under which it is expressed and its function. How the structure of the protein lends itself to this function is also examined.

Chapter 2

Materials and Methods

2.1 General Methods

2.1.1 Bacterial strains and culture conditions

2.1.1.1 Bacterial Strains

All bacterial strains used in this study were derivatives of *S.* Typhimurium strains LT2 and SL1344, *E. coli* strains K-12 and B and *Staphylococcus aureus* strain 8325-4 and are listed in Table 2.1. Permanent stocks were maintained in L broth supplemented with 8.7% (v/v) DMSO and stored at –80 °C.

2.1.1.2 Bacterial Growth Media

All media were prepared using Millipore 18 $M\Omega cm^{-1}$ grade water and chemicals obtained from Difco, Oxoid and Sigma. Media were sterilised by autoclaving at 120 °C for 20 min prior to use. Additives not suitable for autoclaving were sterilised by filtration through 0.2 μm Millex filters (Milipore). The quantities listed below are sufficient for 1 litre of medium.

Lennox L broth and agar:

L broth and agar were used throughout this study for the routine culturing of all gram-negative bacterial strains except where otherwise stated.

L broth: 10 g enzymatic digest of casein, 5 g yeast extract, 5 g NaCl

L agar: 9.14 g enzymatic digest of casein, 4.57 g yeast extract, 4.57 g NaCl, 13.72 g bacteriological agar

Tryptone soy (TS) broth and agar:

TS broth and agar were used throughout this study for the routine culturing of gram-positive bacterial strains.

TS broth: 17 g casein peptone, 2.5 g K_2HPO_4, 2.5 g glucose, 5 g NaCl, 3 g soya peptone (papain digest).

TS agar: 17 g casein peptone, 2.5 g K_2HPO_4, 2.5 g glucose, 5 g NaCl, 3 g soya peptone (papain digest), 15 g bacteriological agar

SOC medium:

SOC medium was used following electroporation of *Salmonella* and *E. coli* strains to increase the recovery of viable bacteria following transformation.

SOC medium: 20 g Oxoid tryptone, 5 g yeast extract, 0.5 g NaCl

After autoclaving 0.95 g $MgCl_2$, 1.2 g $MgSO_4$ and 1.8 g glucose was added.

Minimal medium 5.8:

MOPS [3-(N-morpholino)propanosulfonic acid] minimal medium, adjusted to pH 5.8 with HCl (MM 5.8), is a low pH, minimal medium adapted from media previously described by Neidhardt *et al.* (291) and Kox *et al.* (219). It is used to simulate conditions inside a macrophage and has been shown to activate transcription of SPI-2 and PhoP-activated genes (219).

10X MOPS solution: 83.7 g MOPS, 7.2 g Tricine, 0.03 g $FeSO_4.7H_2O$, 5 g NH_4Cl, 0.5 g K_2SO_4, 1 ml $CaCl_2$ (50 mM), 73.05 g NaCl, 10 ml micronutrients (see below), adjust to 1 L with dH_2O.

Micronutrients: $(NH_4)_5(MO_7)_{24}$, 3 µM; H_3BO_3, 400 µM; $CoCl_2$, 30 µM; CuSO4, 10 µM; $MnCl_2$, 80 µM; $ZnSO_4$, 10 µM

MM 5.8: 100 ml 10X MOPS, 0.23 g K_2HPO_4, 20 ml glycerol, 1 g Casamino acids, adjust volume to 1 L with dH_2O.

The solution was adjusted to pH 5.8 with HCl (1 M)

After filter-sterilisation, 50 µl of filter-sterilised $MgCl_2$ (1M) was added.

Green agar:

Green agar plates were routinely used following bacteriophage P22-mediated generalised transduction to obtain isolates of *S.* Typhimurium free of phages. On these plates phage-free colonies appear light green whereas pseudo-lysogens appear dark green. The dark green colour results from a lowered pH caused by bacterial lysis.

Green agar: 8 g tryptone, 1 g yeast extract, 5 g NaCl, 15 g bacteriological agar

After autoclaving 16.8 ml 50% glucose, 5 ml 62.2 mg/ml Alizarin yellow (freshly prepared) and 5 ml 6.5 mg/ml Aniline blue were added.

Overnight Express™ instant TB Medium:

Overnight express (OnEx™) medium (381) is a medium whose components are metabolised differentially to promote growth to high density and automatically induce protein expression. It consists of three solutions: an induction solution which is a blend of carbon sources optimized for tightly regulated, uninduced growth to high cell density, followed by induction with lactose and continued growth; a buffering solution that controls pH throughout metabolic acid production and provides additional nitrogen support increased protein synthesis; and a magnesium solution which provides high levels of this cation to promote maximal cell density.

2.1.1.3 Bacterial culture conditions

Bacteria were routinely grown on L agar plates and in shaken aerobic liquid cultures at 37 °C, except where otherwise stated. Liquid cultures were inoculated by transferring single colonies from agar plate cultures into an appropriate volume of L broth and grown overnight. Where mid-logarithmic cultures were required, overnight cultures were diluted 1:50 in fresh media and grown to the appropriate optical density at 600 nm.

2.1.1.4 Antibiotics and media additions

All stock antibiotics and media additives were filter sterilised through 0.2 μm Millex filters (Milipore) and stored at –20 °C. Carbenicillin, kanamycin and spectinomycin were prepared as 50 mg/ml stocks in ddH_2O. While carbenicillin and kanamycin were used at a working concentration of 50 μg/ml, spectinomycin was used at a working concentration of 100 μg/ml. Tetracycline was prepared as a 30 mg/ml stock in 70% (v/v) ethanol and used at a working concentration of 30 μg/ml. Chloramphenicol was prepared as a 10-mg/ml stock in 70% (v/v) ethanol and used at a concentration of 10 μg/ml. The *lac* operon inducer IPTG was prepared as a 100 mM stock and used at concentrations of 0.4-1 mM as appropriate. X-Gal, a chromogenic substrate for β-galactosidase, was prepared as a 20 mg/ml stock solution in *N, N*-dimethyl formamide and stored in the dark at –20 °C. X-Gal was used in agar plates at a final concentration of 20 μg/ml.

TABLE 2.1. Bacterial strains used in this study

Strain	Relevant details	Reference or source
S. Typhimurium strains		
CH133	LT2 *galE503*	(186)
CJD365	SL1344 *ompR::tet*	(61)
LT2	Wild type strain	ATCC
ML133	LT2 *galE503 pagN::spc*	This study
ML3	LT2 *galE503 pagN::spc invA::cat*	This study
ML4	LT2 *galE503 invA::cat*	This study
ML5	SL1344 *invA::cat*	This study
ML6	SL1344 *pagN::spc*	This study
ML7	SL1344 *invA::cat pagN::spc*	This study
ML8	SL1344 *pagN::spc galE::kan*	This study
ML9	SL1344 *galE::kan*	This study
ML11	TA2367 *pagN::spc*	This study
MLT2	LT2 *pagN::spc*	This study
SL1344	Wild type mouse-virulent strain	ATCC
TA2362	*PhoP12* (*phoP* null mutant)	(210)
TA2367	*phoQ-24* (constitutively activate *phoQ* mutant)	(210)
Escherichia coli strains		
BL21(DE3)	*F-, ompT, hsdS*(r_B, m_B), *gal, dcm*, λDE3 (*lacI*, *lac*UV5-T7 gene 1, *ind*1, *sam*7, *nin*5)	Stratagene
BZB1107	BL21 *ompF*::Tn5	(201)
DH5α	*F′ endA1 hsdR17* ($r_k^- m_k^+$) *glnV44 thi-1 recA1 gyrA* (Nal^r) *relA1 Δ(lacIZYA-argF)U169 deoR (Φ80dlacΔ (lacZ)M15)*	Invitrogen Life
XL-1 Blue	*recA1 endA1 gyrA96 thi-1 hsdR17 supE44 relA1 lac* [*F′ proAB lac^{q}ZΔM15* Tn*10* (Tet^r)]	Stratagene
Staphylococcus aureus strains		
8325-4	NCTC 8325 cured of prophages ϕ11, ϕ12 & ϕ13.	(302)
DU1090	8325-4 *hla ::ermC*	(305)
DU5720	8325-4 *hla ::ermC hlb ::* ϕ42E	(316)
DU5938	8325-4 *hla ::ermC hlb ::* ϕ42E *hlg ::tetK*	(297)

2.1.2 Eukaryotic cell lines and growth conditions

2.1.2.1 Eukaryotic cell lines

All cell lines used were obtained from ATCC (Manassas, VA, U.S.A.). The mammalian cell lines used were HT-29 (ATCC HTB-38), Caco-2 (ATCC HTB-37), CHO-K1 (ATCC CCL-61) and pgsA-745 (ATCC CRL-2242) cells. The murine, macrophage-like cell line J-774A.1 (ATCC TIB-67) was also used. Stocks of all cell lines were maintained in cell freezing medium/DMSO (Sigma-Aldrich) under liquid nitrogen.

2.1.2.2 Cell growth conditions

Caco-2, CHO-K1 and pgsA-745 cell lines were grown in a 1:1 mixture of DMEM/Ham's F12K medium with 2 mM L-glutamine adjusted to contain 1.5 g/L sodium bicarbonate, supplemented with 10% (v/v) heat-inactivated fetal bovine serum (Life Technologies). HT-29 cells were grown in McCoy's 5a medium with 1.5 mM L-glutamine (Gibco) supplemented with 10% (v/v) heat-inactivated fetal bovine serum. J-774A.1 macrophages were grown in DMEM with 4 mM L-glutamine adjusted to contain 1.5 g/L sodium bicarbonate and 4.5 g/L glucose. Cells were routinely 75 cm^2 flasks at 37 ^{o}C in 5% CO_2. Confluent monolayers were disrupted by treatment with a trypsin/EDTA solution (Sigma-Aldrich) and diluted into fresh medium.

2.1.3 Plasmids, bacteriophage and oligonucleotides

2.1.3.1 Plasmids

All plasmids used in this study are listed in Table 2.2 along with relevant descriptions and sources. For plasmids constructed during this study the details of construction are described in the relevant chapters.

2.1.3.2 Oligonucleotides

The sequences of all oligonucleotides used in this study are listed in Table 2.3. All oligonucleotides were synthesised by MWG-Biotech, Martinsried, Germany.

TABLE 2.2. Plasmids used in this study

Plasmid	Relevant details	Reference or source
pACYC184	Tet^r Cm^r pSC101 replicon, plasmid source of *cat* cassette for gene disruption	(59)
pBluescript SKII	Ap^r ColE1 replicon	Strategene
pBR322	Ap^r Cloning vector	(18)
pD103A	Ap^r *pagN* (D103A) ORF inserted into pTrc99a	This study
pD97A	Ap^r *pagN* (D97A) ORF inserted into pTrc99a	This study
pET-19b	Ap^r encodes 10 histidines upstream of MCS	Novagen
pGalE	Ap^r Kan^r *galE* gene inserted into pBSKII	This study
pGalEKO	Ap^r Kan^r *galE*::*kan* gene fusion inserted into pBSKII	This study
pH12P34	Ap^r *hek::pagN* gene fusion inserted into pTrc99a	This study
pHek6	Ap^r 886 bp of *E. coli* RS218 DNA carrying the *hek* gene inserted into pBSKII	(108)
pHP45Ω	Ap^r Spc^r Plasmid source of spc cassette for gene disruption	(324)
pInvA	Ap^r 1000-bp *invA* gene fragment inserted into pBSKII	This study
pInvAKO	Ap^r *invA*::*cat* gene fusion inserted into pBSKII	This study
pK99A	Ap^r *pagN* (K99A) ORF inserted into pTrc99a	This study
pKOBEGA	Ap^r Temperature-sensitive plasmid carrying the *red* and *gam* genes of λ-phage under control P_{araBAD} promoter	(62)
pOS32	Ap^r Contains the *gfp*mut3b gene under the transcriptional control of the *E. coli rrn*B-P1 promoter	(360)
pKRP11	Kan^r Plasmid source of *kan* cassette for gene disuption	(332)
pLoop1	Ap^r Derivative of pML1 with the DNA sequence corresponding to the first loop of the PagN protein replaced with CGCGCG	This study
pLoop2	Ap^r Derivative of pML1 with the DNA sequence corresponding to the second loop of the PagN protein replaced with CGCGCG	This study
pLoop3	Ap^r Derivative of pML1 with the DNA sequence corresponding to the third loop of the PagN protein replaced with CGCGCG	This study
pLoop4	Ap^r Derivative of pML1 with the DNA sequence corresponding to the fourth loop of the PagN protein replaced with CGCGCG	This study
pLysS	Cm^r p15A replicon, harbours the T7 lysozyme gene	Novagen
pMAL-c2	Ap^r maltose binding protein gene upstream of MCS	New England BioLabs
pML1	Ap^r *pagN* ORF inserted into pTrc99a	This study
pML10	Ap^r *pagN* gene inserted into pBR322	This study
pML4	Ap^r *pagN* ORF inserted into pBSKII	This study
pML7	Ap^r *pagN* ORF, excluding the DNA corresponding to the signal sequence of the PagN protein, inserted into pMAL-c2	This study
pML9	Cm^r *pagN* gene inserted into pPD101	This study
pMompF	Ap^r *ompF* ORF, excluding the DNA corresponding to the signal	This study

	sequence of the OmpF protein, inserted into pMAL-c2	
pPagN1	Cm^r *pagN* gene with 1000 bp flanking DNA inserted into pPD101	This study
pPagN2.3	Ap^r *pagN* gene with 1000 bp flanking DNA cloned into pBSKII	This study
pPagN-GFP	Cm^r putative *pagN* promoter region inserted into pZep08	This study
pPagNHis2.6	Ap^r *pagN* ORF inserted into pET-19b	This study
pPagNKO	Ap^r Spc^r *pagN*::*spc* gene fusion inserted into pBSKII	This study
pPB1020	Ap^r *phoP* ORF inserted into pT7-7	(56)
pPD101	Cm^r Low copy-number inserted vector	(89)
pR93A	Ap^r *pagN* (R93A) ORF inserted into pTrc99a	This study
pRI203	Ap^r *inv* locus inserted into pBR325	(200)
pThek6	Ap^r *hek* ORF inserted into pTrc99a	(107)
pTia5	Ap^r *tia* gene inserted into pBSK II	(108)
pTrc99a	Ap^r Cloning vector with an IPTG-inducible P_{trc} promoter	(10)
pZep08	Cm^r encodes *gfp* downstream of MCS	(166)

TABLE 2.2. Oligonucleotide primers used in this study

Primer	Sequence
CH4F	5′ – CGC AGC ATT AAT GTA TTT ATA ACT GGC GTC –3′
CH4R	5′ – CGC AAT GAC TTC ATG CTC GGC ATT AC –3′
CHBK2	5′ – CGC CAG GTC CGA ATG ACC ACT TAC ATG G –3′
CHBK3	5′ – CGC TTT GCC TGG GGC GCA GGT ATC GG –3′
CHFW2	5′ – CGC AGT GGT ATC CAG TTC TAA ACG TAC TGG –3′
CHFW3	5′ – CGC GAG GCC AAC GCC TGC GCT GAT ATA GG – 3′
D103Af	5′ – GAT GCT AAA GGC GGG CAG GCC ATT ATT GCA TTT GG –3′
D103Ar	5′ – CCA AAT GCA ATA ATG GCC TGC CCG CCT TTA GCA TC –3′
D97Af	5′ – GAG GTG AGA CGG CCG CTA AAG GCG GG –3′
D97Ar	5′ – CCC GCC TTT AGC GGC CGT CTC ACC TC –3′
galEF	5′ – TGC GTA AAA TCA CCA GTG TG –3′
galER	5′ – GCA GCG TTT TAC TGT GAT CG –3′
HekL12-R	5′ – TGG TGT GAA TGC GCT GTC ATT CCG GAA GTC –3′
HekL34-F	5′ – GCA TTT ACT CCC TGG GTA TCC GCA GGG AT –3′
invA-allele-F	5′ – CAA ACG CTG CAA AAC TTC AG –3′
invA-allele-R	5′ – TTG ATT TCC TGA TCG CAC TG –3′
K99Ab	5′ – GGT GAG ACG GAT GCT GCA GGC GGG CAG GAT ATT ATT-3′
K99At	5′ – GCA ATA ATA TCC TGC CCG CCT GCA GCA TCC GTC TCA-3′
Loop1_F	5′ – CGC TTT GGC GGG GTT GCT ATC G –3′
Loop1_R	5′ – CGC GAC TAC GGA TGT CCC CGC TTT CC –3′
mgtApromo_F	5′ – TTG ATT TCC CTA CGA CGC TC –3′
mgtApromo_R	5′ – GTA AAT AAT TTG CGC CGC GG –3′
ML2	5′ – GCT AGG ATC CCG ATA GTG TTT AAA AGG CG –3′
ML3	5′ – GCC TCC ATG GAA AAC TTT GCA GTC TGC –3′
OmpF-R-BamHI	5′ – GCA GAA ATT TAT AAT AAA GAT GGT AAT AAG CTG G –3′
OmpF-SS-F	5′ – CCG GAT CCT CAG AAC TGG TAA G –3′
PagNF	5′ – AGA TAA TTG CTC GCC ATT CG –3′
pagN-F	5′ – AAA GAA GGG ATC TAT ATC ACC GGG AAA G –3′
PagNL12-R	5′ – GGG AGT AAA TGC CGT ACT ATT GTG AAA ATC ATA ATA G-3′
PagNL34-F	5′ – GCA TTC ACA CCA TAT ATC AGC GCA GGC GTT –3′
pagNpromo_F	5′ – CAG TCA GAT TTC TAT GAA GGG AAT TAA –3′
pagNpromo_R	5′ – GGT CTA GAG ACC AGG CTA CCA CAA –3′

PagNR	5′ – ATG GAG GGT TCC AGA TCT CC –3′
pagN-R	5′ – GCT ATC TAG ACG ATA GTG TTT AAA AGG CG –3′
PromoterF	5′ – CAG TCA GAT TTC TAT GAA GGG AAT TAA –3′
PromoterR	5′ – GGT CTA GAG ACC AGG CTA CCA CAA –3′
pTrc99a-MCS-F	5′ – GGA ATT GTG AGC GGA TAA CAA TTT C –3′
pTrc99a-MCS-R	5′ – CTT CTC TCA TCC GCC AAA AC – 3′
R93Ab	5′ – CTG GAT ACC ACT TTC GCC GGT GAG ACG GAT GCT AAA-3′
R93At	5′ – GCC TTT AGC ATC CGT CTC ACC GGC GAA AGT GGT ATC-3′

2.2 Nucleic acid methodologies

2.2.1 Transformation of *Salmonella* and *E. coli* strains

Two distinct methods were used for the introduction of foreign DNA into bacterial cells. Cells were made competent either by repeated washing in an ice-cold calcium chloride solution or ice-cold Millipore grade water and then transformed by heat-shock (256) or electroporation (94) respectively. Significantly greater transformation efficiencies were achieved using the electroporation method. The calcium chloride method was used for routine transformation of intact plasmids into *E. coli* K-12 and *E. coli* B strains. Due to the higher efficiencies achieved, the electroporation method was used with *E. coli* K-12 and B strains when higher efficiencies were required and routinely with *Salmonella* strains.

2.2.1.1 Transformation of *E. coli* K-12 and B strains using calcium chloride method

A 3 ml culture of the strain to be made competent was inoculated from a single colony into L broth and incubated overnight with shaking. This culture was then diluted 1:50 in 100 ml of fresh L broth and grown to an OD_{600nm} of between 0.4 and 0.6. The cultures were then incubated on ice for 20 min and the bacteria were harvested by centrifugation at 6,000 x *g* for 8 min. The pellet was resuspended in 20 ml of cold $CaCl_2$ solution (60 mM $CaCl_2$, 15% (v/v) glycerol, 10 mM PIPES, pH 7) and harvested by centrifugation as before. This pellet was resuspended in 20 ml cold $CaCl_2$ solution and incubated on ice for 30 min before harvesting the bacteria as before. The pellet was then resuspended in a final volume 4 ml of cold $CaCl_2$ and incubated overnight on ice before aliquoting 100 µl volumes and storage at –80 °C.

Competent bacterial cells (100 µl) were mixed with between 10 ng and 1 µg of plasmid DNA and incubated on ice for 10 min. The cells were then transferred to a 42 °C water bath and incubated for 90 s, thus inducing the uptake of the DNA. Cells were immediately transferred to ice. Following a further 1 min incubation on ice the cells were mixed with 1 ml of pre-warmed SOC broth and incubated at 37 °C for 1 h to allow expression of plasmid-borne antibiotic resistance genes. Aliquots of 50 µl and 1 ml of the transformation mixture were then spread on selective L agar plates and incubated overnight at 37 °C. Transformants were single colony purified on fresh L agar plates containing appropriate antibiotics.

2.2.1.2 Transformation of *E. coli* and *S.* Typhimurium strains by electroporation

A 3 ml culture of the strain to be made electro-competent was inoculated from a single colony into L broth and incubated overnight with shaking. This culture was then diluted 1:50 in 50 ml of fresh L broth and grown to an OD_{600nm} of between 0.4 and 0.6. The cultures were then incubated on ice for 5 min, the bacteria were harvested by centrifugation at 6,000 x *g* for 8 min and the pellet was resuspended in 50 ml of sterile, ice-cold water. The bacteria were then harvested as before, resuspended in 25 ml ice-cold water and harvested again. The pellet was then resuspended in 2.5 ml sterile ice-cold 10% (v/v) glycerol, harvested and resuspended again in ice-cold 10% (v/v) glycerol to a final volume of 200 µl. 40 µl aliquots were stored at -80 °C.

Electro-competent bacteria (40 µl) were mixed with between 10 ng and 2 µg of DNA (in a volume not exceeding 4 µl) and immediately transferred into a cold electroporation cuvette (BioSmith, 0.2 cm electrode width). The electroporation was then carried out in a Bio-Rad gene pulser at 12.5 $kVcm^{-1}$, 25 µF and 200 Ω. The bacteria were than mixed with 1 ml of pre-warmed SOC broth and incubated at 37 °C for 1 h to allow expression of plasmid-borne antibiotic resistance markers. Aliquots of 10 µl and 1 ml quantities of the transformation mixture were then spread on selective L agar plates and transformants were single colony purified onto fresh L agar plates following growth overnight at 37 °C.

2.2.2 Transduction with bacteriophage P22

Bacteriophage P22 is a temperate phage that specifically recognises *S.* Typhimurium by binding to the O antigen component of its LPS-based outer membrane. After binding, double stranded linear DNA is injected into the host. The DNA circularises and is replicated first by O replication and then by rolling circle replication which generates long concatemers of double stranded P22 DNA. These concatemers are resolved by cleavage by a phage encoded nuclease, which cuts the DNA at specific sequences, 44 kb apart, called Pac sites. This DNA is packaged into new phage particles, which are released from the host by lysis after 50-100 of these particles have been produced. In this study the P22 derivative used for generalised transduction in *S.* Typhimurium was P22 HT105/1 *int*-201. The high transducing frequency of this phage results from its nuclease having a lower specificity for the Pac sequence. This results in a high proportion of the phage heads carrying chromosomal DNA. Approximately 50% of the P22 HT (high transducing) phage heads carry random transducing fragments of host DNA. The *int* mutation prevents the formation of stable lysogens.

2.2.2.1 Preparation of P22 lysate

P22 lysates were routinely prepared as follows: the donor strain was grown overnight in 2 ml of L broth at 37°C, with antibiotic selection as appropriate. This culture was used to inoculate 5 ml of fresh broth at a 1:200 dilution. This culture was incubated at 37 °C with shaking for 1 h. At this point 10 µl of P22 phage stock (titre of approximately 10^{10} pfu/ml) was added and incubation continued for a further 4 h. 500 µl of chloroform was added, the culture mixed by vortexing and stored for 1 h at 4°C. Cellular debris was removed by centrifugation at 3,800 x g for 20 min. The supernatant, containing the lysate was transferred to a clean, glass tube and stored over chloroform.

2.2.2.2 Transduction with P22 bacteriophage

The recipient strain was grown overnight at 37 °C in 2 ml of L broth. 100 µl of the recipient culture was removed to a sterile Eppendorf tube containing 20 µl of the donor P22 lysate. The mixture was incubated for 1 h at 37 °C. The transduction mixture was then spread on selective L agar plates and incubated overnight at 37 °C. True lysogens were then distinguished from pseudo-lysogens by 3 repeated single colony purifications on Green agar plates.

2.2.3 λ Red-mediated allele replacement

The inactivation of chromosomal genes involved a two-step process whereby mutated alleles were constructed *in vitro* and transferred to the bacterial chromosome using an allele-replacement system based on the gene products of the λ phage *red* operon (83). This system is based on the ability of the *gam*, *bet* and *exo* gene products to inhibit the Exonuclease V activity of RecBCD, allowing the transformation of linear DNA fragments, and promote homologous recombination at regions of homology between the chromosome and the transformed linear DNA fragment. The λ-phage *red*γβα operon was located on the pKOBEGA (62) plasmid under the control of the L-arabinose-inducible P_{BAD} promoter. This plasmid has a temperature sensitive pSC101 replicon, which permits plasmid replication at 30 °C but not at higher temperatures. The plasmid also confers resistance to the antibiotic carbenicillin. The λ Red allele replacement system was employed to interrupt genes within the *S.* Typhimurium strain LT2 and strain SL1344 genome (See Chapter 4).

2.2.3.1 Generation of mutated alleles *in vitro*

In order to generate a mutated allele, the appropriate region of the bacterial chromosome, plus 500 bp of flanking DNA was first cloned into the plasmid vector pBSKII. The allele was then disrupted by insertion of an antibiotic resistance cassette. The details of each gene disruption are described later in detail in the appropriate section. Once the mutant allele had been constructed and confirmed by restriction endonuclease mapping, a linear DNA fragment containing the novel allele was produced either by PCR amplification of the desired region or restriction endonuclease digestion with appropriate enzymes. The linear fragment was isolated and purified from an agarose gel (Section 2.2.5.2) and concentrated by Pellet Paint®-precipitation (Section 2.2.5.5). In the case of PCR products the DNA was digested with the restriction endonuclease *Dpn*I prior to purification to decrease the amount of intact parental plasmid in the PCR mixture.

2.2.3.2 λ Red-mediated allele replacement in *S.* Typhimurium

S. Typhimurium bacteria harbouring the plasmid pKOBEGA were grown to mid-logarithmic phase at 30 °C in the presence of 50 μg/ml carbenicillin. Expression of the Red α, β and γ proteins was induced by addition of 0.2% L-arabinose. The induced bacteria were grown for a further 2 h and made electrocompetent (Section 2.2.1.2). These electrocompetent bacteria were then transformed with 4-5 μg of purified linear DNA containing the relevant disrupted gene as described previously. To increase the transformation frequency, 1 μl TypeOne™ Restriction inhibitor (Epicentre) was added during electroporation. TypeOne™ Restriction inhibitor is a preparation of a phage protein called ocr. This protein acts as a decoy which blocks the DNA binding sites of Type I R-M enzymes which cleave unmodified DNA. *S.* Typhimurium strain LT2 contains the *Sty*L TIII type I R-M system. Bacteria were subsequently incubated for 4 h at 37 °C. Cells were then spread on agar plates containing the appropriate antibiotic. All subsequent steps were carried out at 37 °C in the absence of carbenicillin to ensure rapid loss of the pKOBEGA plasmid. Putative mutants were single-colony purified twice and then screened for the presence of the novel mutant allele by PCR. Loss of the pKOBEGA plasmid was confirmed by testing for carbenicillin sensitivity on agar containing the antibiotic.

2.2.4 Purification of plasmid and chromosomal DNA

2.2.4.1 Small-scale purification of plasmid DNA

The Genelute Plasmid Miniprep kit (Sigma-Aldrich) was used for the routine purification of plasmid DNA from overnight bacterial cultures. Purification was carried out according to the manufacturer's instructions using a modified alkaline lysis method. Briefly, depending on plasmid copy-number, bacteria from a 3-10 ml overnight culture were harvested and lysed in an alkaline solution containing SDS, to denature proteins, and RNase, to degrade RNA. The alkaline conditions also denatured both the chromosomal and plasmid DNA which was released upon cell lysis. The solution was then rapidly neutralised causing the plasmid DNA to re-anneal and the chromosomal DNA to precipitate. The lysate was then cleared by centrifugation to remove cellular debris and chromosomal DNA and the soluble plasmid DNA was purified using a mini cation-exchange column. The purified DNA was eluted from the column in TE buffer following a desalting and washing step.

2.2.4.2 Large-scale purification of DNA

The Qiagen Plasmid Midi kit was used to purify plasmid DNA from 100 ml overnight cultures of *E. coli* according to the manufacturers instructions. Purification was carried out according to the manufacturers instructions using a modified alkaline lysis similar to that described above. Bacteria were lysed as before and the cleared lysate is passed through a cation-exchange column, which binds the re-natured plasmid DNA. The column with bound DNA was washed repeatedly and the DNA is eluted in a high-salt buffer. The DNA is then further purified and desalted by precipitation with isopropanol and resuspended in ddH_2O.

2.2.4.3 Purification of total genomic DNA

Chromosomal DNA was routinely purified using the Puregene genomic DNA purification kit (Gentra Systems). Briefly, bacteria from a 0.5 ml overnight culture were harvested by centrifugation, resuspended in a cell lysis solution, containing Tris [hydroxymethyl] aminomethane, EDTA and SDS and incubated at 80 ^{o}C for 5 min to lyse the bacteria. Contaminating RNA was removed by treatment with RNase and cellular

proteins were removed by protein precipitation using ammonium acetate. The remaining DNA was then precipitated with isopropanol and resuspended in a Tris/EDTA buffer.

2.2.5 *In vitro* manipulation of DNA

2.2.5.1 Restriction endonuclease digestion of DNA

All restriction digests were carried out using enzymes supplied by New England Biolabs (NEB) according to the manufacturers instructions. Briefly, 0.1-2 µg of purified DNA was incubated with 10-20 U of restriction enzyme in the appropriate NEB buffer for 2 h at the appropriate temperature. Digests with multiple enzymes were carried out in the recommended double digest buffer or in an appropriate buffer in which all enzymes had 100% activity. Where no suitable buffer was available sequential digests were performed.

2.2.5.2 Purification of DNA fragments

Following digestion with restriction endonucleases or PCR amplification linear DNA fragments were purified directly from solution or from an agarose gel slice using the HiYield Gel/PCR DNA Fragments Extraction Kit (Real Biotech Corporation). To purify DNA from solution, 5 volumes of DF buffer was added and mixed by vortexing. DF Buffer contains a chaotropic salt, guanidine thiocyanante, which denatures enzymes and dissolves agarose gel. The solution was then added to a spin column where the DNA fragments bind to a glass fibre matrix. Salts, enzymes and unincorporated nucleotides were subsequently removed in 2 wash steps. Purified DNA was eluted from the column in TE buffer. Purification from an agarose gel slice uses a similar protocol with the following addition. The gel slice was first melted at 56 ^{o}C in 500 µl DF buffer (regardless of gel mass). The soluble DNA was then purified as before.

2.2.5.3 Ligation of DNA fragments

The T4 DNA Ligase was used to catalyse the formation of a phosphodiester bond between the exposed 5′ phosphate and 3′ hydroxyl groups of linear DNA fragments in an ATP-dependent fashion (105). These ligations were carried out using the Quick Ligation kit (NEB) and were routinely used for the cloning of DNA fragments into appropriate

plasmid vectors. 50 ng of digested vector DNA was mixed with a three-fold molar excess of digested insert in a total volume of 10 µl and mixed with 10 µl of 2 x Quick Ligation Reaction Buffer. 1 µl of Quick T4 DNA Ligase was added and the reaction was incubated at room temperature for 10 min. The ligated DNA molecules were then transformed into either calcium-chloride or electro-competent *E. coli* XL-1 Blue cells. Where calcium-chloride competent cells were used the whole ligation reaction was directly transformed. For electro-competent cells the ligated DNA was first purified as previously described (Section 2.2.5.2) and concentrated by ethanol or pellet-paint precipitation (Section 2.2.5.6) prior to electroporation.

2.2.5.4 Agarose gel electrophoresis

DNA samples were visualised following separation on a 0.8-2% agarose gel, depending on the size of the DNA. Briefly, for a 1% gel, agarose (1 g) was added to 100 ml of 0.5X TBE buffer (44.5 mM tris borate, pH 8.3, 1 mM EDTA) and heated to 100 °C to dissolve the agarose. Ethidium bromide was added to a final concentration of 1 µg/ml and the molten gel was poured into a gel mould and allowed to set. DNA samples were prepared by adding an appropriate volume of 5X sample loading buffer (25 mM tris pH 7.6, 30% (v/v) glycerol, 0.125% (w/v) bromophenol blue) and these samples were electrophesised through the gel at 135 V for 45 min in 0.5X TBE buffer. The separated DNA fragments were photographed while illuminated under UV light.

2.2.5.5 Purification of DNA samples from solution by ethanol precipitation

Ethanol precipitation of DNA was routinely used for the preparation of desiccated DNA samples for DNA sequencing. Ethanol is added to the aqueous DNA sample to deplete the hydration shell surrounding the DNA molecules exposing the negatively charged phosphate groups. A cation is then added to mask this charge and allow a precipitate to form. Sodium acetate was routinely used as the cation. Briefly, the DNA sample was mixed with 2.5 volumes of ethanol followed by 0.1 volumes of 3 M sodium acetate (pH 5.2) and incubated at –80 °C for 1 h to allow a precipitate to form. The precipitated DNA was then recovered by centrifugation at 21,000 x *g* for 30 min, washed with 500 µl of 70% ethanol to remove contaminating salt and centrifuged again as before. The precipitated DNA was then dried at 55 °C for 10 min. If an aqueous DNA solution was required, the precipitated DNA was dissolved in Millipore grade water at 56 °C for 10 min.

For concentrating dilute DNA samples, Pellet Paint® Co-Precipitant was routinely used. Pellet Paint® Co-Precipitant is a visible dye-labeled carrier formulated specifically for use in alcohol precipitation of nucleic acids. 2 µl of Pellet Paint® Co-Precipitant was added to DNA solution followed by 0.1 volume of 3 M Sodium Acetate and 2 volumes of ethanol. The samples were vortexed briefly and incubated at room temperature for 2 min. Precipitated DNA was collected by centrifugation at 21,000 x *g* for 5 min. DNA was subsequently washed with 70% ethanol and air-dried. The dried DNA pellet was resuspended in an appropriate volume of dH_2O.

2.2.6 Polymerase chain reaction

The polymerase chain reaction (PCR) was used for the amplification of specific DNA fragments for use in cloning reactions and for the confirmation of constructed plasmids and mutant alleles. PCR is based on the ability of certain thermostable DNA polymerases to synthesise a new DNA strand complementary to a provided single-stranded, denatured DNA template when primed with specific complementary oligonucleotides (343). The procedure involves successive rounds of thermal denaturation of a double-stranded DNA template, hybridization of two complementary oligonucleotides (primers) and synthesis of the new DNA strand by the DNA polymerase. The primers are designed to be complementary to opposite strands at either end of the fragment to be amplified and orientated such that their 3′ ends face each other. The new DNA strand is synthesised from provided dNTPs by the DNA polymerase in the presence of Mg^{2+}. Each new strand acts as a template in further rounds of amplification and the procedure thus results in exponential amplification of the desired DNA fragment.

2.2.6.1 Amplification of DNA by polymerase chain reaction

Two different DNA polymerases were used for the routine amplification of DNA fragments. *Taq* DNA polymerase (New England Biolabs), a recombinant purified thermostable polymerase from *Thermus aquaticus* YT-1, which is highly efficient but lacks the 3′-5′ exonuclease activity necessary for error correction (proof-reading), was used in PCR reactions were the sequence accuracy of the amplified DNA was not critical; for example, screening recombinant plasmids for inserts or screening for mutant alleles in purified chromosomal DNA. Where a high degree of sequence fidelity was required, for example to generate DNA fragments for cloning reactions, Platinum *Pfx* polymerase was

used (Life Technologies). *Pfx* is also highly processive but retains the 3′-5′ exonuclease activity necessary for proof-reading resulting in a significant decrease in the rate of nucleotide misincorporation.

Pfx PCR reactions were carried out according to the manufacturers instructions in an MJ Research PTC-200 peltier thermal cycler. Briefly, 10 µl of 10 x *Pfx* buffer was mixed with 0.3 mM of each dNTP, 0.3 µM of each primer, 1 mM $MgSO_4$, 100 pg-10 ng of template DNA, 1 U of Platinum *Pfx* and ddH_2O to a final volume of 50 µl. The PCR reactions were transferred to the thermal cycler and incubated as follows:

1	Denaturation: 94 °C for 5 min
2	Denaturation: 94 °C for 30 sec
3	Oligonucleotide annealing: a temperature corresponding to 1 degree below the lowest melting temperature of the primer pair for 30 sec
4	Extension: 68 °C for 1 min per kilobase of expected DNA product
5	Repeat steps 2-4 for an additional 29 cycles

Taq PCR reactions were carried out as above with some exceptions. *Taq* buffer (10 mM tris-HCl, 50 mM KCl, 1.5 mM $MgCl_2$, pH 8.3) was substituted for *Pfx* buffer in the reaction mixture, $MgCl_2$ (1-3 mM) was used in place of $MgSO_4$ and 1 U of *Taq* polymerase was added to each reaction. In the thermal cycler extension was carried out at 72 °C, the optimal temperature for *Taq* activity and an additional 72 °C for 10 min step was included at the end of the program to complete any unfinished products.

Purified plasmid, genomic DNA or cell lysates were used as templates in PCR reactions. Cell lysates were prepared by transferring a single bacterial colony to a PCR tube containing 20 µl Millipore grade water using a sterile pipette tip and incubating at 100 °C for 5 min. 1 µl of this crude lysate was used in each PCR reaction.

2.3 Analysis and manipulation of proteins

2.3.1 SDS-PAGE

Proteins were separated on discontinuous denaturing polyacrylamide gels by the method of Laemmli (226). Using this method, proteins are denatured in SDS and β-mercaptoethanol and separated on the basis of their size as they travel through a polyacrylamide gel towards the anode. SDS binds to most proteins in a constant weight ratio, masking their natural charge with its own negative charge and giving each protein a similar mass:charge ratio allowing separation on the basis of size rather than charge. The discontinuous gel is formed using buffers of differing composition and pH to firstly focus the separating proteins into narrow well-defined bands and then separate these focused proteins on the basis of their size.

2.3.1.1 Preparation of total cellular extract for SDS-PAGE analysis

The OD_{600nm} of an overnight culture was measured and 1 ml of the culture was then harvested by centrifugation at 15,800 x *g* for 1 min. The pelleted bacteria were then resuspended in an appropriate volume of Laemmli buffer (75 mM tris-HCl, pH 6.8, 20% (v/v) glycerol, 2% (w/v) SDS, 2% (v/v) β-mercaptoethanol, 10 μg/ml bromophenol blue) such that the final concentration was 10 OD_{600nm} units/ml. The samples were boiled at 100 ^{o}C for 5 min and stored at –20 ^{o}C. Prior to use, samples were thawed and boiled again to denature all proteins.

2.3.1.2 Sarcosyl enrichment of outer membrane proteins

Bacterial lysates were enriched for outer-membrane proteins as previously described (88). This procedure is based on the ability of the detergent N-laurylsarcosine (sarcosyl) to disaggregate and solubilise protein and lipid components of the bacterial cytoplasmic membrane while, due to its similar charge density to LPS, leaving the LPS-containing outer-membranes intact and insoluble.

The OD_{600nm} of an overnight culture was measured and 60 OD_{600nm} units (corresponding to 20 ml of a culture with an OD_{600nm} equal to 3) of bacteria were harvested by centrifugation at 6,000 x *g* for 10 min and resuspended in 2 ml of ice-cold sonication

buffer (10% sucrose, 50 mM TrisHCl (pH 7.5), 100 mM NaCl, 1mM EDTA) and incubated with 500 µg/ml lysozyme on ice for 20 min. Complete lysis was achieved by sonication. Cellular debris was removed by centrifugation at 9,300 x *g* for 5 min. The supernatant was then incubated with 0.5% sarcosyl for 30 min at RT with continuous mixing. The sarcosyl-insoluble fraction containing the outer membranes was harvested by centrifugation at 21,000 x *g* for 45 min and resuspended in 100 µl of Laemmli buffer. As before samples were stored at –20 °C and bolied for 5 min prior to use.

2.3.1.3 Crude preparation of lipopolysaccharide from *S.* Typhimurium

Overnight cultures (2 ml) of the bacteria to be examined were grown in the presence of appropriate antibiotics. 1.5 ml of each culture was collected by centrifugation at 19,000 x *g* fo 2 min. Bacteria were resuspended in 100 µl of 2x Laemmli buffer. Lysis of resuspended bacteria was achieved by boiling the samples for 10 min at 100 °C. Lysed bacteria were cooled on ice for 5 min. All protein present in the sample was digested with 20 µl of Proteinase K (10 mg/ml), leaving the lipolysaccharide (LPS) component of the outer membrane intact. Digestion of protein was carried out at 60 °C for 1 h. A 1:6 dilution of each sample was prepared in Laemmli buffer. As before samples were stored at –20 °C and bolied for 5 min prior to use.

2.3.1.4 Electrophoresis of protein samples

Discontinuous gels were prepared using standard protocols (13) and 12 or 15% polyacrylamide gels were routinely used. Typically 10 µl of each boiled Laemmli sample was loaded per well and broad range molecular weight markers (New England Biolabs) were included on all gels. Electrophoresis was carried out in a Bio-Rad Mini-Protean III gel tank at 200 V for 55 min. Gels were stained using Coomassie brilliant blue R-250 (0.25% Coomassie brilliant blue R-250, 45% (v/v) methanol, 10% (v/v) acetic acid) and destained using coomassie destain solution (45% (v/v) methanol, 10% (v/v) acetic acid) or transferred to nitrocellulose or PVDF membranes for use in western immunoblots.

2.3.1.5 Silver-staining of LPS samples separated by SDS-PAGE analysis

LPS samples separated by SDS-PAGE were fixed overnight (O/N) in fixing solution (25% (v/v) isopropanol, 7% (v/v) acetic acid). Gels were then oxidised for 5 min in

oxidation buffer (0.7% (v/v) periodic acid in 2.67% (v/v) fixing solution) and subsequently washed four times (4 x 15 min) with dH_2O. Gels were then stained for 10 min in freshly prepared staining solution (28 ml NaOH (0.1 M), 2 ml conc. NH_4OH, 5 ml 20% (w/v) $AgNO_3$). Excess stain was washed away with 3 x 10 min washes with dH_2O. Gels were subsequently placed in developing solution (0.04% (v/v) formalin, 2% (w/v) Na_2CO_3). Image development was stopped with 10% (v/v) acetic acid.

2.3.1.6 Bradford assay for protein concentration determination

The Bradford reagent was used to determine the concentration of proteins in solution. Proteins form a complex with the Brilliant Blue G dye causing a shift in the maximum absorbance from 465 to 595 nm. The amount of absorbance at 595 nm is proportional to the protein present.

A protein concentration dilution series was made using BSA diluted in PBS with concentrations of 1, 0.5, 0.4, 0.3, 0.2, 0.1 and 0.05 µg/µl. 5 µl of each dilution was added to 95 µl of Bradford Reagent, in duplicate in a 96-well plate. 5 µl of PBS was added to 95 µl of Bradford Reagent, in duplicate, in a 96-well plate. 5 µl of the protein sample of interest was added to 95 µl of Bradford Reagent, in duplicate, in a 96-well plate. The absorbance at 595 nm was read and recorded. A standard protein concentration curve was constructed using the BSA dilution series. The concentration of the protein of interest was extrapolated from the standard curve.

2.3.2 Purification of an MBP-PagN fusion protein, a His_{10}-tagged PagN protein and production of an anti-PagN antiserum

The pET poly-histidine tagging and purification system (Novagen) was used to contruct a plasmid where the *pagN* gene was tagged with ~30 nucleotides (encoding ten histidine residues) at the 5′ end of the ORF. This gives rise to a protein tagged with ten histidine residues at the amino terminus. The pMAL protein fusion and purification system (New England Biolabs) was also used to construct a plasmid where the *pagN* gene was fused to the *malE* gene, encoding the maltose-binding protein MBP; this fusion gene is transcribed under the control of an IPTG-inducible P_{tac} promoter. These plasmids were used to produce large amounts of a His_{10}-PagN protein and an MBP-PagN fusion protein allowing

generation of an anti-PagN antiserum and large-scale purification of the fusion protein. The construction of these plasmids is described in detail in Chapter 3.

2.3.2.1 Large-scale purification of His_{10}-PagN tagged protein

His•Bind® columns (Novagen) were used for rapid one-step purification of His_{10}-PagN by immobilised metal affinity chromatography. The His-Tag sequence (10 consecutive histidine residues) binds to divalent cations (Ni^{2+}) immobilised on His•Bind® resins. After unbound proteins are washed away, the target protein is recovered by elution with imidazole. This system enables the purification of proteins under non-denaturing conditions, or in the presence of 6 M urea.

A 100 ml overnight culture of *E. coli* BL21(DE3) containing the plasmid pPagNHis2.6 was grown in OnEx™ medium. The culture was harvested by centrifugation at 9,000 x *g* for 10 min, resuspended in 10 ml sonication buffer (10% sucrose, 50 mM Tris-HCl, 100 mM NaCl, 1 mM EDTA, pH 7.5) and lysed by sonication. The over-expressed His_{10}-tagged PagN protein was purified under denaturing conditions using a His•Bind® column. A His•Bind® Quick 900 cartridge (Novagen) was equilibrated with 6 ml binding buffer (6 M urea, 0.5 M NaCl, 20 mM Tris-HCl, 5 mM imidazole, pH 7.9). Using a 20 ml syringe, the bacterial cell lysate was pushed through the cartridge at a rate of 2 drops/sec. Unbound protein and cellular debris was removed by washing with 20 ml binding buffer. The column was washed with 10 ml wash buffer (binding buffer with the addition of 60 mM imidazole). Bound, His_{10}-PagN was subsequently eluted in 4 ml elution buffer (binding buffer with the addition of 1 M imidazole), and stored at 4 °C.

2.3.2.2 Large-scale purification of MBP-PagN and MBP-LacZ

A 100 ml overnight culture of *E. coli* BL21(DE3) harbouring the *malE-pagN* fusion plasmid (pML7) was grown in OnEx™ medium. Bacteria was harvested and resuspended in 10 ml sonication buffer lysed by sonication. An MBP affinity column was prepared by pouring amylose resin (3 ml) into a 2.5 x 10 cm column. The column bed was washed with 16 ml column buffer (200 mM NaCl, 20 mM Tris-HCl, 1 mM EDTA, 1 mM DTT, pH 7.4). The soluble lysate was diluted 1:5 in column buffer and loaded onto the column at a rate of approximately 1 ml/min. To remove unbound proteins, the column was washed with 32 ml column buffer. The bound protein was eluted in 10 ml column buffer adjusted to 10 mM maltose (as MBP has a higher affinity for maltose than amylose) and collected

in 10 fractions. The 10 fractions were analysed by SDS-PAGE and the protein-containing fractions were pooled, concentrated in a Vivaspin column (MW cut-off 10,000 kDa), according to the manufacturer's instructions, and stored at 4 °C. Large-scale production of MBP-LacZ was carried out in an identical manner. The plasmid expressing MBP-LacZ is pMAL-c2.

2.3.2.3 PagN antiserum

Immunising a rabbit with a crude protein preparation containing both the His_{10}-PagN and MBP-PagN fusion proteins generated an anti-PagN antiserum. As explained in Chapter 3, the majority of the His_{10}-tagged PagN protein was insoluble while the MBP-PagN fusion protein was mostly soluble. For this reason the MBP-PagN fusion was mixed with the His_{10}-PagN tagged protein making a crude protein preparation. This crude preparation was then used to immunise a rabbit. The initial immunisation consisted of 200 µg protein in Freund's complete adjuvant with two further boosts containing 200 µg of protein in Freund's incomplete adjuvant administered on days 14 and 28. A high antibody titre was detected by western immunoblotting after 38 days and the rabbit was exsanguinated.

The resultant antiserum was absorbed against a pooled lysate of *E. coli* K-12 expressing MBP-LacZ, *E. coli* BL21(DE3) and *S.* Typhimurium strain MLT2 to remove cross-reacting antibodies. The lysate was prepared from a 10 ml culture of each strain. Bacteria were pooled, harvested by centrifugation, resuspended in 3 ml sonication buffer and subsequently lysed by sonication. The lysate was divided in two, and one half was heated at 100 °C for 5 min. The boiled and un-boiled lysates were combined, mixed with 9 ml antiserum and incubated for 2 days at 4 °C with continuous mixing. Insoluble materials, including protein-antibody complexes, were removed by centrifugation at 15,800 x *g* for 30 min. The remaining anti-PagN antibody was precipitated by adding an equal volume of ammonium sulfate, pH 7.0. The precipitate was collected by centrifugation and resuspended in 0.3 volumes of PBS of the original volume (3 ml). The absorbed antiserum was dialysed against 8 L PBS at 4 °C overnight.

2.3.2.4 Small-scale purification of MBP-PagN using amylose magnetic beads

Amylose magnetic beads (NEB) were used for small-scale purification of the MBP-PagN fusion protein. Magentic beads were resuspended thoroughly by vortexing. 100 µl aliquot was washed three times in 500 µl MBP column buffer in a microcentrifuge tube. 500 µl of

cell culture supernatant, containing the MBP-PagN fusion protein, was added to the washed beads. The solution was mixed thoroughly and incubated at 4 °C with agitation for 1 h. A magnet was applied to the solution and supernatant was decanted. The beads were washed three times as before. The MBP-fusion was eluted by adding 250 µl MBP column buffer contining 10 mM maltose to the bead pellet. The resuspended beads were incubated for 10 min at 4 °C with agitation. A magnet was applied and the eluted MBP-fusion protein was removed. The elution process was repeated to collect any fusion protein that had remained bound.

2.3.2.5 Small-scale purification of MBP-PagN using anti-MBP magnetic beads

Anti-MBP magnetic beads (NEB) were also used for small-scale purification of the MBP-PagN fusion protein. Magentic beads were resuspended thoroughly by vortexing. 40 µl aliquot was washed three times in 500 µl sodium phosphate (pH 8.0) buffer in a microcentrifuge tube. 500 µl of cell culture supernatant, containing the MBP-PagN fusion protein, was added to the washed beads. The solution was mixed thoroughly and incubated at 4 °C with aggitation for 1 h. A magnet was applied to the solution and supernatant was decanted. The beads were washed three times as before. The MBP-fusion was eluted in 40 µl 3X SDS sample buffer (187.5 mM Tris-HCl (pH 6.8), 6% (w/v) SDS, 30% glycerol, 150 mM DTT, 0.03% (w/v) Bromophenol blue, 2% β-mercaptoethanol). The resuspended beads were heated for 5 min at 70 °C.

2.3.3 Western immunoblotting

2.3.3.1 Electro-transfer of separated proteins

Proteins were separated on SDS-polyacrylamide gels and transferred to nitrocellulose or PVDF membranes using a Biometra Fastblot semi-dry transfer apparatus. For transfer to nitrocellulose membranes the polyacrylamide gel and the membrane were equilibrated in transfer buffer (25 mM tris, 192 mM glycine, 20% (v/v) methanol) and blotting was carried out according to the manufacturers instructions at 5 mA/cm^2 for 20 min. Where higher sensitivity of detection was required Immobilon-P PVDF membrane (Millipore) was used and transfer was carried out using a three buffer semi-dry system according to the manufacturers instructions. Following transfer all membranes were rinsed briefly with

Millipore grade water and stained with Ponceau S stain (0.5% (w/v) Ponceau S, 1% (v/v) acetic acid) to visualise the transferred proteins. Excess Ponceau S stain was removed by further washes with Millipore purified water before subsequent manipulation of the membranes. Nitrocellulose membranes were blocked by incubation in blocking buffer (5% non-fat powdered milk in phosphate-buffered saline) at 4 °C overnight prior to use. Immobilon-P PVDF membranes were dried overnight at room temperature according to the manufacturers instructions prior to use.

2.3.3.2 Detection of bound proteins

Blocked nitrocellulose membranes or dried PVDF membranes were incubated with anti-PagN antiserum diluted 1:500 in appropriate blocking buffer (5% non-fat powdered milk in PBS for nitrocellulose or 3% non-fat powdered milk in PBS containing 0.01% Tween-20 for PVDF membranes) for 1 h at room temperature. The membrane was then washed three times for 30 min with PBS containing 0.1% Tween-20 and incubated with a secondary HRP-linked anti-rabbit antibody diluted 1:20,000 in blocking buffer for either 1 h (nitrocellulose) or 30 min (PVDF). The blot was then washed as before and developed using the SuperSignal West Pico chemiluminescent HRP substrate (Pierce). Chemiluminescence was detected using BioMax Light Film (Kodak) and films were developed manually using standard Kodak developer and fixer solutions according to the manufacturers instructions. The length of exposure was varied to adapt for the signal strength. Typical exposure lengths were 1-5 min for nitrocellulose and 10 sec -1 min for PVDF membranes.

2.3.3.3 Gel mobility shift analysis of protein/DNA complexes

The association of purified His-PhoP protein with the putative *pagN* promoter region was analysed by gel mobility shift assay using the LightShift® Chemiluminescent EMSA kit (PIERCE). DNA probes were amplified by PCR with *Pfx* polymerase, using *S.* Typhimurium strain LT2 chromosomal DNA as template. During synthesis, the 5′ end of each primer was biotinylated so detection of the resultant PCR product was possible by non-radioactive methods. Amplified probes were gel purified twice as described (Section 2.2.5.2). Approximately 0.3 pg of the *pagN,* biotinylated promoter fragment was incubated with purified His-PhoP at a final concentration range of 52 nM-3.3 µM. The DNA and protein were incubated at 37 °C for 10 min in 20 µl binding reaction containing

binding buffer (100 mM Tris, 500 mM KCl, 10 mM DTT, glycerol 5% (v/v), 3 mM $MgCl_2$ and 50 ng/ml poly-(dI.dC), pH 7.5). Protein/DNA complexes were resolved by electrophoresis through a 5% polyacrylamide gel, for 70 min at 100 V. DNA, protein and DNA/protein complexes were then transferred to a nylon membrane (Biodyne) at 80 V for 1 h. To immobilise the DNA/Protein complexes onto the membrane the membrane was cross-linked using UV-light at 120 mJ/cm^2 for 1 min. Nylon membranes were blocked by incubation in blocking buffer at room temperature for 15 min.

2.3.3.4 Detection of DNA/protein complexes

Blocked nylon membranes were incubated with stabilised streptavidin-horseradish peroxidase conjugate/blocking buffer solution (1:300 dilution) for 15 min at room temperature. The membrane was then washed four times for 5 min with wash solution. The membrane was then incubated with substrate equilibration buffer for 5 min at room temperature. The blot was developed using a 1:1 Luminol enhancer/stable peroxide solution. Chemiluminescence was detected using BioMax Light Film (Kodak) and films were developed manually using standard Kodak developer and fixer solutions according to the manufacturers instructions. The length of exposure was varied to adapt for the signal strength.

2.3.4 Flow cytometry

2.3.4.1 Gene expression profiling of intracellular *Salmonella*

To examine the expression of *pagN* from an intracellular environment Caco-2 cells, CHO-K1 cells or J-774A.1 macrophages were seeded in 12-well tissue culture trays at a density of 2.5 x 10^5, 3.0 x 10^4 or 5 x 10^5 respectively and grown until confluent. Confluent monolayers were challenged with *S.* Typhimurium strain LT2 or TA2362 containing the plasmid pPagN-GFP (Table 2.2). The infected cells were centrifuged at 600 x *g* for 5 min to initiate contact between bacteria and the mammalian cells and incubated at 37 °C in 5% CO_2 for 1 h to allow bacterial internalisation. Following the 1 h infection, cells were incubated at 37 °C in 5% CO_2 with medium containing gentamicin (100 µg/ml) to kill any extracellular bacteria. At times 1, 2, 4 and 6 h post addition of gentamicin, cells were

washed three times with PBS and fixed in 1.5 ml 2% (v/v) formaldehyde. The tray was wrapped in tin foil and stored at 4 °C overnight.

Cells were subsequently washed three times with PBS. Monolayers were incubated at 37 °C for 30 min with 1 ml trypsin/EDTA solution. Cells were removed from the tissue culture trays, washed three times with PBS and resuspended in 400 µl 2% (v/v) formaldehyde. The level of intracellular *pagN* gene expression was determined by measuring the fluorescence of the eukaryotic cells on a Beckman Coulter Epics XL flow cytometer and Expo 32 ADC software according to the manufacturers instructions.

2.3.4.2 Determination of PagN surface exposure

To examine the surface exposure of the PagN protein, intact bacterial cells were labelled with anti-PagN polyclonal antiserum and a fluorescently labeled secondary antibody and analysed by flow-cytometry. Briefly, 1 ml PagN-expressing bacteria (approx. 3 x 10^7 cfu/ml) from an IPTG-induced culture was harvested at 6,000 x *g* for 5 min, and resuspended in PBS containing 2% (v/v) formaldehyde. Fixed bacteria were stored at 4 °C over night. Excess formaldehyde was removed from 100 µl fixed bacteria by three successive washes with PBS. Bacteria were then incubated for 1 h at room temperature in 200 µl of a 1:10 dilution of absorbed anti-PagN antiserum. The labeled bacteria were then washed three times with PBS and incubated with a 1:100 dilution of secondary FITC-conjugated anti-Rabbit antibody for 1 h at room temperature. The labeled samples were then washed again as before and fluorescence was analysed on a Beckman Coulter Epics XL flow cytometer and Expo 32 ADC software.

2.3.5 Mass Spectrometry

The identification of proteins by mass spectrometry was carried out by Dr. Catherine Botting at the Centre for Biomolecular Sciences, University of St. Andrews, Scotland. Protein bands were excised from polyacrylamide gels and cut into 1 mm cubes. These were then subjected to in-gel digestion, using a ProGest Investigator in-gel digestion robot, using standard protocols. Briefly the gel cubes were destained by washing with acetonitrile and subjected to reduction and alkylation before digestion with trypsin at 37 °C. The peptides were extracted with 10% formic acid and concentrated to 20 ml

(SpeedVac, ThemoSavant). They were then separated using an UltiMate nanoLC (LC Packings, Amsterdam) equipped with a PepMap C18 trap & column. The eluent was sprayed into a Q-Star Pulsar XL tandem mass spectrometer (Applied Biosystems, Foster City, CA) and analysed in Information Dependent Acquisition (IDA) mode. MS/MS data for doubly and triply charged precursor ions was converted to centroid data, without smoothing, using the Mascot Daemon 2.1 (Matrix Science, London) data import filter for Sciex Analyst. The MS/MS data file generated was analysed using the Mascot search engine against MSDB May 2006. These data were searched with tolerances of 0.2 Da for the precursor and fragment ions, trypsin as the cleavage enzyme, one missed cleavage, carbamidomethyl modification of cysteines as a fixed modification and methionine oxidation selected as a variable modification. The Mascot search results were accepted if a protein hit included at least one peptide with a score above the homology threshold and the MS/MS interpretation accounted for the major peaks.

2.4 Phenotypic Assays

2.4.1 Haemagglutination assay

The ability of bacterial strains to agglutinate erythrocytes was determined using a 1% suspension of human blood, except where otherwise stated. Briefly, sterile human blood was diluted 1:10 with PBS, centrifuged at 6,000 x *g* for 10 sec to harvest intact erythrocytes and resuspended in the same volume of PBS. This wash step was repeated until the supernatant was clear. Immediately prior to use, this 10% suspension of erythrocytes was diluted 1:10 with PBS containing 100 mM mannose. Mannose was included to inhibit agglutination due to type 1 fimbriae. Overnight bacterial cultures were sub-cultured into 10 ml L broth at a 1:50 dilution. Bacteria were grown to mid-logarithmic phase and recombinant protein expression was induced with IPTG (1 mM). Bacteria were grown for 3 h. Where indicated, protein expression was induced by growing *E. coli* BL21(DE3), harbouring the indicated plasmid, in OnEx^{TM} medium containing the appropriate antibiotic. Upon protein production, bacteria were harvested by centrifugation at 15,800 x *g* for 1 min and resuspended in an equal volume of PBS. The OD_{600nm} was measured and the bacteria were diluted with PBS such that their OD_{600nm} was equal to 10. The bacteria were then serially 2-fold diluted with PBS in a final volume of 100 µl in a 96-

well microtitre plate. To each well was added an equal volume of 1% blood and the plate was incubated at 4 °C overnight to allow un-agglutinated erythrocytes to settle out of suspension.

To investigate whether recombinant, purified MBP-PagN or MBP-LacZ could inhibit PagN-promoted haemagglutination; erythrocytes were incubated with MBP-tagged protein prior to the previously described assay. 100 µl aliquots of 1% blood were incubated with a range of MBP-tagged protein (40, 30, 20, 10, 5, 2 and 1 µg) at 4 °C for 1 h. To remove any unbound protein, cells were subsequently washed 3 times with 500 µl PBS. Erythrocytes were resuspended in 100 µl PBS and 50 µl of this blood was added to wells containing bacteria adjusted to the concentration of the titre as determined by a previous HA assay. This gives a final concentration of 20, 15, 10, 5, 2.5, 1 or 0.5 µg/well of MBP-tagged protein.

2.4.2 Autoaggregation assays

To ascertain if the autoaggregation phenotype associated with the expression of the Hek protein could be transferred to PagN via Hek loops 1 and 2, autoaggregation assays, as developed by Fagan *et al.* (108), were carried out with *E. coli* XL-1 and *E. coli* BL21(DE3) expressing the hybrid protein H12P34. Briefly, overnight cultures (5 ml) of *E. coli* BL21(DE3) expressing Hek, PagN or the hybrid protein H12P34 respectively, were grown in OnEx™ medium, harvested by centrifugation and resuspended in 5 ml PBS. The OD_{600nm} were measured and adjusted to approximately 3.0 by the addition of PBS. 2 ml of each culture was then transferred to a Kahn tube, a 50 µl sample was taken and the OD_{600nm} measured again to determine the starting OD for each culture (T=0). Further 50 µl samples were taken from the surface of the cultures every 20 min and the OD_{600nm} were measured as before. Assays were performed in duplicate and the rate of autoaggregation was determined by the mean decrease in optical density over time.

2.4.3 Adhesion, cell association and invasion assays

2.4.3.1 Qualitative adhesion assay

In order to perform qualitative adhesion assays, HT-29 cells were seeded into chamber slides (Nalge Nunc International, 0.8 cm^2 per well) at a density of approximately 1.0 x 10^5 cells per chamber and grown to confluency at 37 °C in 5% CO_2. *S.* Typhimurium, harbouring plasmid pOS32, were grown overnight in MM5.8 medium and 5 µl quantities were added to each well of cultured HT-29 cells. Infected monolayers were then wrapped in tin-foil and incubated for 3 h at 37 °C in 5% CO_2 and then washed extensively with PBS to remove non-adherent bacteria. The chamber slides were disassembled and the mammalian cells with adherent bacteria were fixed in 70% (v/v) methanol for 5 min. Slides were air-dried and examined by fluorescent microscopy.

2.4.3.2 Quantitative cell association and invasion assays

CHO-K1, pgsA-745 and HT-29 cultured cells were infected with *E. coli* or *Salmonella* as indicated and the total numbers of cell associated and intracellular bacteria were enumerated. All cell lines were grown in 12-well trays in the appropriate tissue culture medium and fed once on the day before the experiment. HT-29 cells were split 5 days prior to infection at a density of 2.5 x 10^5 per well and CHO-K1 and pgsA-745 cells were split 3 days prior to infection at densities of 3.0 x 10^4. Bacterial strains were grown overnight, harvested by centrifugation and resuspended in PBS. The OD_{600nm} were measured and bacteria were diluted 1:500 in warm tissue culture medium. Mammalian cell monolayers were washed once with warm PBS and bacteria-containing medium (1 ml) was added to each well. The infected cells were centrifuged at 600 x *g* for 5 min to initiate contact between bacteria and the mammalian cells and incubated at 37 °C in 5% CO_2 for 1 h to allow adhesion to and invasion of the cultured cells. Samples of the medium containing bacteria were also diluted and spread on L agar plates to determine the numbers of bacteria present in each inoculum. The infected cells were then washed 5 times with warm PBS to remove any non-adherent bacteria. To determine the total number of cell associated bacteria the monolayer was disrupted by treatment with 0.1% Triton X-100 and the released bacteria were enumerated by spreading dilutions on L agar. To determine the number of intracellular bacteria a standard gentamicin protection assay was performed (198). Following the 1 h infection the cells were incubated with medium containing

gentamicin (100 μg/ml) for 90 min at 37 °C in 5% CO_2 to kill any adherent extracellular bacteria, washed twice with PBS, to remove dead bacteria and gentamicin, disrupted with 0.1% Triton X-100 and the released bacteria enumerated as before.

In experiments where exogenous glycosaminoglycans were tested as potential inhibitors of invasion the bacterial inocula were prepared essentially as before but in media containing the inhibitor to be tested and incubated for between 30 min at 37 °C prior to infecting the cultured monolayers. The experiments were then carried out as previously described. Conditions under which the glycosaminoglycan chains are enzymatically removed prior to assays are described in detail in the relevent sections (See Chapter 5).

Chapter 3

Initial characterisation of the PagN protein of *S.* Typhimurium

3.1 Introduction

In 1985, through the systematic screening of an *S.* Typhimurium library, Fitts described five clones containing DNA sequences that were thought to be unique to *Salmonella* (115). Of these five, only one (RF333) was subsequently found to be confined to the *Salmonella* genome. Apart from its presence in *Salmonella*, clone RF321 was also detected in a strain of *Klebsiella pneumoniae*. This DNA sequence was described as a 4.9-kDa fragment, with a G+C content of 44.9%, containing 12 ORFs, one of which encoded a LysR-like protein, which was named *Salmonella*-insert Regulator, SinR (150). Subsequently, several of the other ORFs in this region have been described (119), among which is the PhoP-activated gene N, *pagN* (158). The *pagN* ORF was originally identified in a Tn*phoA* random-mutagenesis screen of the *S* Typhimurium strain 14082s (28). Bacteria with active *phoA* gene-fusions in wild-type strains that showed decreased fusion-protein activity on acquisition of the *phoP12* allele (which results in a PhoP null phenotype) were identified. The *pagN* ORF was one such gene, placing it in the category of a *pag*. At the DNA level, *pagN* displays no similarity to any other gene, however the gene-product PagN is 54% similar to the *E. coli* adhesin Tia (see section 3.2.1.1.) (117, 158). As PhoP primarily regulates genes associated with *Salmonella* virulence, a *pagN*-deficient *S.* Typhimurium strain was used to challenge BABL/c mice, and the mouse LD_{50} was determined. Data from that study indicated that *pagN* did not contribute to *Salmonella* mouse lethality (28).

Through the use of *in vivo* expression technology (IVET), Heithoff *et al.* identified over 100 genes that were specifically expressed during infection of BALB/c mice (172). Of these hundred genes, it was shown that *pagN* (also termed *iviVI-A*), although not expressed in *S.* Typhimurium strains grown on typical laboratory medium, is required for survival in BALB/c mice under the conditions of the IVET selection (172). The *pagN* gene was identified as an IVET-fusion recovered from the spleen of BALB/c mice injected intra-peritoneally, suggesting a role in the more progressive stages of *Salmonella* pathogenesis. In the same screen, the authors identified another *pag* immediately upstream of *pagN*. Mutagenesis of this upstream gene had polar effects on *pagN* expression, indicating that the two genes may form part of an operon, or that the gene-product may positively regulate *pagN* expression either directly or as part of a cascade (173). Subsequently, Conner *et al.* noted a decrease in competiveness for a mutant with deletions in the region of *pagN*/*iviVI-A* when mixed with its parental strain (72).

Expression of the *pagN* gene has been shown to respond to pH and Mg^{2+} concentration *in vitro* (173). As with other *pags*, in a PhoP-dependent manner, *pagN* expression was induced in conditions of acidic pH and low Mg^{2+} concentration (173). Expression of *pagN* has been demonstrated to be highly up-regulated within cultured RAW264.7 macrophages and Henle-407 enterocytes (173). These data suggest that the adhesin-like protein responds to intracellular signals present during both early and late stages of infection.

In contrast to the *Salmonella* chromosome, which has an average G+C content of 52%, the *pagN* gene has a G+C content of 42% (72). This lower G+C content suggests it has been acquired by horizontal transfer during bacterial evolution. The *pagN* gene is located on a highly-characterised *Salmonella enterica* centisome 7 genomic island (SCI) located at the *aspV* loci in *S. enterica* subspecies I strains (Fig. 3.1). This region is flanked by sequences with similarity to the *E. coli* tRNA gene *aspV* and the *yafV* ORF, and has been the target for multiple insertion events (119, 120). In addition to *pagN*, the 47-kb genetic island encodes 36 putative proteins. Situated immediately upstream of *pagN*, is the transcriptional regulator *sinR* and the *Salmonella* atypical fimbrial operon, *saf*. This *saf-pagN* region is flanked by inserted repeats, forming a putative element of 11.1 kb. Of note is a 100 bp region in the coding sequence of *sinR* with a corresponding inverted region upstream of the *saf* operon indicating that multiple insertion events have formed this mosaic region. The *saf-sinR* region of this element is broadly distributed within, but confined to *S. enterica* subspecies I, while *pagN* is found throughout the *Salmonella* species (119). Recently, in a vaccine development study, a recombinant histidine-tagged SafB chaperone complexed with the SafD adhesin was used to immunise BALB/c mice subcutaneously (380). When challenged with *S. enteritidis*, the immunised mice had lower bacterial counts than the untreated control group, highlighting SafB/SafD for potential inclusion in a *Salmonella* vaccine (380). Interestingly, *S.* Typhi contains an additional 10-kb fimbrial operon in the *saf-pagN* intergenic region. This region contains four ORFs termed *tcfA-D* (typhi colonizing factor), predicted to encode proteins TcfA, TcfB, TcfC and TcfD (119), which show significant homology to the enterotoxigenic *E. coli* CS1 fimbrial subunits and chaperone proteins CooA, CooB, CooC and CooD (127, 320, 355). Downstream of the *tcf* operon are two ORFs, one encoding a putative transcriptional regulator TinR and another of unknown function (119).

The nucleotide content is not evenly distributed over the SCI genomic island. The region encoding the *saf-pagN* element, has a lower (45%) content while the rest of the island has a G+C content significantly higher (56%) than the average in *Salmonella* (120). The region of DNA upstream of the *saf* operon contains 25 ORFs denoted *sci A* to *Y* encoding putative

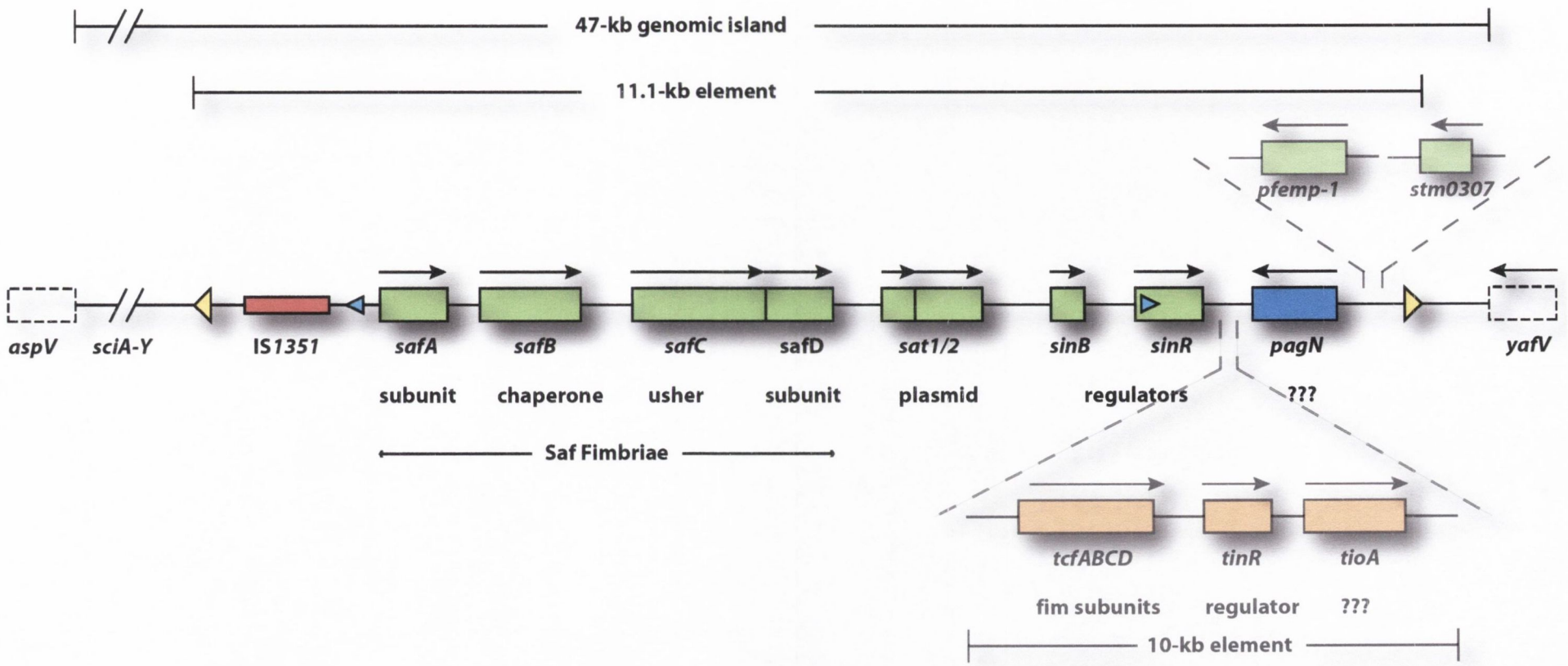

FIG 3.1. Schematic representation of the *Salmonella* centisome 7 genomic island in *S. enterica* serovars Typhimurium and Typhi. Putative genes are represented by coloured boxes. ORFs with a broad distribution within the *Salmonella* genus are coloured dark blue, while *S. enterica* subspecies I-specific genes are green. ORFs specific to *S.* Typhi are faded and coloured orange. ORFs whose presence is not universally confirmed are faded and colured green. The IS*1352* element is red. Inverted repeats are indicated by triangles. White, dashed boxes represent genes common to *E. coli* and *Salmonella* spp. Arrows indicate transcriptional direction. Putative functions are indicated below the genes. Adapted from Folkesson *et al.* (10). Not to scale.

proteins with homologies to virulence-associated proteins in gram-negative bacteria such as *Pseudomonas aeruginosa*, *Yersinia pestis* and enterohaemhorragic *E. coli*. Importantly, the *pagN*-containing region presented by Conner *et al.* lacks sequences of DNA with similarity to the *sinR* gene (72), while the SCI genomic island presented by Folkesson *et al.* lack regions with similarity to two ORFs, one of which was thought to form a putative operon with *pagN* (120). These differences may be due to strain variation as Conner *et al.* used *S.* Typhimurium strain 14028s while Folkesson *et al.* used *S.* Typhimurium strain SR11 χ3181.

The aim of the study presented in this chapter was to characterise the *pagN* gene and the corresponding protein, PagN. In doing so, the most relevant questions to be addressed were:

- Is the *pagN* gene regulated directly by the PhoP/Q system?
- Is PagN an outer membrane protein?
- Under what conditions is it expressed?
- Is the protein an adhesin?

3.2 Results

3.2.1 Cloning and expression of the PagN gene in *S.* Typhimurium

3.2.1.1 Comparative analysis of the *Escherishia coli* adhesins Tia and Hek with PagN

The *E. coli* proteins Tia and Hek are well-characterised adhesins and invasins (108, 255). Tia has been shown to be necessary for invasion by Enterotoxigenic *E. coli* and sufficient to promote invasion by a non-invasive *E. coli* K-12 strain (255); while Hek has a role in the primary attachment of neonatal-meningitic *E. coli* to epithelial cells (108). These are similar proteins (62% identical) and interact with similar receptors on the cell surface ((116), R. Fagan personal communication). Protein-protein BLAST (www.ncbi.nlm.nih.gov/BLAST) analysis of the Hek primary sequence indicated that the *Salmonella*-specific protein PagN is similar to both Hek and Tia. A sequence alignment of all three proteins demonstrates that PagN is 38% identical and 54% similar to Tia; while it shares 37% identity and 54% similarity with Hek (Fig. 3.2). The degree of similarity between Tia, Hek and PagN suggests that PagN may have a similar function to these related adhesin/invasin proteins.

3.2.1.2 Expression of *pagN* from its native promoter

The *pagN* ORF from *S.* Typhimurium strain LT2 and 500 bp of DNA either side of the ORF was amplified by PCR using primers PagNF and PagNR (Table 2.3). The purified *pagN* PCR product was cloned into pBluescript II SK + cloning vector (pBSKII) cut with *Eco*RV creating the multi-copy plasmid pPagN2.3. The pPagN2.3 plasmid was sequenced to confirm the DNA sequence of the insert (Table 2.2 and Fig. 3.3 (A)). As the *E. coli* and *S.* Typhimurium PhoP/Q systems are not inter-changeable and regulate analogous genes differently (424), this plasmid was transformed into *S.* Typhimurium strain LT2. *S.* Typhimurium strain LT2 harbouring plasmid pPagN2.3 was grown in MOPS minimal medium containing $MgCl_2$ [0.05 mM] and adjusted to pH 5.8 (MM5.8) (these conditions have been shown to induce maximal transcription of *pagN* (173)). SDS-PAGE analysis of sarcosyl-extracted outer membrane protein preparations of these bacteria revealed a unique

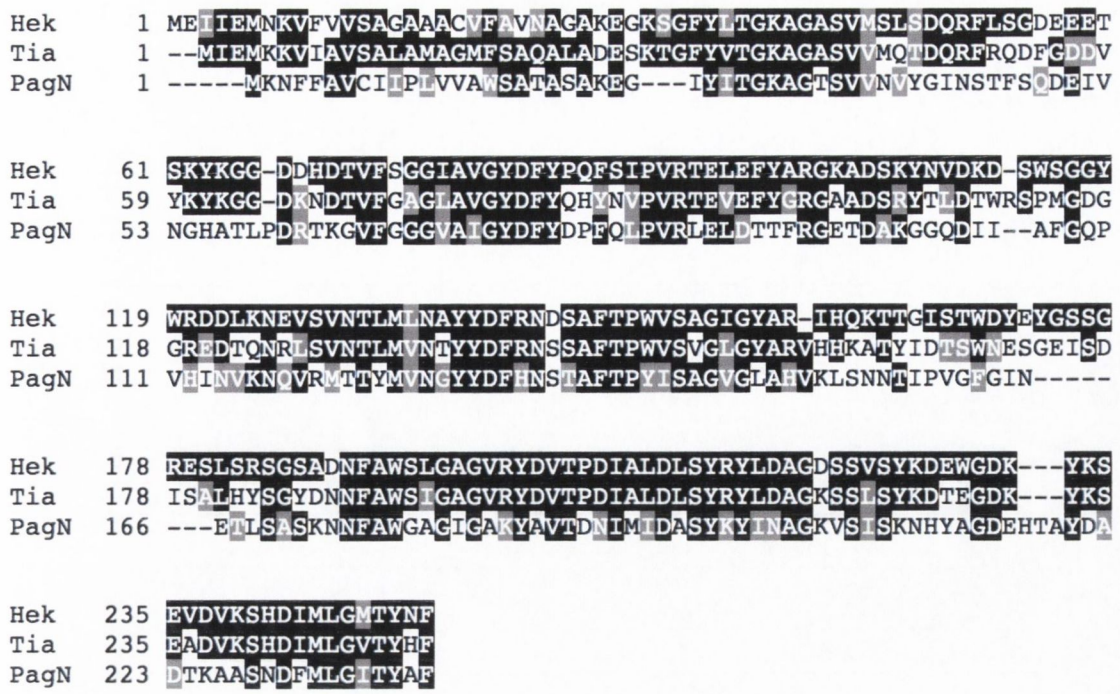

FIG 3.2. Clustal alignment of the primary sequence of the Hek, Tia and PagN proteins from *E. coli* strains RS218, H10407 and *S.* Typhimurium strain LT2 respectively. Identical residues are coloured black while similar residues are coloured grey. Gaps are indicated with hyphens.

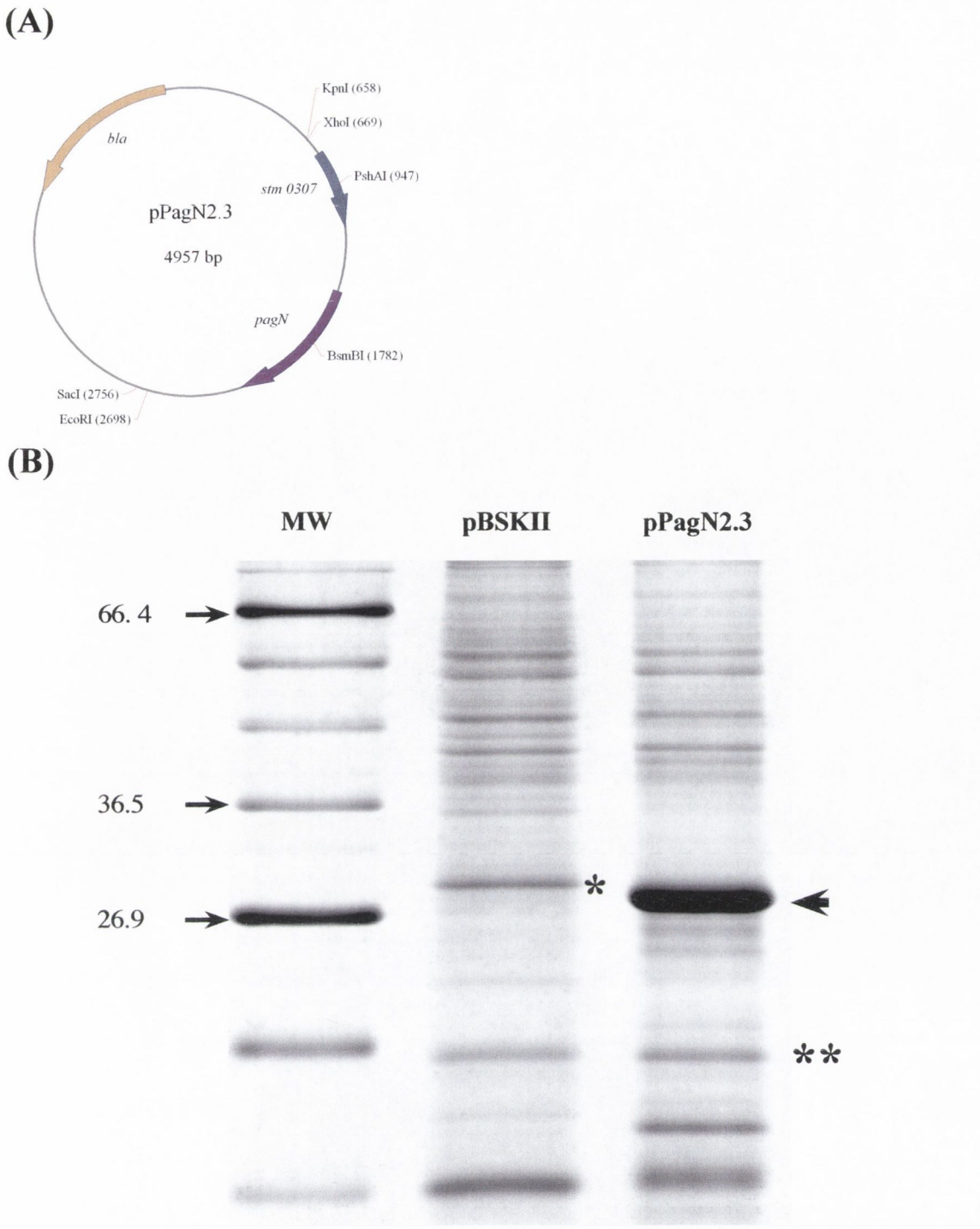

FIG. 3.3. (A) Map of the plasmid pPagN2.3. The positions of the *pagN* gene, *stm0307* ORF and the *bla* gene (encoding beta-lactamase) are indicated. Relevant restriction endonuclease sites are marked. **(B) SDS-PAGE analysis of *S.* Typhimurium outer membrane fractions.** Fractions were prepared from *S.* Typhimurium strain LT2 grown in MM5.8 medium. membrane fraction samples from *S.* Typhimurium carrying the indicated plasmid are loaded in each lane. PagN is indicated on the right. The protein indicated by * was subjected to MALDI-TOF analysis but no identification was determined. The protein indicated by ** was identified as lysozyme, used in the preparation of outer membrane samples. Molecular mass standards (in kilo-daltons) are indicated on the left.

(A)

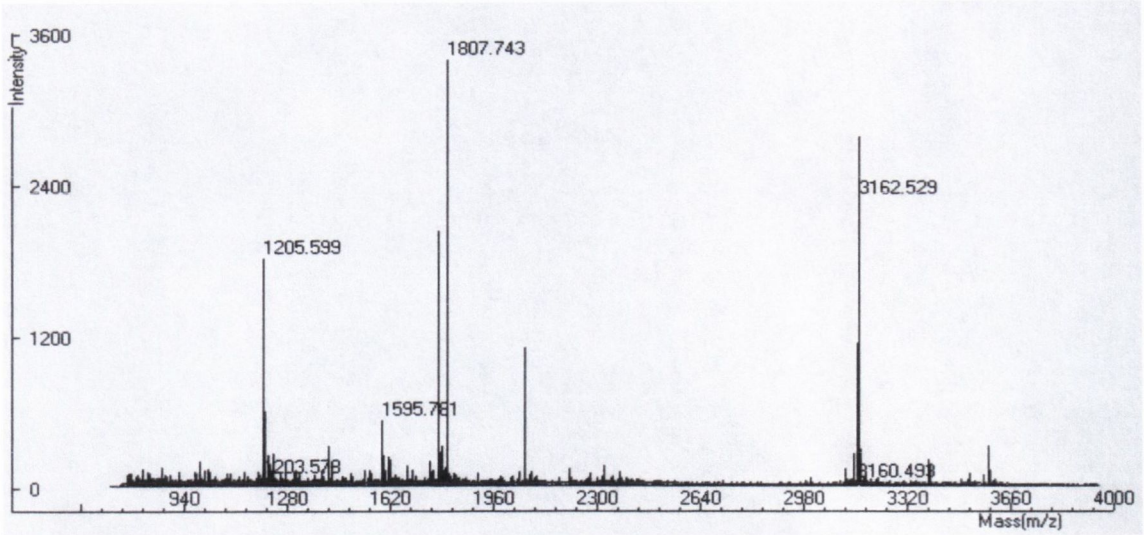

(B)

1. gi|16763689|ref|NP_459304.1 (NC_003197) Homolog of sapA [Salmonella typhimurium LT2]
2. gi|16418808|gb|AAL19263.1 (AE008709) Homolog of sapA [Salmonella typhimurium LT2]

Sample ID : A3 [Pass:0]
Measured peptides : 9
Matched peptides : 5
Min. sequence coverage: 33%

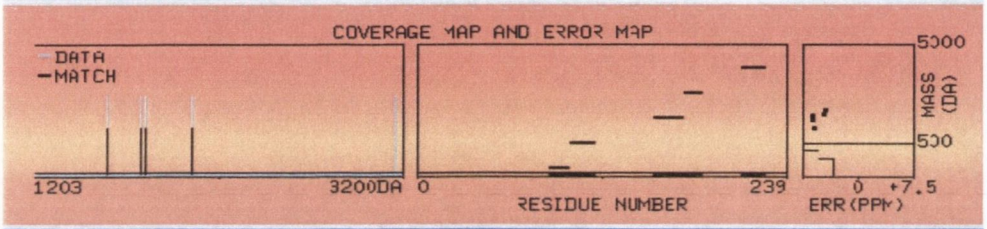

Measured Mass(M)	Avg/ Mono	Computed Mass	Error (ppm)	Residues Start	To	Missed Cut	Peptide sequence
1204.591	M	1204.598	-6	173	184	0	NNFAWGAGIGAK
1594.773	M	1594.783	-6	86	99	1	LKLDTTFRGETDAK
1778.920	M	1778.931	-6	100	116	0	GGQDIIAFGDPVHINVK
1806.736	M	1806.744	-4	210	225	0	NHYAGDEHTAYDADTK
2061.064	M	2061.073	-4	153	172	0	LSNNTIPVGFGINETLSASK

Unmatched Monoisotopic Masses:

3162.530 1805.778 1203.578 3160.463

(C)

KEGIYITGKA GTSVVNVYGI NSTFSQDEIV NGHATLPDRT KGVFGGGVAI
GYDFYDPFQL PVRLELDTTF RGETDAKGGQ DIIAFGDPVH INVKNQVRMT
TYMVNGYYDF HNSTAFTPYI SAGVGLAHVK LSNNTIPVGF GINETLSASK
NNFAWGAGIG AKYAVTDNIM IDASYKYINA GKVSISKNHY AGDEHTAYDA
DTKAASNDFM LGITYAF

FIG. 3.4. MALDI-TOF analysis of the mature PagN protein. (A) Peptide mass fingerprint spectrum of the mature PagN protein. The mass to charge ratio (m/z) of the ionised peptides is indicated. **(B) PagN protein sequence coverage.** The peptides identified by MALDI-TOF analysis of the trypsinised mature PagN protein are aligned with the *in silico* peptide profile prediction. The matched and unmatched measured peptides are indicated. **(C) Sequence coverage of PMF.** The sequence of the predicted mature PagN protein is shown in single letter amino acid code. The measured peptides which matched the protein are coloured green.

protein band with an apparent molecular weight of ~26 kDa, corresponding to the predicted size of the PagN protein (Fig. 3.3 (B)). This band was excised from the gel, digested with trypsin, and subjected to peptide-mass fingerprinting (PMF). Matrix assisted laser desorption/ionization time-of-flight (MALDI-TOF) mass spectrometric analysis confirmed the protein as PagN with a high probability (Expectation: 1.90959 x 10^{-5}) (Fig. 3.4). Five of the nine measured peptides matched the protein corresponding to 33% coverage. The PMF analysis of PagN identified it as a 25.7-kDa protein with homology to SapA. However, PagN is not a SapA homologue; this may represent an error in the initial Sanger Institute database annotation of the *pagN*-containing SCI element. The PMF search criteria were set with a stringency level of 10 p.p.m. therefore, the expectation value of 10^{-5} establishes with confidence that the protein excised from the gel was PagN. As PagN was present in the insoluble fraction of sarcosyl-extracted proteins, it would suggest that in MM 5.8, *pagN* expression is induced, directing the production of a ~26-kDa protein which is targeted to the outer membrane.

3.2.1.3 Construction of a *his*-tagged *pagN* expression plasmid and purification of the recombinant His_{10}-PagN protein

Western immunoblotting is an invaluable method of detecting proteins of interest with antibodies that specifically recognise them. In order to raise antibodies against PagN, a recombinant PagN protein, tagged with ten histidine residues (His_{10}-PagN), was produced and used to immunise an SPF rabbit. The pET-19b plasmid (Table 2.2) was digested with *Nde*I and the resulting 5′ overhangs were filled in with DNA polymerase I, Large Fragment (Klenow). The blunt-ended vector was then digested with *Bam*HI. Using *S.* Typhimurium strain LT2 genomic DNA as a template, the *pagN* ORF was amplified by PCR using the primers ML2 and ML3 (Table 2.3). The PCR product was digested with *Bsa*BI and *Bam*HI and ligated into the previously digested pET-19b vector. The vector was sequenced and the resulting plasmid named pPagNHis2.6 (Table 2.2 and Fig. 3.5 (A)). The plasmid pPagNHis2.6 was transformed into *E. coli* BL21(DE3) containing the pLysS plasmid. The plasmid pLysS constitutively expresses a small amount of T7 lysozyme, a natural inhibitor of T7 RNA polymerase, preventing leaky expression from T7-activated promoters. Upon IPTG induction of such promoters, the presence of lysozyme is comparatively negligible and large-scale gene expression is attained. Protein expression was induced with the addition of IPTG. SDS-PAGE analysis of whole cell lysates of *E. coli* containing pPagNHis2.6, showed the presence of a unique band of ~30 kDa

corresponding to the His_{10}-tagged protein. Whole cell lysates were separated into soluble and insoluble fractions by centrifugation and analysed by SDS-PAGE (Fig 3.5 (B)). The recombinant His_{10}-PagN protein was largely insoluble. The protein was purified from the insoluble fraction by passing the insoluble fraction through a nickel column under denaturing conditions. Bound His_{10}-PagN was eluted and analysed by SDS-PAGE (Fig. 3.5 (C)). Urea and other salts were removed by passing the purified protein fractions through a PD-10 de-salting column, as described by the manufacturers (Amersham). SDS-PAGE analysis of de-salted, eluted protein fractions showed that full-length, relatively pure protein had been isolated (Fig. 3.5 (D)). The fractions were subsequently pooled and concentrated using a Vivaspin R15 ultrafiltration spin column, as described by the manufacturers (Sartorius). Upon examination by eye of the concentrated protein fractions, it was apparent that the His_{10}-tagged protein had formed precipitates. The protein was used to immunise a rabbit. However, the first test-bleed revealed very low antibody titre against PagN. The purified recombinant His_{10}-PagN protein was deemed unsuitable for further immunisations.

3.2.1.4 Construction of a *malE-pagN* gene-fusion expression plasmid and purification of the recombinant MBP-PagN protein

As PagN proved to be insoluble when purified via a poly-histidine tag, an alternative strategy was devised. Indeed PagN is not unusual in this regard; due to the amphipathic nature of their surfaces, solubilisation of outer membrane proteins often requires the addition of vast excess of detergents (310). The maltose binding protein, MBP, has been shown to lend solubility to target proteins when fused to the amino-terminus (207). This allows purification of fusion proteins on an amylose resin affinity column (209), thus facilitating purification of otherwise insoluble proteins.

The *pagN* ORF was amplified by PCR using the primer set ML3 and PagN-R (Table 2.3), and *S.* Typhimurium strain LT2 genomic DNA as a template. The PagN-R primer has an *Xba*I site incorporated into it, resulting in a unique *Xba*I at the 3′ end of the *pagN* ORF. The PCR product was digested with *Xba*I and *Bsa*BI. The *Bsa*BI site is at nucleotide position 75 of the *pagN* ORF, corresponding to amino acid residue number 26. Digesting the ORF at this site results in the corresponding truncated protein being cut just after the predicted signal sequence. The plasmid pMALc-2 was digested with *Eco*RI and the 5′ overhangs were blunted by digestion with Mung Bean Nuclease. The plasmid was digested with *Xba*I. The digested PCR product was cloned downstream, and in frame with

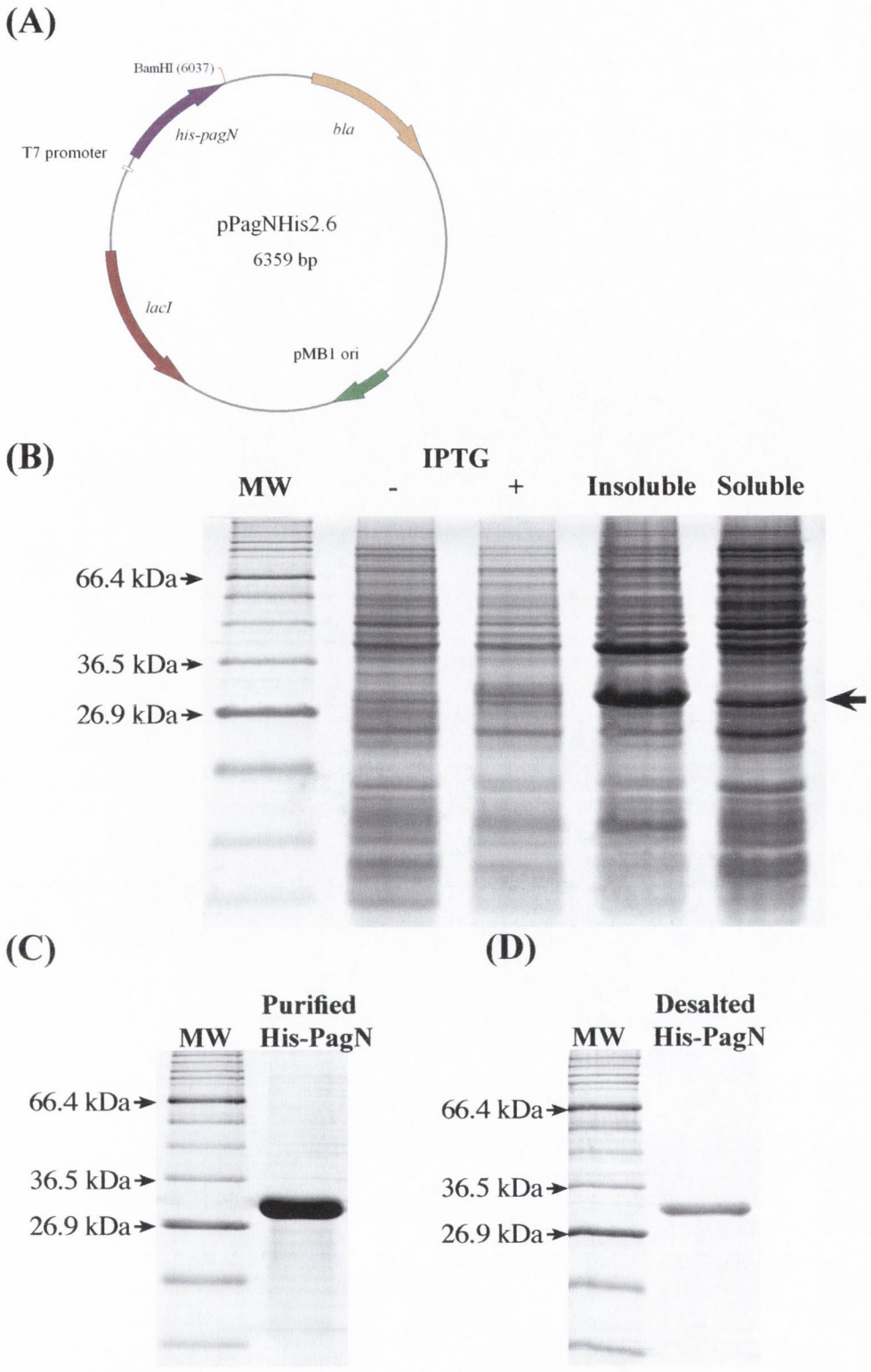

FIG. 3.5. Structure of pPagNHis2.6 and purification of a His-tagged PagN. (A) Map of the plasmid pPagNHis2.6. The position of the *his*$_{10}$*-pagN* gene fusion is noted along with important restriction endonuclease site. **(B)** SDS-PAGE analysis of induced and uninduced cultures as well as insoluble and soluble fractions of the induced culture. Induced protein is marked with ←. **(C)** SDS-PAGE analysis of PagN fusion protein purified under denaturing conditions as described in Section 2.3.2.1. **(D)** SDS-PAGE analysis of desalted purified PagN fusion protein.

(A)

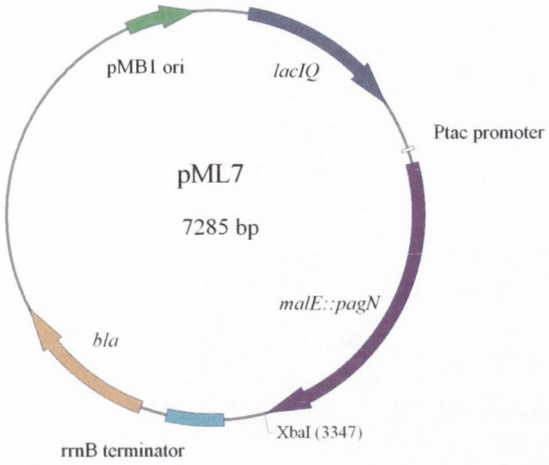

(B)

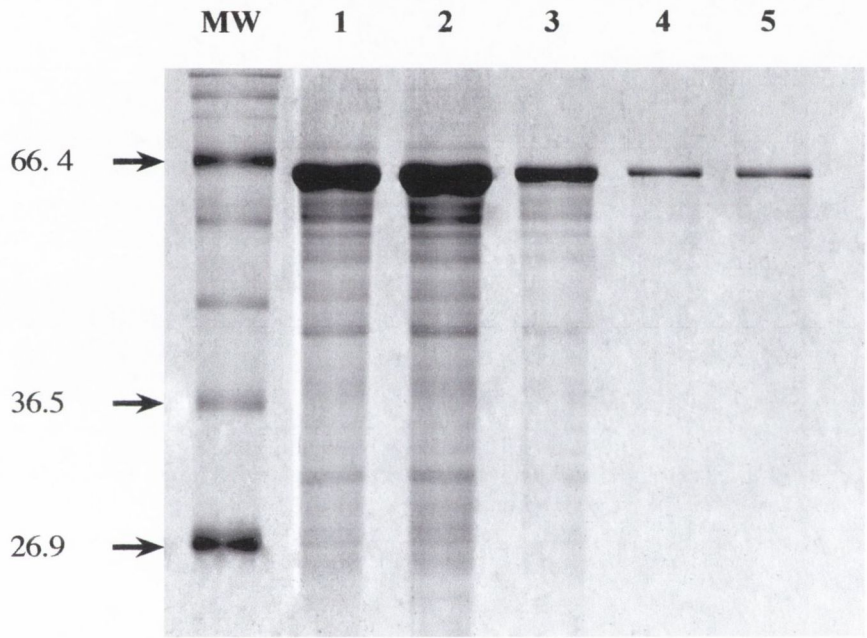

FIG. 3.6. (A) Map of the plasmid pML7. The position of the *malE-pagN* gene fusion is indicated. Restriction endonuclease sites used in the construction of the plasmid are marked. Other relevant features are indicated **(B) SDS-PAGE analysis of fractions eluted from an amylose resin column.** Fractions contain purified MBP-PagN eluted with maltose from a amylose resin column. Molecular mass standards (in kilo-daltons) are indicated on the left.

the *malE* gene of the cut pMALc-2 vector. The plasmid was sequenced to confirm the DNA sequence of the insert and named pML7 (Table 2.2 and Fig. 3.6 (A)). SDS-PAGE analysis of *E. coli* K-12 strain XL-1 containing the pML7 plasmid revealed one major inducible protein with an apparent molecular weight of ~65 kDa, corresponding to the predicted size of the MBP-PagN fusion protein. Smaller MBP-PagN truncates were also noted. These may be due to stalling of the DNA polymerase during translation of mRNA due to the formation of secondary structures such as stem loops (152). The MBP-PagN fusion protein was found to be largely soluble. The soluble fusion-protein was purified on an amylose resin column and analysed by SDS-PAGE (Fig. 3.6 (B)). An aliquot of soluble protein was mixed with Freund's complete adjuvant and used to immunise a rabbit to generate anti-PagN serum.

3.2.2 Transcriptional organization of *pagN*

3.2.2.1 Construction of plasmid pML9, a *pagN*-containing plasmid

The *pagN*-containing insert of pPagN2.3 is flanked by 500 bp of DNA either side of the *pagN* ORF. Upstream of the *pagN* ORF lies a putative promoter region and the gene of unknown function, *stm0307*. To investigate if *pagN* is expressed in a PhoP-dependent manner from its own putative promoter, and to avoid confusion between characteristics attributed to the presence of *pagN* and to *stm0307*, this gene was excised from the plasmid pPagN2.3. The pPagN2.3 insert is 1996 bp in length. Within this insert, the *stm0307* and *pagN* ORFs run from positions 58 to 473 and 803 to 1523 respectively. A unique *Psh*AI restriction site exists within the *stm0307* ORF at position 249 (Fig. 3.7 (B)). In order to excise *stm0307* but retain any putative promoter region that *pagN* may possess, the pPagN2.3 plasmid was digested with *PshA*I and *Xho*I which deleted the first 274 bp of the insert. The digested backbone was gel-purified and ligated to yield the plasmid pML9 (Table 2.2 and Fig. 3.7 (A)). Several diagnostic restriction digests were carried out comparing pML9 to pPagN2.3. The banding-pattern of the digested plasmids confirmed the absence of the *stm0307* ORF in the pML9 plasmid. This plasmid may be used to investigate whether *pagN* is part of a di-cistronic operon with *stm0307* or forms a single transcriptional unit.

3.2.2.2 The *pagN* gene has its own PhoP/Q-dependent promoter

To investigate if *pagN* is transcribed from a promoter directly upstream of the ORF expression of *pagN* from plasmid pPagN2.3 and pML9 was compared. Plasmids pPagN2.3 and pML9 were transformed into *S.* Typhimurium strain TA2362 *(a phoP null mutant,* Table 2.1*)* and strain TA2367 *(a phoPQ constitutively activated mutant,* Table 2.1*)*. Bacteria were grown in MM 5.8 and PagN expression was detected by Western immunoblotting (Fig 3.7 (C)). It was observed that the PagN protein was expressed in strains in which PhoQ was constitutively active. PagN was not detectable in *S.* Typhimurium strain TA2362, indicating that PagN expression is dependent on a functional PhoP/Q system. The presence of either multi-copy plasmid pML9 or pPagN2.3 increased PagN expression, indicating that a PhoP-activated promoter precedes the *pagN* ORF. Interestingly, the presence of the *stm0307* gene in pPagN2.3 promoted further, though marginal, PagN protein expression. Densitometric analysis of the expression of PagN revealed that the presence of the *pagN* gene on the plasmid pPagN2.3 resulted in a ~5.4-fold increase in PagN levels as compared to those detected from *S.* Typhimurium strain TA2367. The presence of *pagN* and *stm0307* on the plasmid pML9 caused a 7.7-fold increase in PagN protein expression. It is important to acknowledge that although it appears that a functional PhoP/Q system is required for the expression of PagN, the level of *pagN* transcription was not measured. It is feasible that due to the highly pleiotropic nature of *phoP* mutants, PagN protein stability may have been affected. Therefore, an alternative and equally valid interpretation of the protein expression data is that in the absence of a functional PhoP/Q system, the PagN protein is highly unstable and degrades. This alterative interpretation of the data was not investigated further.

3.2.2.3 PhoP binds directly to P_{pagN}, the putative *pagN* promoter

As discussed in Sections 1.5.1 and 3.1, the PhoP/Q two-component system controls the expression of many genes in response to levels of Mg^{2+} ions. The *pagN* gene is one such gene. In section 3.2.2.2 it was established that *pagN* expression is dependent upon a functionally active PhoP/Q system. However, it has never been established whether PhoP/Q influences *pagN* expression directly or as part of a cascade. To determine if *pagN* expression is controlled directly by the PhoPQ system, the putative *pagN* promoter region (P_{pagN}) was examined for the presence of PhoP and PmrA binding boxes. The PhoP protein recognises the direct hexanucleotide repeat (T/G)GTTTA, separated by 5 nucleotides while PmrA binds preferentially to the repeat (5'-CTTAAT-N_5-CTTAAT-3')

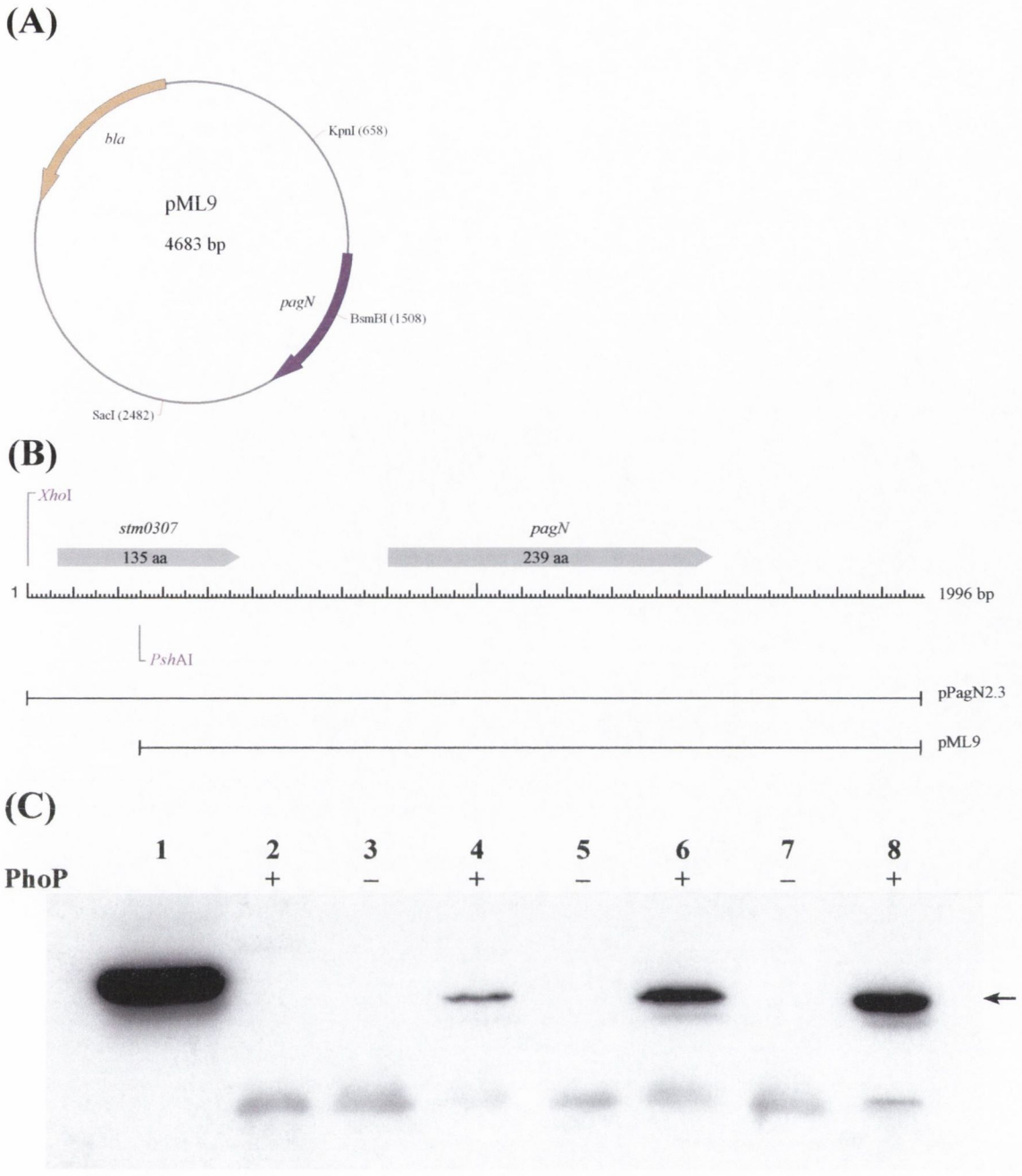

Lane 1: Purified His-PagN
Lane 2: pBSKII
Lane 3 & 4: pBSKII
Lane 5 & 6: pML9
Lane 7 & 8: pPagN2.3

S. Typhimurium strains:
Lane 2: MLT2
Lane 3, 5 & 7: TA2362
Lane 4, 6 & 8: TA2367

FIG. 3.7. (A) Map of the plasmid pML9. The positions of the *pagN* and *bla* genes are indicated. Important restriction endonuclease sites are marked. **(B) Graphical representation of the DNA inserts in the vectors pPagN2.3 and pML9.** Genes are represented by grey arrows, with transcriptional direction indicated. The insert present in each plasmid is represented by a thin black line. The *Psh*AI and *Xho*I sites are indicated. **(C) Western blot analysis of whole cell lysates from *S.* Typhimurium.** Samples were probed with polyclonal anti-PagN serum. The plasmid contained in each strain is indicated. PagN is indicated on the right.

ACCGACGTCA GTCAGATTTC TATGAAGGGA ATTAAAGACG GTGCGCTGAT
AGAGGTGATT AAATCCGGTA AATGGGATGA CGCCGCCGTA AAACAGCAGC
TTGCAGCCTT CAGTAACATA GAACAACAGG CTCGCTATTA TCGGGTTAAA
TATTATTTTG ATTTAAGCAA AGTCTTAACA CCAGAACAGC GTCAACAGGT
ACAACAAGAT CTCGCCCAGG CACTTGAGTA AATATTTTTG CCCGTTATTC
CGGGATAACG GGCTTTATCC AGGTCGGGTA CAAATTCATC TTCATCTTTT
TCTTACAGCA TCGCTCCATC TCACACTACC CGTTACATAA CGTAGAAGTG
AAACCGTACG TGGGGCAATT TGGCGAGGAG ATGGATTTCC ATACCGACGA
TTATCGTATT GTTATTTAAA ATCTTCATCT CATTTTTTAC CCGCTTACAG
AAAACCCAGC GTTACAATAG ACCGTTTTTT GGGCTTCGTT TATGTAATCG
TTATATCACA CCCTATACCG TGAAACTTGT CTTTTAGCCC AATATTAAGG
CAGGTTCTGA AATGAAAAAC TTTTTCGCAG TCTGCATCAT TCCCCTTGTG
GTAGCCTGGT CCGCTACTGC

FIG. 3.8. Putative *pagN* promoter region. The ATG translational start site is marked in bold type and underlined. Putative -10 and -35 boxes are underlined. A possible PmrA box is coloured red and a putative PhoP box is coloured green. The primers pagNpromo_F and pagNpromo_R, used to amplify the putative promoter region for use in mobility shift assays is italisised and coloured blue. The sequence of the primers PromoterF and PromoterR is identical to pagNpromo_F and pagNpromo_R respectively.

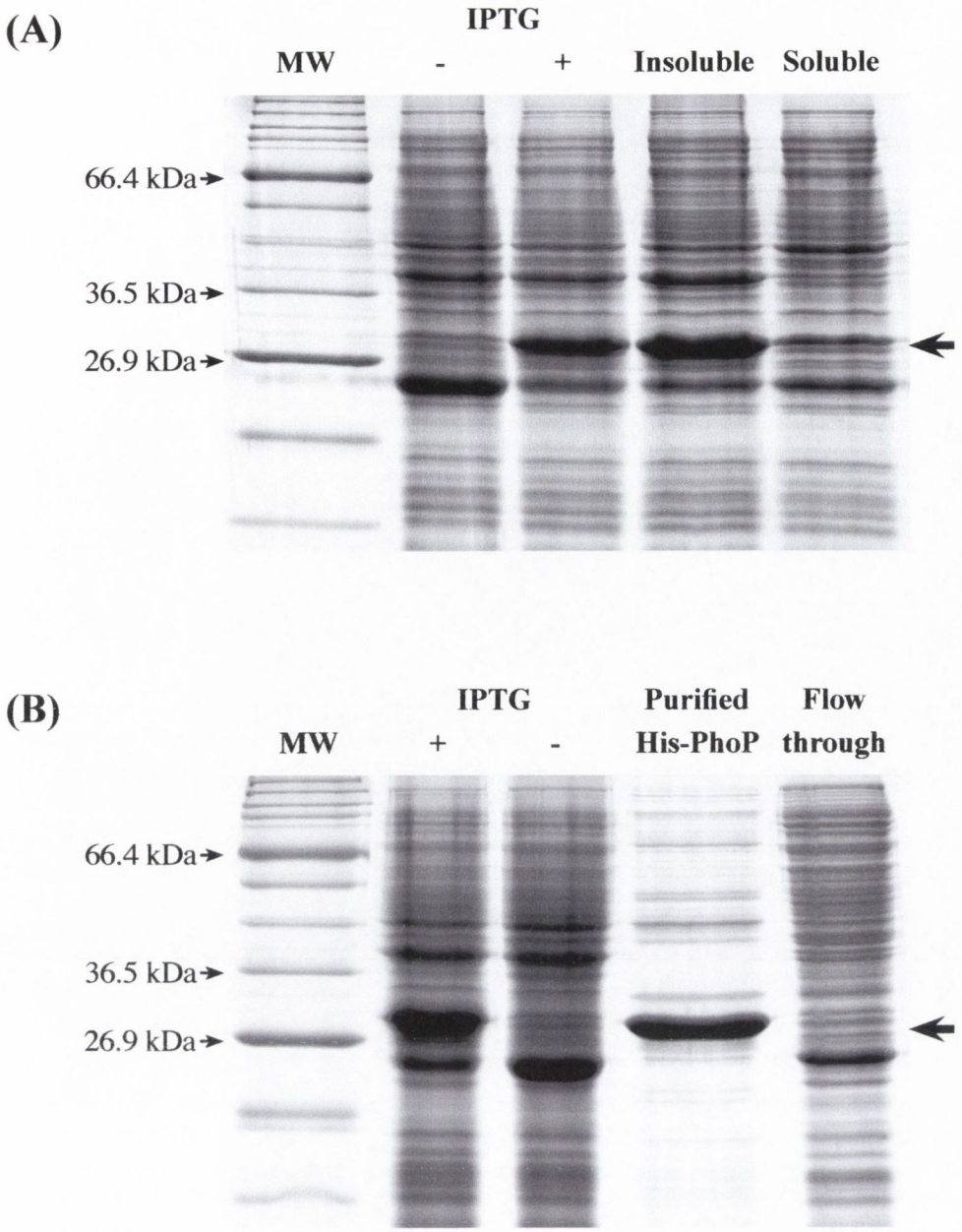

FIG. 3.9. Purification of recombinant His-tagged PhoP. (A) SDS-PAGE analysis of induced and uninduced cultures of *E. coli* BL21(DE3) containing pPB1020 and pDIA17 as well as insoluble and soluble fractions of the induced culture. The His-tagged PhoP protein is indicated on the right. **(B)** SDS-PAGE analysis of the His-tagged PhoP protein purified under non-denaturing conditions. His-tagged PhoP is indicated on the right side of each gel.

(3, 208). Examination of the putative P_{pagN} region identified a strong PmrA box and a more degenerate PhoP box indicating that PhoP may regulate *pagN* expression indirectly through the PmrAB two-component system (Fig 3.8).

To determine if PhoP interacts directly with the putative promoter region, a His-tagged PhoP protein was purified. The plasmid pPB1020 (Table 2.2) was transformed into the *E. coli* strain BL21(DE3) harbouring the plasmid pLysS. SDS-PAGE analysis of *E. coli* strain BL21(DE3) containing pLysS and pPB1020, induced with IPTG, revealed the induction of a protein with an apparent molecular weight of ~27 kDa, corresponding to PhoP (Fig. 3.9 (A)). However, most of this protein was located in the insoluble fraction. Although the majority of the protein was insoluble, the quantity of protein needed for a gel mobility assay is in the pico-molar level and therefore the protein in the soluble fraction was purified using a HIS-Select™ Spin column, as described by the manufacturers (Sigma-Aldridge). The protein concentration was determined by the Bradford assay (Section 2.3.1.6) and the protein profile of the purified His-PhoP protein was analyzed by SDS-PAGE (Fig 3.9 (B)). It was noted that there was a large number of contaminant protein species in the "pure" His-PhoP preparation.

A 565-bp DNA fragment that extends upstream from and including the transcriptional start site was amplified by PCR using the 5′-biotinylated primers pagNpromo_F and pagNpromo_R (Table 2.3 and Fig. 3.8) and *S.* Typhimurium strain LT2 genomic DNA as a template. The *mgtA* promoter region (P_{mgtA}) is known to bind PhoP (419) and was used as a positive control. The *mgtA* promoter was amplified using primers mgtAF and mgtAR (Table 2.3) and the same DNA template. Both the *pagN* and *mgtA* promoter regions were gel-purified twice to ensure purity. The gel mobility assays were performed as described in Section 2.3.3.3 by incubating 52- to 825 nM concentration of purified His-PhoP with 0.3pg of the 565-bp P_{pagN} fragment in 1X binding buffer in a 20-µl assay. An almost complete shift of the DNA fragment was detected when using a concentration of 206 nM of unphosphorylated His-PhoP (Fig. 3.10). Binding of P_{pagN} by His-PhoP was demonstrated by the detection of a shift in DNA at protein concentrations as low as 52 nM. His-PhoP bound to P_{pagN} with the same, or greater affinity as it does the P_{mgtA} promoter region. Of immediate importance is the fact that the His-PhoP preparation used in this band-shift assay contained several contaminant protein species. It may be suggested that the shift in mobility was due to binding of a contaminant to the putative *pagN* promoter and not specifically PhoP. To eliminate this possibility a negative control should be included. By incubating the His-PhoP sample with a DNA promoter fragment known not to interact with PhoP such a possibility would be ruled out.

Although it is not ruled out that PmrA may also bind P_{pagN} it is evident that PhoP is capable of binding directly to the putative *pagN* promoter region.

3.2.2.4 Transcription of *pagN* is affected by the intracellular environment

Previously, using β-galactosidase assays *pagN* has been show to be up regulated in cultured epithelial cells (173). However, these assays involved the lysis of the cells after 4 h and recovery of intracellular bacteria. This method gives only a snapshot of the gene expression profile.

In order to examine the activity of the *pagN* promoter under intra-cellular conditions a *pagN-gfp* transcriptional fusion plasmid was constructed. The putative *pagN* promoter region was amplified by PCR using the primer set PromoterF and PromoterR (Table 2.3 and Fig. 3.8) and *S.* Typhimurium strain LT2 genomic DNA as a template. The PromoterR primer has an *Xba*I recognition-site incorporated into it, resulting in an *Xba*I recognition-site being introduced immediately 3′ of the PCR product. The PCR product was sequenced to ensure faithful amplification of the putative promoter region. It was then digested with *Xba*I and ligated into the pZep08 vector digested with *Xba*I and *Sma*I. This placed the putative promoter region immediately upstream and in-frame of a promoterless *gfp* gene allowing effective reporting on the activity of P_{pagN}. The promoter-*gfp* fusion reporter plasmid was designated pPagN-GFP (Table 2.2). Using this plasmid, *pagN* gene expression can be monitored from an intracellular environment over a specified time period, giving a more informative description of the *pagN* gene expression profile.

The plasmid pPagN-GFP was transformed into wild-type *S.* Typhimurium strain LT2 and *S.* Typhimurium strain TA2362 (a *phoP* null mutant). Gentamicin protection assays were carried out (Section 2.3.4.1) using overnight MM5.8 cultures of these strains. The level of *pagN* transcription was measured by flow cytometry from the intracellular environment of human carcinoma Caco-2 cells. Expression of *pagN* within epithelial cells was found to be somewhat PhoP-independent, suggesting that gene expression in such environments is under the control of a different regulatory network. Maximal expression was observed in Caco-2 cells within the first hour post-invasion. Within 3 h post-invasion, promoter activity was greatly reduced (Fig. 3.11 (A)). These findings suggest that *pagN* expression is induced upon invasion of epithelial cells, and once inside, expression is down regulated. Expression studies with CHO-K1 cells under identical conditions displayed similar patterns to those found in Caco-2 cells (results not shown).

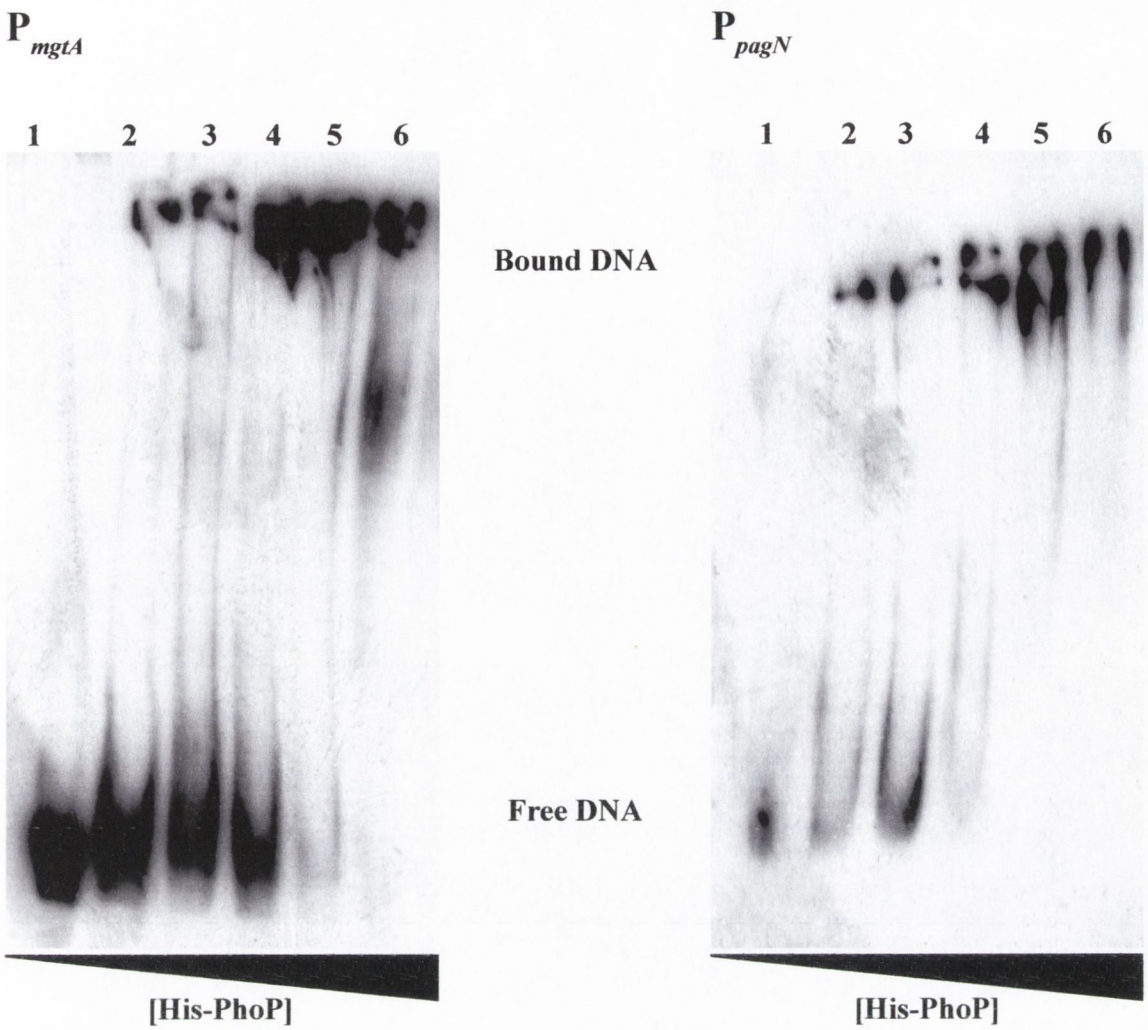

FIG. 3.10. His-PhoP binding to *mgtA* and *pagN* promoter regions. 0.3 pg of *mgtA* or *pagN* biotynylated promoter fragment was incubated without His_{10}-PhoP (lane 1) or with His_{10}-PhoP at a final concentration of 52 nM, 103 nM, 206 nM, 412 nM or 825 nM (lanes 2-6 respectively). Binding of PhoP to the promoter region is seen as a shift in the mobility of the DNA fragment.

3.2.2.5 Intra-macrophage expression of *pagN*

Wild-type *S.* Typhimurium strain LT2 and *S.* Typhimurium strain TA2362 (a *phoP* null mutant) were incubated with cultured J774A.1 murine macrophages in a 12-well culture plate. The co-culture was incubated for 1 h, washed and treated with gentamicin to kill extracellular bacteria. At time-points 1, 2, 4 and 6 hours post inoculation, 2 wells of co-culture were fixed with formalin. The level of *pagN* expression was detected from the intra-macrophage environment by flow cytometry. In agreement with previous findings with RAW 264.7 macrophages (173), the activity of the *pagN* promoter increased within J774A.1 macrophages. More importantly, the activity of the putative *pagN* promoter matched levels of *pagN* mRNA recovered from intra-macrophage *Salmonella* as determined by Eriksson *et al.* (106). Maximal expression of *pagN* was seen 6 hours post-internalisation. Transcription of *pagN* was not completely dependant upon a functional PhoPQ system with the *S.* Typhimurium strain TA2362 strain showing an initial decrease in expression after 2 h followed by an increase after 4 h (Fig. 3.11 (B)). The levels of transcription were overall greater within an intra-macrophage environment. Maximum levels of *pagN* transcription were almost 3-fold greater in macrophages than those observed within Caco-2 epithelial cells.

3.2.2.6 Expression of the PagN protein in *S.* Typhimurium strain SL1344

Using β-galactosidase assays on a *pagN-lacZ* gene fusion, expression of *pagN* has previously been shown to be highly up regulated in MOPS minimal medium with a Mg^{2+} concentration of 0.05 mM and pH of between 5.5 and 6.6 (173). To investigate if high levels of PagN protein expression correlated with the elevated levels of transcription, western immunoblot analysis was carried out on *S.* Typhmurium strains grown in MM 5.8 medium. The sarcosyl-insoluble (outer membrane) fraction of stationary phase *S.* Typhmurium cultures, were separated by SDS-PAGE. The proteins were transferred to a nitrocellulose membrane and probed with anti-PagN serum. Comparison of the fractions extracted from *S.* Typhmurium strain SL1344 and strain ML6 (Section 4.2.2.7) revealed a protein unique to strain SL1344 with an apparent molecular weight corresponding to PagN (Fig. 3.12). This protein was also present in the fraction extracted from *S.* Typhmurium ML6 harbouring pML10 (Table 2.2), a *pagN* containing plasmid.

3.2.3 Phenotypic analysis of the PagN protein

3.2.3.1 Construction of the IPTG-inducible pML1 expression vector

In order to examine the PagN protein independently of its native promoter and to express it in a range of surrogate host cells, namely *E. coli* strains DH5α, XL-1 and BL21(DE3), the *pagN* ORF was amplified by PCR using the primers ML2 and ML3 (Table 2.3). The reverse primer, ML2, has a *Bam*HI restriction endonuclease recognition site incorporated into it. The forward primer, ML3, introduces a base change immediately after the first codon of the *pagN* ORF. This produces an *Nco*I site at the 5′ end of *pagN* while introducing an K2E mutation in the protein sequence. The resultant PCR product was digested with *Bam*HI and cloned into the plasmid pBSKII digested with *Bam*HI and *Eco*RV. The resulting plasmid was sequenced to confirm the sequence of the insert and the plasmid was designated pML4. The *pagN* ORF was excised from pML4 by digestion with *Nco*I and *Bam*HI and cloned into the pTrc99a vector digested with *Nco*I and *Bam*HI producing the plasmid pML1 (Table 2.3 and Fig. 3.13 (A)). This construct places *pagN* expression under the control of the IPTG-inducible P_{trc} promoter. To confirm inducible expression of the PagN protein, *E. coli* K-12 strain XL-1 harboring the pML1 plasmid was grown to mid-logarithmic phase and induced with 1 mM IPTG for 3 h. Sarcosyl-extracted protein samples were analysed by SDS-PAGE (Fig. 3.13 (B)). A ~26-kDa protein corresponding to PagN was visible in pML1-containing samples. This protein band was absent in samples containing the vector control pTrc99a treated with IPTG in an identical fashion. PagN protein expression was not detectable in *E. coli* strains containing pML1, which were un-induced with IPTG (results not shown).

3.2.3.2 PagN binds to, and agglutinates human erythrocytes

The Hek protein from *E. coli* K1 strain RS218 is capable of agglutinating erythrocytes in a heat-resistant manner (108). A close homologue of Hek, the *E. coli* heat-resistant agglutinin, Hra1 also mediates this heat-resistant agglutination (253). As discussed in Section 3.2.1.1, at the protein level, PagN and Hek are 54% similar, indicating that PagN may also promote an erythrocyte agglutination activity. To test this hypothesis, a microtitre haemagglutination (HA) assay was performed as described in Material and Methods. *E. coli* K-12 strain XL-1 containing the *pagN* expression-vector pML1 or the empty vector control, pTrc99a, were incubated with human erythrocytes. The expression

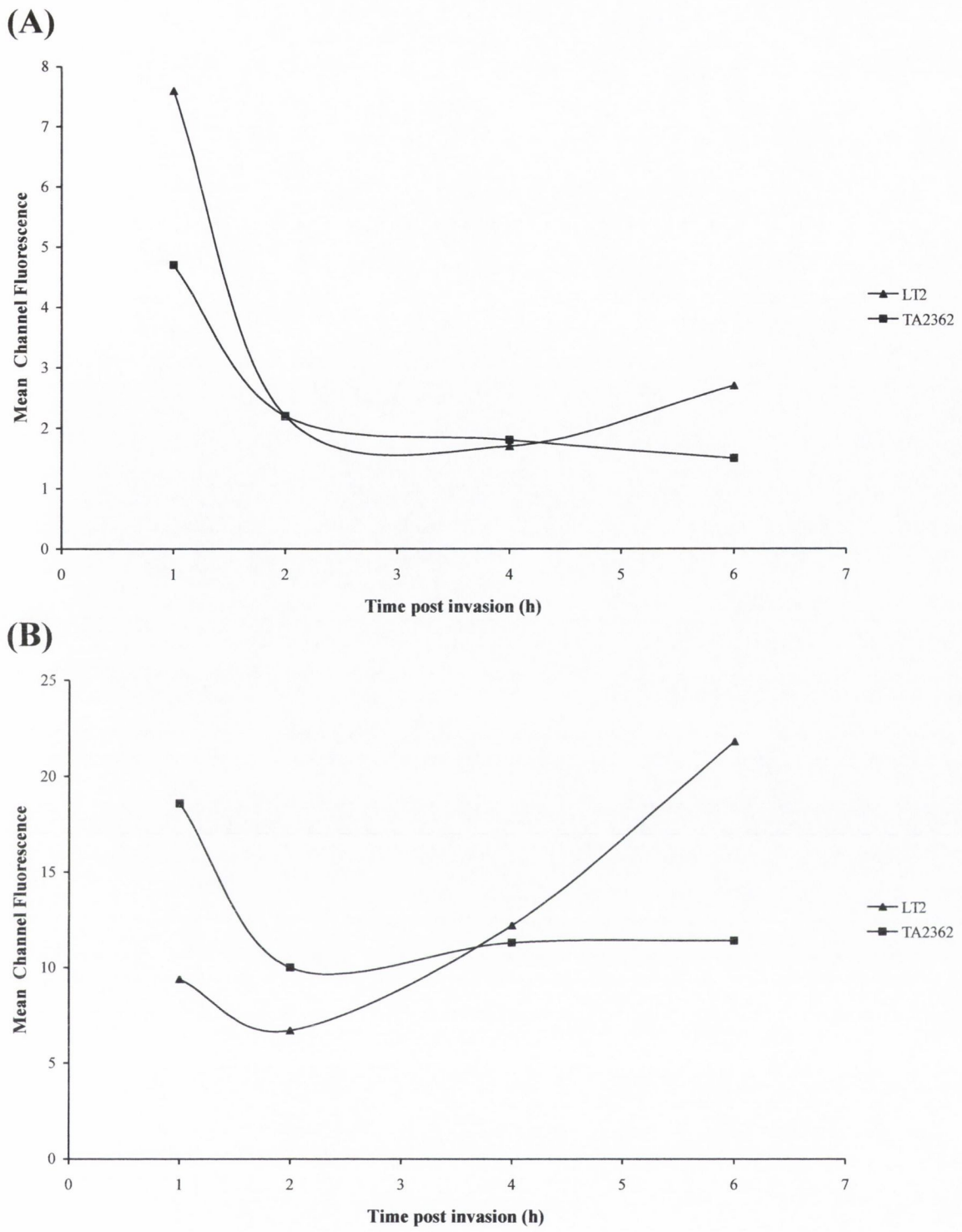

FIG. 3.11. Transcriptional activity of *pagN* as reported by a *gfp* reporter fusion. Gene expression detected in **(A)** Caco-2 human epithelial cells or **(B)** J774A.1 cultured murine macrophages. The level of bacterial fluorescence as measured by flow cytometry indicates the transcriptional activity of *pagN*. The pPagN-GFP reporter fusion is harboured by *S.* Typhimurium strain LT2 (triangles) and strain TA2362 (squares).

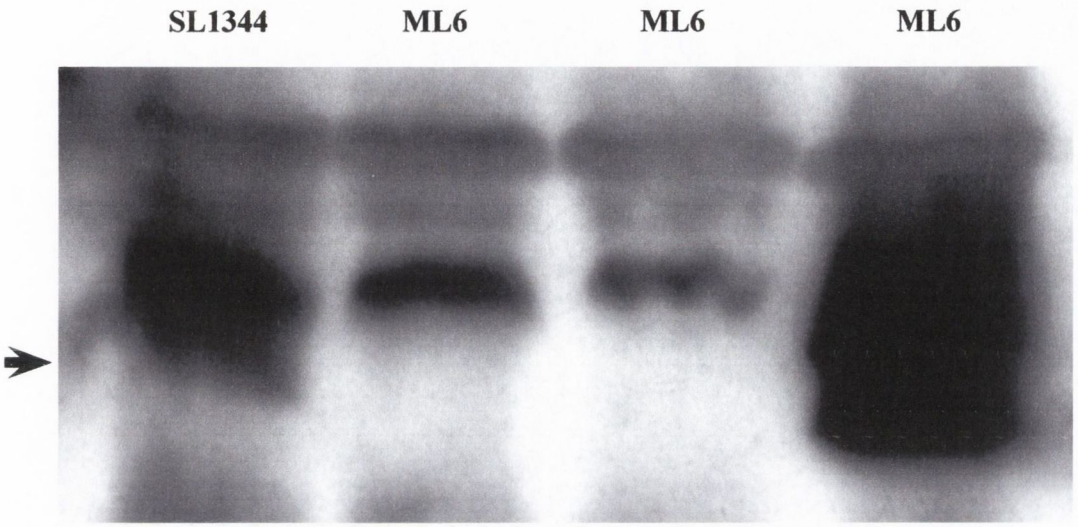

FIG. 3.12. Expression of PagN by *S.* Typhimurium grown in MM5.8 medium. Western immunoblot analysis of sarcosyl-extracted outer membrane fractions of *S.* Typhimurium strains. The fractions in lane 3 & 4 were harvested from *S.* Typhimurium strain ML6 harbouring the plasmids pBR322 (*pagN* –) and pML10 (*pagN* +) respectively. The strains under analysis are indicated above each well. PagN is indicated on the left.

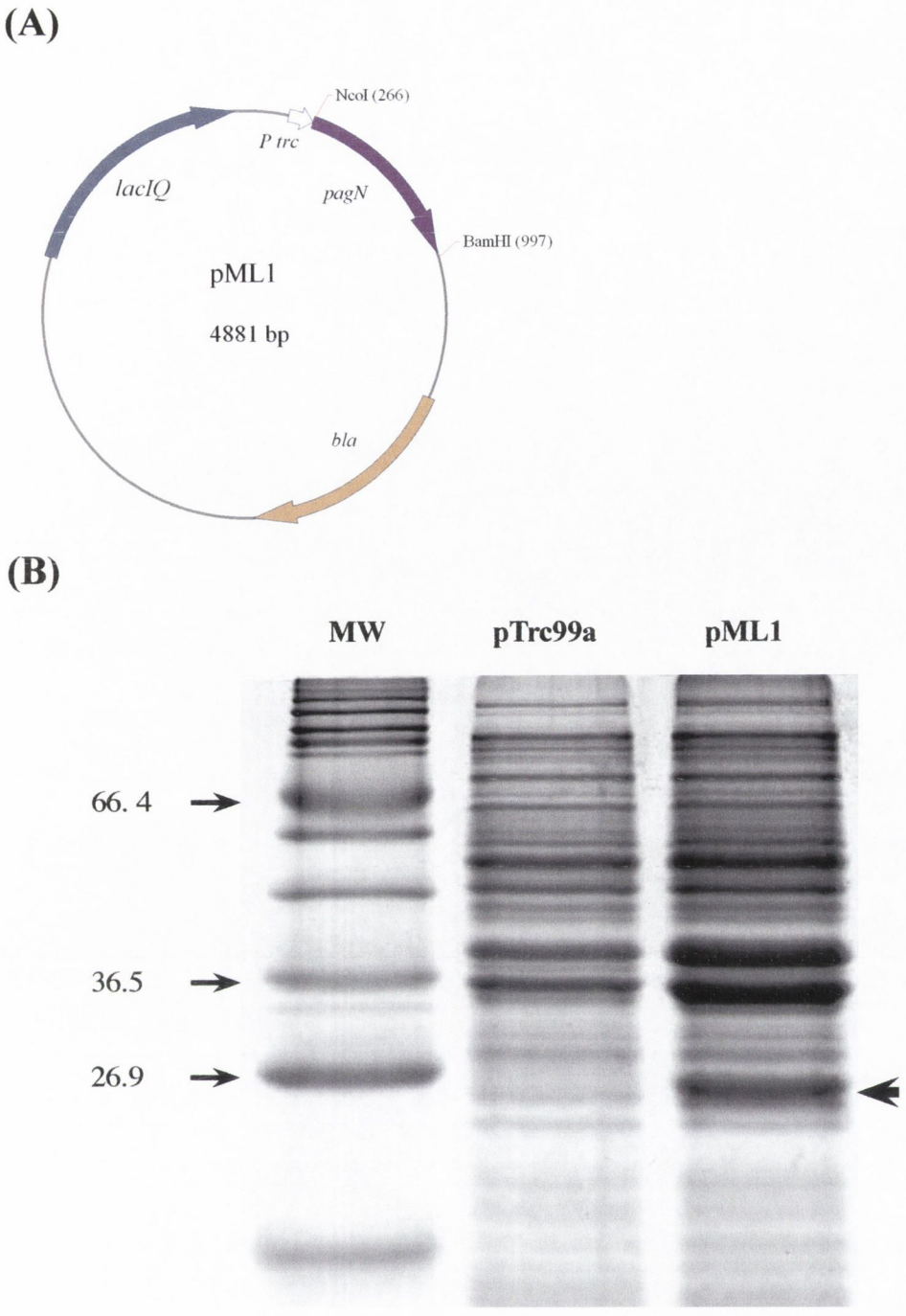

FIG. 3.13. (A) Map of the plasmid pML1. The position of the *pagN* ORF is indicated. Restriction endonuclease sites used in the construction of the plasmid are marked. **(B) SDS-PAGE analysis of *E. coli* K-12 strain XL-1 outer membrane fractions.** Fractions were prepared from *E. coli* strain XL-1 induced with IPTG. Membrane fraction samples from *E. coli* strain XL-1 carrying the indicated plasmid are loaded in each lane. PagN is indicated on the right. Molecular mass standards (in kilo-daltons) are indicated on the left.

of PagN conferred upon recombinant *E. coli* the ability to agglutinate erythrocytes. Using 3-% blood donated by a human female, a bacterial HA titre of 16 was displayed by PagN-expressing *E. coli*, which was higher than that promoted by E. *coli* expressing Hek (HA titre = 8) (Fig 3.14 (A)). Unlike Hek and Hra1, PagN displayed a decrease in HA titre after heating (Fig 3.14 ((B) i and ii)). Interestingly, after protein induction with IPTG, *E. coli* K-12 strain XL-1 lysed upon incubation at 70 °C. In order to avoid IPTG-induction, the assay was carried out using *E. coli* BL21(DE3) cells harbouring pML1 (or pTrc99a) grown overnight in OnEx™ protein induction medium. Following incubation at 70 °C for 30 min bacteria expressing the Hek protein were still capable of agglutinating human erythrocytes whereas *E. coli* strain BL21(DE3) expressing PagN were not (Fig 3.14 ((B) (ii)). Pre-heating caused the bacterial HA titre to be reduced from 8 to 2, which was the same HA titre as the negative control.

It was possible to inhibit PagN-mediated haemagglutination by pre-incubating erythrocytes with purified MBP-PagN (Fig 3.15 (A)). As little as 0.5 μg/well of MBP-PagN prevented PagN-promoted haemagglutination. The fusion protein MBP-LacZ also inhibited PagN-promoted haemagglutination (2.5 μg/well). LacZ would not be expected to inhibit PagN-promoted properties, as it a cytoplasmically located enzyme, so it may be possible that the MBP moiety of the fusion protein inhibited the PagN/erythrocyte interaction sterically. The purity of the MBP-fusion proteins must also be considered; there may be proteases and other unidentified factors co-purified with both fusion proteins. The presence of such contaminants may affect the erythrocytes, enhancing agglutination. PagN did not promote agglutination of horse or guinea pig erythrocytes (results not shown), suggesting that it may bind to an erythrocyte receptor specific to humans. Over-expression of PagN from pML1 in the *S.* Typhimurum strain LT2 failed to promote haemagglutination (results not shown).

3.2.3.3 The effect of lipopolysaccharide O antigen on PagN-mediated haemagglutination

As reported in Section 3.2.3.2, when over-expressed in *S.* Typhimurium strain LT2, PagN did not promote agglutination of human erythrocytes. Laboratory strains of *E. coli* such as K-12 or B completely lack the O antigen component of lipopolysaccharide (LPS) (295). It has been reported that porins in *E. coli* are partially obscured by the LPS core and completely blocked by O antigen sugars (252) and indeed in *S.* Typhimurium the O antigen prevents the outer membrane PgtE protease from interacting with its substrates (225). *S.*

Typhimurium has a large O antigen, which may serve to mask PagN thus limiting access to its receptor. To investigate this hypothesis, the plasmid pPagN2.3 was transformed into *S.* Typhimurium strain CH133, a *galE* mutant. The *galE* gene encodes the enzyme UDP-galactose 4-epimerase which is the first enzyme catalysing O antigen biosynthesis. Therefore *S.* Typhimurium strain CH133 lacks the O antigen component of LPS. Haemagglutination assays using this strain showed that PagN, when over-expressed in a rough strain, was capable of promoting agglutination (Fig. 3.15 (B)). These data suggest that LPS is capable of 'masking' PagN and preventing functional receptor binding.

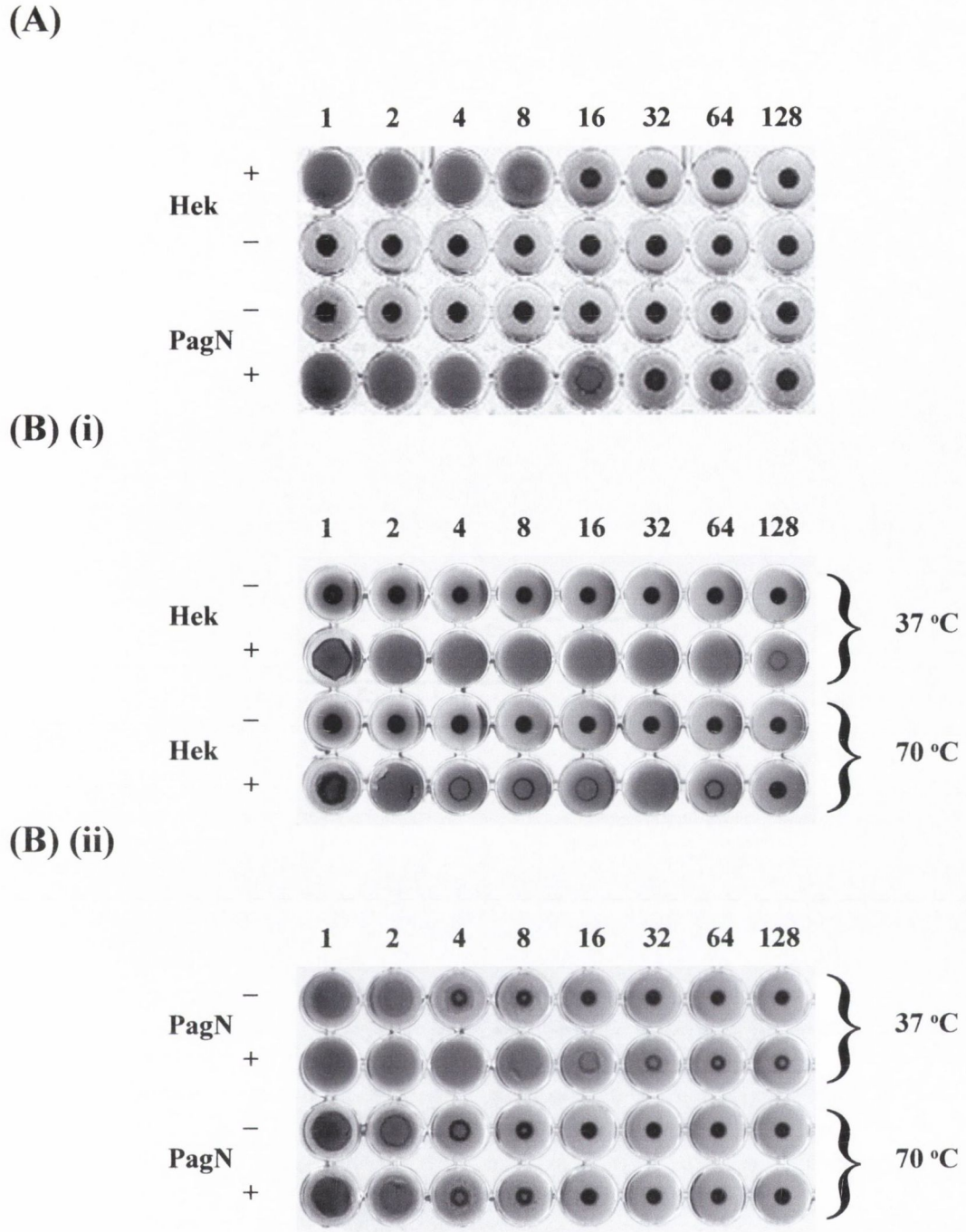

FIG. 3.14. Haemagglutination of *E. coli* K-12 expressing PagN. (A) Cultures of *E. coli* K-12 strain XL-1 harbouring plasmids pML1 (PagN +) or pTrc99a (PagN –) were induced with IPTG, normalised to an optical density of 1.0 at 600 nm (titre=1) and serially two-fold diluted. An equal volume of 1% human blood containing mannose (100 nM) was added to each well. After incubation at 4 °C overnight, agglutination is seen as a diffuse carpet of erythrocytes spread over the whole well surface. Non-agglutinated cells are seen as a tight button in the centre of the wells. Over night cultures of *E. coli* K-12 harbouring plasmids pHek6 (Hek +) and pBSKII (Hek –) were included as a positive control and vector control respectively. **(B) (i & ii)** Assays were carried out as described in (A) with cultures being incubated at 37 °C or 70 °C for 30 min prior to the assay.

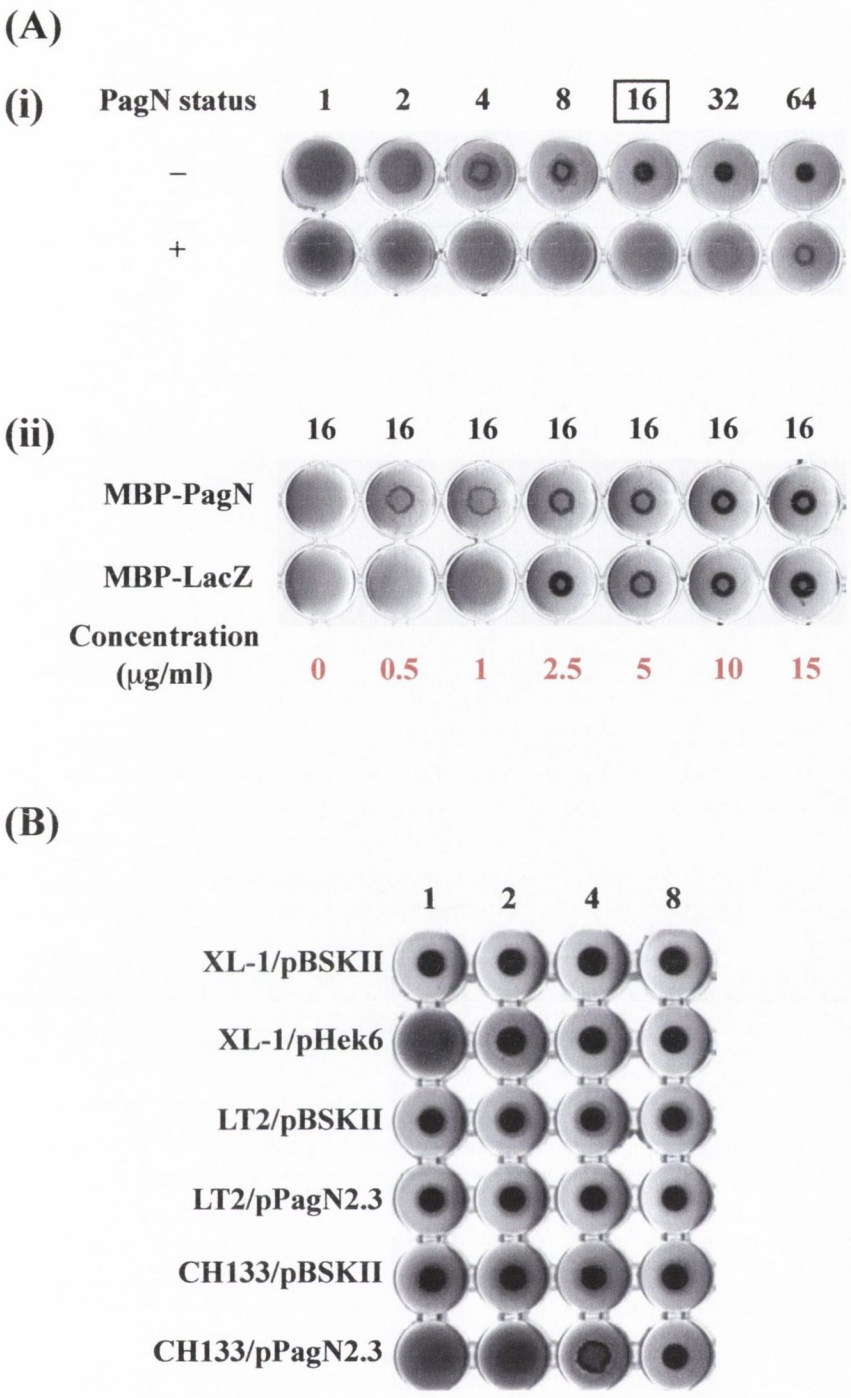

FIG. 3.15. (A) Protein inhibition of PagN-promoted haemagglutination. Protein inhibition was carried out using purified MBP-PagN or MBP-LacZ and titre 16 bacteria from panel (i). **(ii)** Blood (1%) was incubated with the indicated fusion-protein at a concentration of 1, 2, 5, 10, 20 or 30 μg/ml respectively at 4 °C for 1 h, then washed three times in PBS before the assay. 50 μl of pre-treated blood, was mixed with an equal volume of bacteria giving the indicated concentration of MBP-fusion protein per well. **(B) The effect of LPS on PagN-promoted haemagglutination.** Haemagglutination assays were carried out with the bacterial strains indicated on the left. *E. coli* strains were grown to stationary phase in L broth while all *S.* Typhimurium strains were grown to stationary phase in MM5.8 medium.

3.3 Discussion

As outlined in Section 3.1, much is known about the *pagN* gene at the DNA level. Its chromosomal location is well established (119, 120) and some of the conditions under which it is expressed have been elucidated (72, 172, 173). However, the PagN protein is largely uncharacterised. This study was conducted to further characterise PagN at both the genetic and protein level, and based on its homology with known adhesins, assess its possible role as a bacterial haemagglutinin.

At the DNA level *pagN* shows no similarity to other genes (119). However, the predicted mature PagN protein shows similarity over its entire length to both Tia and Hek, both of which promote invasion of and adhesion to cultured mammalian epithelial cells (108, 117). These adhesins are believed to form 8-stranded anti-parallel beta barrels in the outer membrane of *E. coli* (Chapter 6). Due to the modest degree of identity between PagN and these proteins, it is feasible that PagN may occupy a similar location and engage in a similar role. In order to characterise the *pagN* gene and corresponding protein, numerous *pagN* expression vectors were constructed. These vectors placed *pagN* transcription under the control of either its own putative promoter or a foreign, inducible one, P_{trc}. The pML7 and pPagNHis2.6 plasmids allowed for expression of *pagN* as a *malE-pagN* or a *his*$_{10}$*-pagN* gene fusion respectively. With these tools it was possible to express PagN in non-pathogenic laboratory strains of *E. coli* K-12 as well as raise polyclonal antibodies against the His$_{10}$-tagged and MBP-PagN fusion proteins. The reporter plasmid pPagN-GFP allowed for further transcriptional analysis of the *pagN* gene.

The *pagN* gene was shown to encode a 26-kDa outer membrane protein. Differential extraction of outer membrane proteins with sarcosyl has been carefully evaluated with use in enteric bacteria, and as such is the most widely used method (294). However, the procedure, although specific for outer membrane proteins, fails to remove some residual cytoplasmic membrane proteins (64). This fact although relevant, may be discounted, as PagN, when expressed from its own promoter or an inducible P_{trc} promoter was present in sarcosyl-extracted fractions with a comparable or greater intensity than established outer membrane proteins. Tia, Hek and a Tia homologue (referred to as Omp21) exhibit multiple species upon examination by SDS-PAGE, with some species migrating faster than others. It has been suggested that such a migration pattern may be a characteristic of this protein family (255). However, PagN differs in this regard migrating as a single protein moiety. It may be that Tia and its homologues are structurally more rigid and resistant to

denaturation by boiling in SDS, as is the case with the *E. coli* outer membrane protein OmpA (216) . PagN is denatured in the presence of SDS suggesting a less rigid structure.

Western immunoblot analysis of PagN revealed that the *pagN* gene is expressed from a PhoP-dependent promoter directly upstream of the ORF. PagN production is dependent upon a functional PhoP/Q two-component system. Although data presented does not rule out the possibility that *pagN* may be part of a larger operon, it does show that the gene is expressed from a promoter residing immediately upstream. Conner *et al.*, studying *S.* Typhimurium strain 14028s, reported on a PhoP-activated gene with homology to PfEMP-1 directly upstream of *pagN* (72) (Fig. 3.1). In the present study this gene was not identified, however an uncharacterised ORF termed *stm0307* exists immediately upstream of the *pagN* gene. The predicted gene product shows similarity to CpxP, a periplasmic adaptor protein that enhances the specificity of the DegP protease for mis-folded outer-membrane proteins (197). Expression of PagN was seen to be elevated when *stm0307* was present on the same multi-copy plasmid as the *pagN* gene. This may indicate several possibilities. The first is that *stm0307* and *pagN* form a di-cistronic operon. The *pagN* gene may be expressed from a promoter upstream of *stm0307* as well as its own. It is equally feasible that the *stm0307* gene product may regulate the expression of *pagN*. This is strengthened by reports of a PhoP-activated gene directly upstream of *pagN* which elicits polar effects on *pagN* gene expression (172). Thirdly, the CpxP-homologue may help target any incorrectly-folded PagN protein for degradation, thus increasing the relative proportion of correctly-folded PagN in the outer membrane. Indeed this has been shown to be the case for the PapE pilin subunit and the PapG adhesin of *E. coli* (90, 197). Therefore, when it itself is over-expressed PagN production is increased. In this particular study none of these avenues were explored, and these theories remain un-tested.

The PhoP/Q regulon is a complex network of genes and regulatory proteins. Within this network there are two-component systems positioned downstream of PhoPQ such as PmrA/B (Section 1.5.1). The promoter region of many PhoP-activated genes are not directly bound by the response regulator PhoP (424). Indeed, analysis of the putative promoter region of *pagN* showed the presence of a possible PmrA-binding box indicating that *pagN* may be controlled indirectly by PhoP. In this study, PmrA-binding was not investigated and therefore may not be ruled out. However, the putative promoter region of *pagN* showed a similar affinity for a His-tagged PhoP as the PhoP-regulated gene *mgtA*. These data indicate that *pagN* is indeed directly regulated by the PhoP response regulator, however as stated in Section 3.2.2.3, inclusion of a negative control would further strengthen this claim. At the protein level, signals typical to PhoP-activated genes induced

expression of PagN. When grown in MM5.8 medium the PagN protein was detected in the sarcosyl-extracted outer membrane fractions of *S.* Typhimurium. PagN expression could not be detected from strains grown in nutrient-rich laboratory L broth.

Transcriptional analysis of the *pagN* gene in intracellular environments expanded insights into its expression pattern and qualified previously published data (106, 173). Heithoff *et al.* reported that *pagN* is highly up-regulated within human epithelial cells 4 h post invasion. In agreement with this, it was observed that within Caco-2 cells, expression of *pagN* is switched on during the first 1.5 hours of invasion, suggesting a role for the protein in the invasion process. However, once internalised, transcription of the gene is reduced rapidly, indicating that PagN may be required only during the initial stages of bacterial internalisation. The control of *pagN* expression within the early stages of invasion is seen to be independent of PhoP/Q, suggesting that signals other than Mg^{2+} and Ca^{2+} concentration stimulate *pagN* gene expression. The *pagN* gene was shown not to be expressed in DMEM culture medium (data not shown) verifying that the gene was up-regulated upon initial contact and entry into epithelial cells. It is feasible that *pagN* expression may be induced in a contact-dependant manner, during initial adhesion to epithelial cells. Contact-dependent gene regulation is common in bacteria and has been established as one of the stimuli of the *E. coli* Cpx two-component system (312).

The observed expression of *pagN* within macrophages agreed with previous findings (106, 173), indicating that PagN has a role in the more progressive stages of pathogenesis. Eriksson *et al.* have established that for *S.* Typhimurium strain SL1344 *pagN* gene expression increases within cultured J774A.1 cells. Expression was shown to increase by 4.03-fold, 1.04-fold and 5.21-fold over a course of 4, 8 and 12 h respectively (106). The data presented here, although over a shorter time scale, agreed with Eriksson *et al.* Expression of *pagN* was seen to increase over the course of the experiment. Within macrophages, expression was seen to be dependent upon PhoP, indicating that it is induced in response to limiting Ca^{2+} and Mg^{2+} levels. Expression of *pagN* is more than doubled over the course of 6 h indicating a functional requirement within the SCV. It has been previously shown that *Salmonella* does not replicate in J744A.1 macrophages over a time course of 6 h (377), and indeed Eriksson *et al.* did not observe a statistically significant increase in *S.* Typhimurium numbers over the course of 4 h (106), therefore the increase in fluorescence detected by flow cytometry from intracellular bacteria can be considered a true increase in gene expression and not just in bacterial numbers due to replication.

When expressed in *E. coli* K-12 strain XL-1, PagN conferred the ability to agglutinate human erythrocytes. Unlike Hek, this phenotype was not resistant to heat-treatment.

Haemagglutination is not required for infection *per se*. However, it is a useful tool for the classification of putative novel adhesins indicating an ability to bind specifically to human cells. The specificity of the PagN/erythrocyte interaction was strengthened by the ability of exogenously added MBP-PagN to inhibit PagN-promoted haemagglutination. Interestingly *S.* Typhimurium strain LT2 over-expressing PagN from a native promoter or the PagN expression vector pML1 failed to agglutinate erythrocytes (results not shown). This inability to promote haemagglutination may be explained by examination of the LPS on *E. coli* laboratory strains and *S.* Typhimurium strain LT2. Laboratory strains of *E. coli* such as K-12 and B completely lack the O antigen component of LPS (295) whereas *S.* Typhimurium has a large O antigen containing OAc, Abe, Man, Gal, and Glc. When over-expressd in the rough *S.* Typhimurium strain CH1344, PagN promoted haemagglutination. With this in mind it is possible that PagN does not gain access to its cell-located receptor until initial binding has been established through some other means and the bacteria are close enough so that LPS masking is no longer a factor. Interestingly, several genes both directly (*pagP*) and indirectly *(pmrE, pmrC* and *cptA*) regulated by PhoP are involved in restructuring of LPS *in vivo* (269). This restructuring may result in a more exposed PagN protein facilitating easy receptor binding within the SCV of macrophages.

Chapter 4

Functional analysis of PagN

4.1 Introduction

Colonisation of the intestinal epithelial mucosa is a key virulence mechanism of many enteric bacteria such as *E. coli* and *Salmonella*. Initial long-range adherence of these pathogens to the intestinal epithelium is established by fimbrial adhesins such as the bundle-forming pili of enteropathogenic *E. coli* (370) and Type 1 fimbriae of *Salmonella* (98, 99). In addition to fimbriae, these bacteria are capable of producing non-capsular, afimbrial adhesins thought to mediate a more intimate association with the epithelium.

Non-capsular, afimbrial protein adhesins are located in the LPS-based outer membrane of gram-negative bacteria. They are typically composed of a number of anti-parallel β-sheets which associate to form a membrane-spanning barrel, giving rise to several hydrophilic, surface-exposed loops (See Chapter 6). Inter-species structural similarity between such proteins is often common, with proteins forming families with similar functions. However, many protein families consist of proteins that share structural and sequence identity but have very distinct functions. One such family of proteins is that containing Ail from *Y. enterocolitica* (276), Rck from *S.* Typhimurium (169), PagC from *S.* Typhimurium (274) and OmpX from *E. coli* (267). These proteins are all predicted to encode 8-stranded β-barrels giving rise to 4 surface-exposed loops. However, although Ail and Rck are considered adhesins (66, 275), PagC mediates macrophage survival (274) and OmpX promotes resistance to β-lactam antibiotics (267). These proteins often share similarity in regions encoding the membrane-buried β-strands of the barrel (217). The sequences of the surface-exposed loops can be very different among family members, and hence the function of the proteins may differ accordingly.

The Ail protein from *Y. enterocolitica* is distantly related to the Tia protein from enterotoxigenic *E. coli* (ETEC). Although Tia is not part of a family of proteins, it is classified as a member of the cluster of orthologous groups of proteins (COGs) 3637, all of which are predicted to form outer membrane β-barrels. The Tia homologues, the heat-resistant agglutinin 1 (Hra-1) from porcine ETEC (253), the opacity-associated (Opa) protein OpaA of *Neisseria* (34) and the Hek protein of neonatal meningitic *E. coli* (108), are also grouped in this COG 3637; although OpaA is also a member of the Opa COG. These proteins have all been shown to promote adhesion and invasion of human, epithelial cells.

As outlined in section 3.2.1.1, the PagN protein displays 54% sequence similarity to Tia and Hek, and thus can also be grouped in COG 3637. The areas of PagN showing most similarity to these proteins are predicted to be located in the β-sheets of the protein (Chapter 6). This is often common amongst β-barrel proteins as the membrane-spanning domains are composed of alternating hydrophobic and hydrophilic residues giving rise to an amphipathic barrel (217). The sequences of the predicted surface-exposed loop regions display considerably less similarity, indicating that PagN may not share the same adhesive and invasive properties as these similar proteins.

The purpose of this study was to determine if PagN is an adhesin and/or invasin and to assess its contribution during binding to and entry into epithelial cells by *Salmonella*. The questions deemed most relevant in this study were:

- Can PagN promote adhesion to and invasion of epithelial cells when expressed in avirulent laboratory strains of *E. coli*?
- Does PagN contribute to adhesion/invasion by *S.* Typhimurium?
- Is LPS involved in masking PagN thus affecting access to its receptor?
- Does PagN promote invasion independently of the SPI-1 TTSS?
- Is there a role for PagN in an intra-macrophage environment?

4.2 Results

4.2.1 Quantitative cell association and invasion assays on PagN-expressing bacteria

4.2.1.1 Interaction of PagN-expressing *E. coli* with human HT-29 cells

In common with Hek (108), PagN agglutinates erythrocytes when expressed in the surrogate host, *E. coli* K-12 strain XL-1 (Section 3.2.3.2). It has been established that both the Hek and Tia adhesins promote attachment of *E. coli* to human epithelial cells (108, 255). To investigate if PagN supports binding to other human cell-types, cell association and gentamicin protection (invasion) assays were performed with confluent monolayers of HT-29 cells as described in Materials and Methods. HT-29 cells, described previously (118), are human colonic cells with epithelial morphology originally isolated from a 44-year-old female, diagnosed with a colorectal adenocarcinoma. They have been used extensively in culture models of the human intestinal tract (176-178, 410) and represent a useful model for bacterial/colon interaction studies. *E. coli* K-12 strain DH5α containing the *pagN* expression plasmid pML1 or the vector control pTrc99a were incubated with confluent HT-29 monolayers. Approximately 1% of the bacteria expressing PagN bound to the eukaryotic cells. This was 6-fold greater than the negative control (Fig 4.1). Of the bound bacteria, ~2% had actually invaded the cell monolayer.

4.2.1.2 Interaction of PagN- or Tia-expressing *E. coli* with CHO-K1 epithelial cells

Chinese hamster ovary (CHO-K1) cells display typical epithelial cell morphology. However, as the CHO-K1 cell line is not of human origin, it is not a valid model for the study of the sequelae of human *Salmonella* infection. The CHO-K1 cell line is often used in adhesin/receptor studies as a number of mutant cell lines, lacking various cell-surface components, are available (335). These cells are easily cultured and are readily invaded by strains of pathogenic *S.* Typhimurium (91) and *E. coli* (116).

To investigate if PagN could promote adhesion to and invasion of CHO-K1 monlayers, cell association and invasion assays, similar to those described in Section 4.2.1.1, were performed. *E. coli* carrying the pTia5 plasmid (Table 2.2) was included as a positive

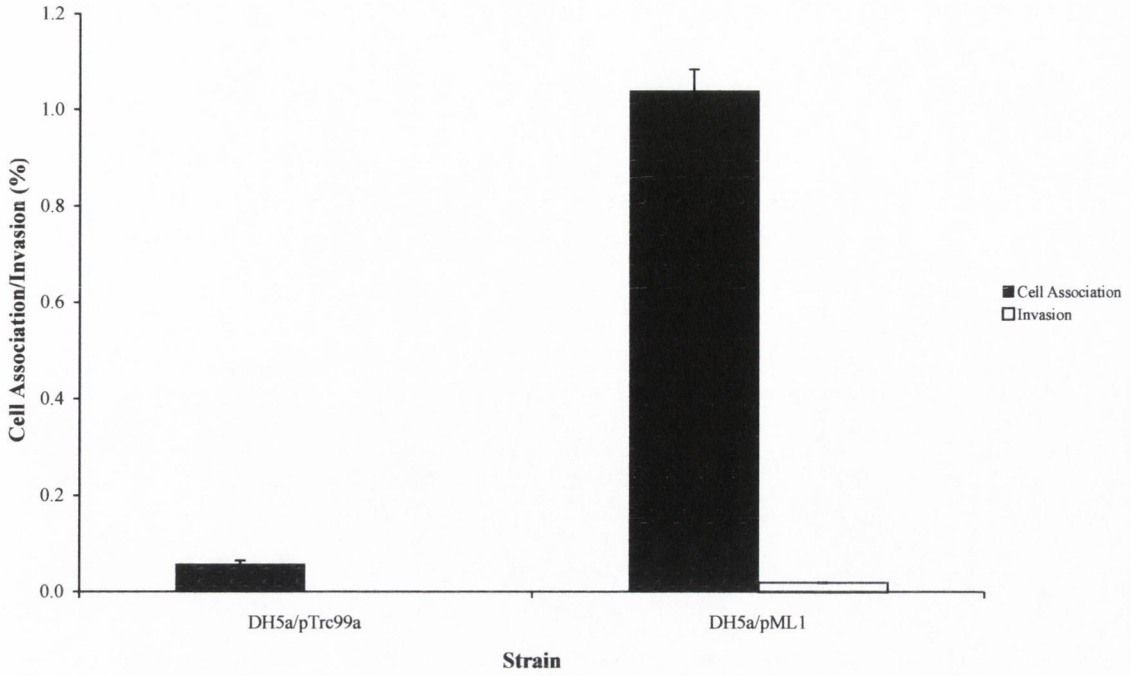

FIG. 4.1. Interaction of *E. coli* K-12 expressing PagN with HT-29 cells. Percentage cell association and invasion is calculated as the viable number of bacteria after the assay as compared to the initial innocula size. The strains tested are indicated. Data represents averages of triplicate wells, and standard error bars are shown. The value for invasion displayed by *E. coli* K-12 strain DH5α harbouring plasmid pTrc99a was 0.00 ± 0.00%.

control. This plasmid contains the *tia* gene thus allowing for the expression of *tia* from its native promoter. The Tia protein has been shown to promote strong adhesion and invasion of CHO-K1 cells (116).

TABLE 4.1. Interaction of *E. coli* K-12 expressing PagN or Tia with CHO-K1 cells

Adhesin Expressed	Cell Association	Invasion
None	1	1
PagN	25-fold	11-fold
Tia	9-fold	3-fold

Cell association and invasion levels for the negative control are adjusted to 1. The level of cell association and invasion promoted by the expression of the indicated protein is indicated as a fold-increase relative to the negative control.

When PagN was over expressed in *E. coli* K-12 strain DH5α more than 70% of the inoculum bound to CHO-K1 cells. The fold-increase in cell association promoted by PagN was significantly greater than that mediated by the positive control Tia (25-fold vs 9-fold, $P < 0.01$). Upon binding, large-scale uptake of bacteria into the non-phagocytic CHO-K1 monolayer took place. Almost 1/6 of the adherent PagN-expressing bacteria were internalised. However, although PagN mediated significantly greater cell invasion levels than Tia (11-fold vs 3-fold, $P < 0.01$), ~1/8 of the adherent Tia-expressing bacteria were internalised. These data indicate that PagN is a both an adhesin and invasin promoting the internalisation of *E. coli* by epithelial cells.

4.2.1.3 PagN-promoted invasion requires actin rearrangements in CHO-K1 cells

As discussed in Section 1.3.4, *Salmonella* induce a complex array of cytoplasmic and nuclear responses during invasion of host intestinal epithelial cells. The most dramatic of these effects is the initiation of host cytoskeletal rearrangements leading to membrane ruffling. To investigate whether PagN-mediated invasion of epithelial cells induces cytoplasmic rearrangements, invasion assays were performed with CHO-K1 cells, which had been pre-incubated with cytochalasin D. Cytoplasmic rearrangements involve the polymerization of actin filaments. Actin filaments have a fast and slow growing end; cytochalasins inhibit elongation at the fast growing end (141). Specifically, cytochalasin D affects the polymerisation of actin in two ways: it increases the initial rate but markedly

reduces the final extent of the Mg^{2+}-induced polymerisation process (141). To assess the role of actin filament polymerisation in PagN-mediated invasion, confluent CHO-K1 monolayers were pre-incubated with cytochalasin D (1 μg/ml) for 30 min at 37 °C before infection with bacteria. Cytochalasin D was present throughout the invasion assay.

TABLE. 4.2. PagN-promoted invasion of epithelial cells requires actin polymerisation

Adhesin Expressed	**Invasion (%) – cytochalasin D**	**Invasion (%) + cytochalasin D**
None	2.24 ± 0.17	0.00 ± 0.00
PagN	60.07 ± 3.08	2.28 ± 0.10

In the presence of the actin polymerisation inhibitor, invasion by *E. coli* expressing PagN was reduced by 30-fold. This dramatically reduced level was comparable to that of the negative vector control, *E. coli* containing pTrc99a. These data show that PagN promotes internalisation of *E. coli* into CHO-K1 epithelial cells by an actin polymerisation-dependent process.

4.2.2 The role of PagN in adhesion to and invasion of cultured epithelial cells *in vitro*

4.2.2.1 Construction of *S.* Typhimurium strain LT2 *pagN* mutant

To determine the contribution of PagN to cell association and invasion of epithelial cells by *S.* Typhimurium, an *S.* Typhimurium *pagN* mutant was constructed. The interrupted *pagN* gene was constructed on a plasmid and transferred to the chromosome of *S.* Typhimurium strain LT2 using the λ Red allele replacement system as described in Section 2.2.3. The plasmid pPagN2.3 was digested with *Bsm*BI and the resulting 5′ overhangs were filled in with Klenow (Fig. 4.2 (A) (i)). A 2.2-kb fragment containing a spectinomycin resistance (*spc*) cassette was excised from plasmid pHP45Ω (Table 2.2) by digesting with *Sma*I and *Pst*I (Fig. 4.2 (A) (i)). The resulting blunt-ended *spc* cassette was ligated into the Klenow-filled in pPagN2.3 plasmid, thus interrupting the *pagN* gene (Fig. 4.2 (A) (ii)). The structure of the resulting plasmid was confirmed by restriction endonuclease mapping and the plasmid was named pPagNKO (Table 2.2 and Fig. 4.2 (A)

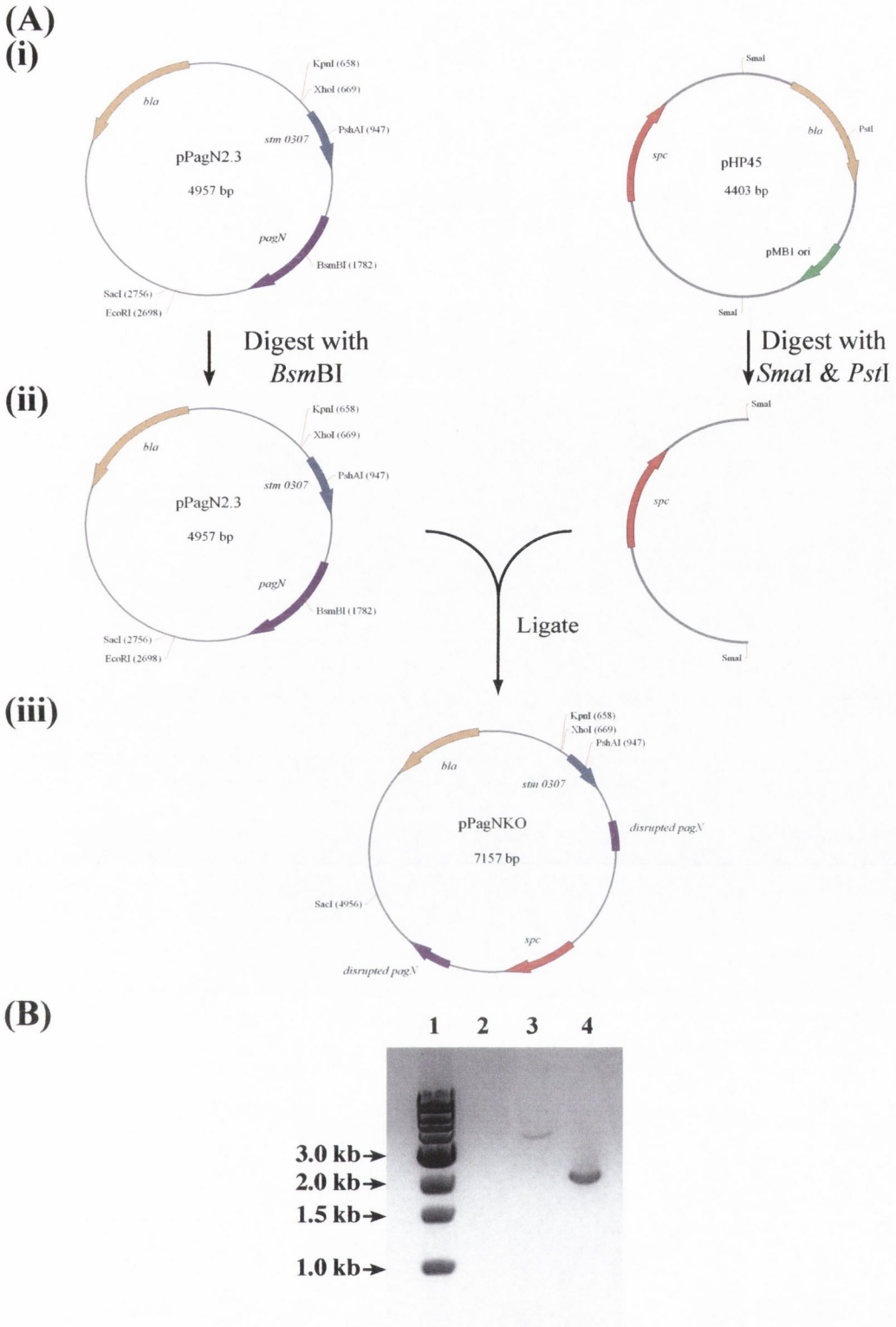

FIG. 4.2. (A) Schematic of the construction of the plasmid pPagNKO. (i) The plasmid pPagN2.3 was digested with *Bsm*BI. The plasmid pHP45Ω was digested with *Sma*I and *Pst*I. **(ii)** The blunt-ended *spc* cassette was ligated into the digested pPagN2.3 plasmid, interrupting the *pagN* gene. **(iii)** The structure of the resulting plasmid was confirmed by restriction endonuclease mapping and the plasmid was called pPagNKO. **(B) Confirmation of the chromosomal *pagN*::*spc* gene fusion of *S.* Typhimurium strain MLT2.** Boiled bacterial colonies from wild-type (Lane 4) or *pagN* mutant (Lane 3) strains of *S.* Typhimurium were used as a template for PCR amplification of the *pagN* gene. Lane 2 contains a no-DNA negative control. Primers PagNF and PagNR were used for PCR.

(iii)). The pPagNKO plasmid was digested with *Kpn*I and *Sac*I and used a template for PCR amplification of the interrupted *pagN* gene. Following amplification, the template was digested with *Dpn*I. *Dpn*I is specific for methylated DNA and therefore does not digest the un-methylated PCR product. The PCR product was then gel-purified and transformed into *S.* Typhimurium strain LT2 containing the pKOBEGA plasmid (Table 2.2). *S.* Typhimurium had elevated levels of the λ Red proteins due to the induction of these genes from pKOBEGA by the addition of L-arabinose, thus facilitating transfer of the interrupted gene to the bacterial chromosome. Putative mutants were confirmed by PCR (Fig 4.2 (B)). The newly generated *pagN* mutant was designated *S.* Typhimurium strain MLT-2 (Table 2.1).

4.2.2.2 Construction of a low copy-number *pagN*-containing plasmid

The plasmid pBSKII has a copy number of ~300 plasmids/cell resulting from a mutated *rop* gene which controls replication of ColE1 origins (420). To avoid dose-dependent effects from expressing the *pagN* gene from the multi-copy plasmid pPagN2.3 and hence to allow expression of PagN at levels close to those observed in *S.* Typhimurium, the *pagN*-containing insert from pPagN2.3 was transferred into a low-copy vector, pPD101 (Table 2.2). The plasmid pPD101 has a pSC101 *ori* which giving rise to a copy number of ~2-4 plasmids/cell. The 1996-bp *pagN*-containing insert was excised from pPagN2.3 by digestion with *Kpn*I and *Sac*I. This fragment was cloned into the multiple cloning site (MCS) of pPD101 which had been digested with *Kpn*I and *Sac*I. The resulting low copy-number plasmid was called pPagN1 (Table 2.2 and Fig. 4.3).

4.2.2.3 Invasion of CHO-K1 epithelial cells by an *S.* Typhimurium strain LT2 *pagN* mutant

The use of CHO-K1 cells to study epithelial cell invasion by *S.* Typhimurium is widespread and has been employed by several high-profile laboratories worldwide (91, 114, 189, 379, 420). The contribution of the PagN protein to the invasion of these cells by *S.* Typhimurium was tested. Invasion promoted by *S.* Typhimurium strain LT2 and its *pagN* mutant derivative, MLT2, was determined with non-polarised cells and a standard invasion assay. Relative to the initial inoculum, wild-type *S.* Typhimurium were recovered in significantly greater numbers than PagN-defective bacteria (Fig. 4.4). Bacterial invasion levels were found to be highly variable when comparing data sets from individual

experiments carried out on different days. However, the overall pattern displayed by strains was reproducible. Analysis of data from simultaneous experiments showed that the *pagN* mutant strain was less well able to invade CHO-K1 cells. Data from triplicate wells showed that wild-type levels were reduced from 22.16 ± 1.23% to 18.08 ± 0.36% for a *pagN* mutant ($P < 0.05$).

In order to confirm that the loss of a functional *pagN* gene was responsible for the reduction in invasion, it was important to complement the mutant MLT2 strain with a *pagN*-containing plasmid. To do this *S.* Typhimurium strain MLT2 was transformed with the low-copy number plasmid pPagN1. Invasion of CHO-K1 cells by the complemented strain was compared to that of strain MLT2 containing pPD101, the parental vector. The complementation with a functional *pagN* gene promoted a considerable increase in invasion as compared to either the empty vector control or indeed levels displayed by wild-type *S.* Typhimurium (29.01 ± 1.23% compared to 11.01 ± 1.34% and 22.16 ± 1.23% respectively). This pattern was reproduced in subsequent experiments. However, it was noted that on occasion the pPD101 vector appeared to increase the level of invasion displayed by *S.* Typhimurium strain MLT2.

4.2.3 Analysis of PagN in the mouse-virulent strain SL1344

4.2.3.1. Comparison of *S.* Typhimurium strain LT2 and strain SL1344

S. Typhimurium strains LT2 and SL1344 have been used in hundreds of publications studying diverse aspects of *Salmonella* biology. Over the course of these studies several independent groups have reported differences between these two strains at both the genetic level (411) and the phenotypic level (39, 232). Strain LT2 has been shown to be less virulent in a mouse model than its SL1344 counterpart with SL1344 displaying an LD_{50} of < 65 as compared to 3.6×10^4 for LT2. Strain LT2 has also been shown to be less invasive of intestinal 407 (Int-407) cells in *in vitro* gentamicin protection assays (411). However, these differences in virulence have been shown to be in both directions. Boddicker *et al.* demonstrated that strain LB5010, an LT2 derivative, displays a greater ability than strain SL1344 to adhere to HEp-2 cells *in vitro*. Incubation of strain LB5010 with HEp-2 cells resulted in extensive biofilm formation as compared to the limited ability to grow on these cells displayed by strain SL1344 (39). Indeed in my hands I have noted that *S.* Typhimurium strain LT2 displayed a slightly greater ability to invade CHO-K1 cells than

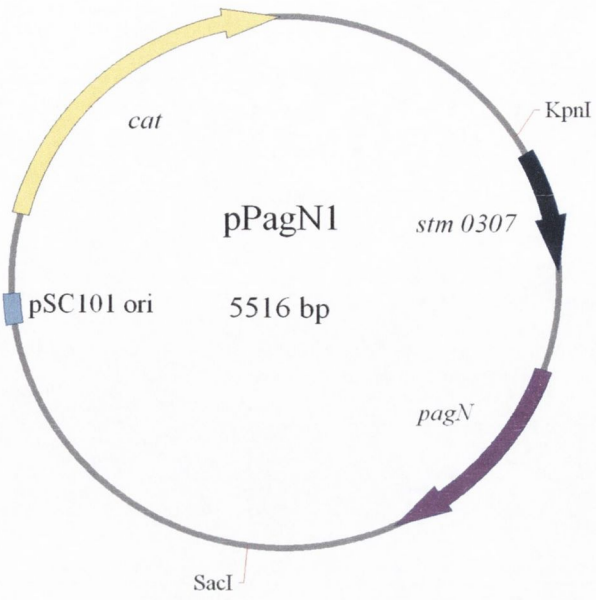

FIG. 4.3. Map of the plasmid pPagN1. The positions of the *pagN* gene, *stm0307* ORF and the *cat* gene are indicated. Restriction endonuclease sites used in the construction of the plasmid are marked. The pSC101 origin of replication is indicated which gives rise to a copy number of ~ 4-5 plasmids/cell.

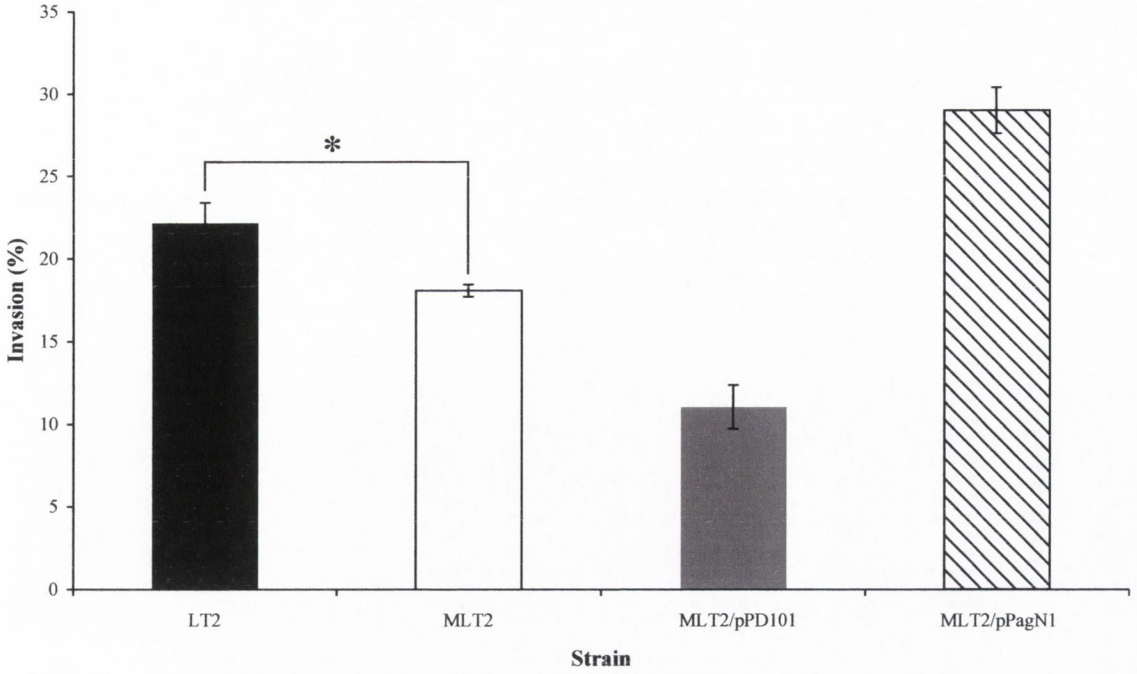

FIG. 4.4. Invasion of CHO-K1 cells by *S.* Typhimurium. *S.* Typhimurium strains and any plasmids they harbour are indicated on the horizontal axis. Data represents averages of triplicate wells, and standard error bars are shown. * indicates statistical significance, $P < 0.05$.

its more virulent relative *S.* Typhimurium strain SL1344. Strain LT2 promoted 20.31% invasion compared to 18.26% for strain SL1344. The occurrence of such differences therefore made it necessary to determine the contribution of PagN in strain SL1344 to the invasion of epithelial cells.

4.2.3.2 Construction of *S.* Typhimurium strain SL1344 *pagN* mutant

An *S.* Typhimurium strain SL1344 *pagN* mutant was constructed in an identical manner to strain MLT2. Putative mutants were confirmed by PCR (Fig 4.5). The newly generated *pagN* mutant was designated *S.* Typhimurium strain ML6 (Table 2.1). The mutant strain produced no detectable PagN protein when analysed by western immunoblotting (Fig. 3.12).

4.2.3.3 Construction of pML10, a *pagN*-containing plasmid

As reported in Section 4.2.2.3, while performing invasion assays with *S.* Typhimurium LT2-derived strains, inconsistencies between pPagN1-complemented strains and the pPD101 vector control were noted. To avoid such errors during analysis of *S.* Typhimurium strain SL1344 and *S.* Typhimurium strain ML6, a further *pagN*-containing vector was constructed. The *pagN*-containing insert (exluding *stm0307*) was excised from pPagN2.3 and cloned into the MCS of the established and well-published *bla*-containing cloning vector pBR322. The pBR322 plasmid has a ColE1 *ori* which gives rise to ~25 plasmids/cell. Although this is not as low as the pPD101-derived plasmids, it is sufficiently low to avoid major dose-dependent effects that may have been introduced by pBSKII-derived plasmids. The plasmid pPagN2.3 was digested with *Eco*RI and *Psh*AI. This gives rise to two DNA fragments of 3202 bp and 1755 bp respectively. The smaller *pagN*-containing DNA fragment was ligated into the pBR322 vector which had been digested with *Eco*RI and *Eco*RV (Fig. 4.6). Putative clones were screened by digesting isolated plasmids with *Bam*HI and *Pst*I. Plasmids with the correctly sized insert were subjected to a series of diagnostic digests. The restriction digest pattern of successful clones were compared to that of pBR322 when digested with *Hind*III, *Dra*I and the double digest *Aat*II and *Psh*AI. These digests confirmed that the *pagN*-containing DNA fragment had been cloned successfully into pBR322. The resultant plasmid was named pML10 (Table 2.2).

4.2.3.4 Invasion of CHO-K1 epithelial cells by an *S.* Typhimurium strain SL1344 *pagN* mutant

The contribution of PagN to the invasion of CHO-K1 cells by *S.* Typhimurium strain SL1344 was determined. Invasion promoted by *S.* Typhimurium strain SL1344 and its *pagN* mutant derivative, ML6, were tested with non-polarised cells and a standard invasion assay. These data established that wild type *S.* Typhimurium strain SL1344 was internalised in significantly greater numbers than the *pagN* mutant strain ML6 (Fig. 4.7). Data from triplicate wells revealed that wild-type levels were reduced from 18.26 ± 2.35% to 9.99 ± 1.37% for a *pagN* mutant ($P < 0.05$). The PagN-defective bacteria displayed a ~2-fold reduction in CHO-K1 cell invasion as compared to the wild-type parent. Interestingly, the invasion defects due to a non-functional *pagN* gene were more marked in SL1344-derived bacteria than LT2-derived bacteria (2-fold as compared to 1.2), indicating that the PagN protein may have a larger role to play in SL1344 and its derivative strains.

As with *S.* Typhimurium strain LT2, the loss of a functional *pagN* gene was shown to be responsible for the reduction in CHO-K1 invasion by complementing the mutant ML6 strain with a *pagN*-containing plasmid. To do this PagN-defective bacteria were transformed with the plasmid pML10. As seen in Fig. 4.7. the invasion defect of the *pagN* mutant could be partially restored by complementation with a functional *pagN* gene.

4.2.3.5 Adhesion to human HT-29 cells by a *S.* Typhimurium strain SL1344 *pagN* mutant

Adhesion to the human colonic HT-29 cell line by *S.* Typhimurium strain SL1344 and adhesion-defects due to the absence of the PagN protein in strain ML6 were investigated. Standard cell association assays were performed comparing levels of cell association displayed by wild type and PagN-defective *S.* Typhimurium.

TABLE 4.3. Contribution of PagN to the adhesion of *Salmonella* to HT-29 cells

***S.* Typhimurium strain**	**Cell association (%)**
SL1344	0.98 ± 0.09
ML6	0.48 ± 0.01 **
ML6/pBR322	0.72 ± 0.06
ML6/pML10	10.95 ± 1.69

Cell association levels were calculated for wild-type *S.* Typhimurium strain SL1344 and the *pagN* mutant, strain ML6. Levels were also calculated for the *pagN* mutant harbouring the plasmid

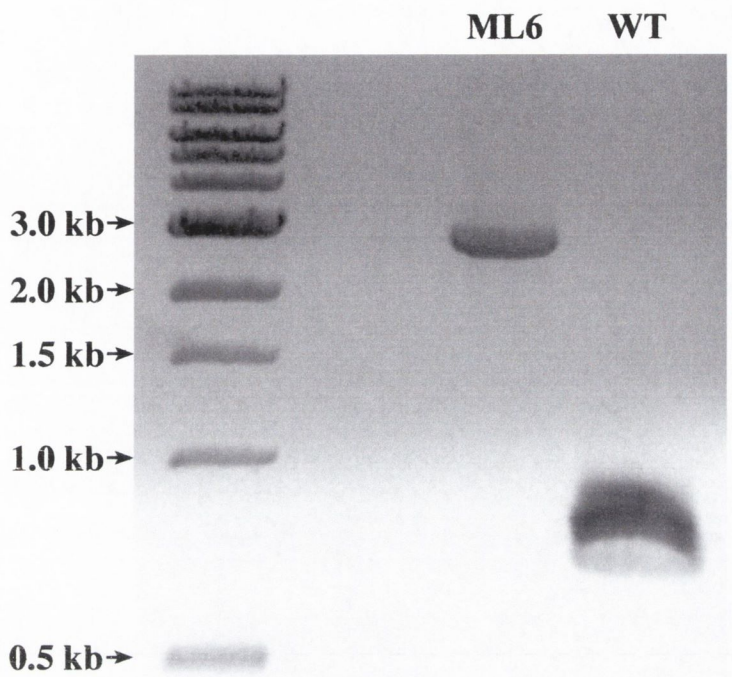

FIG. 4.5. Confirmation of the chromosomal *pagN*::*spc* gene fusion of *S.* Typhimurium strain ML6. Boiled bacterial colonies from wild-type (WT) or *pagN* mutant (ML6) strains of *S.* Typhimurium were used as a template for PCR amplification of the *pagN* gene. Lane 2 contains a no-DNA negative control. DNA fragment length is indicated on the left.

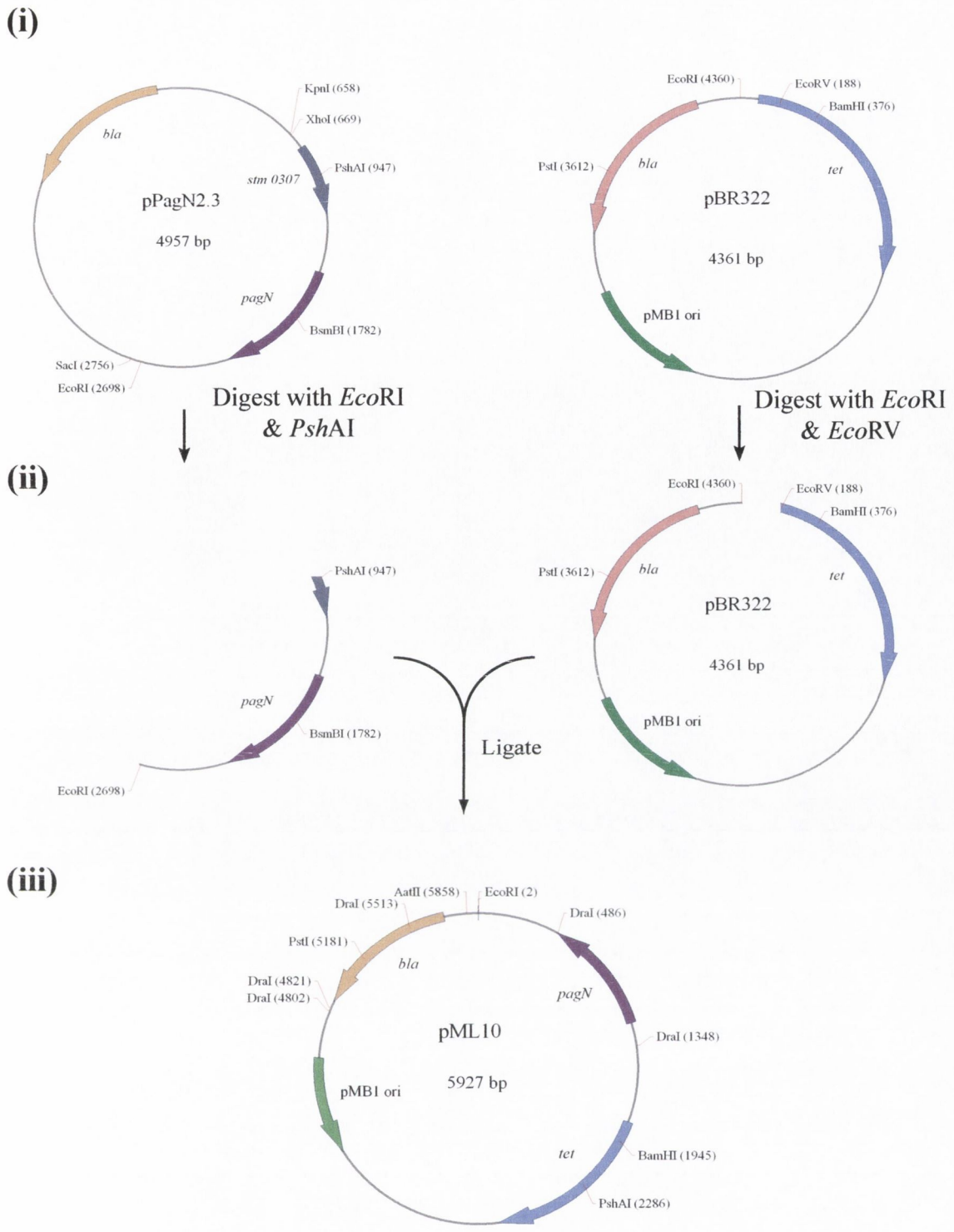

FIG. 4.6. Schematic of the construction of the plasmid pML10. (i) The plasmid pPagN2.3 was digested with *Eco*RI and *Psh*AI. The pBR322 vector was digested with *Eco*RI and *Eco*RV **(ii)** The 1755-bp *pagN*-containing DNA fragment from pPagN2.3 was ligated into the digested pBR322 plasmid giving rise to **(iii)** plasmid pML10. The positions of the *pagN* and the *bla* genes are indicated. The ColE1(pMB1) origin of replication is indicated; this gives rise to a copy number of ~ 25 plasmids/cell. Restriction endonuclease sites used in the construction of the plasmid, and those used for diagnostic digests are marked.

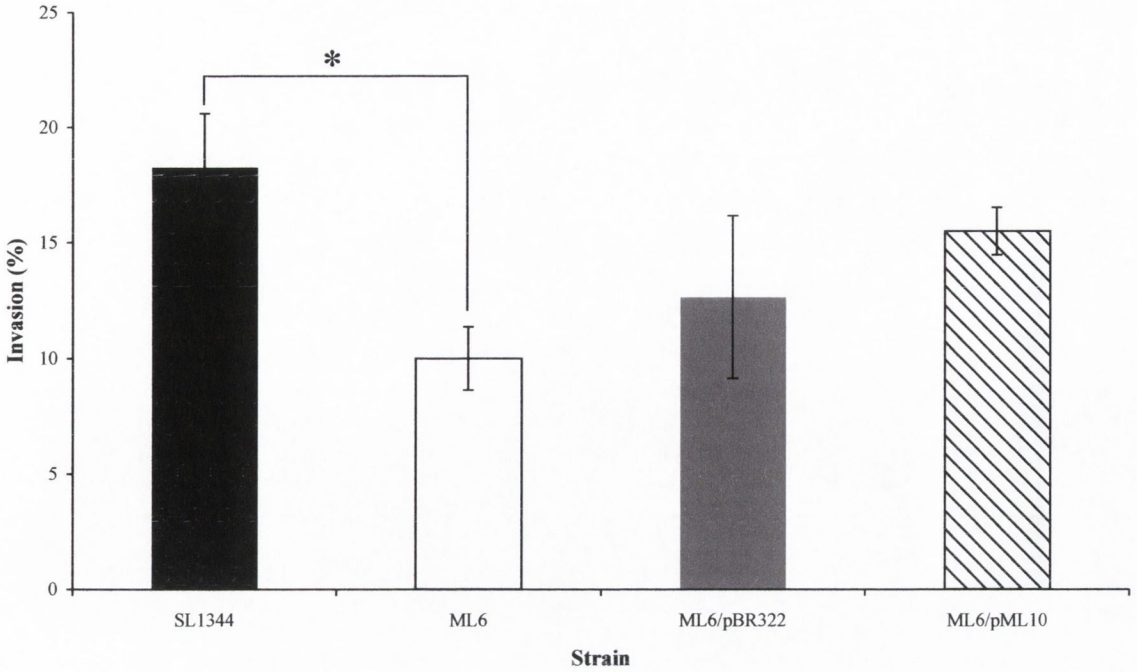

FIG. 4.7. Invasion of CHO-K1 cells by *S.* Typhimurium strain SL1344 and a *pagN* mutant. Invasion levels are calculated for wild-type *S.* Typhimurium strain SL1344 and the *pagN* mutant derivative, strain ML6. Levels are also calcultaed for the mutant ML6 strain harbouring the plasmid pML10 (PagN +) or the vector control pBR322. Data represents averages of triplicate wells, and standard error bars are shown. * indicates statistical significance, $P < 0.05$.

pML10 (PagN$^+$) or the vector control pBR322. Data represents averages of triplicate wells. ** indicates statistical significance, $P < 0.01$.

Wild-type bacteria were recovered in higher numbers compared to PagN-defective bacteria (0.98 ± 0.093% as compared to 0.48 ± 0.01%). Complementation of the *pagN* mutation with the *pagN*-containing plasmid pML10 increased cell association to 10-fold greater than that exhibited by wild-type *S.* Typhimurium.

4.2.3.6 Invasion of human HT-29 cells by an *S.* Typhimurium strain SL1344 *pagN* mutant

To determine if the PagN protein contributes to the invasion of the HT-29 cell line by *S.* Typhimurium strain SL1344, wild-type and *pagN* mutant bacteria were compared in gentamicin protection assays. As with the cell association assays described in Section 4.2.3.4, the overall level of invasion of HT-29 cells displayed by *S.* Typhimurium strain SL1344 was very low. Internalisation of wild-type bacteria was as low as ~0.1%. However, relative to these bacteria, PagN-defective bacteria displayed an ~80-% reduction in internalisation (Fig. 4.8). These data suggest that PagN may contribute largely to *Salmonella* invasion of HT-29 cells. The invasion defect of the *pagN* mutant bacteria was completely restored by complementation with pML10.

4.2.3.7 Qualitative adhesion assays on *S.* Typhimurium strain SL1344 and a *pagN* mutant using human HT-29 colonic epithelial cells

Quantitative cell association and invasion assays outlined in previous sections revealed that PagN has a role in adhesion to and invasion of epithelial cells. Data indicates that a *pagN* defective strain of *S.* Typhimurium adheres to and subsequently invades epithelial cells less well than its wild-type parent. In order to discern any adhesive defects of *S.* Typhimurium due to the loss of *pagN*, adhesion assays with wild-type and PagN-defective bacteria were performed. *S.* Typhimurium strains SL1344 and ML6, were both transformed with the plasmid pOS32 (Table 2.2). The plasmid pOS32 contains the *gfp*mut3b gene under transcriptional control of the *E. coli rrnB*-P1 promoter. As such, the *gfp*mut3b gene is constitutively expressed allowing for labeling of bacteria (360). Bacteria containing the pOS32 plasmid appear fluorescent green when viewed through a fluorescent microscope.

Human HT-29 cells were grown at 37 °C in 5% CO_2 on plastic chamber-slides and incubated with *S.* Typhimurium strains SL1344 (wt) or ML6 (*pagN*⁻), both harbouring the plasmid pOS32. Non-adherent bacteria were removed and the infected monolayers were fixed in methanol. Adherence bacteria were visualised by fluorescence light microscopy. When HT-29 cells were incubated with wild-type *S.* Typhimurium strain SL1344, large, highly fluorescent microcolonies were observed distributed evenly across the monolayer surface. In some areas cells appeared to be completely covered with fluorescent bacteria. In contrast, *S.* Typhimurium strain ML6 displayed a more diffuse pattern. The microcolonies were less intensely fluorescent and appeared smaller in size. Although mutant microcolonies were also evenly distributed across the monolayer surface, they occurred less frequently. These data suggest that the loss of PagN causes *S.* Typhimurium strain SL1344 to form smaller microcolonies, containing less bacteria, distributed with a lower frequency across the target cell surface area (Fig 4.9).

4.2.4 The LPS O antigen masks the PagN protein

4.2.4.1 Construction of an *S.* Typhimurium strain CH133 *pagN* mutant

HA assays demonstrated that the LPS O antigen masks PagN preventing it from reaching its target receptor (Section 3.2.3.3). To determine the effect of LPS O antigen on PagN during invasion of CHO-K1 cells, an *S.* Typhimurium strain CH133 *pagN* mutant was constructed. This mutant was made in an identical manner to *S.* Typhimurium strains MLT2 and ML6. Putative mutants were confirmed by PCR (Fig. 4.10) and the *pagN* mutant was designated *S.* Typhimurium strain ML133 (Table 2.1). Unsurprisingly, in invasion assays, the level of invasion displayed by this rough *S.* Typhimurium was less than that observed for smooth *S.* Typhimurium (7.40 ± 1.27% compared to 22.16 ± 1.23%). As LPS is a known virulence factor, the loss of the O antigen component was expected to correlate with a loss of invasivity. Indeed smooth strains have been shown to have a superior ability to bind and colonise HeLa cells *in vitro* (284) or murine epithelial cells *in vivo* (240). Invasion assays performed with strains CH133 and ML133 established that a reduction in invasion due to the loss of *pagN* was more pronounced in rough *S.* Typhimurium strains than the smooth parental LT2 strains. These data suggest that PagN may have more access to its receptor in rough bacteria and therefore may contribute more

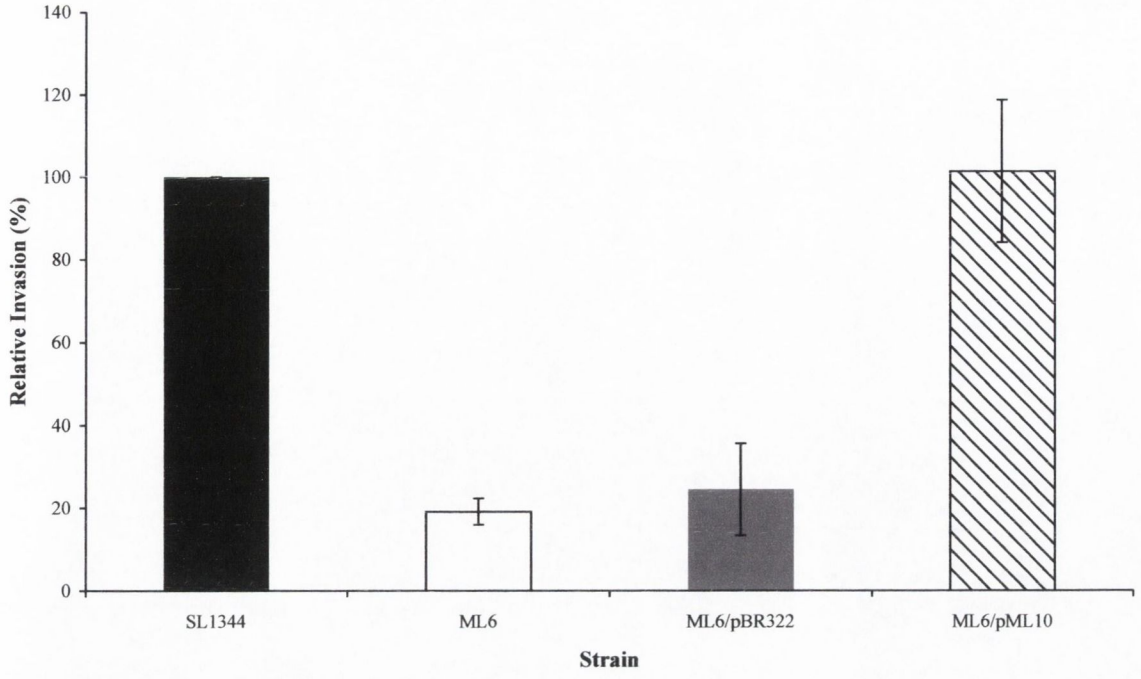

FIG. 4.8. Invasion of human HT-29 cells by *S.* Typhimurium strain SL1344 and a *pagN* mutant. Invasion levels are calculated for wild-type *S.* Typhimurium strain SL1344 and a *pagN* mutant derivative, strain ML6. Levels are also calculated for the mutant ML6 strain harbouring the plasmid pML10 (PagN +) or the vector control pBR322. Data represents averages of triplicate wells, and standard error bars are shown. The invasion efficiencies were expressed as a percentage of the wild-type.

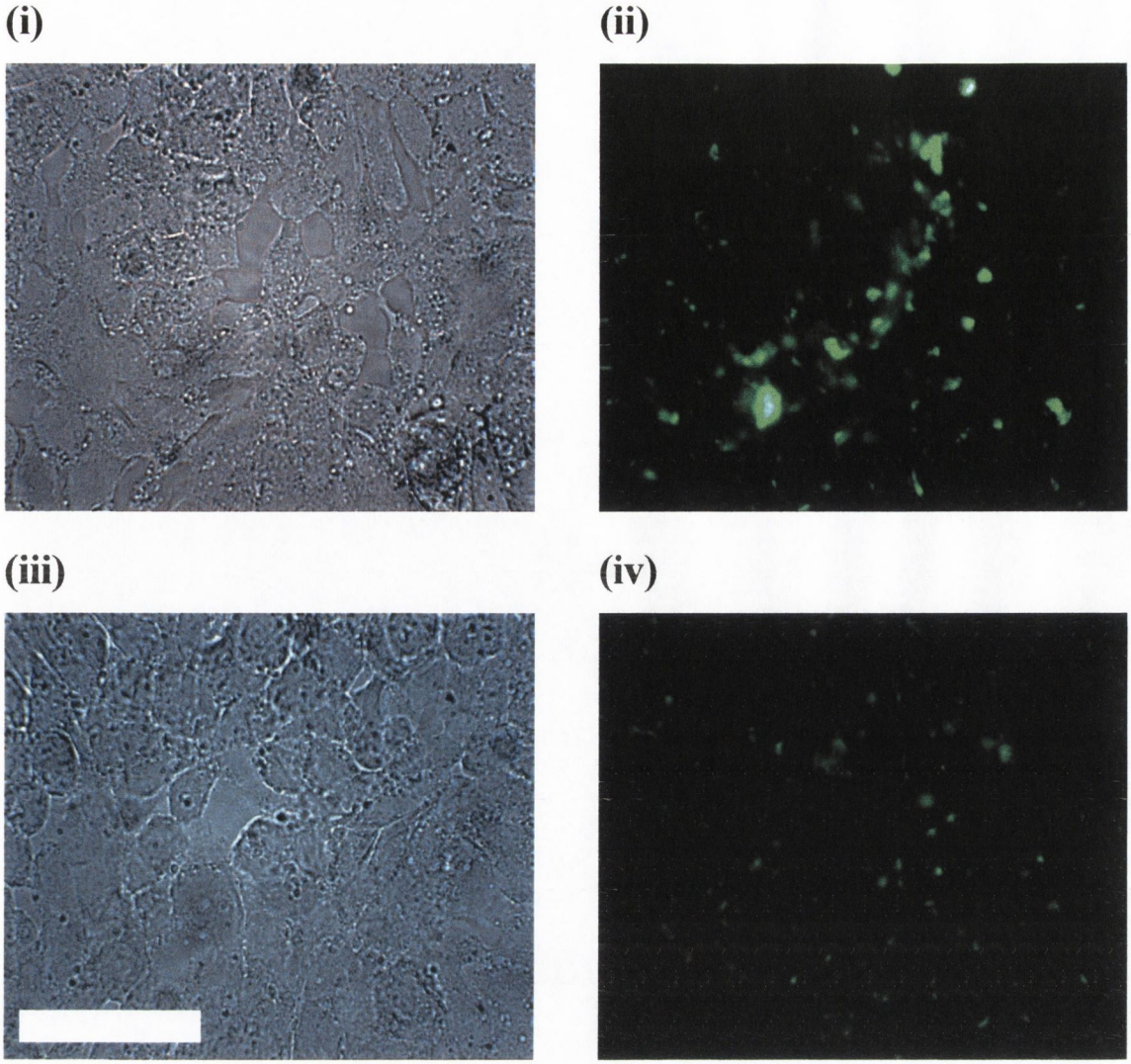

FIG. 4.9. Adherence of *S.* Typhimurium to HT-29 cells *in vitro*. The adherence of the parental wild-type *S.* Typhimurium strain SL1344 harbouring plasmid pOS32 can be seen in panel (ii). The adherence pattern of the *pagN* mutant, ML6, harbouring pOS32 is shown in panel (iv). The un-stained confluent HT-29 monolayers that the bacteria are binding to are seen in panels (i) and (iii) respectively. Scale bar in panel (iii) represents 5 mm.

to the invasion process. The invasion defect due to the *pagN* mutation was completely restored by complementation with the plasmid pPagN2.3.

4.2.4.2 Construction of an *S.* Typhimurium strain SL1344 *galE* mutant

To investigate if the LPS O antigen of *S.* Typhimurium strain SL1344 has the ability to mask PagN during invasion of CHO-K1 epithelial cells, a *galE* mutant was constructed. The interrupted *galE* gene was constructed on a plasmid and transferred to the chromosome of *S.* Typhimurium strain SL1344 using the λ Red allele replacement system. The *galE* ORF of *S.* Typhimurium strain SL1344 including ~50 bp of upstream and 250 bp of downstream DNA was amplified by PCR using the primers galEF and galER. The 1496-bp PCR product was cloned into the pBSKII plasmid digested with *Eco*RV creating the plasmid pGalE (Table2.2 and Fig. 4.11 (i)). A large section of the *galE*-containing insert of pGalE was removed by digestion of the plasmid with *Psh*AI. A 1.4 kb fragment containing a kanamycin resistance (*kan*) cassette was excised from plasmid pKRP11 (Table 2.2) by digestion with *Sma*I. The resulting blunt-ended *kan* cassette was ligated into the digested pGalE plasmid, thus interrupting the *galE* gene (Fig. 4.11 (ii)). The structure of the resulting plasmid was confirmed by restriction endonuclease mapping and the plasmid was designated pGalEKO (Table 2.2 and Fig 4.11 (iii)). The pGalEKO plasmid was digested with *Kpn*I and *Sac*I and used as a template for PCR amplification of the interrupted *galE* gene. Following amplification, the template was digested with *Dpn*I and then gel-purified. Approximately 4-5 μg of DNA was transformed into electrocompetent, *S.* Typhimurium strain SL1344 containing the pKOBEGA plasmid (Table 2.2). Putative mutants proved impossible to confirm by PCR. PCR amplification of putative mutants resulted in a smaller rather than larger product as compared to the wild-type *galE* gene (Fig 4.12. (A)). Putative mutants were confirmed by SDS-PAGE analysis of their LPS profile (Fig 4.12. (B)). The newly generated *galE* mutant was designated *S.* Typhimurium strain ML9 (Table 2.1).

4.2.4.3 Construction of an *S.* Typhimurium strain ML6 *galE* mutant

To compare the *S.* Typhimurium *galE* mutant strain ML9 with a *pagN* mutant of the same genetic background, a *galE pagN* double mutant was constructed. The *galE* gene of *S.* Typhimurium strain ML6 was interrupted in an identical manner to that of the *S.* Typhimurium strain SL1344. Confirmation of putative mutants proved impossible by PCR

(Fig 4.12. (A)). Putative mutants were confirmed by SDS-PAGE analysis of their LPS profile (Fig 4.12. (B)). The *galE pagN* double mutant was designated *S.* Typhimurium strain ML8 (Table 2.1).

Invasion assays with CHO-K1 cells, involving *S.* Typhimurium strains ML9 (*galE*) and ML8 (*galE pagN*) revealed little discernable difference between strains. This may have been due to the overall reduction in invasion mediated by rough bacteria. The levels may have been reduced to such an extent that small changes due the presence or absence of PagN could go un-noticed. However, the introduction of a functional *pagN* gene on the plasmid pML10 increased invasion levels from 2.59 ± 0.68% to 22.17 ± 2.62% representing a 8.5-fold increase. This large increase due to the presence of PagN would indicate that the protein has greater access to its receptor when expressed in a rough *S.* Typhimurium strain (Fig. 4.13).

4.2.4. Contribution of PagN to a functional SPI-1-encoded TTSS during PagN-promoted invasion

4.2.4.1 Construction of an *S.* Typhimurium strain CH133 *invA* mutant

As discussed in Section 1.3.4, *S.* Typhimurium primarily use a TTSS encoded by SPI-1 to gain entry into human colonic cells. However, in its arsenal *S.* Typhimurium has fimbrial and afimrial adhesins which act independently of this TTSS. The InvA protein is involved in the synthesis of the needle complex of the TTSS (Fig. 1.3 (C)). It is widely published that *invA* mutants lack a functional TTSS and are highly attenuated, indeed an *invA* mutant has been reported to be 360-fold less invasive than wild-type bacteria (135). To investigate if PagN acts independently of the SPI-1-encoded TTSS, an *S.* Typhimurium *invA* mutant was constructed. As with other chromosomally located mutations, the interrupted *invA* gene was constructed on a plasmid first and then transferred to the chromosome of *S.* Typhimurium strain CH133 using the λ Red allele replacement system. A 1499-bp fragment of the 2058-bp *invA* gene of *S.* Typhimurium strain LT2 was amplified by PCR using the primers invA-allele-F and invA-allele-R. The PCR product was cloned into the pBSKII plasmid digested with *Eco*RV creating the plasmid pInvA (Fig. 4.14 (i) and Table2.2). The pInvA plasmid was opened by digestion with *Sna*BI. A 1.6-kb fragment containing a chloramphenicol resistance (*cat*) cassette was excised from

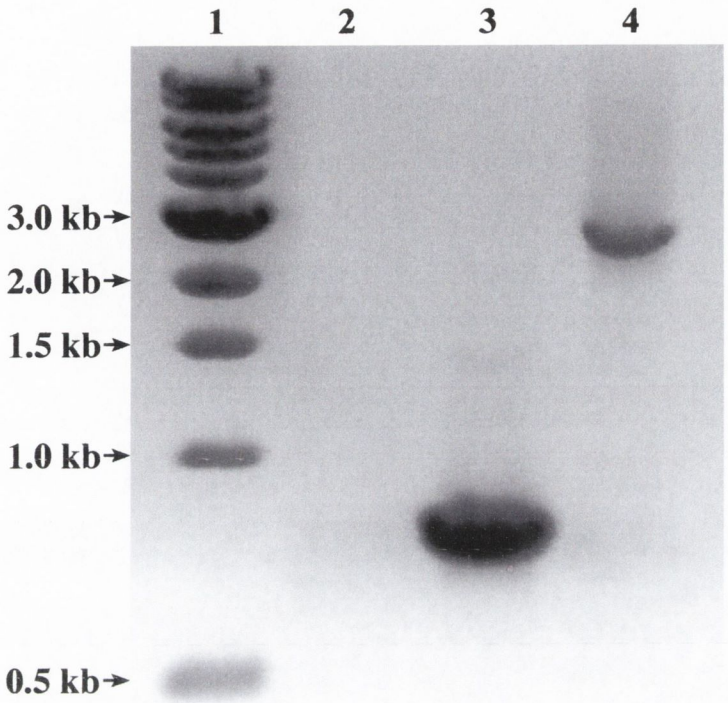

FIG. 4.10. Confirmation of the chromosomal *pagN*::*spc* gene fusion of *S.* Typhimurium strain ML133. Boiled bacterial colonies from wild-type (Lane 3) or *pagN* mutant (ML133; Lane 4) strains of *S.* Typhimurium were used as a template for PCR amplification of the *pagN* gene. A 1-kb DNA ladder is in Lane 1. Lane 2 contains a no-DNA negative control. DNA fragment length is indicated on the left.

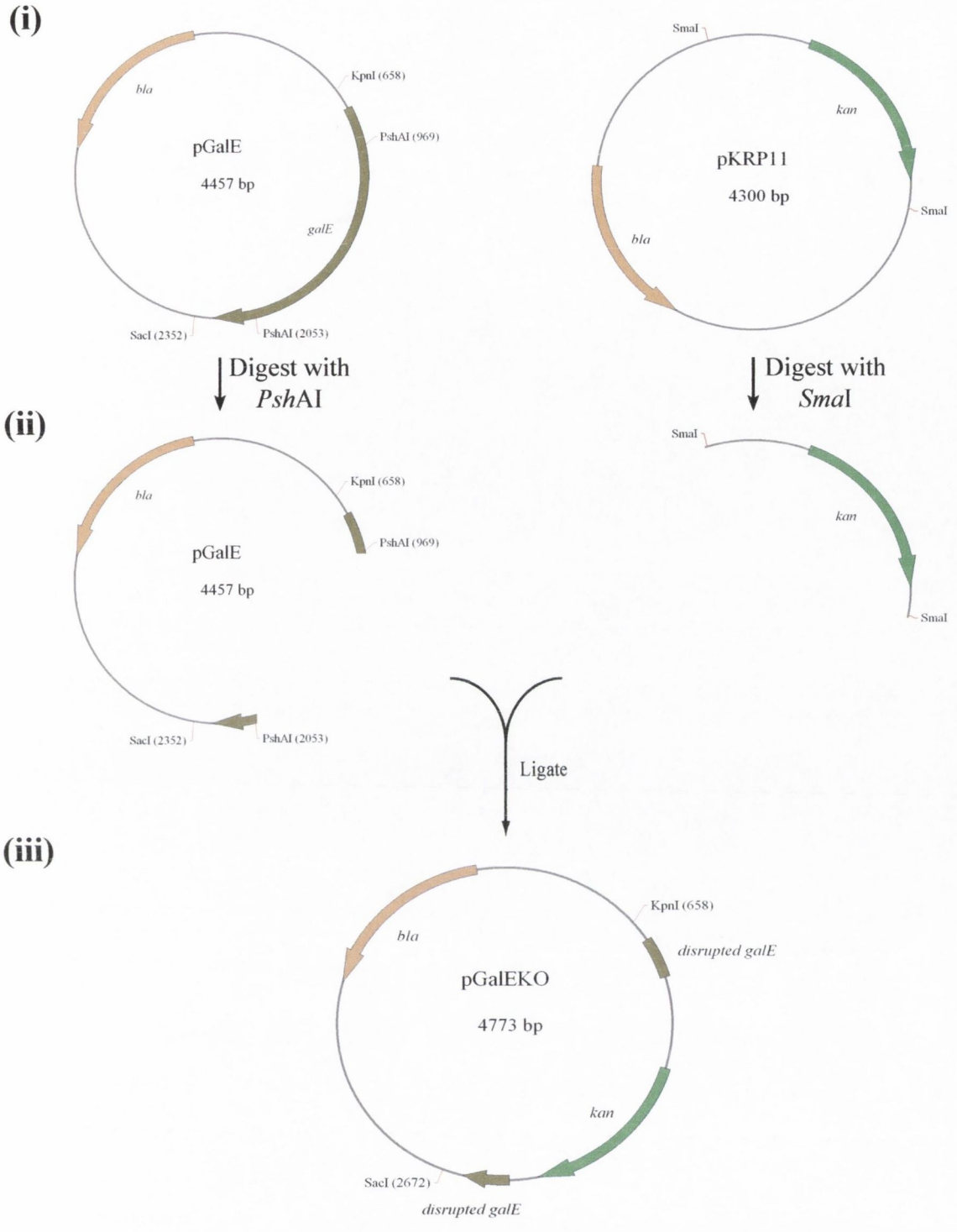

FIG. 4.11. Schematic of the construction of the plasmid pGalEKO. **(i)** The plasmid pGalE was digested with *Psh*AI. The pKRP11 plasmid was digested with *Sma*I **(ii)** The *kan*-containing DNA fragment from pKRP11 was ligated into the digested pGalE plasmid giving rise to **(iii)** plasmid pGalEKO. The *Sac*I/*Kpn*I fragment from pGalEKO was the source of template for amplification of the interrupted *galE* gene used to construct rough strains of *S.* Typhimurium.

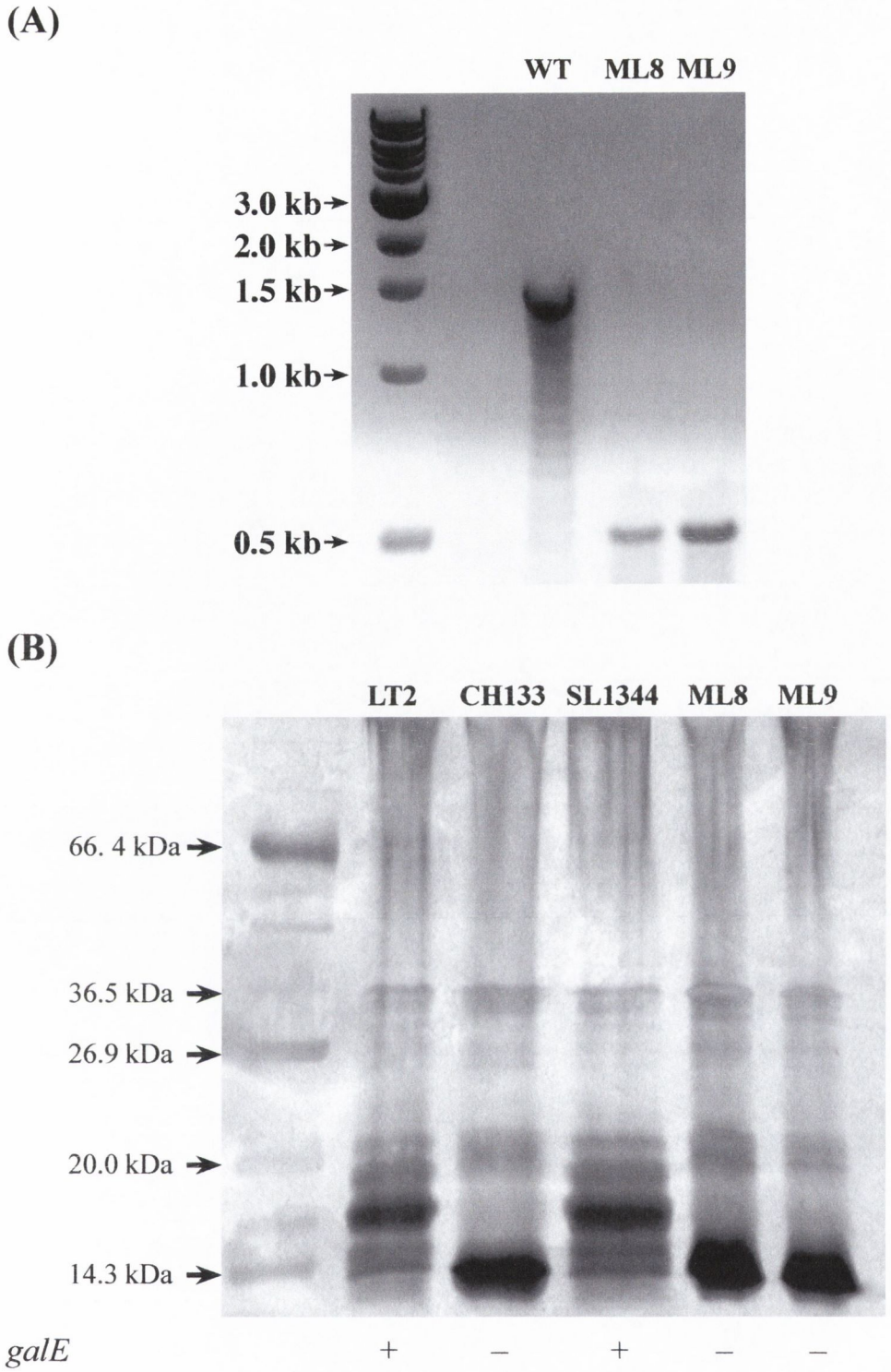

FIG. 4.12 (A) PCR analysis of the *galE* gene from *S.* Typhimurium strains SL1344, ML8 and ML9. Boiled bacterial colonies from wild-type (WT) or *galE* mutant (ML8 & ML9) strains of *S.* Typhimurium were used as a template for PCR amplification of the *galE* gene. Lane 2 contains a no-DNA negative control. DNA fragment length is indicated on the left. **(B) Confirmation of the rough LPS status of *S.* Typhimurium strains ML8 and ML9.** Bacterial cultures were treated with proteinase K to completely degrade protinacious structures. The bacterial strains are indicated above each lane. The *galE* status is indicated below the gel.

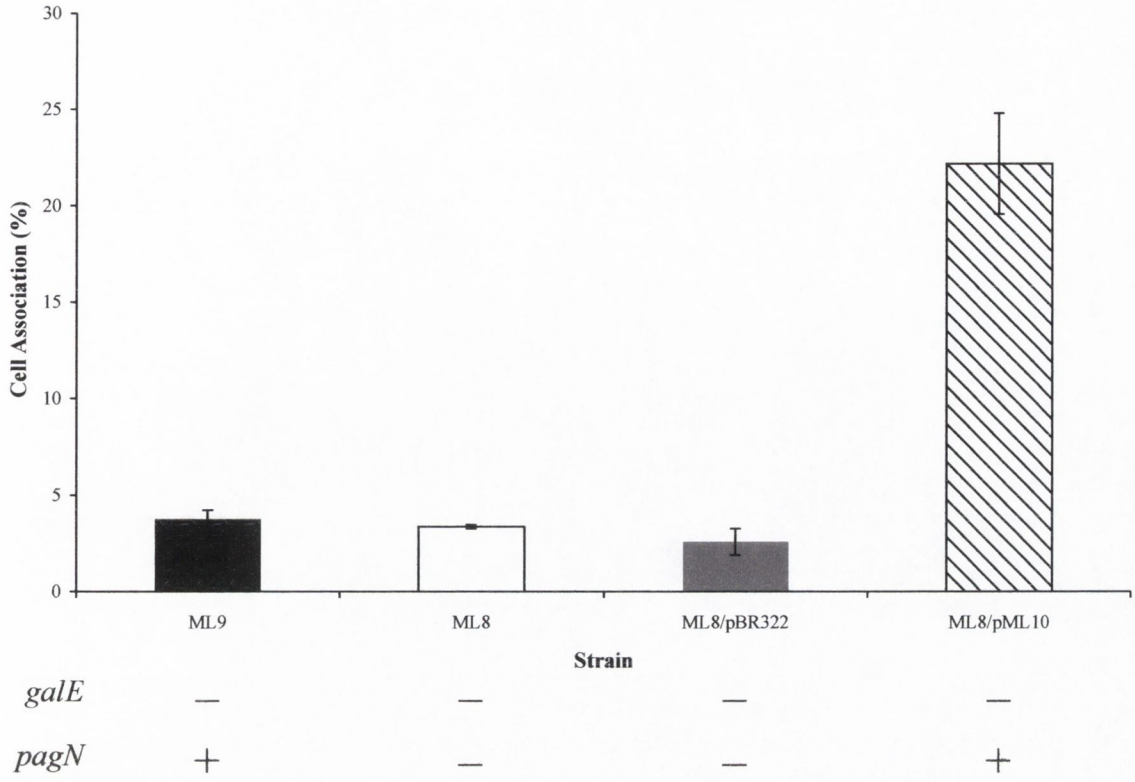

FIG. 4.13. Invasion of human HT-29 cells by rough *S.* Typhimurium. Invasion levels are calculated for rough *S.* Typhimurium strains ML9 (PagN +) and ML8 (PagN –). Levels are also calcultaed for the mutant ML8 strain harbouring the plasmid pML10 (PagN +) or the vector control pBR322. The *galE* and *pagN* status of each strain is indicated below the histogram. Data represents averages of triplicate wells, and standard error bars are shown.

plasmid pACYC184 (Fig. 4.17 (i) and Table 2.1) by digestion with *Hinc*II and *Xmn*I. The resulting blunt-ended *cat* cassette was ligated into the digested pInvA plasmid, thus interrupting the *invA* gene. The structure of the resulting plasmid was confirmed by restriction endonuclease mapping and the plasmid was called pInvAKO (Fig. 4.14 (ii & iii) and Table 2.2). The pInvAKO plasmid was digested with *Kpn*I and *Sac*I and used as a template for PCR amplification of the interrupted *invA* gene. Following amplification, the template was digested with *Dpn*I, gel-purified and transformed into electrocompetent, *S.* Typhimurium strain CH133 containing the pKOBEGA plasmid. Putative mutants were confirmed by PCR (Fig 4.15. (A)). The newly generated *invA* mutant was designated *S.* Typhimurium strain ML4 (Table 2.1).

4.2.4.2 Construction of an *S.* Typhimurium strain ML1344 *invA* mutant

To determine differences in the invasion capabilities of wt and PagN-defective *S.* Typhimurium in an *invA*⁻ background, the *invA* gene of the *pagN*-defective strain ML133 was interrupted. The mutant was constructed in an identical manner to the *S.* Typhimurium strain ML4. Putative mutants were confirmed by PCR (Fig 4.15. (B)). The newly generated *pagN invA* double mutant was designated *S.* Typhimurium strain ML3 (Table 2.1).

4.2.4.3 PagN promotes TTSS-1-independent invasion of CHO-K1 cells

Invasion assays performed with CHO-K1 cells and *S.* Typhimurium strains ML4 (*galE invA*) and ML3 (*galE invA pagN*) revealed that PagN mediates bacterial internalisation independently of a functional SPI-1-encoded TTSS. The absence of PagN caused no discernable difference in the percentage invasion displayed by strain ML3 as compared to strain ML4. However, *S.* Typhimurium strain ML3 harbouring the plasmid pPagN2.3 showed a highly elevated ability to invade CHO-K1 cells as compared to either strain ML4 or strain ML3 (Fig. 4.16). The level of invasion promoted by pPagN2.3 was far in excess of the parental *S.* Typhimurium strain CH133, suggesting that PagN has better access to its cognate receptor in the absence of the LPS O antigen.

4.2.4.4 Construction of an *S.* Typhimurium strain SL1344 *invA* mutant and an *invA pagN* double mutant

Considering the observations presented in Section 4.2.3.1, in which phenotypic differences between *S.* Typhimurium strains LT2 and SL1344 were highlighted, it was important to ascertain whether PagN expressed by strain SL1344 also promoted SPI-1-encoded TTSS-independent invasion of epithelial cells. Using λ Red allele replacement, the *invA* gene of *S.* Typhimurium strains SL1344 and ML6 were interrupted creating the new mutant *S.* Typhimurium strains ML5 (*invA*) and ML7 (*pagN invA*) respectively (Fig. 4.17 (A) & (B)). Gentamicin protection assays with the human cell line HT-29 and these *invA*$^-$ bacteria established that for *S.* Typhimurium strain SL1344, *invA* is necessary for invasion. As the invasion levels were so reduced in the absence of the *invA* gene, it was impossible to discern any differences attributable to the loss of *pagN* (Fig. 4.17(B)). However, *S.* Typhimurium strain ML7 harbouring the plasmid pML10 gave rise to a 7-fold increase in invasion as compared to strain ML7 carrying the empty vector pBR322, showing that PagN can promote invasion of human HT-29 independently of the SPI-1-encoded TTSS.

4.2.5 The role of PagN in cultured macrophages

4.2.5.1 PagN promotes cell survival in cultured J774A.1 murine macrophages

To determine any advantage wild type *S.* Typhimurium strain LT2 or strain SL1344 may have over a *pagN* mutant in an intra-macrophage environment, gentamicin survival assays were performed. In contrast to assays with epithelial cells, bacteria were incubated with J774A.1 cultured macrophages for 2 h rather than 1 h before addition of gentamicin.

TABLE 4.4. Contribution of PagN to the survival of *Salmonella* J774A.1 macrophages

***S.* Typhimurium genotype**	**Survival (%)**	
	LT2	**SL1344**
Wild-type	56.52 ± 3.05	6.26 ± 0.75
pagN mutant	48.15 ± 1.72 *	5.28 ± 0.65
Vector control	43.01 ± 1.55	4.76 ± 0.75
Complemented mutant	29.01 ± 1.90	7.28 ± 0.11

Bacterial survival levels were calculated for wild-type *S.* Typhimurium and *pagN*-defective bacteria. Survival levels were also calculated for the *pagN* mutant complemented with a *pagN*-containing plasmid or the corresponding vector control. Data represents averages of triplicate wells. * indicates

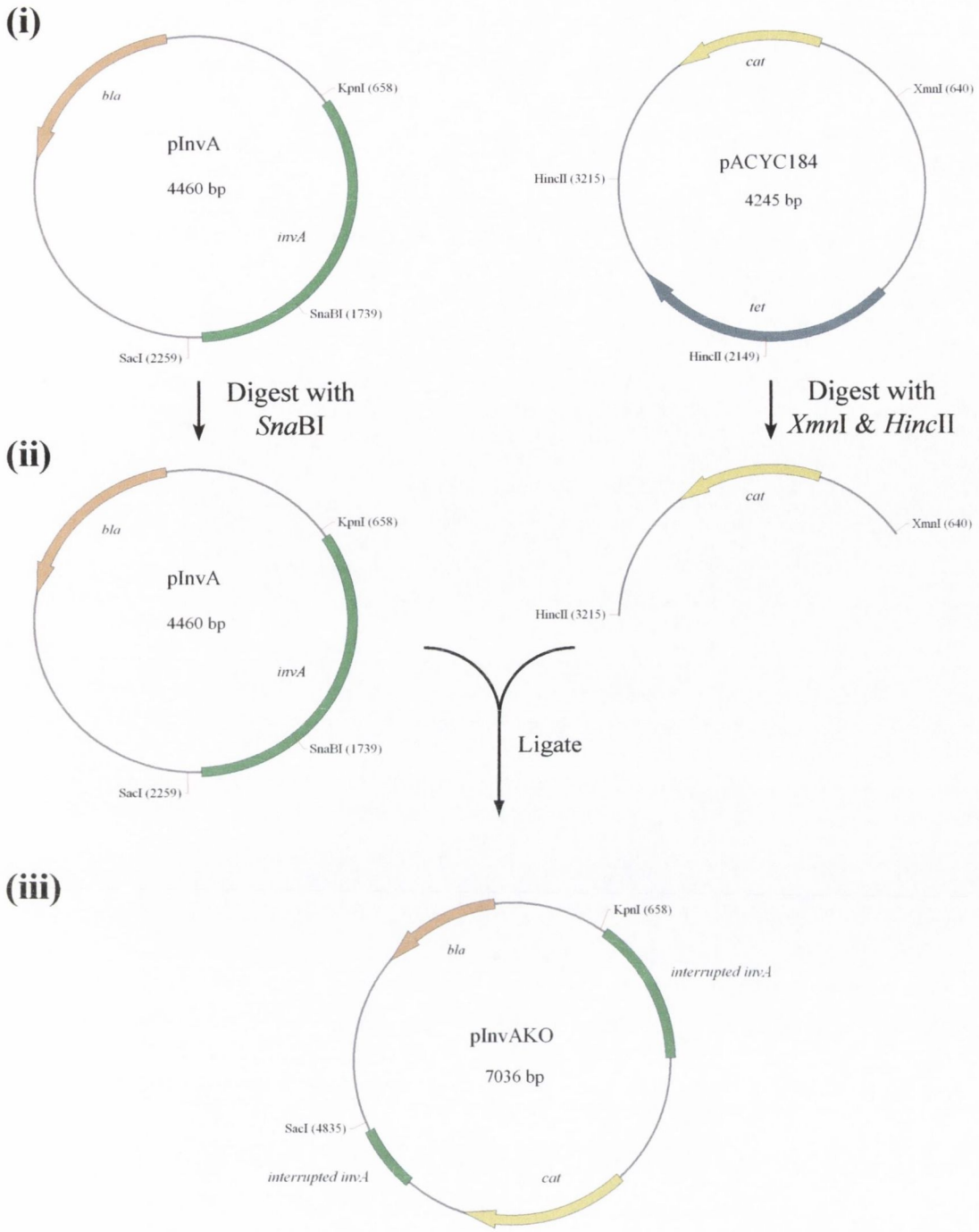

FIG. 4.14. Schematic of the construction of the plasmid pInvAKO. (i) The plasmid pInvA was digested with *Sna*BI. The *cat*-containing vector pACYC184 was digested with *Xmn*I and *Hinc*II. **(ii)** The 1.6-kb *cat* DNA fragment from pACYC184 was ligated into the digested pInvA plasmid interrupted the *invA* fragment and giving rise to **(iii)** plasmid pInvAKO. The *Sac*I/*Kpn*I fragment from pInvAKO was the source of template for amplification of the interrupted *invA* gene used to construct *invA*::*cat* mutant strains of *S.* Typhimurium.

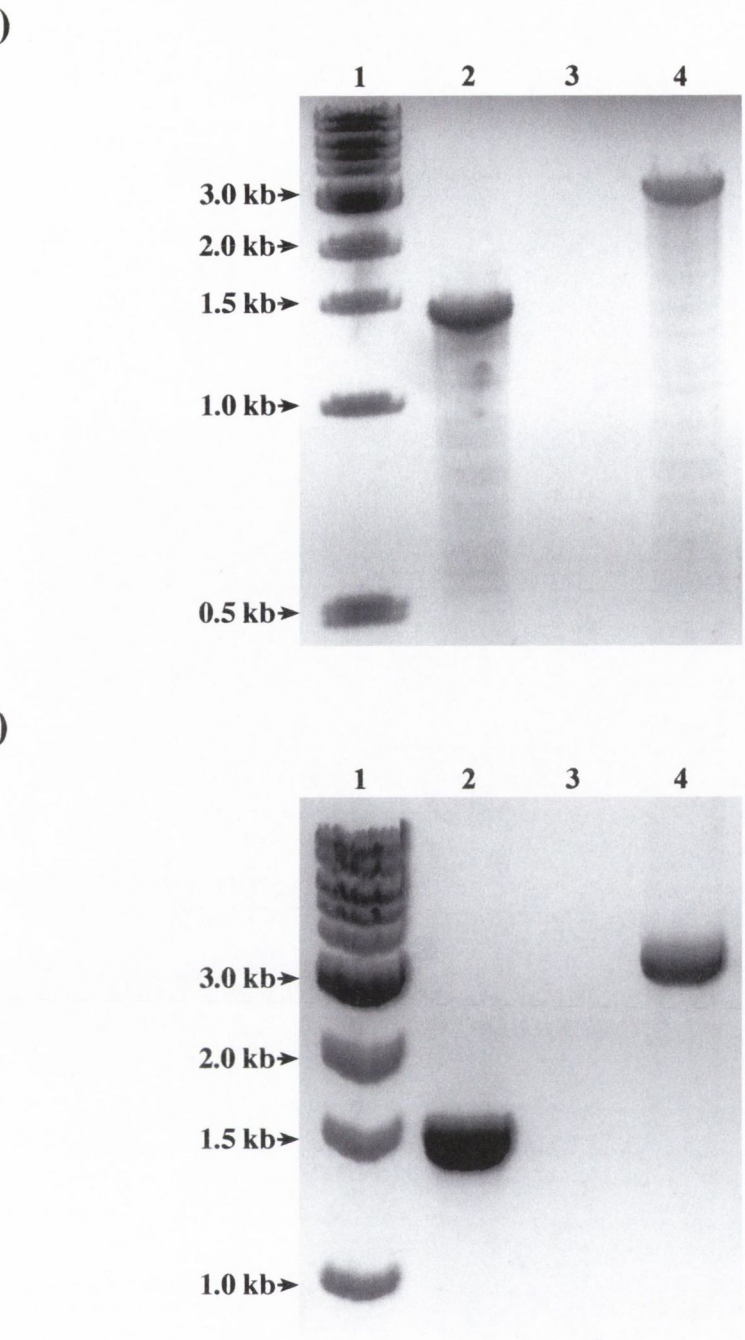

FIG. 4.15. Confirmation of the chromosomal *invA*::*cat* gene fusion of *S.* Typhimurium strain ML4 (A) and ML3 (B). (A) Boiled bacterial colonies from wild-type (CH133; Lane 2) or *invA* mutant (ML4; Lane 4) strains of *S.* Typhimurium were used as a template for PCR amplification of the *invA* gene. **(B)** Boiled bacterial colonies from wild-type (ML133; Lane 2) or *invA* mutant (ML3; Lane 4) strains of *S.* Typhimurium were used as a template for PCR amplification of the *invA* gene. In both (A) and (B) a 1-kb DNA ladder is in Lane 1. Lane 3 contains a no-DNA negative control. DNA fragment length is indicated on the left.

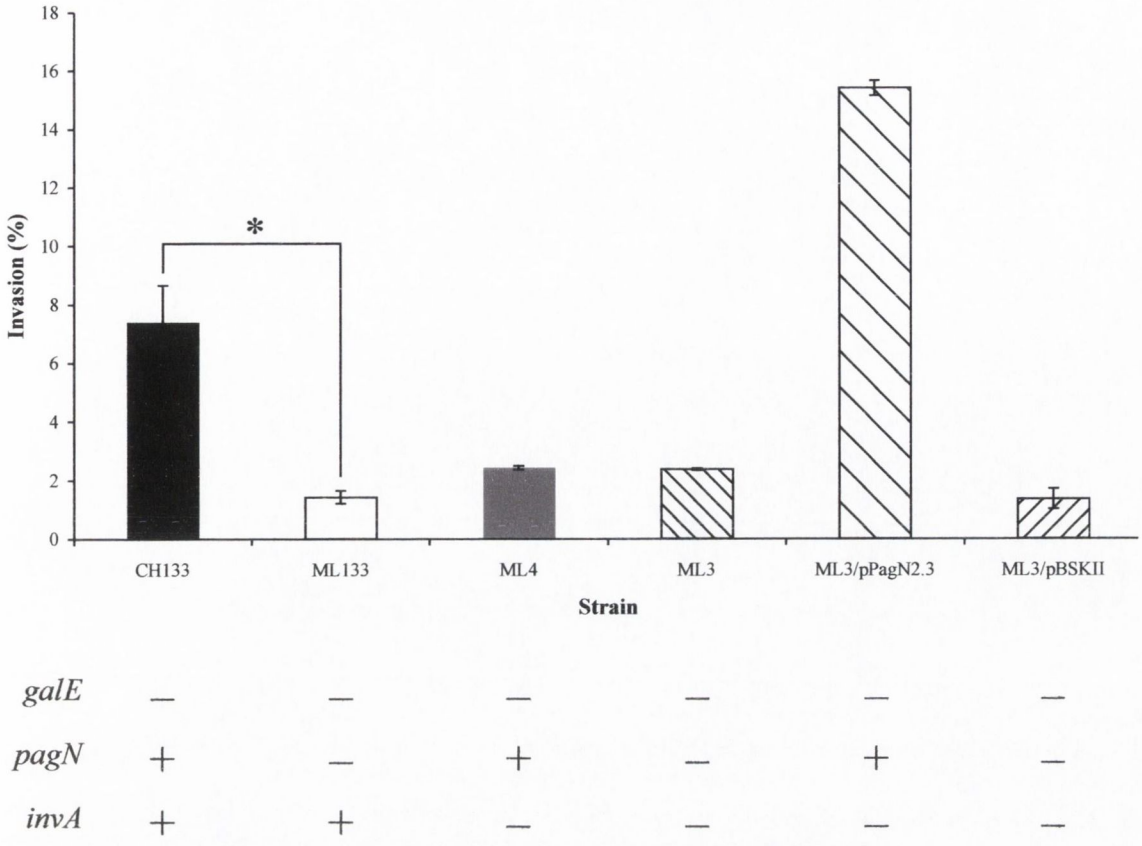

FIG. 4.16. Invasion of CHO-K1 cells by rough *S.* Typhimurium lacking a functional SPI-1-encoded TTSS. Invasion levels are calculated for rough *S.* Typhimurium strains with a functional TTSS, CH133 (PagN +) and ML133 (PagN –) and strains without a functional TTSS, ML4 (PagN +, InvA –) and ML3 (PagN –, InvA –). Levels are also calcultaed for the mutant ML3 strain harbouring the plasmid pPagN2.3 (PagN +) or the vector control pBSKII. The *galE*, *pagN* and *invA* status of each strain is indicated below the histogram. Data represents averages of triplicate wells, and standard error bars are shown. * indicates statistical significance, $P < 0.05$.

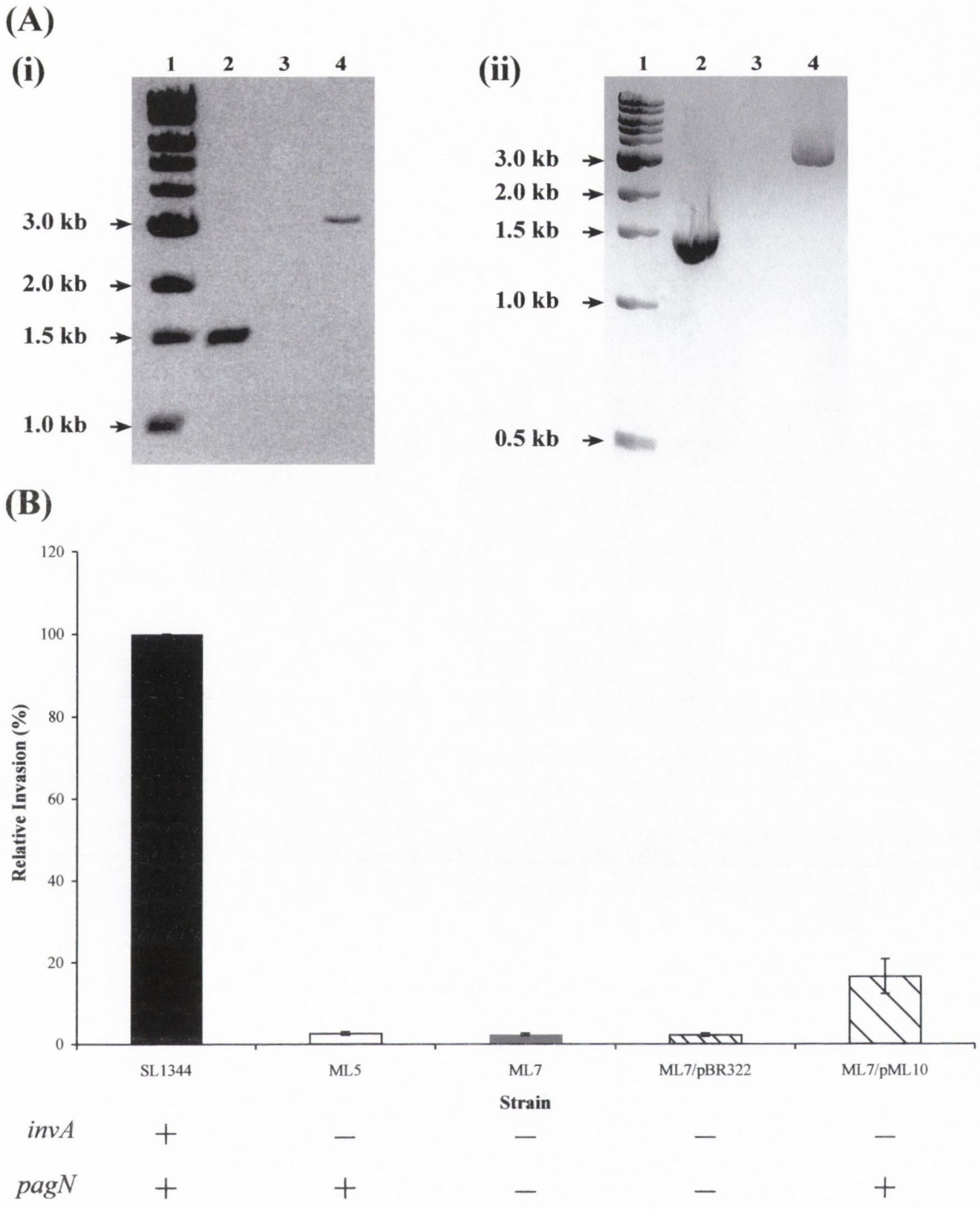

FIG. 4.17. (A) Confirmation of the chromosomal *invA*::*cat* gene fusion of *S.* Typhimurium strain (i) ML5 and (ii) ML7. (i) Boiled bacterial colonies from wild-type (SL1344; Lane 2) or *invA* mutant (ML5; Lane 4) strains of *S.* Typhimurium were used as a template for PCR amplification of the *invA* gene. **(ii)** Bacterial strains SL1344 (Lane 2) and ML3 (Lane 4) analysed as in panel (i). In both (i) and (ii) a 1-kb DNA ladder is in Lane 1. Lane 3 contains a no-DNA negative control. DNA fragment length is indicated on the left. **(B) Invasion of human HT-29 cells by *S.* Typhimurium lacking a functional SPI-1-encoded TTSS.** Invasion levels are calculated for *S.* Typhimurium strains with or without a functional TTSS. Levels are also calculated for the mutant ML7 strain harbouring the plasmid pML10 (PagN +) or the vector control pBR322. The *invA* and *pagN* status of each strain is indicated below the histogram. Data represents averages of triplicate wells, and standard error bars are shown. The invasion efficiencies were expressed as a percentage of the wild-type.

statistical significance, $P < 0.05$.

Strikingly, the overall percentage recovery of LT2 and its derivative strains was far greater than that of the more virulent SL1344 strain and its corresponding mutant derivatives. The percentage recovery of strain LT2 and its derivative strains was ~10-fold higher than that of strain SL1344 and its derivatives again highlighting the occurrence of strain variation within the Typhimurium serovar.

Wild-type bacteria were recovered in greater numbers relative to a *pagN* mutant. For strain LT2, the recovery of bacteria was significantly reduced from 56.52 ± 2.16% to 48.15 ± 1.22%, while the reduction for strain SL1344 was less pronounced. For LT2-derived bacteria the reduction due to a defective *pagN* gene could not be fully complemented by the plasmid pPagN1. This contrasted sharply to data obtained with strain SL1344. The reduction in bacterial survival was fully complemented by introducing the cloned *pagN* gene on plasmid pML10. It must be noted that *S.* Typhimurium strain ML6 was complemented with the *pagN*-containing plasmid pML10. This plasmid is a derivative of pBR322 which has an approximately 10-fold higher copy number than pPagN1. The possibility of a gene dosage effect from pML10 may account for the differences in data regarding complementation from both *S.* Typhimurium strains.

It is important to note that not all uptake of bacteria by J774A.1 cells is by passive phagocytosis. It may therefore not be ruled out that the apparent defect in intracellular survival may reflect a reduction in the initial invasion. To investigate such a possibility, initial uptake rates and kinetics of survival over time could be determined. Bacterial survival kinetics may be ascertained by enumerating intra-macrophage bacteria at the time of incubation with gentamicin, and at subsequent time-points over the course of several hours. This data would illustrate more definitively the level of bacterial survival within the macrophage.

4.3 Discussion

The ability of *Salmonella* to bind to, and enter host intestinal cells is central to its pathogenesis. *Salmonella* must first attach to the host cell using capsular proteins and fimbriate projections; recently subunits encoded by 11 different fimbrial operons were shown to be up-regulated *in vivo* (194). Once initial attachment has taken place, the bacteria gain more intimate association where upon they employ the use of a TTSS encoded by SPI-1. This TTSS injects effector proteins into the host cell bringing about phagocytosis by an otherwise non-phagocytic cell (Sections 1.3.3 & 1.3.4).

Before employing the TTSS, *Salmonella* must move from a state of initial cellular contact to a more intimate association with the target cell. It is thought that the bacteria use shorter, non-capsular, afimbrial adhesins to facilitate the transition between initial and intimate contact. Indeed, *Salmonella* has a varied arsenal of adhesins and invasins thought to effect this transition. Examples of these afimbrial adhesins include the mannose-sensitive haemagglutinin (273), and autotransporter proteins such as MisL (93) and ShdA (212). These have been established as adhesins capable of promoting invasion of intestinal epithelial cells. It is likely that many proteins with adhesion and invasion capabilities are yet to be characterised.

Data from cell association and invasion assays indicate that PagN is an adhesin and invasin. PagN conferred upon recombinant *E. coli* the ability to adhere to and invade both human (HT-29) and non-human (CHO-K1) epithelial cells. Expression of PagN in the poorly adhesive *E. coli* K-12 strain DH5α promoted ~1% cell association with a HT-29 monolayer. Low-level invasion was also promoted. In comparison to levels observed with HT-29 cells, PagN promoted high-level adhesion to and subsequent invasion of CHO-K1 cells. These data suggest that CHO-K1 cells display greater levels of the PagN receptor than HT-29 cells. HT-29 cells may possess lower levels of the target receptor, or may be more difficult to invade due to the production of bacteriocidal peptides such as defensins (77, 344). Studies with HT-29 cells and T84 cells have revealed that differences between human colon carcinoma cell lines significantly influence the levels of invasion and the mechanisms available for *S.* Typhimurium to enter into host cells (328); it is therefore not surprising that bacteria display disparate levels of invasion for cell lines from different host animals.

The high levels of both adhesion and invasion mediated by PagN when compared to the known invasin Tia, indicates that PagN is a potent adhesin. PagN-mediated internalisation

of epithelial cells was dependent upon actin polymeristaion. Pre-incubation of eukaryotic cells with cytochalasin D abolished PagN-promoted invasion of eukaryotic cells, suggesting that PagN promotes invasion by the Trigger Mechanism whereby the host machinery is hijacked resulting in actin polymerisation and cytoplasmic rearrangements.

The phenotypes of *S.* Typhimurium strains LT2 and SL1344 has been shown to differ with regards to the same adhesin (39), however, regarding PagN, both strains displayed a reduction in invasion when a functional PagN protein was absent. Disruption of the chromosomal *pagN* gene resulted in a decrease in the number of *Salmonella* internalised by CHO-K1 cells. Surprisingly *S.* Typhimurium strain LT2 displayed slightly more elevated levels of invasion than the mouse-virulent strain SL1344, although the loss of a functional *pagN* gene had a more detrimental effect in an SL1344 background. The reduction in invasion due to the loss of PagN in strain SL1344 was 1.8-fold whereas in strain LT2 was 1.2-fold. These data are summarised below.

TABLE 4.5. Invasion of CHO-K1 cells by *S.* Typhimurium

***S.* Typhimurium strain**	**Invasion (%)**	
	Wild-type	***pagN* mutant**
LT2	~22	~18
SL1344	~18	~10

These data, especially that comparing SL1344 and ML6, suggest that PagN may have a role in *Salmonella* pathogenesis. The reduced ability of PagN-defective *Salmonella* to invade CHO-K1 cells taken together with the fact that *pagN* mutants are less competitive than wild-type bacteria, in a BALB/c mouse competitive index assay (72), suggests that PagN is a virulence determinant.

The defect in *S.* Typhimurium strain MLT2 was fully restored by complementation with the low-copy number vector pPagN1; while complementation of the SL1344-derived mutant, ML6 was partially achieved with the plasmid pML10. Surprisingly, it was noted that the vector control *S.* Typhimurium strain MLT2/pPD101 often displayed elevated levels of invasion. A possible explanation may be considered with reference to recent findings that the *tet* gene from pSC101 cloning vectors impairs *Salmonella* survival in macrophages (1). It has also been revealed that cloning vectors and fluorescent proteins can affect *Salmonella* virulence in both epithelial cells and macrophages (214), it is therefore feasible that the pPD101 plasmid has uncharacterised affects on *Salmonella* virulence. However, these possibilities were not investigated, and without further study it

is impossible to explain fully why the pPD101 plasmid sometimes increases bacterial invasion of epithelial cells.

As the reduction in virulence due to a defective PagN was most apparent in SL1344 strains, the PagN/HT-29 interaction seen when PagN was over-expressed in *E. coli* was further characterised in an SL1344 background. Levels of adhesion and invasion of HT-29 cells were very low, possibly due to bacterial killing by anti-microbial peptides and/or other host cell defense mechanisms. Cell association was reduced by 50% when the *pagN* gene was interrupted while invasion levels were decreased to as little as 20% of wild-type levels. These data suggest that PagN may play a significant role in the attachment of *Salmonella* to the colon of a human host.

The possibility, highlighted in Chapter 3, that LPS can mask PagN was expanded upon here. The phenomenon of LPS masking of outer membrane proteins has been observed for many bacteria including *Neisseria gonorrheae*, in which LPS prevents binding of cathepsin B to three outer membrane proteins (357) and *S.* Typhimurium where steric hindrance by the O antigen prevents the PgtE protease from interacting with its substrates (225). The loss of *pagN* in a rough strain of *S.* Typhimurium (ML133) had a more detrimental effect than in its smooth parental strain LT2. This suggests that PagN has a greater invasive role to play in rough strains; this is possibly due to the protein having greater access to its receptor and therefore its role is exaggerated with respect to a wild-type setting. Complementation of either *pagN* mutant, strain ML1344 or ML8, lead to a large increase in invasion of epithelial cells. These data indicate that LPS masks PagN. However, as PagN is not likely to have a role in the very initial, non-intimate, attachment to epithelial cells this masking effect may be of limited relevance. The predicted β-barrel structure of PagN (see Chapter 6) would suggest that it has a role in establishing more intimate cell/cell interactions at a distance where LPS projections may be inconsequential.

The interference of LPS with PagN function within macrophages may be explained by consideration of the PhoP/Q system. The PhoP/Q system controls the length of the O antigen (159). Upon entry into macrophages, *pagN* expression is up-regulated whereas genes for LPS synthesis and modification are down-regulated (106). This would enable PagN to overcome any steric hindrance caused by the LPS O antigen, thus gaining greater access to its receptor. It is apparent that PagN plays a role in intracellular survival within macrophages. PagN was established as having a protective role within macrophages. PagN-defective *S.* Typhimurium survived less well in macrophages than their wild-type parents. For strain LT2, the loss of PagN resulted in a significant reduction in intra-macrophage survival, while the reduction for strain SL1344 was less pronounced.

Interestingly, the mouse-virulent strain was not able to survive within macrophages with the success displayed by the less virulent LT2 strain. The exact role of PagN within the acidic SCV of macrophages was not investigated and remains undefined at present.

The large number of adhesins and invasins possessed by *Salmonella* indicates a great functional redundancy, and suggests that *Salmonella* may have several auxiliary invasion systems. The possibility that PagN may serve as an auxiliary adhesin in such a system is strengthened by the fact that PagN is capable of acting independently of the SPI-1-encoded TTSS. In both an LT2 and an SL1344 background complementation, with a *pagN*-containing plasmid, of a *pagN invA* double mutant resulted in elevated levels of epithelial cell invasion. This result indicates that for PagN-mediated invasion, a functional SPI-1-encoded TTSS is not required. PagN may have an invasive role in *Salmonella* strains during growth periods where SPI-1 genes are down regulated, or where a functional SPI-1 is absent. Indeed, it is likely that auxiliary invasion systems become up regulated in the absence of a functional SPI-1, as is the case in the *Δspi-1 S.* Typhimurium strain reported on by Murray *et al.* which displayed no loss of invasion capabilities (288).

The vast array of data presented in this chapter establishes PagN as an adhesin and invasin. They expand upon the possible roles of PagN and some contributing factors. I have demonstrated that PagN, is capable of promoting adhesion and subsequent invasion of epithelial cells in a process requiring actin polymerisation. It has been established that PagN contributes to *S.* Typhimurium invasion of human colonic cells in an SPI-1-encoded TTSS-independent manner, is masked by the LPS O antigen, and promotes bacterial survival within cultured macrophages.

Chapter 5

Identification of the PagN receptor

5.1 Introduction

The surfaces of animal cells are largely decorated with negatively-charged complex macromolecules called proteoglycans (335). Proteoglycans consist of a core protein domain, to which one or more glycosaminoglycan (GAG) chains are covalently linked. Based on their linkage to the cell membrane, these glycoproteins can be divided into two sub-families, syndecans and glypicans. Syndecans are type 1 transmembrane proteoglycans while the glypicans are glycosylphosphatidylinositol-anchored. Glypicans in general, are expressed predominantly during development (113). Expression levels change in a stage- and tissue-specific manner, suggesting that they are involved in the regulation of morphogenesis (235, 244, 346). In contrast, syndecans are more widely distributed in developed tissue, and found on epithelium (syndecan-1), mesenchymal tissue (syndecan-2), neural cells (syndecan-3) and ubiquitously (syndecan-4) (32, 84). The name syndecan, comes from the Greek "syndein", to bind together, as they are involved in linking the ECM to the intracellular cytoskeleton (331).

Of interest in this study are the syndecans located on the epithelium, namely syndecan-1 and -4. These syndecans may be considered hybrid proteoglycans as they are composed of a mixture of the two major types of GAG chains, heparan sulphate and chondroitin sulphate. GAGs are heteropolysaccharides made up of a repeated structure containing an N-acetylated hexosamine in a repeated disaccharide unit. Based on their disaccharide repeat structure, GAGs can be divided into different classes, including chondroitin sulphate (CS), dermatan sulphate (DS), heparan sulphate (HS) and heparin (213). HS is based on the disaccharide repeat $(GlcUA\beta1\text{-}4GlcNAc\alpha1\text{-}4)_n$ while the unit disaccharide of CS is $(GlcUA\beta1\text{-}3GalNAc\beta1\text{-}4)_n$ (Fig. 5.1) (32). During chain synthesis, GAGs can undergo both epimerisation and sulphation to varying degrees. These processes lead to a highly heterogeneous population of GAG chains. A HS or CS population may contain GAG chains of varying lengths containing epimers with various sulfation levels. The heterologous nature of GAG chains is thought to allow the proteoglycans to interact with a multitude of different receptors. Indeed, syndecans have been shown to interact with ECM components, morphogens, host defense factors, and proteins involved in energy metabolism (for a review see (31)).

A number of pathogens, including viruses (317, 362), gram-negative bacteria (116, 123), gram-positive bacteria (236, 237) and protozoans (124), are known to interact specifically with HS proteoglycans (HSPGs). Researchers have used a variety of tools to study these

interactions. Of great importance in the study of microbe/HSPG interactions is the cell line CHO-K1. A large array of fully characterised CHO-K1 mutant cell lines, defective in GAG biosynthesis are available. These have been reviewed by Rostand *et al.* (335). One such cell line, pgsA-745, which is defective in GAG production, is especially useful for initial studies with suspected HSPG-binding proteins. The interactions can then be fine-tuned with cell lines such as pgsD-677, which lacks only HS, or cells lacking a functional *ldlD* gene, which fail to express CS. The indicated HSPG/adhesin interaction can then be further and more thoroughly characterised by the use of exogenously added GAG moieties and enzymatic removal of the GAGs from the proteoglycan core protein.

The purpose of this study was to determine whether PagN uses proteoglycans on the surface of epithelial cells for invasion, and if so, characterise this interaction more fully. The main questions addressed included:

- Are glycosylated proteoglycans required for PagN-mediated invasion?
- Does the PagN protein interact with all GAGs or a specific subset?
- Do serum factors contribute to these interactions?
- Does *Salmonella* use proteoglycans for epithelial cell adhesion and invasion?
- If so, which category of proteoglycans are involved?

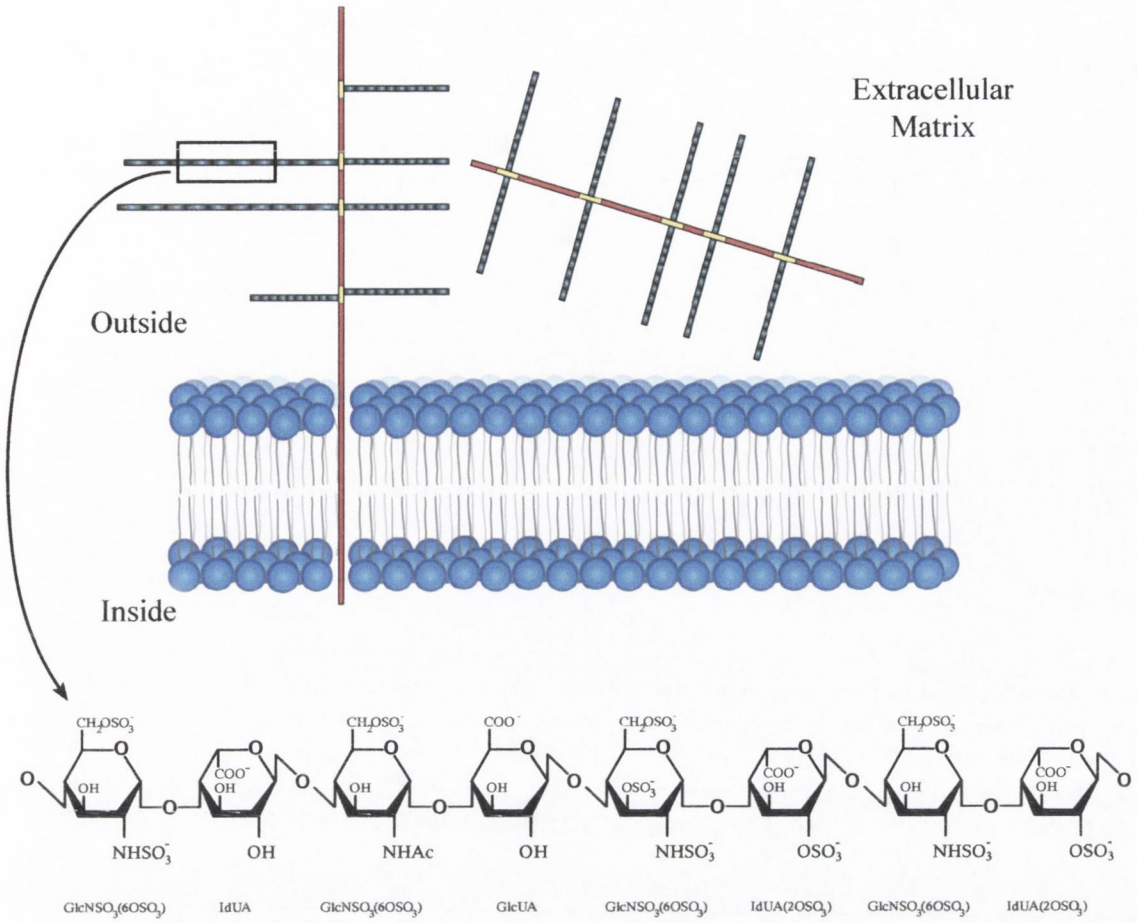

FIG 5.1. Partial structure of a heparan sulphate membrane proteoglycan. The coloured section of the diagram depicts the membrane lipid bilayer with proteoglycan decorating the surface and shed into the extracellular matrix. The proteoglycan core protein can be seen with glycosaminoglycan chains eminating from it like branches of a tree. The black and white section of the diagram shows the chemical structure of the glycosaminoglycan chains of heparan sulphate.

5.2 Results

5.2.1 Interaction of PagN with glycosaminoglycans

5.2.1.1 Are proteoglycans required for host cell interaction by PagN?

Both Tia and OpaA have been shown to promote invasion of cultured epithelial cells through interactions with HSPGs (116, 401). PagN is 54% similar to Tia; while this is not a hugely elevated degree of similarity, it suggests that PagN might also utilise GAGs during adhesion to epithelial cells. To determine if PagN interacts with the GAG moieties of proteoglycans, PagN-mediated adhesion was assessed using CHO-K1 cells with defects in GAG biosynthesis. Firstly, CHO-K1 cells were seeded in media containing p-nitrophyl β-D-xylopyranoside (4 mM, 24-48 h). This chemical resembles a biosynthetic intermediate in GAG chain synthesis and acts as a competitive substrate for the enzyme xylosyltransferase (272), thus diverting the synthesis of chains from endogenous proteoglycans, resulting in under-glycosylation of surface-expressed proteins. Cell association of *E. coli* K-12 strain DH5α expressing recombinant PagN was markedly reduced when CHO-K1 cells were grown in the presence of this inhibitor.

TABLE 5.1. The effect of under-glycosylation on PagN-promoted CHO-K1 binding

Adhesin Expressed	**Cell Association (%) – xylopyranoside**	**Cell Association (%) + xylopyranoside**
None	3.08 ± 0.51	3.19 ± 0.74
PagN	76.81 ± 16.49	13.12 ± 2.23
Tia	28.87 ± 12.78	11.00 ± 1.82

The levels of cell association were reduced from ~77% to ~13% representing a ~6-fold decrease. This compared to the ~3-fold decrease displayed by the known GAG-binding protein Tia, indicates that PagN interacts with the GAG chains of proteoglycans.

The interaction between PagN and GAGs was further characterised through analysis of interactions with the CHO-K1 xylotransferase mutant cell line pgsA-745. pgsA-745 cells have a defective xylotransferase, the enzyme required for the addition of nascent GAG chains to the core protein of proteoglycans, and therefore completely lack HS or CS.

TABLE 5.2. Non-glycosylated CHO-K1 cells do not support PagN-promoted invasion

Adhesin Expressed	Invasion (%) CHO-K1 cells	Invasion (%) pgsA-745 cells
None	1.20 ± 0.26	0.03 ± 0.00
PagN	13.30 ± 0.22	0.03 ± 0.01
Tia	5.14 ± 0.48	0.07 ± 0.01

PagN-mediated invasion of CHO-K1 cells was all but abolished in the absence of glycosylated proteoglycans. Invasion levels were decreased to that displayed by *E. coli* harbouring the vector control, pTrc99a. These data indicate that the production of eukaryotic cell surface GAGs is an absolute requirement for interactions of PagN with CHO-K1 epithelial cells. Interestingly, the level of invasion of *E. coli* containing pTrc99a, the negative control, was reduced from 1.20 ± 0.26% to 0.031 ± 0.004% indicating that the *E. coli* strain has some low-level GAG-binding capabilities.

5.2.1.2 Exogenous addition of GAGs inhibits PagN/cell interactions

To investigate whether PagN interacts with all GAG chains or solely HSPGs, PagN-mediated internalisation of CHO-K1 cells was assessed in the presence and absence of exogenously added GAGs. Recombinant *E. coli* K-12 strain DH5α expressing PagN was incubated with heparin (100 μg/ml), CS (100 μg/ml) or both at 37 °C for 30 min. Unbound, potential competitive inhibitors were removed during three washes with sterile PBS. Invasion assays with the pre-incubated bacteria and cultured CHO-K1 cells were performed as before. Pre-treated cultures were compared to untreated *E. coli* K-12 containing the PagN expression vector, pML1 or pTrc99a. The invasion efficiencies were expressed as a percentage of the untreated positive control, *E. coli* DH5α/pML1. Addition of heparin to bacterial cells resulted in a marked decrease in PagN-promoted invasion of CHO-K1 cells. Invasion levels were reduced by 92% in the presence of heparin. In comparison, a reduction of only 30% resulted from the addition of CS (Fig 5.2(A)). However, the addition of CS did not reduce PagN-promoted invasion of CHO-K1 in a statistically significant manner ($P > 0.05$). Therefore, it may be concluded that the addition of CS had only a minor effect on PagN-promoted invasion. The relative decrease seen for the addition of heparin was identical to that obtained when both heparin and CS were added, indicating that the contribution of CS was minimal when compared to the drastic reduction displayed by heparin. These data suggest that PagN binds

preferentially to heparin-containing GAG chains.

Interactions between GAGs and their ligands are often mediated by ionic forces (340). The role of GAG charge in the interaction with PagN was investigated using dextran sulphate, a polyanionic synthetic carbohydrate with a similar charge to mass density and molecular mass to heparin (322). Dextran sulphate had a marginal inhibitory effect on PagN-mediated invasion of CHO-K1 cells (results not shown), reducing levels of invasion from 38.17 ± 6.74% to 25.51 ± 5.34% ($P > 0.1$). These statistically insignificant data may suggest a minor role for charge in PagN-promoted interactions with epithelial cells, but indicate that the interaction may be a specific adhesin/receptor binding one and not merely electrostatic.

5.2.1.3 Heparin specifically inhibits PagN-mediated invasion

To determine if PagN interacts with heparin specifically, inhibition studies were performed using soluble heparin. The ability of soluble heparin to inhibit PagN-promoted invasion of CHO-K1 cells in a dose-dependent manner was assessed. *E. coli* K-12 strain DH5α harbouring the plasmid pML1 was pre-incubated with increasing concentrations of heparin for 30 min prior to CHO-K1 cell invasion. Heparin was seen to reduce PagN-promoted invasion of CHO-K1 cells dose-dependently (Fig. 5.2 (B)). A heparin concentration of 1 μg/ml reduced PagN-promoted invasion of CHO-K1 cells by 50%, while 80-% inhibition was achieved by the addition of 100 μg/ml. These data show conclusively that PagN binds to GAGs in a specific receptor/ligand interaction. The ability of PagN to bind specifically, in a dose-dependent manner, to CS was also investigated. It was revealed that PagN does not bind to CS in a dose-dependent, specific manner (results not shown).

5.2.1.4 Inhibition of PagN-promoted invasion by alteration of the host cell surface

To further establish the significance of proteoglycans in the PagN-mediated invasion of epithelial cells, eukaryotic cells were treated with several glycolytic and proteolytic enzymes prior to gentamicin protection assays. CHO-K1 cells were incubated at 37 °C with either heparinase III from *Flavobacterium heparinum* (75 mU/ml) or chondroitinase ABC from *Proteus vulgaris* (75 Um/ml) for 3 h prior to addition of bacteria. Heparinase III is a heparin-degrading lyase that recognises HSPG as its primary substrate, specifically hydrolysing the glycosidic linkage present in HS (248, 323) while chondroitinase ABC

cleaves chondroitin sulphate A, B and C moieties and dermatan sulphate from the host cell surface (418). These GAG lyases have been previously shown to fully remove HS and CS GAG moieties from proteoglycan core proteins (9, 116, 401). Cells were alternatively incubated at room temperature for 5 min with the proteolytic enzymes trypsin (100 μg/ml) or α-chymotrypsin (100 μg/ml). Post-treatment with trypsin or α-chymotrypsin, enzyme inactivation was accomplished by incubation of the cell monolayers at 37 °C for 5 min with soybean trypsin inhibitor (500 μg/ml).

Removal of HS by heparinase III resulted in a ~20% decrease in PagN-mediated invasion (Fig. 5.3). Surprisingly, CHO-K1 cells lacking CS showed a greater reduction in bacterial internalisation as compared to heparinase III-treated cells. Eukaryotic cells treated with chondroitinase ABC showed a 30% decrease in PagN-promoted invasion. These data strengthen previous findings that PagN interacts with GAGs during CHO-K1 interactions. Mild cleavage of host cell surface proteins using either α-chymotrypsin or trypsin greatly reduced *E. coli* entry of CHO-K1 cells. Invasion levels were reduced by 60% and 90% respectively, supplying the first evidence that PagN interacts with protein-linked GAGs during entry into CHO-K1 cells. These data, combined with data presented in previous sections, demonstrate that together, cell surface HSPGs and CS proteoglycans (CSPGs) play a crucial role in PagN-promoted invasion of epithelial cells.

5.2.2. PagN interacts with GAGs directly and indirectly

5.2.2.1 Does PagN interact directly with GAGs?

It has been reported previously that OpaA, a HSPG-binding protein from *Neisseria gonorrhoeae* mediates adhesion to CHO-K1 cells via a vitronectin (Vn) cross-bridge (96). OpaA mediates Vn-dependent invasion of CHO-K1 cells and Vn-independent invasion of Chang conjunctiva epithelial cells (401). Interestingly, in the Chang cell system, foetal calf serum (FCS) was not required for internalisation of OpaA-expressing *N. gonorrhoeae*, whereas invasion of CHO-K1 depended upon the presence of FCS, and specifically Vn from FCS (96, 401).

To determine if PagN-promoted invasion of CHO-K1 cells was dependent upon the presence of fetal bovine serum (FBS), invasion assays were performed with CHO-K1 cells in the presence and absence of FBS. Cells were seeded in 12-well trays in normal growth

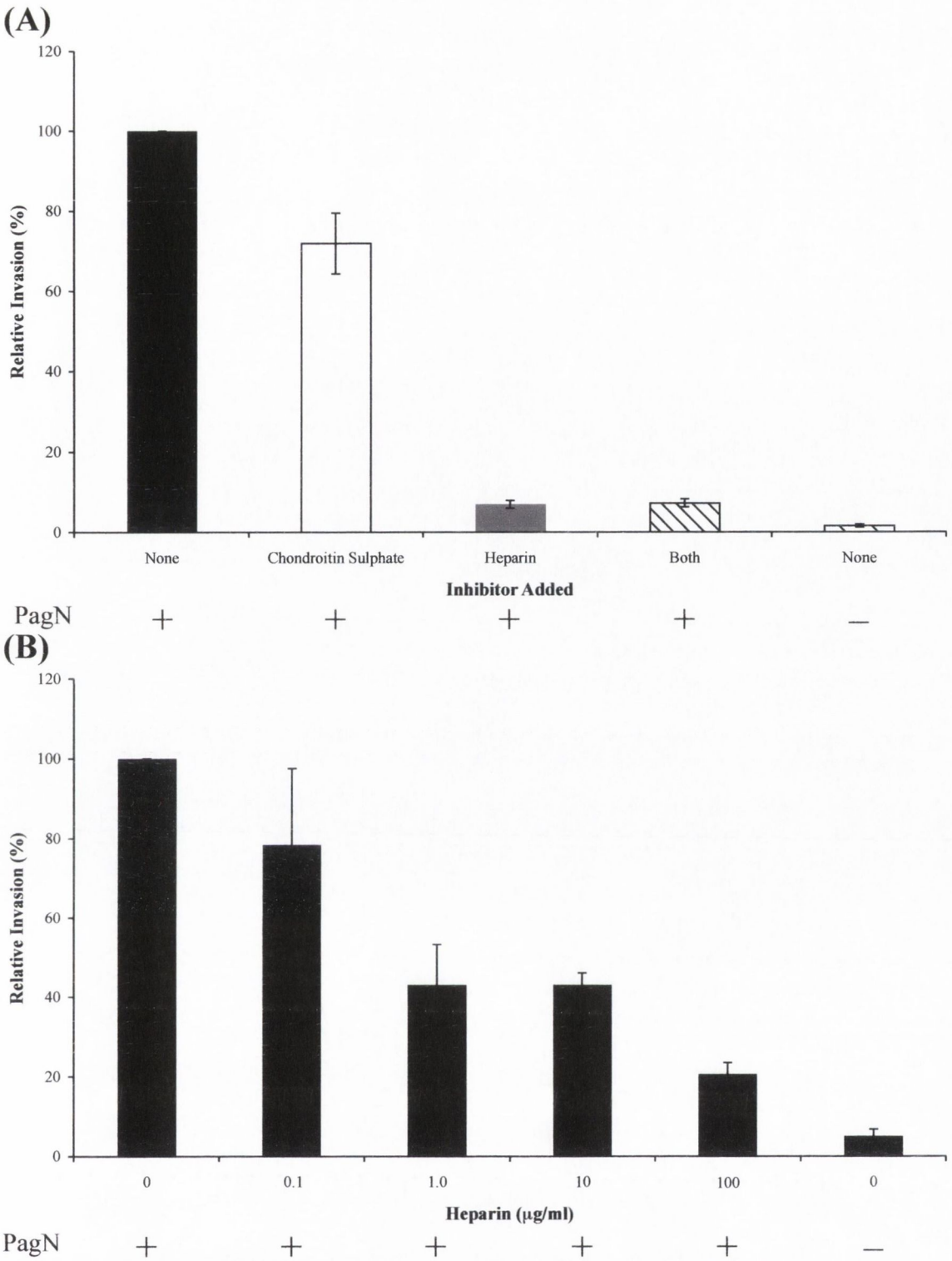

FIG. 5.2. (A) Inhibition of PagN-promoted invasion by exogenous GAGs. CS, heparin, or both (100 μg/ml) were incubated with *E. coli* K-12 expressing PagN at 37 °C for 30 min prior to the invasion assay. These cultures were compaired to untreated *E. coli* K-12 containing pML1 or pTrc99a. The invasion efficiencies were expressed as a percentage of the untreated positive control. **(B) Inhibition of PagN-promoted invasion by heparin.** Heparin (0.1, 1, 10, or 100 μg/ml) was incubated with cultures of *E. coli* K-12 DH5α harbouring pML1, at 37 °C for 30 min prior to the invasion assay. Pre-incubated cultures were compared to untreated *E. coli* containing the plasmid pML1 or pTrc99a as positive and negative controls. The PagN status of the bacteria is indicated below each column. The invasion efficiencies were expressed as a percentage of the untreated positive control.

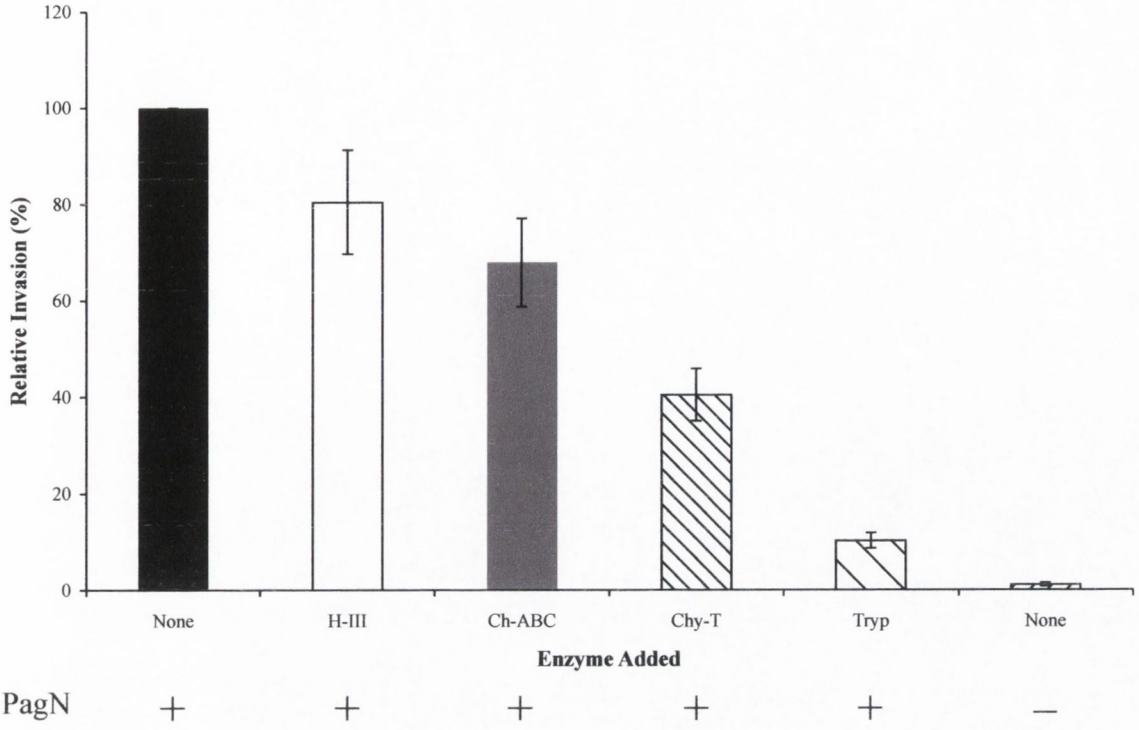

FIG. 5.3. Invasion of CHO-K1 cells after modification of host cell surface constituents. Entry into CHO-K1 cells was determined after pre-treatment of the cultured eukaryotic cells with heparinase-III (H-III; 75 mU/ml), chondroitinase-ABC (Ch-ABC; 75 mU/ml), α-chymotrypsin (Chy-T; 100 μg/ml), or trypsin (Tryp; 100 μg/ml). The PagN status of the bacteria is indicated below each column. The invasion efficiencies were expressed as a percentage of the untreated positive control.

medium (FBS 10% (v/v)) and grown until confluent. Prior to invasion assays, cell monolayers were washed several times with pre-warmed, serum-free medium. Eukaryotic cells were then challenged with *E. coli* K-12 strain DH5α, harbouring the plasmid pML1 or pTrc99a, suspended in medium with or without FBS.

TABLE 5.3. The effect of FBS on PagN-promoted CHO-K1 invasion

Adhesin Expressed	**Invasion (%) + FBS**	**Invasion (%) – FBS**
None	00.79 ± 0.24	00.46 ± 0.74
PagN	50.03 ± 5.69	12.00 ± 2.36

In the absence of FBS, PagN-promoted invasion displayed an ~4-fold decrease as compared to levels in serum$^+$ medium. The absence of FBS did not correlate with an abolition of PagN-promoted invasion of CHO-K1 cells. In the absence of FBS, *E. coli* expressing PagN were still capable of invading CHO-K1 cells, suggesting that PagN may promote two separate methods of invasion. Similar to the OpaA protein of *N. gonorrhoeae*, PagN may bind directly to proteoglycans on the cell surface and may also interact with epithelial cells through a serum-protein-based cross-bridge.

5.2.2.2 Are serum factors required for PagN-mediated invasion of CHO-K1 cells

To determine whether the serum factors were contributing to PagN-promoted invasion of epithelial cells at either the eukaryotic or prokaryotic cell surface, invasion assays were performed with increasing concentrations of FBS. *E. coli* expressing PagN were suspended in tissue culture medium containing 0, 5, 10 or 20% FBS. These preparations were used to challenge CHO-K1 cells and the percentage invasion was determined. Bacteria were more efficiently internalised in the presence of FBS at concentrations of 5% and 10%. At higher concentrations of FBS (20%), invasion by PagN$^+$ bacteria appeared to decrease as compared to the samples with normal (10%) FBS levels, indicating that the binding domains of the PagN protein may have become saturated by serum factors (Fig. 5.4 (A)).

As the CHO-K1 cells were cultured in medium containing FBS (10% (v/v)) prior to the invasion assay, it was unlikely that the invasion-promoting factor in FBS mediated its activity by binding directly to the epithelial cells. If this were the case, the factor would already have bound to its surface-located receptor and would therefore still be present after

washing with serum-free medium. To determine if the serum factor(s) was binding directly to the bacteria, PagN-expressing *E. coli* K-12 were incubated in tissue culture medium with different concentrations of FBS. Prior to serum-free invasion assays, bacteria were incubated with 10, 20 or 30% FBS at 37 ^{o}C for 30 min, then washed 3 times in serum-free media. In comparison to invasion levels achieved in serum-free media, PagN-expressing *E. coli*, pre-incubated with FBS, displayed elevated levels of invasion. As with assays where FBS was added back into the media, high concentrations of FBS (30%) seemed to inhibit invasion (Fig. 5.4 (B)). These data suggest that the serum-factor facilitating invasion was mediating its effect by directly interacting with the bacteria.

5.2.2.3 Does fibronectin or vitronectin contribute to PagN-promoted invasion of epithelial cells

As proteoglycans function as a link between the ECM and the cell cytoplasm, many ECM proteins have been identified as binding HS (for a review see (31)). It is thought that many of these ECM proteins may form cross-bridges between bacterial adhesins and their HSPG target receptors. In particular fibronectin (Fn), Vn, and platelet factor-4 (PF-4) have been implicated in interactions between bacterial adhesins and their HSPG receptors (9, 96, 116). To establish whether ECM proteins could restore the invasion defect displayed by PagN-expressing *E. coli* in serum-free media, Fn (15 μg/ml) and Vn (15 μg/ml) were added separately to invasion assays in which serum-free media was used. The level of invasion of treated cells was expressed as a percentage of normal invasion promoted by PagN in FBS^{+} media (Fig. 5.5). The addition of Fn failed to increase PagN-promoted invasion. Vn increased serum-free levels of invasion from 35% of the positive control to 61% of the control suggesting that PagN may bind to HSPGs through a Vn cross-bridge. However in repeated assays the effect of adding Vn was reduced suggesting that its contribution to PagN/HSPG binding may have been over estimated. It is important to note at this stage that the Vn Sigma-Aldridge product sheet comes with the following disclaimer "*Vitronectin rapidly absorbs to glass and polystyrene plastic surfaces. This property, together with its high affinity for other plasma proteins, makes it difficult to handle*". This may explain why on initial analysis, Vn seems to increase PagN-promoted invasion in serum-free media but on subsequent experiments does so to a lesser extent. PF-4 (5 μg/ml) was also tested in this manner but failed to increase PagN-promoted invasion (results not shown).

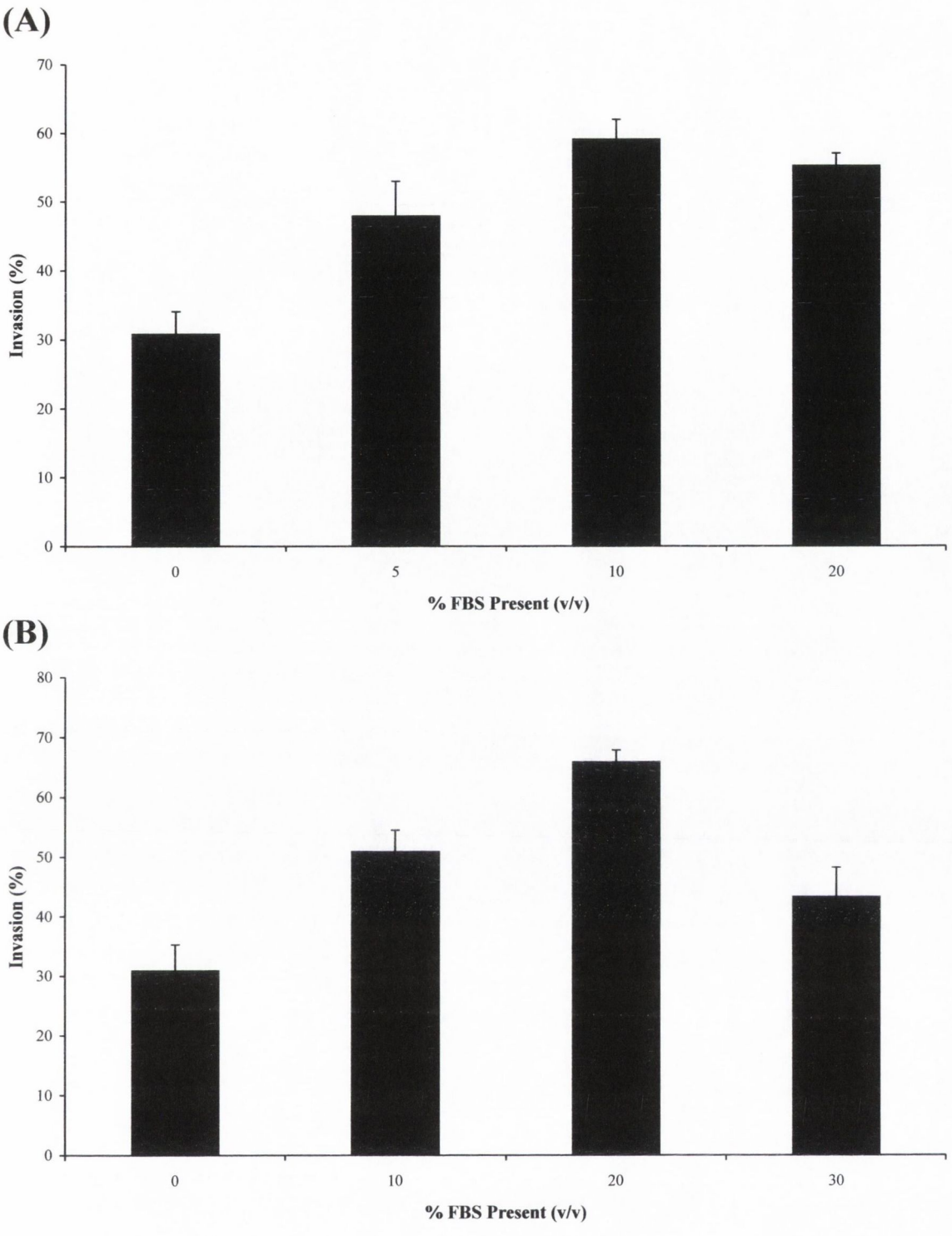

FIG. 5.4. Internalisation of PagN$^+$ *E. coli* in the presence of FBS. **(A)** CHO-K1 were washed with PBS and infected with *E. coli* DH5α harbouring the plasmid pML1 in the absence and presence of increasing concentraions of FBS. **(B)** *E. coli* expressing PagN were incubated with FBS and washed in PBS before addition to CHO-K1 cells. The percentage FBS present is indicated for each assay. Data represents averages from triplicate wells, and standard error bars are shown.

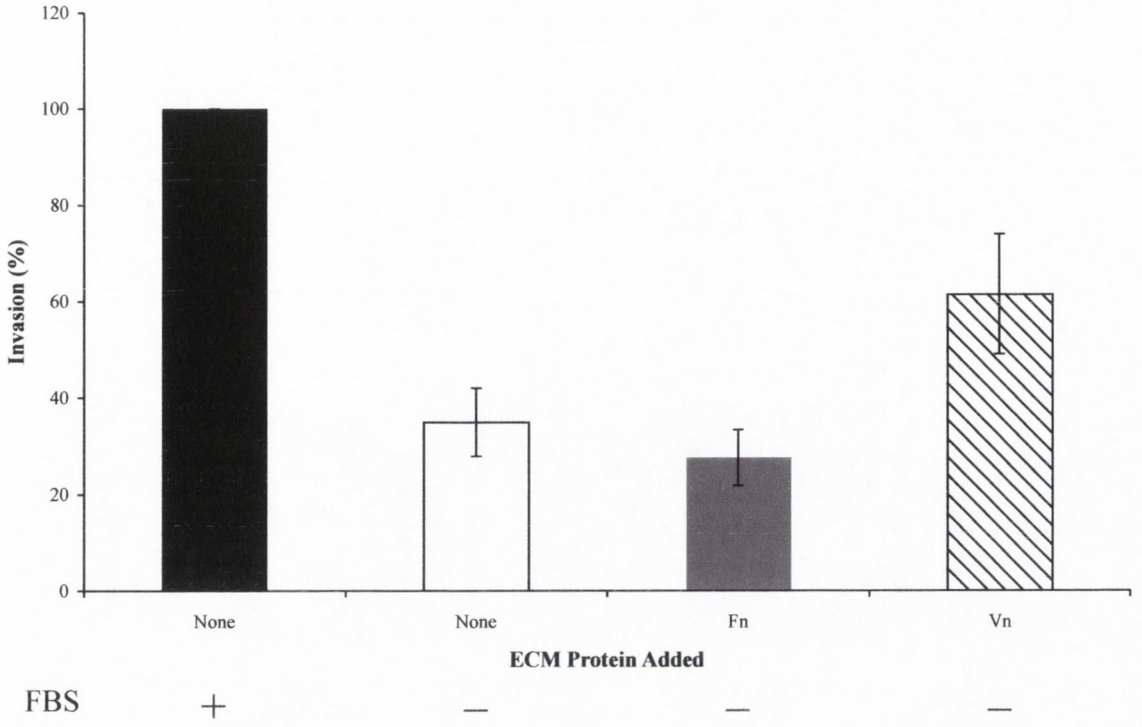

FIG. 5.5. Vitronectin may contribute to the entry of PagN$^+$ *E. coli* into CHO-K1 cells. Fibronectin (Fn) and vitronectin (Vn) (both at 15 μg/ml) were tested for their ability to confer entry of PagN-expressing *E. coli* into CHO-K1 cells. The FBS status of each triplicate set is indicated below each column. The invasion efficiencies were expressed as a percentage of the positive control, *E.coli* K-12 expressing PagN assayed in medium containing 10% (v/v) FBS. Data represents averages of triplicate wells, and standard error bars are shown.

5.2.2.4 Immunoprecipitation of PagN-binding proteins from FBS

As the selected testing of individual ECM proteins in Section 5.2.2.3 yielded only one candidate protein for enhancement of PagN-promoted invasion, a different approach was employed. Identification of serum-factors that bind directly to an MBP-PagN fusion protein was attempted. To do this, *E. coli* BL21(DE3) harbouring pML7 (Section 3.2.1.4 and Table 2.2) was grown overnight in OnEx^{TM} medium. *E. coli* expressing MBP-PagN were lysed by sonication. An aliquot of cell-lysate was incubated with FBS, with continuous mixing, at 4 ^{o}C for 1 h. The MBP-PagN fusion protein, along with any bound serum-factors, was removed from solution using amylose coupled to magnetic beads. The sample was incubated at 4 ^{o}C for 1h with continuous mixing. The amylose/MBP-PagN complex was washed several times in MBP column buffer to remove any serum proteins displaying non-specific binding. Any MBP-PagN/serum-protein complexes were further purified using an anti-MBP monoclonal antibody coupled to magnetic beads. Again any proteins binding non-specifically were removed. The procedure was performed in parallel with the negative control, *E. coli* BL21(DE3) harbouring the plasmid pMALc-2 (Table 2.2). MBP-PagN/serum-protein complexes were analysed by SDS-PAGE. *E. coli* BL21(DE3) harbouring pML7 incubated with PBS rather than FBS was used as a negative control (Fig. 5.6).

Comparison of samples purified from bacteria expressing MBP-PagN, incubated with either FBS or PBS, did not reveal any proteins unique to the FBS samples. However, 3 protein bands appeared to be bound by MBP-PagN isolated from *E. coli* incubated with PBS but not FBS. This analysis would suggest that the purification technique employed failed to identify any serum-factors that PagN may be binding during invasion of CHO-K1 cells. However, the 3 protein bands that appear to bind to MBP-PagN when bacterial lysates, containing MBP-PagN, are incubated with PBS warrant further investigation (See Chapter 6).

5.2.3 Proteoglycan binding by *S.* Typhimurium

5.2.3.1 Does *S.* Typhimurium interact with proteoglycans?

In previous sections, the *Salmonella*-specific adhesin PagN was conclusively proven to bind to proteoglycans. The abolition of PagN-promoted invasion in pgsA-745 cells was complete, indicating that for PagN-mediated invasion, host cell GAG-expression is absolutely required. Previously, *S.* Typhimurium has been reported to show no preference for heparin binding, and has even been used as a negative control for studies investigating bacterial/proteoglycan interactions (176, 177). To resolve these conflicting data, and more fully characterise the apparent presence of heparin-binding displayed by *S.* Typhimurium, cell association and invasion assays using *S.* Typhimurium, CHO-K1 and pgsA-745 cells were performed. *S.* Typhimurium strain SL1344 was grown to stationary phase in MM5.8 medium. These bacteria were washed and resuspended in sterile PBS and used to challenge both CHO-K1 and pgsA-745 cells in cell association and invasion assays (Fig. 5.7 (A)). In the absence of surface-expressed GAGs, cell association and invasion of CHO-K1 cells by SL1344 was reduced from 5.87 ± 0.83% to 1.05 ± 0.14% and 2.83 ± 0.28% to 0.16 ± 0.12% respectively. These data represent a ~6-fold and ~18-fold decrease for cell association and invasion respectively, indicating that *S.* Typhimurium binds to the GAG moieties of proteoglycans.

It was surprising that in the absence of GAGs, *Salmonella* invasion of CHO-K1 cells was reduced by more than 93%. As the reduction in invasion levels was so marked it was deemed necessary to test if pgsA-745 cells were capable of supporting internalisation of *S.* Typhimurium. This cell line was previously shown to support internalisation of several gram-positive and gram-negative strains (177); but *S.* Typhimurium was not tested in these studies. Bacterial invasion of epithelial cells can be divided into two mechanistic categories, the Zipper and Trigger mechanisms (73). *Yersinia* uses the Zipper mechanism while *Salmonella* generally employs the Trigger mechanism (73). Therefore, the ability of pgsA-745 cells to support *S.* Typhimurium invasion was evaluated using recombinant *S.* Typhimurium carrying the invasin of *Y. pseudotuberculosis.* The plasmid pRI203 (Table 2.2) contains the *inv* locus which encodes the INV protein, shown to promote attachment and invasion of epithelial cells by binding to the β1 chain of integrins (199). Previously, it has been established that *Y. pseudotuberculosis* with a wild-type *inv* gene invades CHO-K1 cells displaying 2.5-% invasion while those with an interrupted allele display 0.18-% invasion (365). The pRI203 plasmid was transformed into *S.* Typhimurium strain SL1344. Overnight bacterial cultures, grown at 37 °C in MM5.8 medium, were washed once in PBS and adjusted to an A_{600} of 2. These cultures were used to infect CHO-K1 and pgsA-745 cells in a standard invasion assay. Invasion levels displayed by *S.* Typhimurium strain SL1344 were compared to those of *S.* Typhimurium harbouring pRI203. The presence of

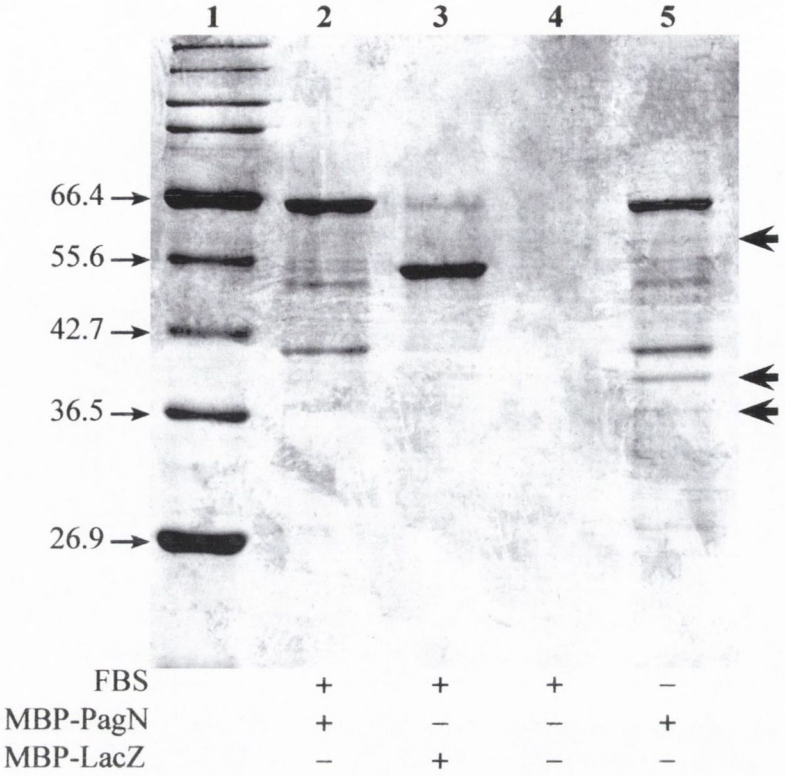

FIG. 5.6. SDS-PAGE analysis of purified MBP-PagN complexes. Lane 1 : Molecular weight standards in kDa. Lane 2: Purified MBP-PagN from lysate incubated with FBS. Lane 3: Purified MBP-LacZ from lysate incubated with FBS. Lane: 4 FBS and PBS incubated together and subjected to purification regime. Lane 5: Purified MBP-PagN from lysate incubated with PBS. Differences between MBP-PagN incubated with FBS and PBS are indicated on right.

the pRI203 plasmid promoted an 80-% increase in invasion. As previously seen (Fig. 5.7. (A)), *S.* Typhimurium invasion of CHO-K1 cells was abolished in the absence of GAGs (7.16 ± 0.28% reduced to 0.05 ± 0.01%), however *S.* Typhimurium expressing the INV protein displayed ~1-% invasion of pgsA-745 cells (Fig. 5.7 (B)). These data indicate that pgsA-745 cells support internalisation of *S.* Typhimurium and strengthens findings that *S.* Typhimurium binds to GAG moieties of proteoglycans during invasion of CHO-K1 cells.

5.2.3.2 Shedding of syndecans from the cell surface of HT-29 cells

Adhesion and invasion of CHO-K1 cells by *S.* Typhimurium was not inhibited by the addition of exogenous heparin (100 μg/ml), CS (100 μg/ml) or both (results not shown). Likewise, enzymatic removal of GAG moieties from CHO-K1 cell surfaces by heparinase III or chondroitinase ABC did not affect the invasion levels of *S.* Typhimurium with any statistical significance (results not shown). However, as the number of adhesins, with GAG-binding capabilities, expressed by *S.* Typhimurium is unknown, it was impossible to determine the appropriate level of exogenous inhibitor to add to the system. Similarly it was impossible to rule out compensatory effects of other adhesion loci during *S.* Typhimurium invasion of lyase-treated cells. Therefore, to investigate further the proteoglycan-binding capabilities of *Salmonella*, syndecan-1 and syndecan-4 were focused upon. As discussed in section 5.1, syndecan-1 and -4 are located on epithelial cells. Therefore, if *Salmonella* does bind to proteoglycans, it is likely to bind to either syndecan-1 or -4. Syndecans are mainly expressed on the basolateral surface of epithelial cells, however in non-polarised cultured cells, they are expressed ubiquitously over the entire cell surface (176).

It has been reported that host factors, such as TNF-α and IFN-γ (178) and bacterial proteins such as LasA of *Pseudomonas aeruginosa* (314) and α- and β-toxin of *S. aureus* (313) can cause syndecan shedding from the host cell surface. In particular, the *S. aureus* β-toxin promotes shedding of both syndecan-1 and -4 while α-toxin causes shedding of syndecan-1 only (313). These toxins were used to enhance shedding of syndecans from the surface of epithelial cells and subsequently determine the contribution of syndecan-binding during *S.* Typhimurium adhesion to epithelial cells.

It is established that bacterial supernatants from overnight cultures of *S. aureus*, when incubated with cultured NMuMG epithelial cells, enhance syndecan shedding (313). Therefore *S. aureus* strain 8325-4 was grown overnight in TS broth. The supernatant was filter-sterilised and diluted to 20% (v/v) in fresh tissue culture media. Confluent CHO-K1

monolayers were incubated at 37 °C, for 4 h, in the presence of this 20% (v/v) supernatant. However, microscopic examination revealed that such treatment resulted in over 90-% CHO-K1 cell lysis (results not shown), deeming this cell line unsuitable for further experimentation.

It has been demonstrated that artificial enhancement of syndecan-shedding by HT-29 cells resulted in neither a loss of viability or change in morphology (178). This cell line was therefore used in further studies. As was performed with CHO-K1 cells, confluent HT-29 monolayers were incubated with filter-sterilised *S. aureus* supernatant (20% (v/v)) for 4 h. As a negative control, monolayers were also incubated with 20% warmed TS broth. Cells were then washed several times with PBS to remove any bacterial proteins and shed syndecans. After incubation, cells were examined for any morphological changes; none were exhibited. Cell monolayers were then probed with the syndecan-1-specific, phycoerythrin-conjugated, monoclonal antibody DL-101. Comparison of untreated cell monolayers with TS broth- and supernatant-treated cells revealed that *S. aureus* supernatant causes the shedding of syndecan-1 from the HT-29 cell surface (Fig. 5.8). In an identical set of experiments, cells were analysed for the expression of syndecan-4 with the phycoerythrin-conjugated monoclonal antibody 5G9. Syndecan-4 was undetectable on the surface of HT-29 cells (results not shown).

5.2.3.3 *S.* Typhimurium does not bind to syndecan-1 on the surface of HT-29 cells

Studies by Henry-Stanley *et al.* have established that *S.* Typhimurium does not bind syndecan-1 (177). However, this group also failed to show that *E. coli* bound to syndecan-1 and reported that heparin-binding proteins were undetectable in 9 different strains of enterobacteria including *E. coli* and *S.* Typhimurium. This group used *S.* Typhimurium strain 10428, which may display phenotypic differences to strain SL1344. Therefore, the system outlined in section 5.2.3.2 was used to investigate the ability of *S.* Typhimurium strain SL1344 to bind syndecan-1.

Confluent HT-29 monolayers were incubated with filter-sterilised supernatants from *S. aureus* strain 8325-4, strain DU1090 (an α-toxin mutant), strain DU5719 (a β-toxin mutant) or strain DU5720 (an α- and β-toxin double mutant). Respectively, supernatant from these strains enhances shedding of both syndecan-1 and -4, low levels of syndecan-1 and -4, reduced amounts of syndecan-1, and no shedding. Therefore, as syndecan-4 was undetectable on HT-29 cells, the binding of *S.* Typhimurium to proteoglycans can be directly determined as different levels of syndecan-1 proteoglycan should be expressed by

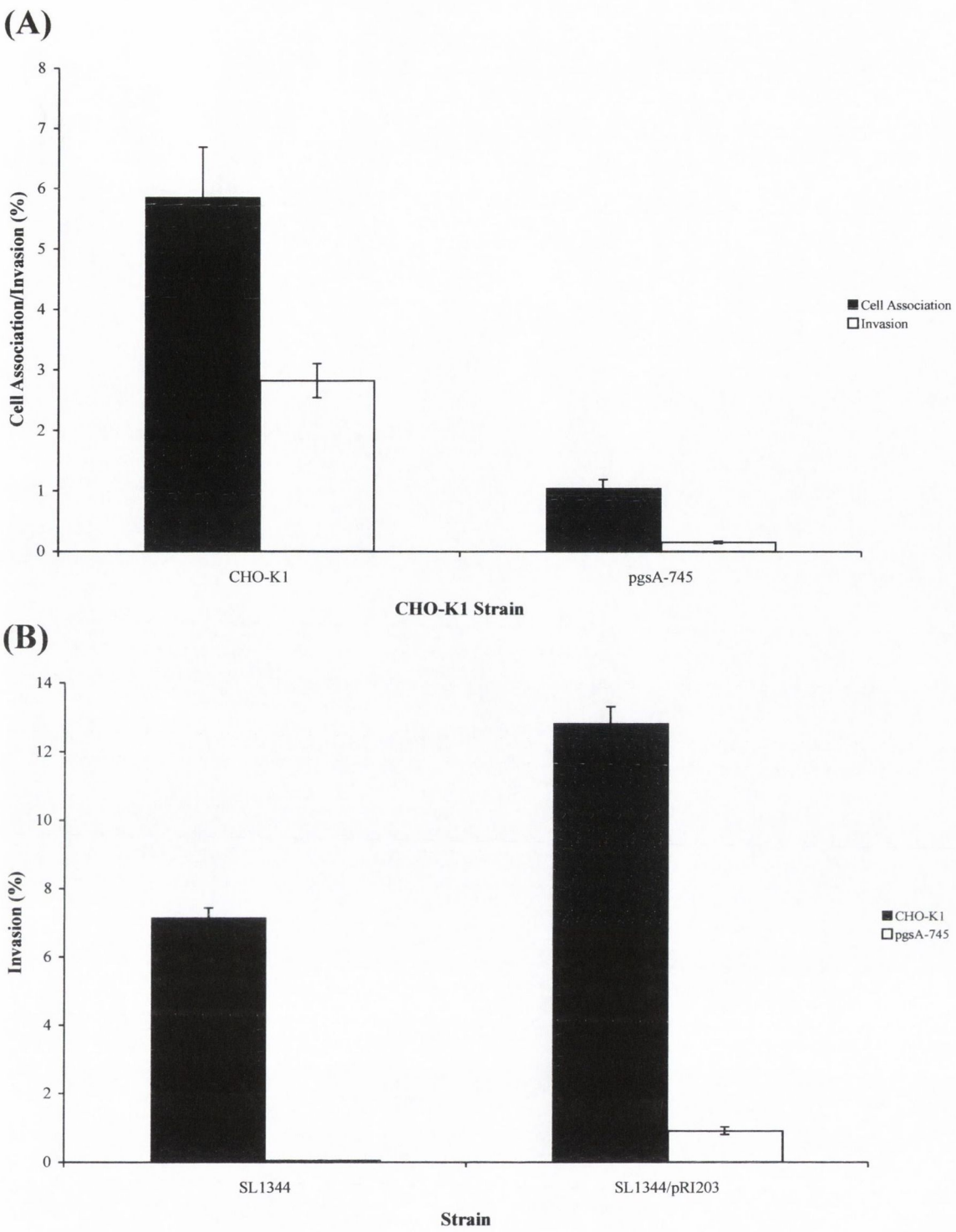

FIG. 5.7. *S.* Typhimurium interacts with glycosaminoglycans. (A) *S.* Typhimurium strain SL1344, grown to stationary-phase in MM5.8 medium, was incubated with wild-type (CHO-K1) or mutant (pgsA-745) cell-lines in standard cell association and gentamicin protection assays. **(B)** *S.* Typhimurium strain SL1344 and strain SL1344 harbouring the pRI203 plasmid were incubated with CHO-K1 and pgsA-745 cells and the level of invasion determined. Data represents averages from triplicate wells, and standard error bars are shown.

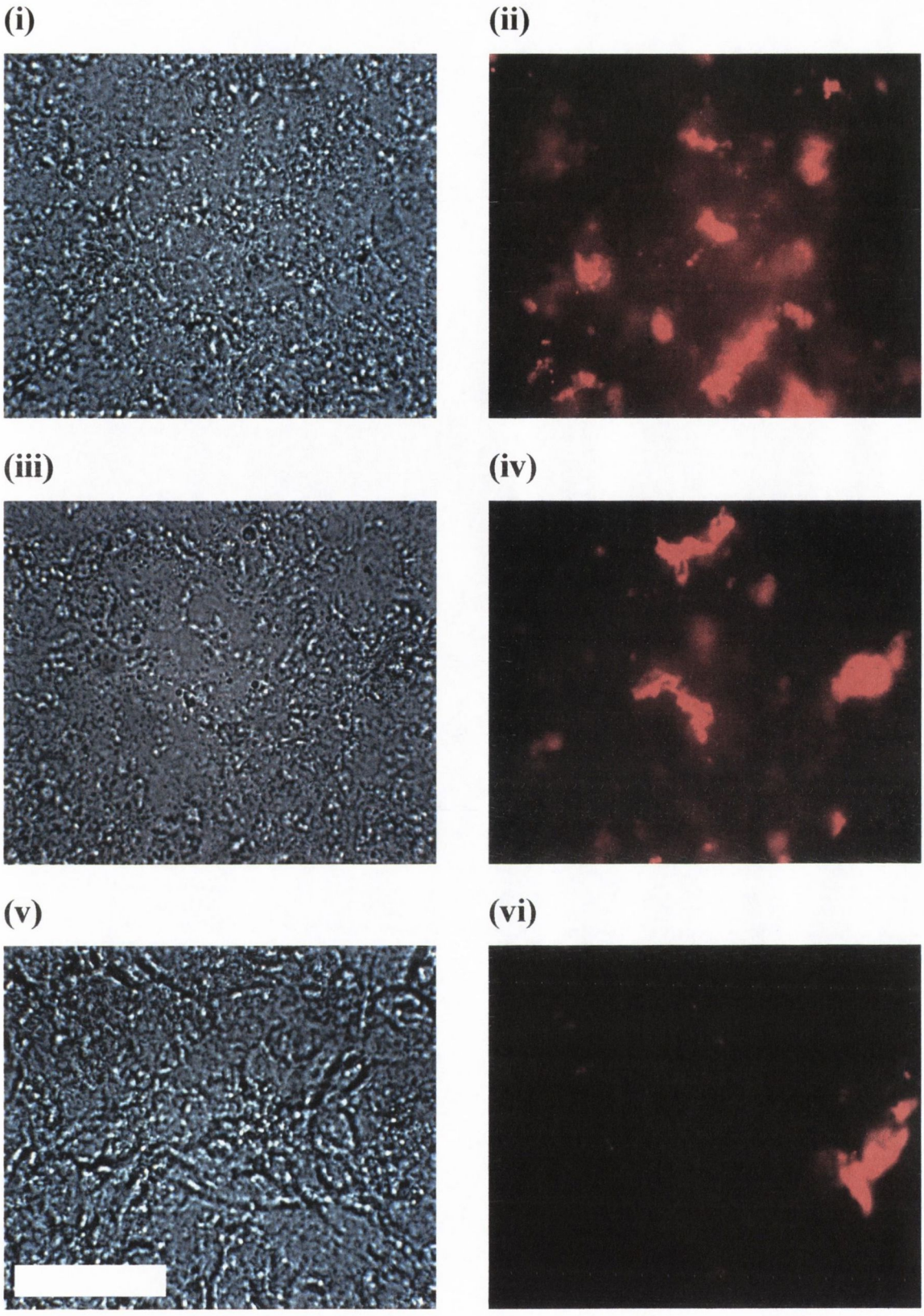

FIG. 5.8. Immunofluorescent localisation of syndecan-1 on mature confluent cultures of HT-29 cells. Panels (ii) and (iv) show intense staining of control enterocytes not exposed to *S. aureus* supernatant. Panel (vi) shows a marked decrease in staining after incubation with supernatant harvested from overnight cultures of *S. aureus* strain 8325-4. Panels (i), (iii) and (v) show the corresppponding light-microscope photograph to more clearly show the distribution of eneterocytes. Scale bar in panel (v) represents 5 mm.

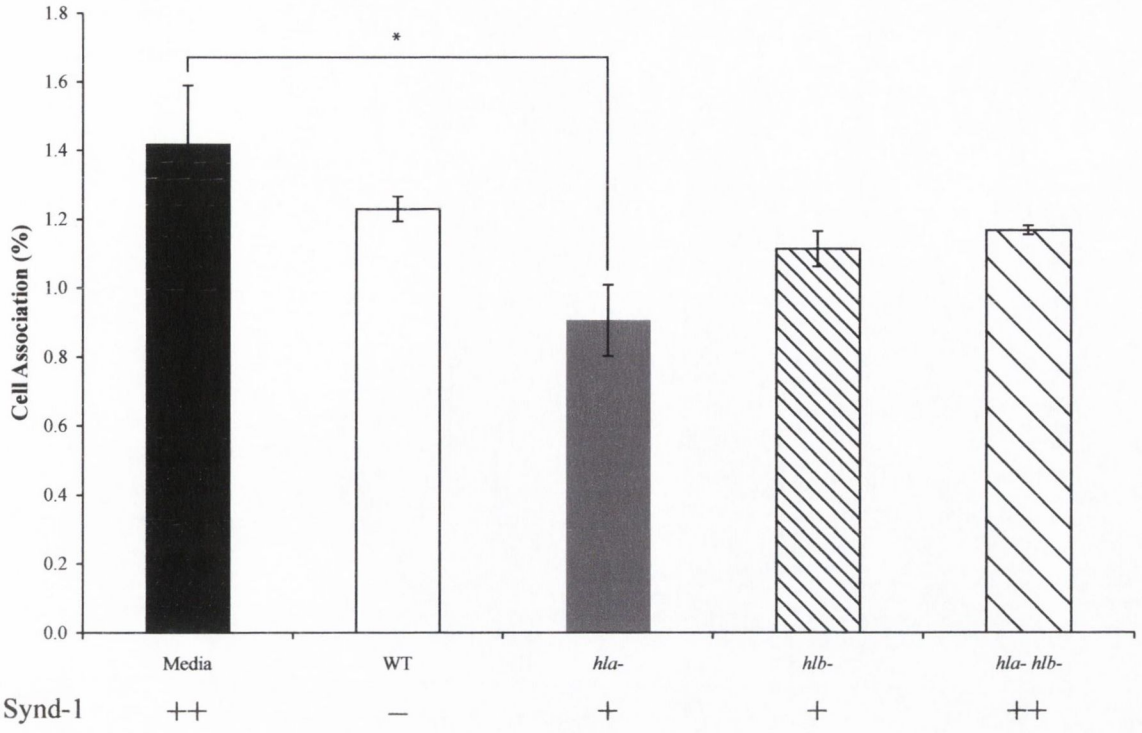

FIG. 5.9. Adhesion of *S.* Typhimurium to HT-29 cells after modification of host cell syndecan-1 distribution. Cell association of *S.* Typhimurium strain SL1344 with HT-29 cells was determined after pre-treatment of the eukaryotic cells with supernatants from overnight cultures of *S. aureus*. *S. aureus* strains used were the parent 8325-4 strain (WT), and mutant 8325-4 strains lacking α-toxin (*hla*–), β-toxin (*hlb*–) and α- and β-toxin (*hla*–*hlb*–). Prior to the assay, HT-29 cells were incubated at 37 °C for 4 h with 20% (v/v) *S. aureus* supernatants or fresh TSB (Media).

the differently treated monolayers. Fig 5.9 shows that the removal of syndecan-1 by supernatant from *S. aureus* strain 8325-4 did not result in a significant reduction of cell association. Counter intuitively, cells treated with supernatant from an α-toxin mutant displayed a reduction in cell association. However, overall, the level of cell association was not affected by syndecan-1 removal from the eukaryotic cell surface indicating that *S.* Typhimurium does not bind to syndecan-1 proteoglycans.

5.3 Discussion

As the Tia, Hek and OpaA adhesins are known to bind HSPGs (107, 116, 400), it was deemed necessary to investigate the ability of PagN to bind proteoglycans. Initial experiments with CHO-K1 cells, deficient in proper GAG presentation, indicated that PagN was capable of binding to the GAG chains of proteoglycans. When mammalian cells were grown in p-nitrophenyl β-D-xylopyranoside normal levels of adhesion were reduced by ~60%. These initial indications of a GAG binding capability of PagN were strengthened with assays using the CHO-K1 mutant cell line pgsA-745. Without GAG production, CHO-K1 cells were unable to support PagN-mediated internalisation of recombinant *E. coli*. Internalisation of bacteria due to the presence of PagN was completely abolished. Surprisingly, invasion levels of the negative control, *E. coli* DH5α containing the plasmid pTrc99a, were also completely abolished in pgsA-745 cells, indicating that the strain of *E. coli* used may have residual GAG-binding capabilities.

To further characterise the interaction of PagN with proteoglycans, exogenous GAGs were used to inhibit invasion of CHO-K1 cells by PagN-expressing *E. coli* K-12. The addition of the HS analogue, heparin, inhibited invasion by over 90%. Addition of CS caused much lower levels of inhibition suggesting that PagN binds preferentially to HSPGs. The preference of PagN to bind to HS over CS may be explained by consideration of the GAG chain placement on syndecan-1. Syndecan-1 is the major proteoglycan on epithelial cell surfaces. As PagN binds to proteoglycans its target could be syndecan-1. On syndecan-1, the most distal GAG substitution sites are predominantly HS, whereas the substitution sites closer to the cell surface are usually occupied by CS (31). Therefore, PagN/HS interactions are more likely to occur than interactions with the less accessible CS-containing GAG chains.

The specificity of the PagN/HS interaction was demonstrated by the ability of exogenously added heparin to inhibit PagN-promoted invasion in a dose-dependant manner. Often, heparin-binding proteins display motifs such as, R-X-B where B denotes a basic residue, and X denotes any amino acid (9) or X-B-B-X-B-X, where B represents a basic amino acid and X represents a hydrophilic amino acid (378). PagN has such a motif in loop 1 of the predicted structure; it also possesses several basic residues in the other predicted loop domains (See Chapter 6). These loops are thought to be flexible and thus heparin-binding pockets may be formed, lined with positively charged amino acids. These features supply further proof that PagN interacts with HSPGs. Exogenous addition of

dextran sulphate reduced PagN-promoted invasion marginally suggesting only a minor role for electrostatic forces between the positively charged PagN residues and the predominantly negatively charged HS. This inhibition was not statistically significant and must be considered with caution. The inability of CS to inhibit invasion and the dose-dependency of heparin inhibition of PagN suggests that the PagN/Heparin interaction is specific and relies not only on charge but also on specific conformational features. Final and conclusive proof that PagN binds to GAG moieties decorating the cell surface of CHO-K1 cells comes from data attained from assays involving enzymatic modification of host cell surfaces. Removal of HS, CS and core protein components of proteoglycans resulted in decreased levels of PagN-promoted invasion. Surprisingly, the removal of CS had a more deleterious affect upon invasion than removal of HS. This apparently aberrant result may be due to differential expression of CS and HS on CHO-K1 cell surfaces. As both enzymes were added at an identical concentration of 75 mU/ml for the same time period, it would be expected that they would process the same amount of substrate. However, the levels of HS and CS present on the surface of CHO-K1 cells may be vastly different, resulting in a greater proportion of HS, relative to CS, expressed on the cell surface after the enzymes are removed. This was not addressed during this study and therefore cannot be commented upon further. A second consideration is that apart from CS, chondroitinase ABC is known to catalyze the eliminative degradation of dermatan sulphate and hyaluronate (418). It is feasible that PagN may bind to either dermatan suphate or hyaluronate; thus their removal may reduce PagN-mediated invasion of CHO-K1 cells. Proteolytic removal of the core proteins of proteoglycans had the most detrimental affect on PagN-mediated internalisation of *E. coli*. However, the removal of core proteoglycan proteins did not fully abolish invasion, suggesting that PagN may bind to another cell-surface receptor. This possibility was not investigated.

In the absence of serum, PagN-promoted invasion of CHO-K1 cells was greatly reduced. During invasion assays, involving serum-free media, internalisation of *E. coli* expressing PagN, was reduced by ~75%; but not abolished. This would suggest that the presence of serum-factors enhance PagN adhesion to epithelial cells. The serum factors were seen to promote binding of CHO-K1 cells by interacting directly with the bacteria rather than at the eukaryotic cell surface. This has been seen previously for the OpaA adhesin of *N. gonorrhoeae* (96). The addition of Vn to serum-free assays contributed slightly to the invasion phenotype. This suggests that Vn may be involved in PagN/cell interactions. Indeed PagN/cell interactions may fit into a paradigm proposed for heparin-binding proteins (HBPs). Duensing *et al.* reported that bacteria may use heparin-binding adhesins

to recruit a diverse array of HBPs to their surfaces, bypassing the need to synthesise individual receptors for each of these proteins (97). Considering this, it may have been more prudent to incubate PagN-expressing *E. coli* with heparin prior to the addition of ECM proteins to the system. This method was adapted by Fleckenstein *et al.* resulting in the dose-dependant binding of Vn and Fn by Tia (116).

The identification of serum-factors capable of binding to PagN was attempted but no factors were identified. However three protein bands were selected as possible bacterial PagN-interacting proteins. Further analysis of these was carried out, and is discussed in Chapter 6. There are several possible explanations for the inability to isolate PagN-binding proteins from serum to be considered. The vector, pMALc-2, used to construct the MBP-PagN fusion protein is a derivative of pMALp-2. The difference between the two vectors is that pMALc-2 encodes an MBP-fusion protein lacking a signal sequence. Therefore, the pML7 plasmid gives rise to a cytoplasmically located MBP-PagN fusion protein, which will not be exported to the outer membrane where PagN is normally located. As it is not resident in its native location, PagN may be incorrectly folded. PagN may form multimers in the outer membrane, or even function in conjunction with other outer membrane proteins. Without these factors, the protein may not adopt its native conformation and may therefore be incapable of binding proteins with wild-type levels of affinity. Another factor to consider is that the MBP moiety of the fusion may sterically hinder PagN in binding to its cognate receptor. The bulky amino-terminal protein may prevent PagN from gaining access to the serum-factors it is capable of binding when expressed in it native form. Indeed in Chapter 3 it was noted that the MBP was capable of inhibiting PagN-promoted haemagglutination. Again, it may have been advisable to incubate the bacterial lysates with heparin prior to serum. In this way, a PagN-heparin-serum factor complex may have been established more easily.

Interestingly, data presented suggests that *S.* Typhimurium depends upon eukaryotic GAG expression when invading CHO-K1 cells. Wild-type bacteria displayed highly reduced adhesion and invasion levels of pgsA-745 cells, indicating that *S.* Typhimurium strain SL1344 may bind to the GAG moieties of proteoglycans. The reduction in cell association was far less dramatic than that seen for invasion (5.6-fold and 17.7-fold decrease respectively). These data would suggest that although GAG moieties may be involved somewhat in the initial attachment of *Salmonella* to the epithelium surface, their role during invasion may be more substantial. This role was strengthened by the fact that pgsA-745 cells were shown to support internalisation of *S.* Typhimurium as can be seen with *S.* Typhimurium expressing INV from the pRI203 plasmid.

In order to more fully characterise this apparent reliance upon cell surface GAG expression, the ability of *S.* Typhimurium to bind to syndecans was investigated. In contrast to cell lines such as Caco-2, HT-29 enterocytes express high levels of syndecan-1 (176). This cell line is therefore ideal for investigating syndecan-1 binding. Analysis of confluent HT-29 monolayers revealed that syndecan-4 was not detectable on the cells surface. Supernatants from *S. aureus* were used to enhance syndecan-1 shedding thereby decreasing the level of expression on the HT-29 cell surface. When treated with supernatant from wild-type *S. aureus*, *S.* Typhimurium adhesion was not decreased by any significant amount indicating that *S.* Typhimurium does not bind to syndecan-1 proteoglycans. HT-29 cells treated with supernatant from α-toxin-defective *S. aureus* displayed significantly reduced levels of bacterial binding ($P < 0.05$). However, greater adhesion levels were supported by cells treated with supernatant from a *hla hlb* double mutant of *S. aureus*, indicating this reduction may be an artifact. It is feasible that HT-29 cells treated with bacterial supernatants may display physiological changes affecting the levels of bacterial interaction they support. It must also be noted that HSPGs have recently been implicated in *S. aureus* interactions with intestinal epithelium (185). It is likely that *S. aureus* interact with these HSPGs using one or more of the highly promiscuous microbial surface components recognising adhesive matrix molecules (MSCRAMMs). MSCRAMMs, such as clumping factor B, are subject to proteolysis by the *S. aureus* metalloprotease aureolysin (263), which causes shedding of the MSCRAMM into the bacterial supernatant. Therefore, treatment of HT-29 monolayers with *S. aureus* supernatant may allow shed MSCRAMMs to bind to surface-located *Salmonella* receptors, thus inhibiting cell association. The α-toxin defective *S. aureus* strain DU1090 may secrete/shed elevated levels of protein, capable of interacting with *S.* Typhimurium receptors, into the supernatant thus increasing the inhibitory effect. Further studies would be required to verify any of these hypotheses.

The use of siRNA to silence the syndecan-1 gene may serve to further explain the apparently disparate results attained during these studies. Without further experimentation, the ability of *S.* Typhimurium to interact with syndecan-1 cells remains in question. However, it would appear that *S.* Typhimurium interacts with GAG chains of proteoglycans as demonstrated by pgsA-745 cells. *S.* Typhimurium may interact with CHO-K1 cells via syndecan-4 which were not identified on the surface of HT-29 cells.

Data presented in this chapter has revealed that PagN promotes bacterial attachment to and invasion of epithelial cells through interactions with proteoglycans. In particular, it was demonstrated that the protein interacts specifically with heparin, suggesting that it

binds preferentially to HSPGs and secondarily to CSPGs. It is thought that bacterial interactions with proteoglycans may cause uptake of bacteria through reorganisation of actin filaments. In epithelial cells, syndecans transduce signals from the cell exterior to the interior via their syndecan-specific variable domain. Indeed it has been established that syndecan-4 complexes with protein kinase Cα (PKCα) and PtdIns(4,5)P_2 and is then thought to phosphorylate regulators of Rho-family GTPases and actin associated proteins (74). Syndecan-2 has also been shown to cause cytoskeletal rearrangements in neuronal cells via activation of the Rho GTPase Cdc42 (196). With this is mind, it may be suggested that PagN-mediated interactions with HSPGs on epithelial surfaces promote reorganisation of actin filaments thus enabling bacterial internalisation.

It was established that PagN can interact with HSPGs independently of serum-factors as well as in a manner enhanced by unidentified serum-factors. These serum-factors may serve as a bridging protein between PagN and surface-expressed HSPGs; whatever their mode of action, it was demonstrated that they enhance bacterial internalisation by eliciting their effects at the bacterial surface rather than the mammalian cell surface.

Chapter 6

Structure/function analysis of PagN

6.1 Introduction

The cytoplasm of gram-negative bacteria is encased by two radically different lipid bilayer membranes, themselves separated by a periplasmic space. Although both membranes contain proteins which assist in the communication of information across the membrane barrier, the overall composition and function of these semi-permeable barriers is markedly different (337). The inner membrane is a typical lipid bilayer composed exclusively of phospholipids distributed equally between the inner and outer leaflets (337). By contrast, the composition of the outer membrane differs significantly. The inner leaflet of the outer membrane (consisting of phospholipids) is similar to the inner membrane (295). However, the outer leaflet of this highly asymmetrical outer membrane is composed of lipopolysaccharides (295). Both membranes contain high concentrations of proteins.

Integral membrane proteins either consist of α-helical bundles or β-pleated sheets. These two structural classes not only serve to categorise membrane proteins but also defines their location. Transmembrane α-helical proteins are typically embedded in the inner membrane while proteins (in the form of a closed barrel), consisting of β-sheets are confined to the LPS-based outer membrane (217). Roughly one half of the outer membrane consists of protein (217). This can be divided into murein lipoprotein and integral, membrane-spanning β-barrels. The amino-terminus of murein lipoproteins consists of three fatty acid groups which penetrate into the inner leaflet of the outer membrane. The rest of the protein, in α-helical form, is located in the periplasm (295). The rest of the outer membrane protein complement consists of β-barrel proteins.

Integral membrane proteins expose a hydrophobic surface to the lipid bilayer core. Long before the first crystal structure of a membrane protein was solved it was predicted that, in order to saturate the entire hydrogen-bonding potential of the protein, only regular secondary structural elements (α-helices and β-sheets) were feasible within the lipid bilayer. The first crystal structure of an outer membrane protein was the porin of *Rhodobacter capsulatus* (409). This structure confirmed previous predictions that outer membrane proteins form β-barrels. Subsequent crystal structures have strengthens the hypothesis that all outer membrane proteins of gram-negative bacteria adopt a β-barrel structure.

Transmembrane β-barrel proteins fulfill a set of criteria, some being more exact than others. They consist of an even number of β-sheets with the amino- and carboxy-termini

located in the periplasm. The number of anti-parallel β-sheets may range from 8 to 22 (217) and their tilt range from 20 to 45° (412). These sheets are connected by short periplasmic turns and longer extra-cellular loops. The predicted size for periplasmic turns ranges from 2 to 8 amino acids while the lowest number predicted to be feasible for loop formation is 5 (406). This topology gives rise to a tightly rolled cylindrical shape reminiscent of a wine barrel. It has been noted that the β-sheets of proteins functional as monomers are longer than those of multimeric proteins (384), specifically 11 amino acids for trimeric proteins and 13-14 residues for monomeric β-barrels (384). The tilt of the β-strands is generally higher in longer sequences therefore the minimum number of residues required to span the membrane is greater.

The primary amino acid composition of the β-sheets gives rise to an amphipathic barrel. Residues facing the bilayer are mostly hydrophobic while those exposed to the channel interior are polar. The size and hydrophobicity of the protein channel varies between β-barrels. For example porins such as OmpF from *S.* Typhimurium have water-filled, hydrophilic channels while the membrane adhesin OpcA of *Neisseria meningitidis* has a closed channel (325). A conserved feature amongst β-barrels is the overrepresentation of aromatic residues found in two rings at the interface between the sheet and loop domains and the sheets and turns. This aromatic girdle is thought to bridge the polar and non-polar environments present at the protein/bilayer interface.

The purpose of this study was to predict the structure of PagN and determine how this structure lends itself to the protein function. The questions deemed most relevant in this study were:

- What is the predicted topology of PagN?
- Which regions of the protein are required for its role as an adhesin?
- Do basic residues have specific functions?
- How does the structure/function relationship of PagN compare to that of Hek?
- Does PagN associate with any bacterial proteins?

6.2 Results

6.2.1 Predicting the structure of PagN

6.2.1.1 Analysis of the amino-terminal sequence of the PagN protein

The *pagN* ORF consists of 720 bp corresponding to 239 amino acids. Analysis of the primary sequence revealed the presence of a putative amino-terminal signal peptide, displaying the characteristic hallmarks of a Sec-dependent signal sequence. This proposed signal peptide, 22 residues in length, displays several features typical of bacterial proteins translocated across the inner membrane via the Sec secretion system. The peptide can be split into three domains. The N-domain, as expected, is highly polar and contains a lysine residue at position 2 supplying an overall positive charge. The H-domain (F5 to W16) is highly hydrophobic and devoid of strongly polar residues (although a cysteine residue is present at position 8). Finally, within the C-domain the putative leader peptide contains alanine residues at positions -3 and -1 relative to the start of the predicted mature protein. Amino acids with short side chains, such as alanine, are typically located in these positions and act as a recognition signal for the signal peptidase (326). This prediction was supported by sequence similarity between PagN and the Hek adhesin (Fig. 3.2). The mature Hek protein starts with an identical Lys residue at the amino-terminal end of the protein which is preceded by identical alanine residues at positions –1 and –3 relative to the start of the mature protein.

The presence of the predicted signal sequence was strengthened by sequence analysis using the SignalP 3.0 program (29). The program agreed with predictions that the first 22 amino acids of the primary sequence form a signal sequence with a cleavage site immediately after the Ala, the twenty-second residue (Fig. 6.1 (A)). The proposed division of the signal peptide was also confirmed (Fig. 6.1 (B)), establishing that residues 1-4 form the N-domain, while the H-domain runs from F5-W16 and the C-domain contains residues 17-23. Final confirmation of the signal peptide came from sequence analysis using the web-based program LipoP 1.0 (204). This program agreed with predictions that PagN has an amino-terminal signal sequence which is cleaved between position 22 and 23. LipoP 1.0 gave a log-odds score of 16.54 where a value of -3 was the cutoff. These data demonstrate that PagN has a signal sequence, suggesting that it is translocated across the inner membrane via the Sec secretion system.

(A)

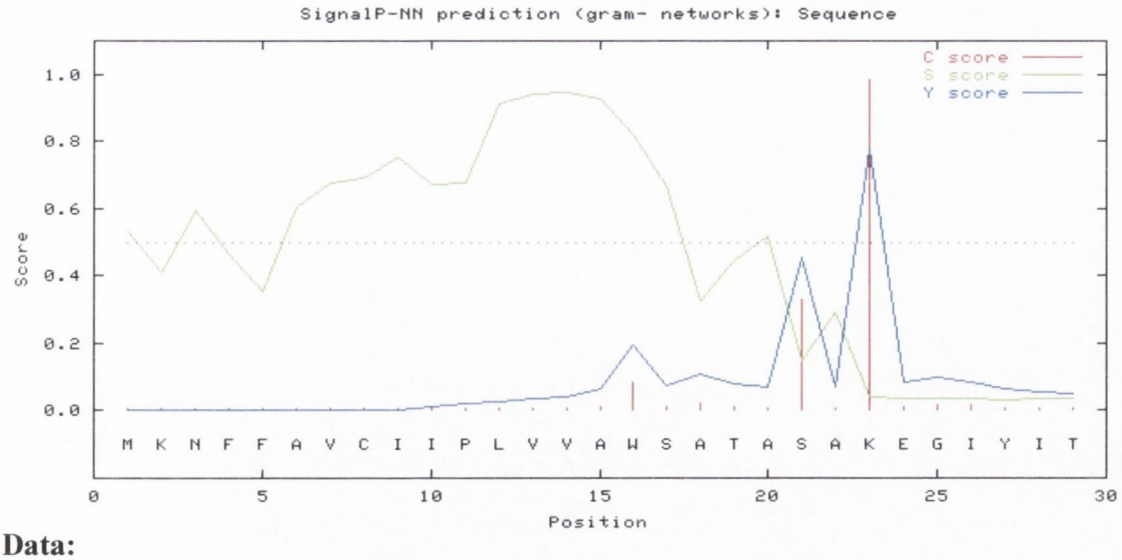

Data:

Measure	*Position*	*Value*	*Cutoff*	*Sig. Peptide?*
max. C	23	0.798	0.52	Yes
max. S	3	0.981	0.92	Yes
mean D	1-22	0.787	0.44	Yes

Most likely cleavage site between positions 22 and 23: ASA-KEG

(B)

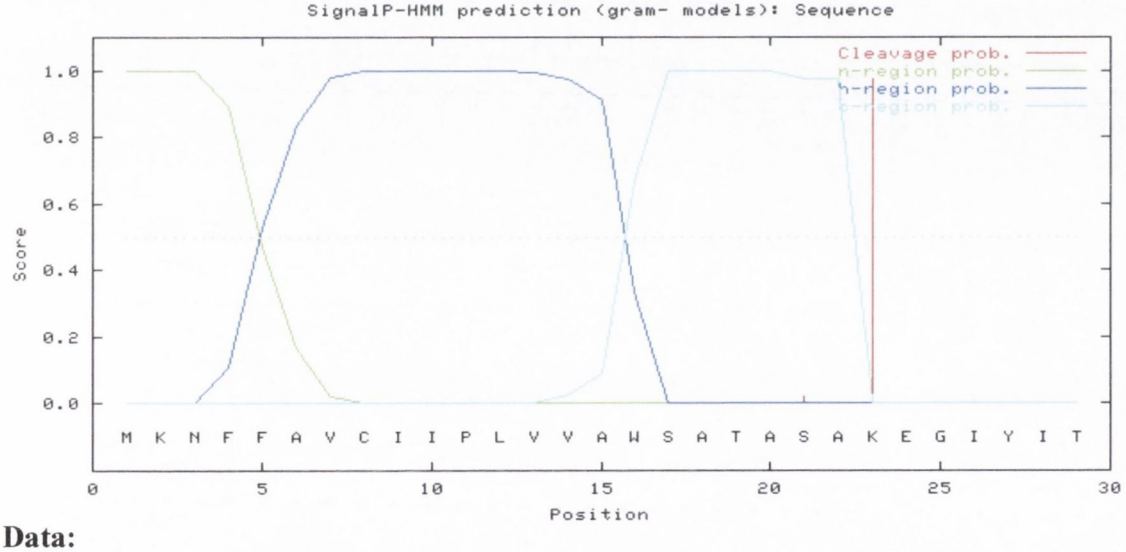

Data:

Prediction: signal sequence
Signal peptide probability: 1.00
Maximum cleavage site probability: 0.807 between positions 22 & 23

FIG. 6.1. (A) SignalP-NN result. The C score is the "cleavage site" site score. For each position in the sequence submitted, a C-score is reported which should only be significantly high at the cleavage site. The S-score is reported for every amino acid in the submitted sequence, with high scores indicating that the corresponding amino acid is part of a signal peptide. The D-score is a derivative of the average of the C- and S-scores which discriminates between secretory and non-secretory proteins. **(B) SignalP-HMM result.** The predicted domains of the signal peptide are shown along with the probability that the submitted sequence forms a signal peptide.

6.2.1.2 PagN is predicted to adopt a beta-barrel secondary conformation

The secondary structure of the mature 217-residue PagN protein was predicted using four web-based structural modeling programs: PredictProtein (www.predictprotein.org), PORES (http://garlic.mefos.hr/pores), PSIPRED (http://bioinf.cs.ucl.ac.uk/psipred) and transFold (http://bioinformatics.bc.edu/clotelab/transFold/). The mature protein sequence met all criteria set out by PORES with an "excellent" score. Most β-barrel proteins have few cysteines and prolines and a relatively large number of glycines and alanines; the mature PagN protein has no cysteines and only 7 prolines, while it contains 46 glycines and alanines. The protein is predicted to contain 8 amphipathic β-sheets separated by alternating short (2-6) or long (26-29) stretches of amino acids. Characteristic of β-barrel proteins, each β-sheet consists of alternating hydrophobic residues (217). β-barrel proteins often possess an aromatic girdle at the interface where the hydrophobic core ends and polar interface begins (217). Many of the β-sheets of PagN are flanked by aromatic residues, creating such a girdle. Based on these observations, PagN is likely to adopt a β-barrel conformation in the outer membrane consisting of 8 anti-parallel β-sheets, connected by 4 long, flexible, surface-exposed loops and 3 short periplasmic turns. The predicted surface-exposed loops were found to contain a large number of charged residues. A model of PagN is predicted in Fig. 6.2 highlighting the main secondary structural features.

6.2.2 Structure/function analysis of the PagN protein

6.2.2.1 Construction of *pagN* loop-deletion mutants

The predicted structure of PagN suggests that the β-barrel protein possesses four surface-exposed loops. Structural consideration of other β-barrel outer membrane proteins reveals that the β-sheets are buried within the outer membrane and it is only the hydrophilic loops that are exposed to the external environment (217). It is therefore likely that it is one or more of these four loops that interacts with the PagN receptor. To determine which of these loops is involved in PagN-mediated bacterial adhesion, a series of loop-deletion mutant ORFs were constructed based on the PagN expression vector, pML1. Inverse PCR, using divergent primers, which flank the region to be deleted (Table. 2.3), was used to generate a linear fragment lacking the DNA sequence corresponding to a particular loop domain. Ligation of this linear DNA produced an expression vector capable of expressing

a mutant PagN protein, lacking one of the four loop domains. In order to retain a correctly folded protein, the individual loops were replaced with Arg-Ala di-amino acid sequence (Fig. 6.2). Arginine was chosen for its turn-promoting properties (342) and Ala as it has a short side chain. Conveniently, the DNA coding sequence for Ala and Arg, GCG CGC, introduces a *Bss*HII restriction endonuclease recognition site, allowing for fast and easy screening of putative mutant vectors. In this manner, four expression vectors were constructed each one lacking the DNA coding for one of the four predicted loops domains. The structure of putative mutant plasmids was confirmed by PCR and diagnostic endonuclease digests. Each plasmid was sequenced to confirm the DNA sequence of the insert and they were designated pLoop1, pLoop2, pLoop3, pLoop4 indicating which loops had been removed. The extent of each loop-deletion is indicated on the predicted topological model depicted in Fig. 6.2.

6.2.2.2 Expression of PagN loop-deletion mutants

To confirm the expression and surface-location of all four loop-deletion mutant proteins, sarcosyl-extracted outer membrane fractions from *E. coli* K-12 containing each of the four mutant expression vectors and the parental construct pML1 were separated by SDS-PAGE, transferred to a nitrocellulose membrane and analysed by western immunoblotting using PagN-specific polyclonal antiserum (Fig. 6.3 (A)). Proteins of the correct predicted size were detected for all four mutants.

To determine if the truncated proteins were inserted correctly into the outer membrane and presented in a functional form, *E. coli* K-12 strain DH5α containing the plasmids pML1 or pLoop1-4 were grown to mid-logarithmic phase and induced with IPTG. Bacteria expressing mutant or wild-type PagN protein were fixed in formaldehyde and probed with PagN-specific polyclonal antiserum. PagN expression was detected using a FITC-labeled anti-rabbit secondary antibody by flow cytometry (Fig. 6.3 (B i and ii)). The mean channel fluorescence displayed by the mutant proteins, with the exception of the loop 1 mutant, was greater than wild-type levels. The plasmid pLoop4 gave rise to ~6-fold greater fluorescence than pML1, while pLoop2 and pLoop3 displayed levels ~2-fold greater. These data indicate that all mutant proteins are inserted in the outer membrane and with the exception of the loop 1 deletion mutant, display greater antibody-accessibility when probed with anti-PagN polyclonal antiserum.

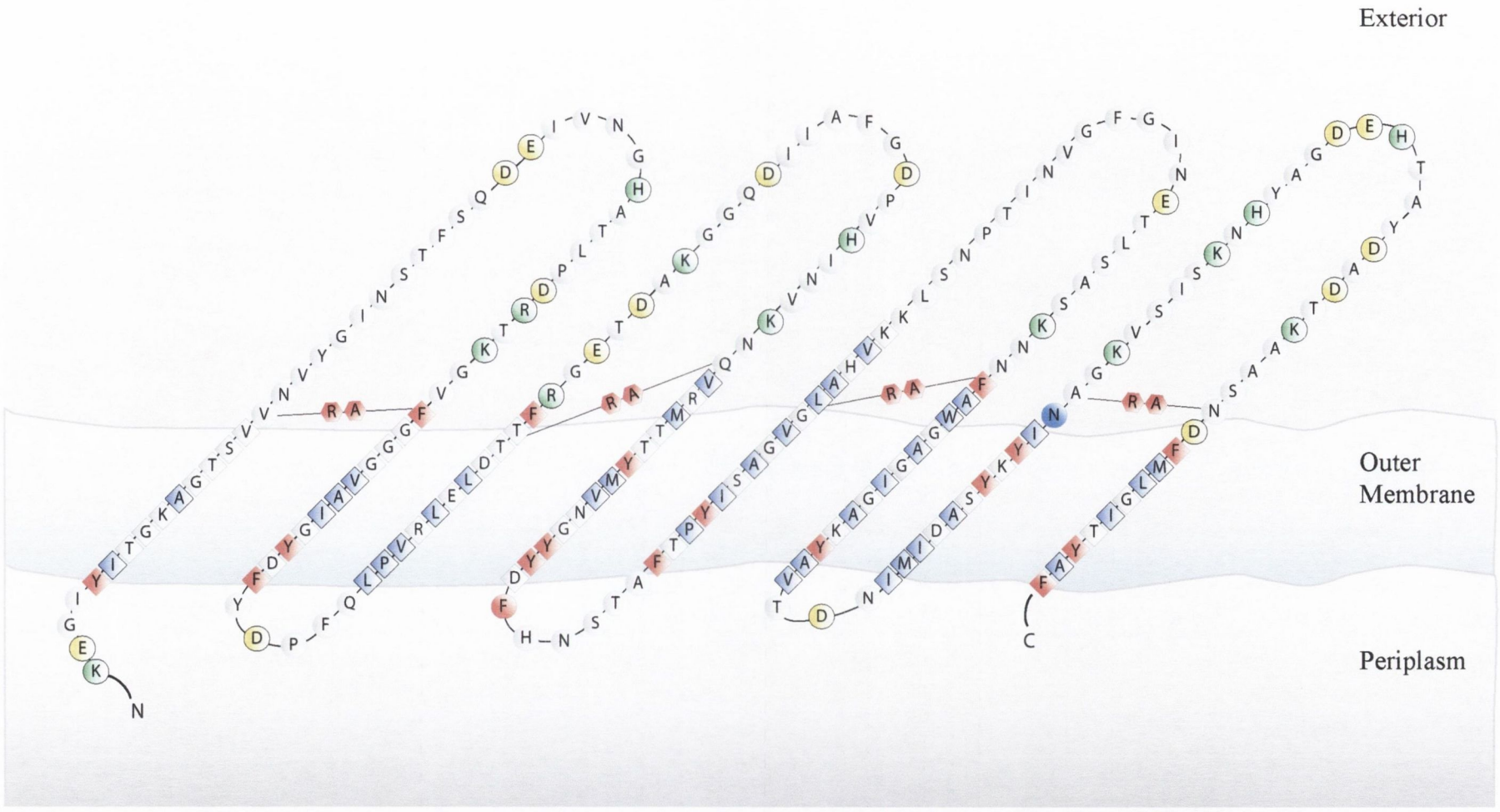

FIG 6.2. Topological model of the mature PagN protein. Residues predicted to form β-sheets are indicated by diamond-shapes, while those predicted to be contained within loops are represented as circles. The pattern of alternating hydrophobic amino acids is highlighted in blue and the aromatic residues which may form girdles around the barrel are coloured red. Surface-exposed basic and acidic residues are coloured green and yellow respectively. The Arg and Ala residues in red hexagons show the extent of each loop deletion as described in Section 6.2.2.1.

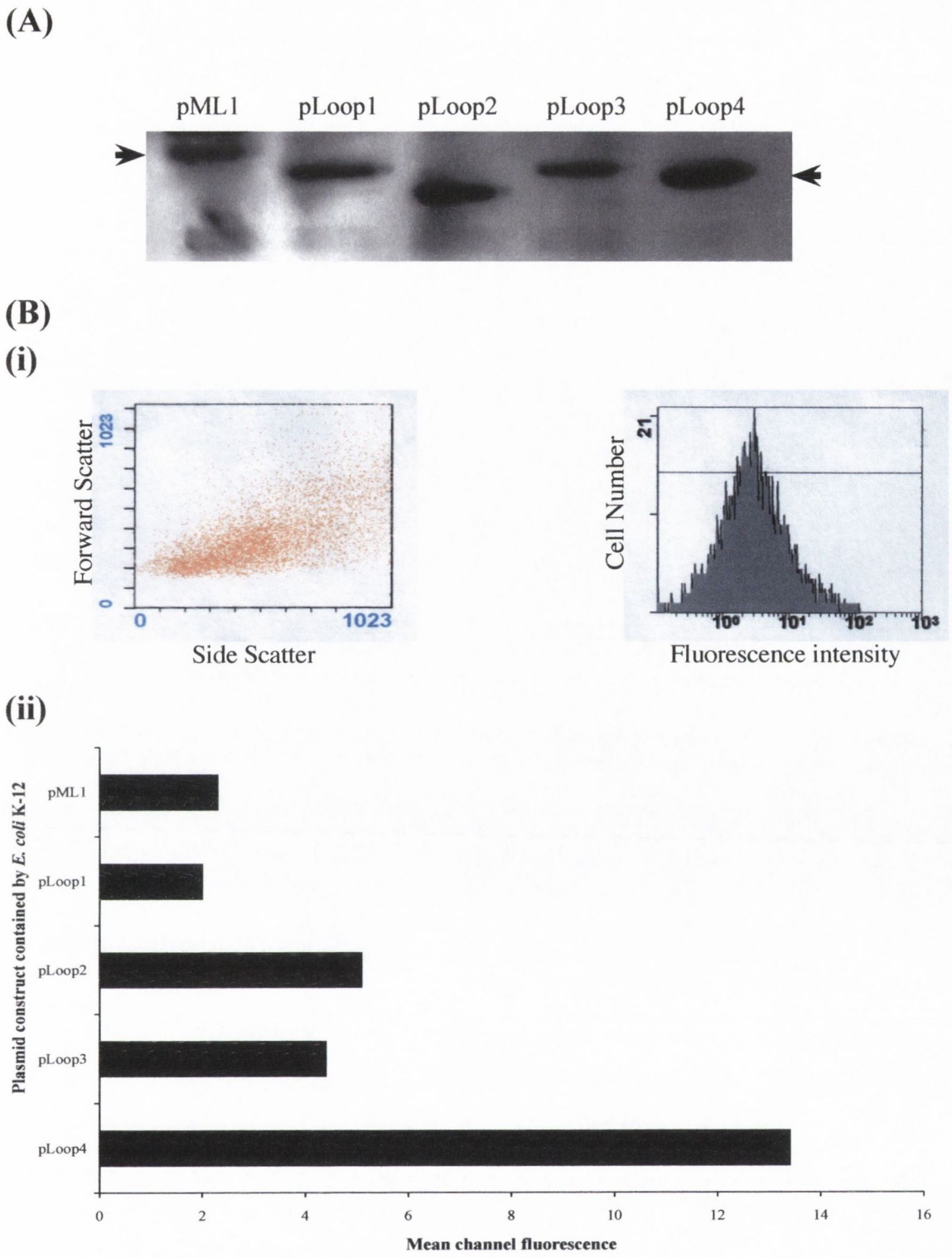

FIG. 6.3. (A) Western blot analysis of outer membrane fractions from recombinant *E. coli*. PagN was detected with polyclonal anti-PagN serum. The plasmid contained in each strain is indicated. Wild-type PagN is indicated on the left, while mutant loop deletion proteins are indicated on the right. **(B) (i) Flow cytometry sample data.** Panels show fluorescence intensity of bacteria probed with anti-PagN serum detected with FITC-conjugated anti-rabbit antibody. **(ii) Surface exposure of PagN loop-deletion mutants.** The fluorescence of 10,000 unique events was detected by flow cytometry and averaged. The levels of PagN exposure is expressed as the mean channel fluorescence.

6.2.2.3 Interaction of loop-deletion mutants with mammalian epithelial cells

The ability of the mutant PagN proteins to mediate invasion of epithelial cells was determined. Truncated PagN proteins were expressed in a non-invasive *E. coli* K-12 strain DH5α background. Standard gentamicin protection assays were performed with CHO-K1 cells and the level of invasion promoted by mutant PagN proteins was compared to that of the wild-type protein (Fig. 6.4). The CHO-K1 cell line was chosen over the more relevant HT-29 cell line as *E. coli*, expressing PagN, more easily invades CHO-K1 cells. Therefore, any small differences in the levels of invasion promoted by mutant PagN proteins will be magnified in assays involving CHO-K1 monolayers. Deletion of loops 1, 2 or 3 reduced wild-type levels of invasion by over 98% while deletion of loop 4 conferred a 94% reduction. These data establish that for PagN-mediated adhesion to and invasion of epithelial cells all four loops are absolutely required. The abolition of invasion upon loss of any one loop suggests that PagN loops may have a more stabilising, structural role as compared to other un-structured β-barrel surface-exposed loops.

6.2.3 The requirement for selected, conserved residues within loop two

6.2.3.1 Single amino acid substitutions in loop 2

In the previous section, it was revealed that all the loops of PagN are of equal importance with regards to the promotion of invasion of epithelial cells. In contrast, analysis of the Hek protein revealed that individual loops contribute to this ability to varying degrees. Loop 2 was established as contributing most to Hek function (personal communication with Fagan, R.P.). Comparison of the primary sequence of PagN, Hek and Tia reveal that there are several identical residues in the amino acid sequence predicted to form loop 2. An alignment of this sequence from the aforementioned proteins from several species of both *Salmonella* and *E. coli* revealed that there are 5 identical residues conserved throughout this region (Fig. 6.5). This would suggest that these residues may be involved in the function of the protein; indeed many of these residues are charged amino acids and may participate in receptor binding. To investigate the contribution of selected residues, namely Arg 93, Asp 97, Lys 99 and Asp 103, site-directed mutagenesis was performed on the plasmid pML1. Using the QuikChange® Site-Directed Mutagenesis Kit (Stratagene) and the primers R93At, R93Ab, D97Af, D97Ar, K99At, K99Ab, D103Af and D103Ar in the appropriate pairing, each one of the residues was individually changed to Ala creating

the plasmids pR93A, pD97A, pK99A and pD103A respectively. The mutated *pagN* ORF of each plasmid was sequenced to ensure that the mutation had occurred.

To confirm the expression and surface-location of all four mutant proteins, sarcosyl-extracted outer membrane fractions from *E. coli* K-12 containing each of the four mutant expression vectors and the parental construct, pML1, were separated by SDS-PAGE, transferred to a nitrocellulose membrane and analysed by western immunoblotting using anti-PagN polyclonal antiserum. Proteins of the correct predicted size were detected for all four mutants (results not shown).

6.2.3.2 The effect of individual PagN amino acid substitutions on haemagglutination

The contribution of the individually selected residues to PagN-mediated haemagglutination was investigated using *E. coli* K-12 strain BL21(DE3) expressing wild-type PagN or one of the four mutant derivatives. HA assays were performed, and the effect of mutating each residue was assessed (Fig. 6.6 (A)). Mutating Arg 93 to Ala had no noticeable effect on the level of haemagglutination promoted by PagN. Altering Asp 97 to Ala increased the ability of PagN to agglutinate erythrocytes. The HA titre was increased from 16 to 32 indicating that the loss of the negatively-charged side chain increased the ability of the protein to bind and agglutinate erythrocytes. Both Ala substitutions at positions K99 and D103 resulted in a decrease in the HA titre. The titres were both reduced to 8 demonstrating that the loss of the charged amino acids decreased the haemagglutination capabilities of PagN.

6.2.3.3 Single amino acid substitutions within loop 2 effect PagN-mediated invasion of mammalian epithelial cells

As Ala substitution of the selected loop 2 amino acids effected the ability of PagN to agglutinate erythrocytes, it was deemed necessary to test all four mutant derivatives for the ability to promote invasion of epithelial cells. Again using CHO-K1 cells and recombinant *E. coli* BL21(DE3), the ability of PagN to promote invasion was compared to that promoted by mutant proteins in a standard invasion assay (Fig. 6.6 (B)). In an identical pattern to that seen with the HA assay data presented in Section 6.2.3.2, the substitution of the four residues had different effects on PagN-mediated invasion of epithelial cells. Substitution of Arg 93 with Ala had no significant effect on the level of invasion promoted by PagN. However, mutating Asp 97 to Ala increased invasion relative to wild-type levels

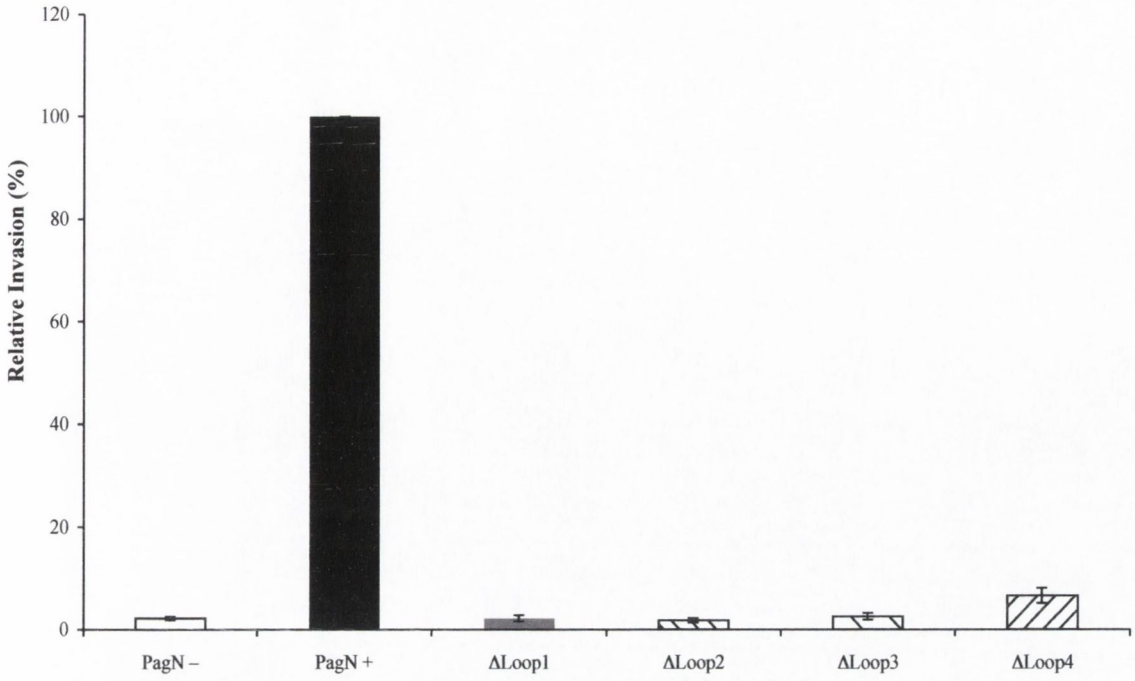

FIG. 6.4. Invasion of CHO-K1 cells *E. coli* DH5α expressing PagN. Invasion levels are calculated for *E. coli* expressing wild-type PagN or the indicated loop-deletion truncated protein. Data represents averages of triplicate wells, and standard error bars are shown. The invasion efficiencies are expressed as a percentage of the invasion promoted by expression of wild-type PagN.

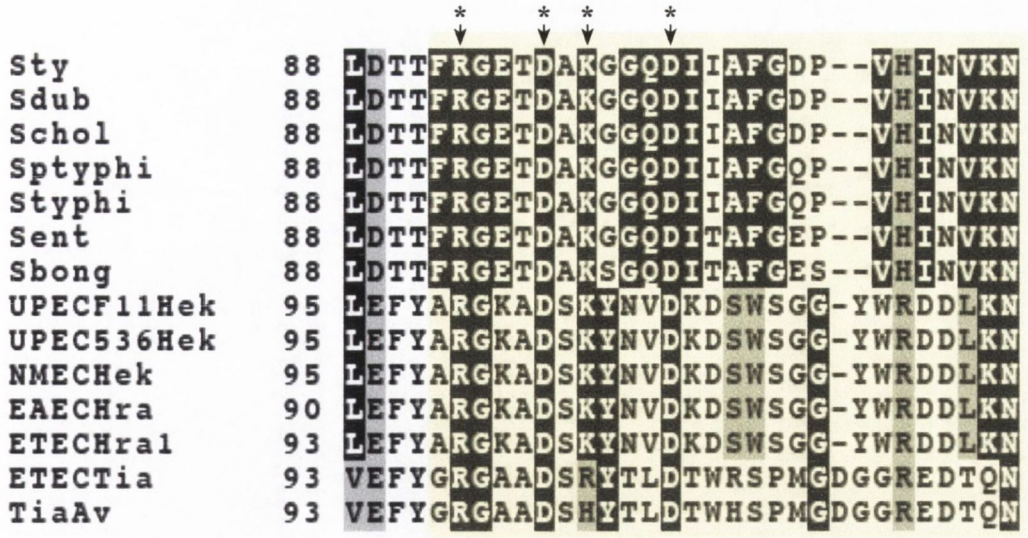

FIG 6.5. Clustal alignment of the primary sequence, predicted to encode loop 2, of the PagN, Hek and Tia proteins from *Salmonella* and *E. coli*. Identical residues are coloured black while similar residues are coloured grey. Gaps are indicated with hyphens. The yellow colour indicates residues predicted to be within the loops. The species or serovar of *Salmonella* and the pathotype of *E. coli* is indicated on the left. Amino acids are numbered relative to the start of the corresponding mature protein. The residues mutated in Section 6.2.3.1 are indicated by a star and an arrow.

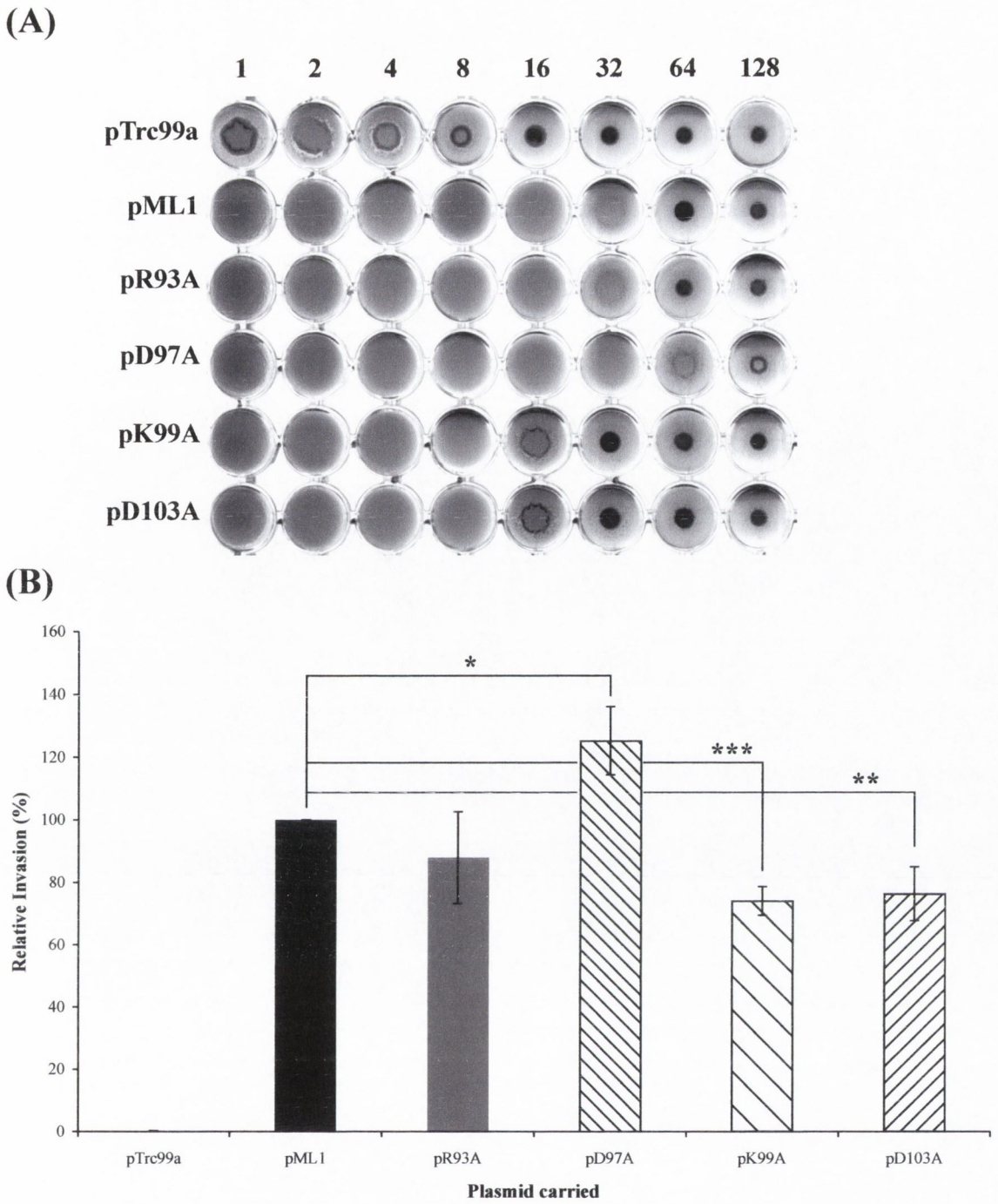

FIG. 6.6. (A) Haemagglutinataion of *E. coli* BL21(DE3) expressing PagN. Cultures of *E. coli* BL21(DE3) harbouring the indicated plasmid are tested in each row. Cultures were washed in PBS and normalised to an optical density of 10 at 600 nm (titre=1) and serially two-fold diluted. An equal volume of 1% human blood containing mannose (100 nM) was added to each well and the HA titre was determined. **(B) Invasion of CHO-K1 cells by *E. coli* BL21(DE3) expressing PagN.** Invasion levels are calculated for *E. coli* expressing PagN from the expression vectors indicated. Data represents averages of triplicate wells, and standard error bars are shown. The invasion efficiencies were expressed as a percentage of the that promoted by expression of wild-type PagN. Statistical significance is indictated by *,** or ***, with $P < 0.05$, < 0.01 and < 0.001 respectively.

by 25%, while Ala substitutions at positions K99 and D103 reduced invasion levels relative to wild-type by 26% and 24% respectively.

6.2.4 Structure/function relationship between PagN and Hek

As stated in Section 3.2.3.2, the Hek protein promotes auto aggregation and heat-resistant haemagglutination when expressed in *E. coli* K-12 strains (108). PagN supports neither of these capabilities. To investigate whether Hek-specific phenotypes could be assigned to PagN by replacing PagN loops with loops from the Hek protein, a hybrid-protein expression vector was constructed using overlap PCR (Fig. 6.7 (A) & (B)). Within Hek and PagN there is a stretch of 4 conserved residues at the beginning of the amino acid sequence predicted to form the sixth β-strand (Fig. 6.2). This sequence consists of Ala, Phe, Tyr and Pro. Although at a DNA level it is quite different, at the protein level the conserved AFTP sequence served as a common region for the construction of two PagN-Hek hybrid-protein expression vectors. These vectors would serve to express proteins in which the two halves of each protein were fused together making a protein with loops 1 and 2 from Hek and loops 3 and 4 from PagN and vice versa (Fig. 6.7 (A)).

6.2.4.1 Construction of the Hek-PagN hybrid-protein expression plasmid pH12P34

The pH12P34 expression vector was to contain DNA coding for the amino terminal 148 amino acids of the Hek protein, containing loops 1 and 2, fused to DNA coding for loops 3 and 4 of the PagN protein, contained within the carboxy terminus.

485 bp of the *hek* ORF, corresponding to 148 amino acids of the amino-terminus of the Hek protein, were amplified by PCR using the primer set pTrc99a-MCS-F and HekL12-R (Table. 2.3) and the plasmid pThek6 as a DNA template. The pTrc99a-MCS-F primer corresponds to DNA within the MCS of the pTrc99a plasmid directly 5′ to the cloned *hek* ORF in the plasmid pThek6. The reverse primer, HekL12-R, corresponds to DNA encoding the AFTP sequence of the mature Hek protein.

DNA (381 bp), corresponding to 99 amino acids of the PagN carboxy terminus was amplified using the primer set PagNL34-F and pTrc99a-MCS-R (Table. 2.3) and the plasmid pML1 as a DNA template. The forward primer, PagNL34-F, corresponds to DNA directly downstream of that encoding the AFTP sequence of the mature PagN protein.

This primer has a 5′-tail incorporating DNA which is complimentary to the HekL12-R reverse primer. The pTrc99a-MCS-R primer corresponds to DNA within the MCS of the pTrc99a plasmid directly 3′ to the cloned *pagN* ORF in the plasmid pML1.

Using equi-molar quantities of both PCR products as a DNA template, and the primer set pTrc99a-MCS-F and pTrc99a-MCS-R, a hybrid PCR product of 854 bp was generated. This PCR product corresponded to the MCS of pTrc99a with a *hek::pagN* gene fusion inserted between the *Nco*I and *Bam*HI sites. The newly generated DNA was digested with *Nco*I and *Pst*I and cloned into pTrc99a digested with *Nco*I and *Pst*I. The resulting plasmid was sequenced to confirm the sequence of the insert (Table 2.2). The plasmid was named pH12P34, indicating that the protein expressed from this plasmid contains loops 1 and 2 from Hek and loops 3 and 4 from PagN.

Despite several attempts, construction of the plasmid pP12H34 (encoding a PagN-Hek chimeric protein) was unsuccessful.

6.2.4.2 The Hek-PagN hybrid protein inserts into the outer membrane

To confirm inducible expression of the Hek-PagN hybrid protein, *E. coli* K-12 strain XL-1 harboring the pH12P34 plasmid was grown to mid-logarithmic phase and induced with 1 mM IPTG for 3 h. Sarcosyl-extracted protein samples were analysed by SDS-PAGE. A 26-kDa protein corresponding to the hybrid was visible in pH12P34-containing samples. This protein band was absent in samples containing the vector control pTrc99a incubated with IPTG in an identical fashion. Hybrid protein expression was not detectable in *E. coli* strains containing pH12P34, which were un-induced with IPTG (results not shown).

6.2.4.4 Loops one and two of Hek do not promote autoaggregation by PagN

To test whether the Hek-PagN hybrid protein expressed from the pH12P34 vector could promote autoaggregation, pH12P34 was transformed into *E. coli* strain BL21(DE3). *E. coli* BL21(BE3) containing the plasmid pH12P34, pML1, or pTrc99a were grown over night in OnEx^{TM} medium. *E. coli* K-12 strain XL-1 containing the plasmid pHek6 or pBSKII were also grown over night in L broth. Autoaggregation assays were performed on these bacterial cultures, as described in Section 2.4.2. The rate of bacterial aggregation promoted by the expression of each protein was determined. Expression of the Hek protein caused bacteria to settle out of solution at a rate of 0.024 OD_{600nm} units/min while bacteria expressing either PagN or the Hek-PagN hybrid protein displayed rates of 0.0035

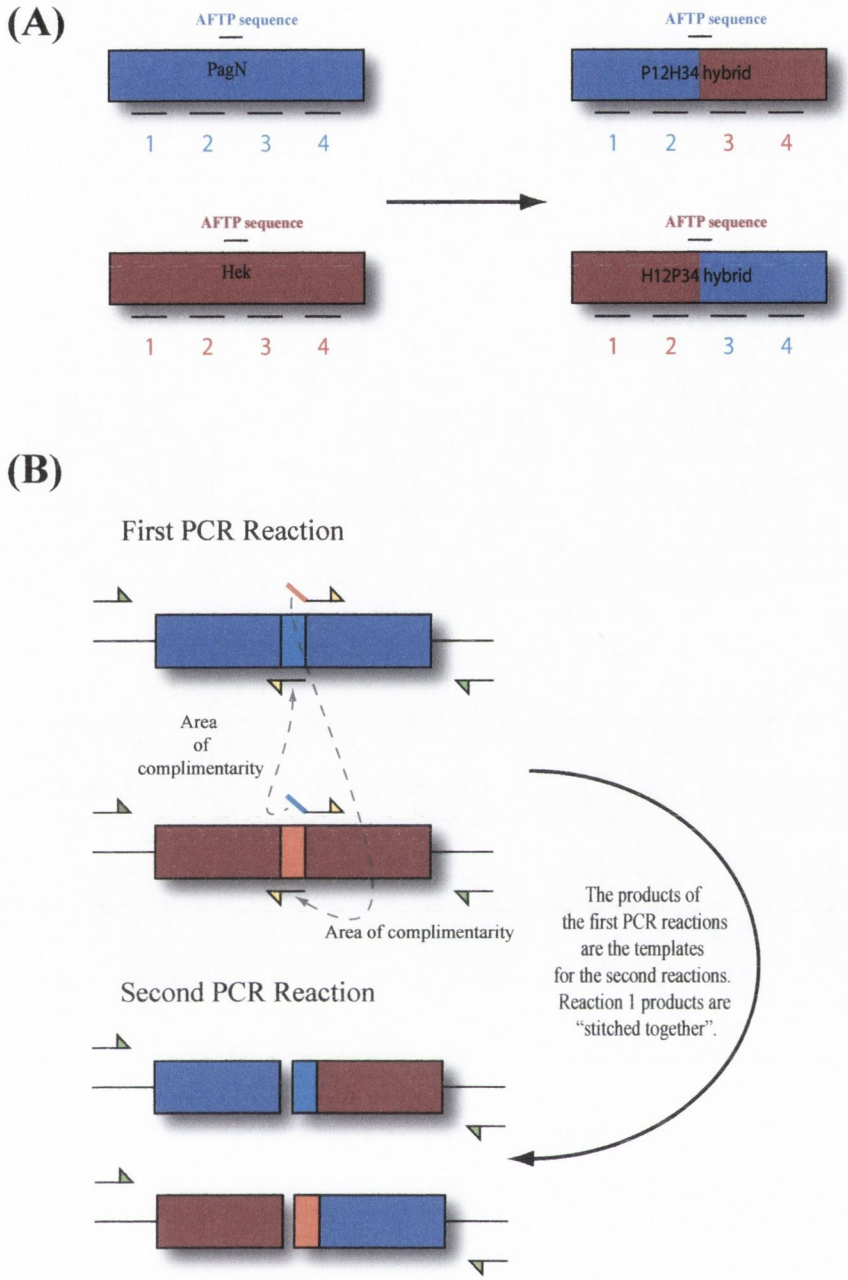

FIG. 6.7. (A) Schematic of fusion proteins. (A) The common ATFP sequence is indicated. The fusion proteins are a combination of the amino-terminus of PagN fused to the carboxy-terminus of Hek with the ATFP sequence common. The second fusion protein is the exact opposite of the first fusion. **(B) Schematic of overlap PCR used to construct the fusion-protein expression vectors.** The first PCR reaction is used to make four different products each encoding two loop domains and the corresponding β-sheets. The second PCR reaction stitches these products together in the desired combination.

OD_{600nm} units/min. These slower rates were identical to those of the negative control strains. These data indicate the amino-terminus of Hek does not endow PagN with autoaggregation capabilities.

6.2.4.5 H12P34, the Hek-PagN hybrid protein, displays an identical HA titre to PagN

As Hek and PagN promote haemagglutination to different extents the haemagglutination ability of the Hek-PagN hybrid protein was investigated. Microtitre HA assays were performed. *E. coli* BL21(DE3) containing the hybrid expression-vector pH12P34, pML1 or the empty vector control, pTrc99a, were incubated with human erythrocytes. The expression of the hybrid protein conferred upon *E. coli* the ability to agglutinate erythrocytes. Using 1% blood donated by a human male, a bacterial HA titre of 16 was displayed by both hybrid-, and PagN-expressing *E. coli* indicating that the fusion protein promoted identical levels of agglutination as compared to PagN.

6.2.4.6 The amino-terminus of Hek increase the thermal stability of PagN

As reported in Section 3.2.3.2, PagN does not support heat-resistant haemagglutination. To determine whether the Hek-PagN hybrid protein supports haemagglutination after incubation at 70 °C, *E. coli* BL21(DE3) harbouring pH12P34, pML1 or pTrc99a were grown overnight in OnEx™ medium. Bacterial cultures were adjusted to 10 OD_{600} units and used in HA assays. Following incubation at 70 °C for 30 min bacteria expressing the Hek-PagN fusion protein were still capable of agglutinating human erythrocytes whereas *E. coli* strain BL21(DE3) expressing PagN were not (results not shown). These data indicate that the Hek amino-terminus lends more stability to PagN and hence the PagN protein is resistant to the de-stabilising effects of heating.

6.2.5 The interaction of PagN with other bacterial proteins

6.2.5.1 Identification of bacterial PagN-interacting proteins

In Section 5.2.2.4, immunoprecipitation of PagN-binding proteins from FBS was attempted. Although no serum proteins were identified as binding to PagN, several bacterial proteins were revealed with which PagN interacted. To further analyse these

putative interacting proteins, immunoprecipitation reactions, as described in Section 5.2.2.4, were performed. *E. coli* BL21(DE3) harbouring the MBP-PagN expression vector pML7 were grown overnight in OnEx™ medium and subsequently lysed by sonication. An aliquot of cell-lysate was incubated with PBS, with continuous mixing, at 4 °C for 1 h. As before, any proteins putatively interacting with MBP-PagN were immunoprecitated first using amylose coupled to magnetic beads and then with an anti-MBP monoclonal antibody coupled to magnetic beads. MBP-PagN/protein complexes were analysed by SDS-PAGE. *E. coli* BL21(DE3) harbouring pMALc-2 incubated with PBS was used as a negative control (Fig. 6.8. (A) (i) & (ii)).

Comparison of samples purified from bacteria expressing MBP-PagN and LacZ, revealed 4 strong protein bands that were unique to the sample from MBP-PagN-expressing bacteria (Fig. 6.8 (A) (i)). These four proteins were excised from the gel and identified by mass spectrometry, as described in Section 2.3.5. For comprehensive results see Appendix I.

TABLE 6.1. Identification of bacterial PagN-interacting proteins

Band Number	Apparent MW	Molecular Mass (Da)	Identification
1	39	39309	OmpF
2	37	39309	OmpF
3	20.5	18553	Dps
4	15.0	15764	Heat-shock protein

Both protein bands marked 1 and 2 on Fig. 6.8 were identified as the outer membrane porin OmpF. Many proteins are known to travel aberrantly through SDS-polyacrylamide gels and may migrate as two bands rather than one single band. This is known to be the case for OmpF (88), and is not surprising. The ability of MBP-PagN to immunoprecipitate OmpF suggests that PagN may interact with OmpF in the outer membrane. The other proteins identified as PagN-binding proteins were the DNA-protective protein Dps and a heat-shock protein. Dps is a cytoplasmic protein (7), and would not be expected to bind PagN in a physiological environment. This interaction may be considered an artifact due to the cytoplasmic location of the MBP-PagN fusion protein and the abundance of Dps produced during stationary phase (7). The identification of a small heat-shock protein as interacting with MBP-PagN is unlikely as again this protein is likely to reside within the cell cytosol and would not easily interact with PagN in its physiological location.

In order to confirm the PagN-OmpF interaction, the previously described immunoprecipitation experiments were performed in an identical manner with the OmpF-defective strain *E. coli* BZB1107. Comparison of SDS-PAGE profiles from samples purified from *E. coli* BZB1107 and *E. coli* BL21(DE3) grown in OnEx^{TM}, revealed a protein band specific to the MBP-PagN-containing sample which migrated to the same level as OmpF (Fig. 6.8. (B) (i)). This protein band was excised from the gel and identified by mass spectrometry (see Appendix I). The protein was identified as the lactose operon repressor, suggesting that the PagN-OmpF interaction is a real interaction and may occur in a physiological environment.

6.2.5.2 PagN/OmpF interactions in *S.* Typhimurium

The MBP-PagN/OmpF interaction identified in the previous section was in an *E. coli* background. To determine if PagN could interact with OmpF expressed by *S.* Typhimurium the plasmids pML7 and pMALc-2 were transformed into *S.* Typhimurium strains SL1344 and CJD365 (Table 2.1) respectively. *S.* Typhimurium strain CJD365 has a defective *ompR* gene. The OmpR protein is the response regulator of the EnvZ/OmpR two-component system known to control expression of OmpF (298). *S.* Typhimurium lacking a functional OmpR protein do not express OmpF. Immunoprecipitation experiments as described in the previous sections were performed with *S.* Typhimurium expressing MBP-PagN or MBP-LacZ from the plasmids pML7 or pMALc-2 respectively. Identical immunoprecitation reactions were performed with the *ompR* mutant strain CJD365. SDS-PAGE analysis of samples from these reactions revealed 2 protein bands which migrated to the same positions as the OmpF protein from *E. coli* (Fig. 6.9). These protein bands seemed to be absent from the sample isolated from the *ompR*$^{-}$ strain, although 1 very feint band was discernable corresponding to the lower OmpF band. However, in the BZB1107 strain, this protein band was identified as the *lac* repressor and not OmpF. These data suggest that PagN interacts with OmpF in an *S.* Typhimurium background. This is of immediate physiological relevance as both OmpF and PagN are located in the outer membrane of *S.* Typhimurium.

Interestingly, there were several more protein bands specific to the MBP-PagN-containing samples which were absent in the MBP-LacZ-containing negative control. However, these possible PagN-interacting proteins were not investigated further.

6.2.5.3 Construction of a *malE::ompF* gene-fusion expression plasmid

To determine if the MBP-PagN/OmpF interaction was reciprocal an MBP-OmpF expression vector was constructed. The *ompF* ORF (excluding the DNA encoding the signal sequence) was amplified by PCR using the primer set OmpF-SS-F and OmpF-R-BamHI (Table 2.3) and *S.* Typhimurium strain SL1344 genomic DNA as a template. The reverse primer, OmpF-R-BamHI, has a *Bam*HI restriction site engineered into its 5′ end, resulting in the PCR product having a *Bam*HI endonuclease recognition site incorporated into the 3′ end. The PCR product was digested with *Bam*HI. The pMALc-2 plasmid was digested with *Xmn*I and *Bam*HI. The digested PCR product was cloned downstream, and in frame with the *malE* gene of the digested pMALc-2 vector. The plasmid was sequenced to confirm the insert and the resulting plasmid was designated pMompF (Table 2.2). SDS-PAGE analysis of *E. coli* K-12 strain DH5α containing the pMompF plasmid, grown grown to mid-logarithmic phase and induced with 0.4 mM for 3h, revealed one inducible protein band with an apparent molecular mass > 66 kDa, corresponded to the predicted size of the MBP-OmpF fusion protein (Fig. 6.10).

6.2.5.4 Construction of an *S.* Typhimurium strain TA2367 *pagN* mutant

To analyse the ability of the MBP-OmpF fusion protein to interact with PagN, a *pagN* mutant was constructed in a PhoP-constitutive *S.* Typhimurium mutant strain TA2367 background. The *pagN*::*spc* gene fusion from the chromosome of *S.* Typhimurium strain ML6 was transferred to the chromosome of strain TA2367 using P22 phage transduction as described in Section 2.2.2. Putative mutants were confirmed by PCR. The newly generated *pagN* mutant was designated *S.* Typhimurium strain ML11 (Table 2.1)

6.2.5.5 Recombinant OmpF does not bind to PagN

To confirm the observed interaction between PagN and OmpF, it was investigated whether an MBP-OmpF fusion protein could immunoprecipitate PagN in an analogous manner to that in which MBP-PagN immunoprecipitated OmpF. The MBP-OmpF expression vector pMompF was transformed into *S.* Typhimurium strain TA2367. This strain has a mutation that maps in or near the *phoP* gene, resulting in constitutive activation of the PhoP/Q system. PhoP-activated genes, including *pagN*, are therefore highly expressed in this strain (confirmed in Section 3.2.2.2). Artificially high levels of PagN within this strain combined with IPTG-induced expression of OmpF from pMompF

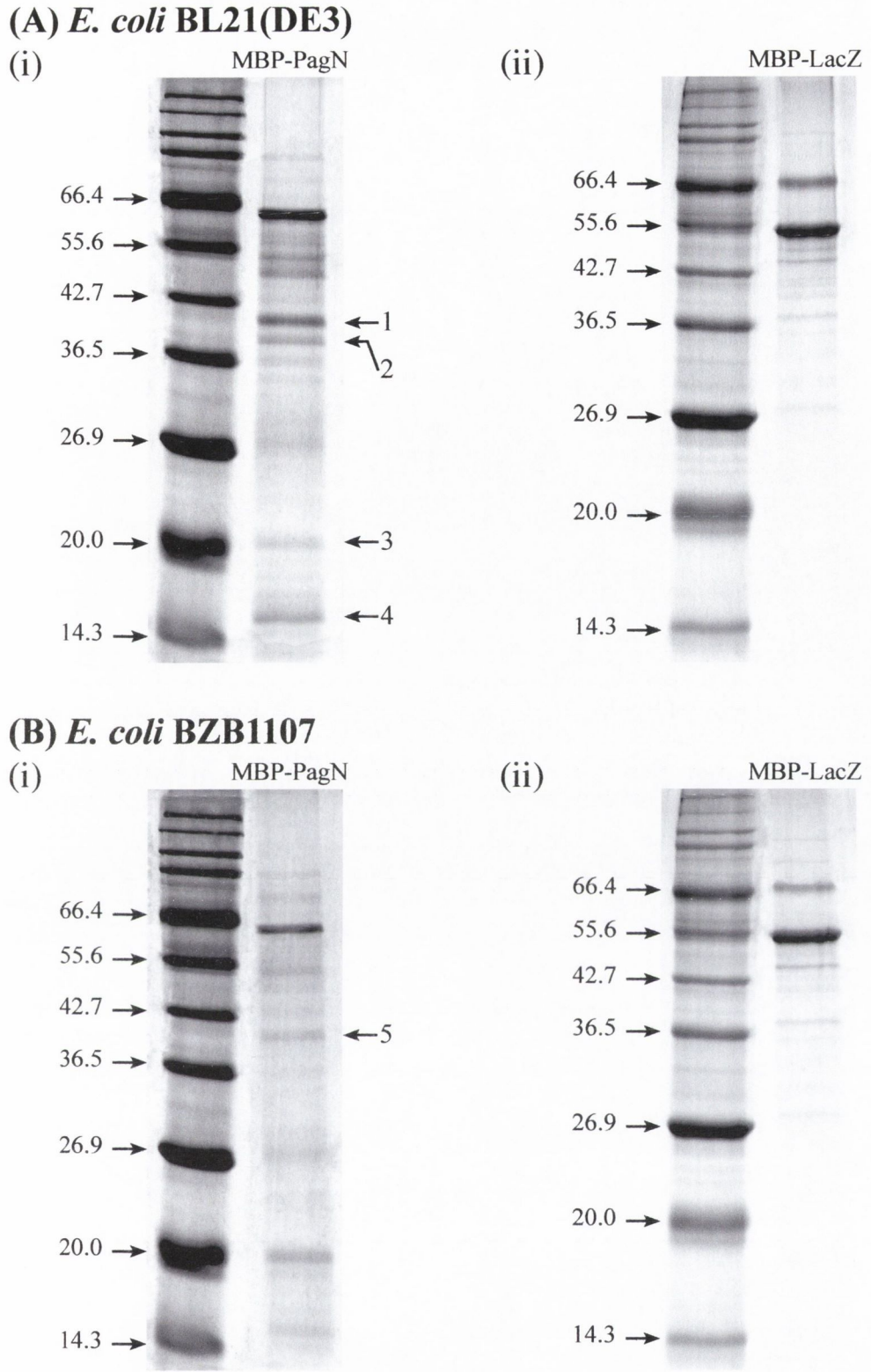

FIG. 6.8. (A) SDS-PAGE analysis of purified MBP-PagN complexes from *E. coli* BL21(DE3). Gels **(i)** and **(ii)** contain purified MBP-PagN or MBP-LacZ respectively. Proteins that were identified by mass spectrometry are indicated and numbered on the right of the gels. **(B) SDS-PAGE analysis of purified MBP-PagN complexes from *E. coli* BZB1107.** Gels **(i)** and **(ii)** contain purified MBP-PagN or MBP-LacZ respectively. Proteins that were identified by mass spectrometry are indicated and numbered on the right of the gels. Molecular mass standards (in kilo-daltons) are indicated on the left.

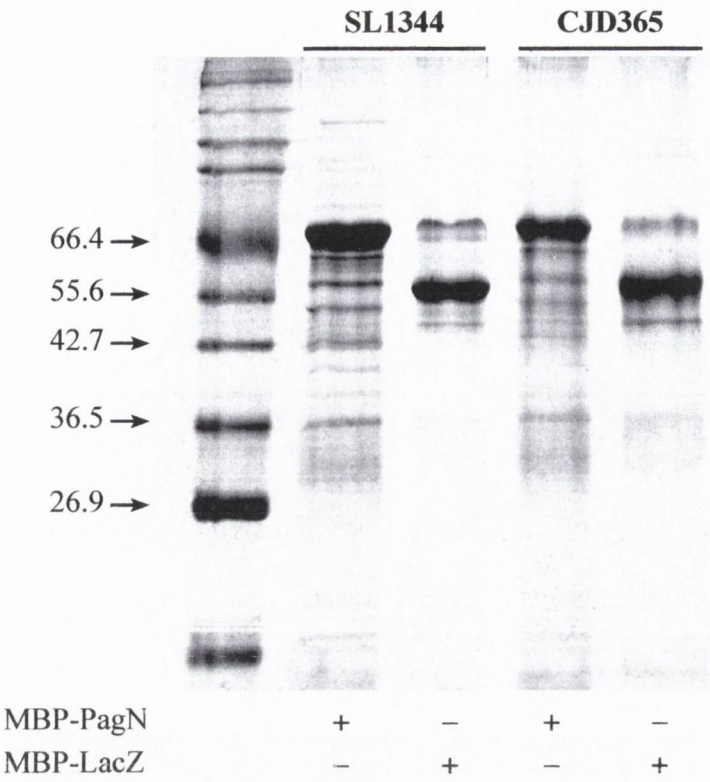

FIG. 6.9. SDS-PAGE analysis of purified MBP-PagN complexes. Lanes 2 and 3 contain purified MBP-PagN or MBP-LacZ respectively. Both samples are purified from *S.* Typhimurium strain SL1344. Lanes 4 and 5 contain identical samples to lanes 2 and 3, except that they are purified from *S.* Typhimurium strain CJD365 (*ompR*::*tet*). Molecular mass standards (in kilo-daltons) are indicated on the left.

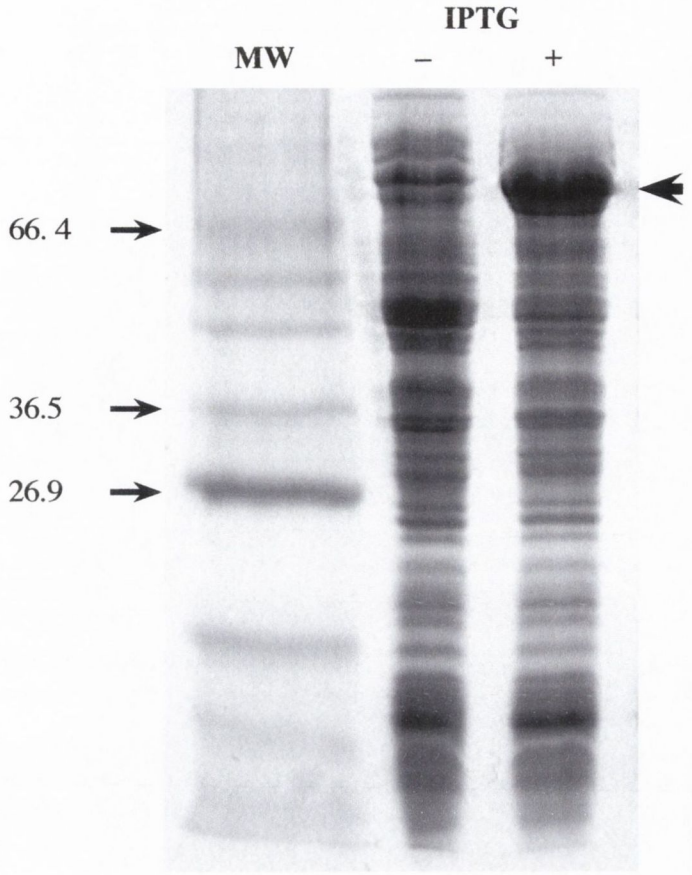

FIG. 6.10. SDS-PAGE analysis of *E. coli* K-12 strain DH5α over-expressing MBP-OmpF. Whole cell lysates were prepared from *E. coli* strain DH5α uninduced and induced with 0.4 mM IPTG. Samples from *E. coli* strain DH5α carrying the pMompF plasmid are loaded in each lane. The MBP-OmpF fusion protein is indicated on the right. Molecular mass standards (in kilo-daltons) are indicated on the left.

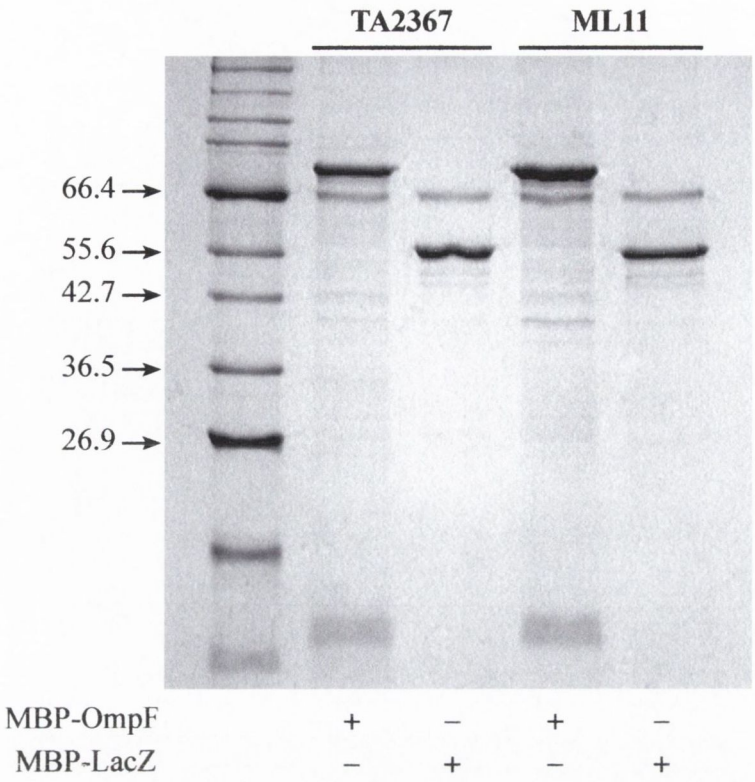

FIG. 6.11. SDS-PAGE analysis of purified MBP-OmpF complexes. Lanes 2 and 3 contain purified MBP-OmpF or MBP-LacZ restectively. Both samples are purified from *S.* Typhimurium strain TA2367. Lanes 4 and 5 contain identical samples to lanes 2 and 3, except that they are purified from *S.* Typhimurium strain ML11. Molecular mass standards (in kilo-daltons) are indicated on the left.

will enrich for any potential OmpF/PagN interactions. *S.* Typhimurium strain TA2367 containing pMompF or pMALc-2 was grown to mid-logarithmic phase in MM 5.8 medium. Expression of MBP-OmpF was induced by the addition of 0.4 mM IPTG. Bacteria were grown for 3 h where upon an immunoprecipitation experiment analogous to those described in Section 6.2.5.1 was performed. The interactions experiment was also carried out with *S.* Typhimurium strain ML11 containing pMompF and pMALc-2.

SDS-PAGE analysis of samples contaning purified MBP-OmpF and MBP-LacZ respectively revealed that MBP-OmpF does not interact with PagN (Fig. 6.11). The constitutively expressed PagN protein was not isolated from solution upon incubation with MBP-PagN suggesting that the PagN/OmpF interaction is not reciprocal.

In the event of a very weak interaction there may be an insufficient quantity of PagN within the polyacrylamide gel to enable visualisation by Coomassie staining. The samples were therefore re-analysed by SDS-PAGE and the gel was subsequently transferred to a nitrocellulose membrane and probed with anti-PagN polyclonal serum. Western immunoblot analysis also failed to identify PagN, confirming that OmpF does not interact with PagN under the condition of this experiment (results not shown).

6.3 Discussion

The PagN protein was predicted to possess a Sec-dependent signal sequence at the amino-terminus. This coupled with its presence in sarcosyl-extracted cell lysates strongly indicates an outer membrane location. Computational modeling programs were employed to predict secondary features of the protein. Using several web-based programs these features were combined to propose a model for the tertiary structure of this outer membrane protein. The PagN protein displays many of the features possessed by proteins established as being integral membrane β-barrels. The mature protein is predicted to contain 8 amphipathic anti-parallel β-sheets spanning the outer membrane. Hydrophilic residues within these sheets are predicted to face into the barrel, while hydrophobic amino acids interact with the lipid bilayer at the outside of the barrel surface. These sheets are connected in the periplasmic space by short turns and on the extracellular side by long, hydrophilic loops. In common with other β-barrel proteins, PagN possesses two putative rings of aromatic residues flanking the top an bottom of the barrel (21, 325).

The four surface-exposed loops are predicted to protrude above the membrane surface and are likely to provide the means by which PagN interacts with target receptor molecules. Of particular note is the number of charged residues located within the four loops of PagN. There are a total of 13 basic residues and 13 acidic residues distributed between the four loops. Basic residues, present in the surface-exposed loops of afimbrial adhesins have been established as being involved in receptor binding (325). Of particular interest is the protein OpcA of *Neisseria meningitidis* which uses a cleft, lined with positively-charged residues, to interact with its proteoglycan receptor. The crystal structure of OpcA revealed that the protein organises its five loop regions into a cleft lined with basic residues contributed by different loops (325). Indeed structural studies in many heparin-binding protein have shown a tendency towards basic side chains at the binding domain (239, 241, 319). It is therefore feasible that PagN may use the basic residues of its extracellular loops to interact with HSPGs. Although originally thought to be unstructured and highly flexible, the crystal structures of many β-barrel proteins have revealed that extracellular loops often form rigid, defined structures. Loop regions are known to fold back into the barrel interacting with the β-strands to form highly ordered 3-dimensional domains. PagN may conform to such a model. The loops of PagN may coordinate so that many of the basic residues within the four loops will associate in close proximity forming a

pocket with a positively charged surface area capable of interacting with the negatively charged GAG moieties of proteoglycans.

To assess the contribution of the extracellular loops of PagN during protein function, a series of mutant PagN expression vectors were constructed. Each plasmid encoded a mutant PagN protein lacking a single loop. All four proteins could be expressed in *E. coli* K-12 and reached their native location as determined by western immunoblotting and flow cytometric analysis.

Investigation of the contribution of each of the four loops revealed that all four are required for a functional protein. Western immunoblotting confirmed membrane location of these mutant proteins while flow cytometry established that they were surface-exposed in live bacteria. The accessibility of the protein to anti-PagN antibodies was highly increased in mutant proteins. It must be noted that the increase in mean fluorescence measured by flow cytometry is not necessarily an indication of the quantity of protein expressed but rather reflects the exposure of epitopes at the bacterial surface. The large increase in fluorescence displayed by loop-deletion mutants would suggest that the mutation of these proteins caused serious structural changes within. This increase in fluorescence coupled with the inability of mutant proteins to support normal PagN-promoted activities indicates that each loop plays a specific role regarding protein structure. These data suggests that unlike many other β-barrel proteins, that are thought to have highly un-structured loops (217), PagN relies upon each loop to maintain structural integrity. Further studies are necessary to establish the contribution of each loop to structural integrity. Definitive information would be supplied by the crystal structure of the protein, but until such time as one is solved many questions will remain unanswered.

The predicted loop 2 of both Hek and Tia are established as contributing maximally to protein function (107, 255). Within these loops, there are 6 amino acids that are highly conserved throughout proteins and species. These include four charged residues, two basic and two acidic. The contribution of these charged amino acids to the function of PagN was investigated. Data from HA assays exactly matched that of invasion assays. Mutagenesis of the Arg at position 93 had little or no effect upon PagN function. However, a D97A mutation increased the ability of PagN to promote both haemagglutination and invasion of epithelial cells. Mutating the negatively charged Asp residue to Ala may indirectly increase the net positive charge of the loop and thus may account for the additive effects. Erythrocytes have a net negative charge at pH 7 (356), therefore it is feasible that increasing the charge of loop 2 would increase the erythrocyte binding-capacity of the protein. As the proteoglycans are also negatively charged, the binding capabilities of PagN

for these may also be increased in an analogous manner. Mutating residues K99 and D103 to Ala decreased PagN-promoted phenotypes. These decreases in function may reflect possible structural roles for these residues. The charged side chains of these residues may be involved in protein structure at a quaternary level. Their absence reduces the ability of the protein to bind to its target receptor. The distinct phenotype associated with mutating each residue reflects the complex structure of the PagN protein. Three out of the four residue substitutions affected the function of the protein. In future experiments a more random mutagenic approach may identify further residues with important contributions to function. By generating a library of PagN mutants with randomly mutagenised loops, further residues involved in receptor-binding may be identified.

As a means to further define how the structure of PagN lends itself to function, hybrid chimeric proteins were generated with the related Hek adhesin. A plasmid capable of expressing a Hek-PagN fusion protein containing the amino-terminus of Hek fused to the carboxy-terminus of PagN was generated. Several characteristics specific to Hek but absent for PagN were investigated. The chimeric protein was unaffected in its ability to agglutinate cells. HA titres were identical to those promoted by the expression of PagN. Loop 2 of Hek, although responsible for autoaggregation in its native location, failed to endow upon PagN the ability to promote bacterial autoaggregation. Interestingly however, the hybrid protein did promote heat-resistant haemagglutination. As discussed in Chapter 3, both Hek and Tia are considered very stable proteins, resisting full denaturation in SDS and promoting heat-resistant haemagglutination. The hybrid protein must therefore be more stable and rigid than PagN. The stability lent to PagN by the 4 β-sheets and 2 loops of Hek suggests that although the sequence of the proteins is similar, the conformation that they adopt is highly different and promotes vastly different phenotypes.

In Chapter 5, several putative bacterial PagN-interacting proteins were revealed. The identity of these proteins was established in this chapter. Of the four putative PagN-interacting proteins, two were dismissed as artifacts due to the experimental design. The third and fourth protein bands were both determined to be OmpF. The MBP-PagN fusion protein was shown to bind to OmpF expressed by both *E. coli* and *S.* Typhimurium. OmpF is an outer membrane porin found in both *E. coli* and *S.* Typhimurium (296). It functions in the membrane as a trimer and forms a relatively non-specific channel that allows the passage of small hydrophilic molecules across the membrane. OmpF also enhances the ability of the vitamin B12 receptor, BtuB, to protect bacteria against the endonuclease colicin E9 (228). PagN may interact with OmpF for a number of reasons. It is feasible that a PagN-OmpF interaction may be responsible for the apparent protective role of PagN

within macrophages. PagN may bind to OmpF inducing conformational changes within the porin. These changes may then promote OmpF, through an undefined mechanism, to provide a protective activity within the harsh intra-macrophage environment. The PagN protein may also simply interact with OmpF as a means of promoting protein stability. The OmpF trimer is a highly rigid structure that resists denaturation by SDS and boiling. The interaction of PagN with such a trimer in the outer membrane may lend rigidity to an otherwise less structured protein. In this manner, PagN may form a heterologous oligomer with OmpF trimers establishing a stable and rigid membrane-anchored structure.

The PagN/OmpF interaction was demonstrated not to be reciprocal as MBP-OmpF failed to interact with PagN. The inability of the MBP-OmpF fusion protein to isolate PagN from lysed bacteria may be explained with reference to the oligomeric state of the OmpF protein within the confines of the experiment. The large MBP moiety may prevent OmpF from adopting its native trimeric conformation. The fact that the MBP-OmpF fusion lacks a signal sequence and is therefore cytoplasmically located may also prevent trimer formation. Therefore the monomeric MBP-OmpF may be in such a conformation that PagN will not interact with it. This lack of interaction would explain why PagN was not identified as binding to OmpF in an analogous manner as that in which OmpF was proven to bind to PagN.

Another point to consider is that PagN interacted with OmpF when over-expressed in *E. coli* BL21(DE3). However, the sequence of the *E. coli* OmpF protein is more similar to the *S.* Typhimurium OmpD protein sequence than it is to the OmpF primary sequence. OmpF from *E. coli* displays 60% similarity to OmpD and 59% similarity to OmpF from *S.* Typhimurium. Therefore, the two protein bands visible in Fig. 6.9 may in fact be OmpD and not OmpF. As OmpD is an established adhesin with a protective function within macrophages (162), it is quite feasible that PagN might interact with this protein, enhancing both its own and the ability of OmpD to promote adhesion to epithelial cells and survival within macrophages.

Chapter 7

General Discussion

The PhoP-activated gene *pagN* has been studied with regard to both its distribution throughout the *Salmonella* genus and its chromosomal location. Although many groups have predicted that PagN may be an invasin (72, 172), the protein remains uncharacterised. The purpose of this study was to characterise PagN at a molecular level.

Analysis of the primary protein sequence predicted that PagN possesses an amino-terminal signal sequence of the type recognised by the Sec membrane translocation machinery. This sequence can be divided into 3 domains which fulfill criteria set about by general signal peptides. Processing by the Sec apparatus is predicted to result in cleavage of the signal peptide between Ala 22 and Lys 23. The result is a 217-residue mature protein predicted to traverse the inner bacterial membrane reaching at least the periplasmic space.

Protein structure prediction software was employed to generate a model for the secondary and tertiary conformation adopted by the PagN protein. The mature protein exhibited many characteristics of known outer membrane β-barrel proteins (217). A model was constructed in which PagN forms 8 anti-parallel β-pleated sheets composed of alternating hydrophobic and hydrophilic residues which span the outer membrane. These sheets are connected in the periplasm by short turns and by long loops on the extracellular side of the membrane. The combination of β-sheets, periplasmic turns and extracellular loops are presumed to fold into a membrane-spanning β-barrel protein.

Initial protein-protein BLAST analysis of the PagN primary sequence identified both the Hek (108), and Tia (117), β-barrel invasins as being similar to PagN, with both displaying 54% overall similarity. However, the areas of highest identity were largely located within the amphipathic membrane-spanning regions, while the occurrence of identical and similar residues in the putative extracellular loops was much more infrequent. This pattern has also been demonstrated for other homologous β-barrel proteins (169, 276). Because the loops are the only part of the protein likely to be extra-membranous, it is predicted, as with other β-barrels, that they are responsible for the function of the protein. The loop regions displayed such low levels of similarity to both Hek and Tia that it was not immediately concluded that PagN might share a similar function.

Cloning the *pagN* ORF, with 500 bp of flanking DNA, into a multi-copy plasmid facilitated the initial characterisation of PagN. SDS-PAGE analysis of sarcosyl-insoluble outer membrane fractions of *S.* Typhimurium harbouring this *pagN*-containing vector revealed the expression of a ~26-kDa protein. The protein was expressed in conditions that mimic the SCV environment, thus acknowledging the PhoP-dependent nature of the protein. Peptide-mass fingerprinting of this heavily induced protein positively identified it

as PagN. The presence of PagN in the outer membrane fractions isolated from *S.* Typhimurium coupled with the possession of a putative signal peptide, confirmed PagN as being an integral outer membrane protein. As all outer membrane proteins of gram-negative bacteria described thus far display a β-barrel conformation, it was concluded that the computer-based predicted structure for PagN was highly accurate.

Although the activation of *pagN* transcription has been established as being PhoP-dependent (158), an analysis of the PhoP-dependency of PagN protein expression has never been performed. To investigate this principal, *pagN*-containing vectors were transformed into two *S.* Typhimurium strains. These strains, TA2362 and TA2367 are defective and constitutive for PhoP expression respectively. As determined by western immunoblotting, a functional PhoP/Q system was necessary for PagN expression. This set of experiments indicated that *pagN* expression was induced from a promoter directly upstream of the ORF. Upon examination of the putative *pagN* promoter region it was demonstrated that *pagN* expression was initiated from a promoter directly upstream of the ORF. This region contains a somewhat degenerative PhoP box along with a putative PmrA-binding sequence. Mobility shift assays with purified His-tagged PhoP and the putative promoter region established that PhoP binds specifically to the promoter, supplying the first evidence that *pagN* is regulated directly by PhoP.

As discussed in Section 1.5.1, many PhoP-regulated genes are controlled indirectly. It is believed that in terms of *Salmonella* evolution, the PhoP/Q system directly controls the expression of the majority of ancestral genes, while it indirectly exerts Mg^{2+} regulation on most of the horizontally acquired *pag* genes (233). Although *pagN* is thought to have been acquired by horizontal transfer, the ability of PhoP to bind directly to its putative promoter region suggests that this horizontal transfer event occurred very early in the evolution of *Salmonella*.

The transcription of *pagN* has been proven to be up-regulated within both epithelial and macrophage cells (173). Analysis of the intra-cellular expression of *pagN* revealed that transcription occurs early within epithelial cells and is then subsequently reduced. Maximal expression occurred within the first hour post-invasion. This initial surge in expression was reduced to more steady-state levels during the next hour. These data suggest that the PagN protein has a role in the initial internalisation of bacteria; once established within the SCV, expression of the protein was reduced. Further analysis is required to determine the level of *pagN* expression within this initial surge of activity. It would be advantageous to conduct a set of time-course experiments in which the time

interval between measurements during the first two hours post-invasion is in terms of minutes and not hours. This would supply a more accurate picture of when and for how long *pagN* expression is induced. Of note is the fact that *pagN* expression within epithelial cells seemed independent of a functional PhoP protein. This may indicate that expression of *pagN* during the more enteric aspects of *Salmonella* virulence is controlled by a different regulatory system. As *pags* are generally not expressed during invasion of the intestinal epithelium, this PhoP-independence would strengthen a role for the protein in the initial stages of infection.

Interestingly, the overall level of *pagN* transcription within macrophages was much greater than that observed in an intra-epithelium environment. Transcription of the *pagN* gene increased dramatically during a 6-hour post-internalisation period. This would suggest a role for PagN within macrophages, and the more progressive, systemic stages of *Salmonella* infection. Within the 6-hour time frame, *pagN* transcription did not plateau, indicating a continued requirement for expression of the gene. Additional longer time-course experiments may provide a clearer indication of the maximal level of *pagN* expression. These initial experiments indicate that the PagN protein has a role in the intestinal stages of *Salmonella* pathogenesis as well as the systemic phase. The apparent independence from PhoP regulation within the early phases of intestinal invasion may facilitate this dual role.

The construction of a PagN expression vector, pML1, facilitated phenotypic analysis of the protein. As many reports suggest that PagN resembles a protein invasin, and the related Hek and Tia β-barrels are both established adhesins and invasins, the ability of PagN to promote haemagglutination was investigated. Over-expression of PagN in *E. coli* K-12 promoted agglutination of human erythrocytes. Unlike the Hek protein, PagN-mediated haemagglutination was not heat-resistant, suggesting that PagN may not be as structurally rigid as the Hek protein. The erythrocyte/PagN interaction was further demonstrated by inhibition experiments. It was possible to inhibit PagN-mediated haemagglutination by pre-incubating erythrocytes with purified MBP-PagN. These assays revealed that PagN is indeed an adhesin, and due to its predicted structure and location may be classified as an afimbrial adhesin.

Interestingly, when over-expressed in *S.* Typhimurium strain LT2, PagN failed to promote haemagglutination. However *S.* Typhimurium lacking the O antigen component of LPS supported PagN-promoted haemagglutination, suggesting that the LPS of *S.* Typhimurium may mask PagN during receptor binding. LPS masking of outer membrane

proteins is not uncommon in bacteria and has been observed previously (225, 252). It is feasible that PhoP/Q-promoted LPS remodeling within the SCV may facilitate PagN/receptor interactions while in the earlier stages of infection, LPS may indeed prevent PagN from accessing its target receptor until more intimate bacterial/cell interactions are established.

As the *pagN* expression studies suggested that PagN has a role in the initial aspects of epithelial cell invasion and the HA assays established PagN as an adhesin, it was deemed appropriate to investigate the ability of PagN to promote adhesion to HT-29 human colonic cells. Over-expression of PagN in *E. coli* K-12 promoted both adhesion to and invasion of epithelial cells, proving that PagN is an adhesin and invasin. The contribution of PagN to *S.* Typhimurium invasion of both HT-29 cells and CHO-K1 cells was determined. Mutation of the *pagN* gene in *S.* Typhimurium was found to reduce invasion of both cell lines. Complementation of this defect with a *pagN*-containing vector proved that the reduction was due to the loss of PagN. PagN-mediated internalisation was dependent upon host cell actin polymerisation and was independent of the expression of a functional bacterial SPI-1-encoded TTSS.

The data obtained from invasion assays with wild-type and *pagN*-defective bacteria conclusively re-established PagN as an adhesin and invasion capable of promoting *Salmonella* internalisation in a process involving actin polymerisation. The ability of PagN to promote invasion in a TTSS-independent manner may imply that this process does not result in the formation of typical membrane ruffles. In the absence of a functional SPI-1-encoded TTSS, none of the required effector proteins will be delivered into the cell cytosol and thus ruffles formation may not take place. Electron microscopic examination of bacteria entering epithelial cells in a PagN-promoted process would determine whether the required actin polymerisation triggers ruffle formation.

The apparent ability of LPS to hinder PagN/receptor interactions was investigated further using mutant *S.* Typhimurium strains defective in *galE*. When a *galE pagN* double mutant was complemented with a *pagN*-containing plasmid, invasion levels far greater than those displayed by wild-type *S.* Typhimurium were supported. These data coupled with the fact that the loss of PagN in a rough strain had a more detrimental effect than in smooth strains, indicate that the O antigen of LPS exhibits a masking effect upon PagN/receptor binding. During epithelial cell invasion, the limited access of PagN to its receptor may be overcome by structural changes induced upon initial cell contact. It has been reported that binding of *E. coli* to abiotic surfaces via Type 1 fimbriae alters the protein composition of the

bacterial outer membrane (311). It has also been demonstrated that the attachment of *E. coli* Type 1 fimbriae to D-mannose receptors down-regulates the *kps* capsular assembly operon (352). In a similar manner, initial binding of *S.* Typhimurium to epithelial cells via fimbriae, may cause alterations in the outer membrane protein profile as well as down-regulation of capsular components. These changes may be accompanied by a change in LPS structure facilitating the employment of afimbrial adhesins, like PagN, to effect the transition from initial binding to a more intimate association with the epithelial surface.

As well a mediating bacterial attachment and invasion of epithelial cells, PagN has a protective role within macrophages. A *pagN*-defective *S.* Typhimurium mutant was recovered in fewer numbers from infected macrophages compared to wild-type strains. These data suggest that PagN promotes bacterial survival within an intra-macrophage environment. The function of PagN within the SCV is undefined, and was not investigated. However, it is attractive to speculate that PagN might be involved in anchoring the bacteria to the inside of the SCV membrane in preparation for secretion of effector molecules via the SPI-2-encoded TTSS. Fimbrial adhesins are not likely to be expressed within the acidic environs of the SCV. Therefore *S.* Typhimurium must use alternative adhesins to establish a position in close proximity to the internal side of the SCV membrane. PagN may serve such a function. The structure of the bacterial LPS is redefined within the SCV (106). This down-regulation of LPS may reduce PagN masking, and therefore lead to exposure of a PagN protein capable of interacting with the SCV membrane. Electron and confocal microscopic analysis of macrophages containing wild-type and *pagN*-defective bacteria may supply an insight into the function of the protein within an intra-macrophage location.

Many bacterial and viral pathogens are known to interact with proteoglycans which emanate from the surface of mammalian cells (123, 236, 317, 362). Proteoglycans are negatively charged cell surface molecules composed of a core protein domain from which long GAG chains branch. Indeed both Tia and Hek have been shown to target proteoglycans during adhesion to epithelial cells (107, 116). It was therefore investigated whether PagN also binds to these host cell appendages during invasion of epithelial cells.

Gentamicin protection assays using CHO-K1 cells with defects in GAG biosynthesis resulted in a reduction in PagN-promoted invasion levels. Growth of CHO-K1 cells in media containing p-nitrophyl β-D-xylopyranoside results in abnormally low GAG expression at the mammalian cell surface. PagN-mediated invasion of such cells displayed

a ~6-fold decrease relative to normal CHO-K1 cells. The CHO-K1 mutant cell line pgsA-745, which is completely deficient in GAG production, did not support PagN-promoted bacterial internalisation. These data indicate that epithelial cell GAG biosynthesis is a requirement for PagN-mediated interactions. Enzymatic removal of both the heparin and CS GAG moieties provided additional evidence that PagN interacts with GAGs. Proteolytic removal of the proteoglycan core reduced PagN-mediated invasion of CHO-K1 cells dramatically, providing the first evidence that PagN interacts with proteoglycans displayed on the surface of epithelial cells. Individual GAG components were tested for their ability to inhibit PagN/cell interactions in a dose-dependent manner. Heparin displayed such a capability. Dose-dependent inhibition of adhesin/receptor interactions is an indication that the interaction is a specific one. Taken together these data suggest that PagN interacts with heparinated proteoglycans. The cytoskeletal rearrangements, established as being essential for PagN-mediated invasion of epithelial cells, may be induced through proteoglycan signaling events. In epithelial cells, proteoglycans transduce signals from the cell exterior to the interior. Indeed, syndecan-4 is capable of activating regulators of Rho-family GTPases (74). Interaction of PagN with proteoglycans such as syndecan-4 may activate Rho GTPases. This activation may then induce the necessary actin nucleation and polymerisation required for bacterial endocytosis.

The proposed roles for PagN during the pathogenic life cycle of *Salmonella* can be summarised diagrammatically. Fig 7.1 illustrates how the proposed function of PagN correlates with the observed *pagN* expression profile.

Interestingly, it was revealed that PagN/cell interactions were dependent, but not solely dependent, upon the presence of serum factors. In the absence of such factors PagN-promoted invasion of CHO-K1 cells was reduced substantially, but not abolished. This finding suggests that PagN may be capable of binding to its target receptor both directly and by utilising a serum-located cross bridge. These cross bridge serum factors elicited their effect at the bacterial surface rather than the mammalian cell surface, suggesting that PagN binds to the cross bridge first and then uses this new extended projection to interact with the host cell. Although attempted, the identification of these factors was not established. In future experiments a possible strategy to identify such serum-based cross bridging proteins could entail the following: Fractionating the serum by size-exclusion chromatography would give rise to distinct groups of proteins. Determining the ability of each of these fractions to enhance PagN-mediated invasion of CHO-K1 cells in serum-free media would then identify any "active" fractions. The protein composition of these

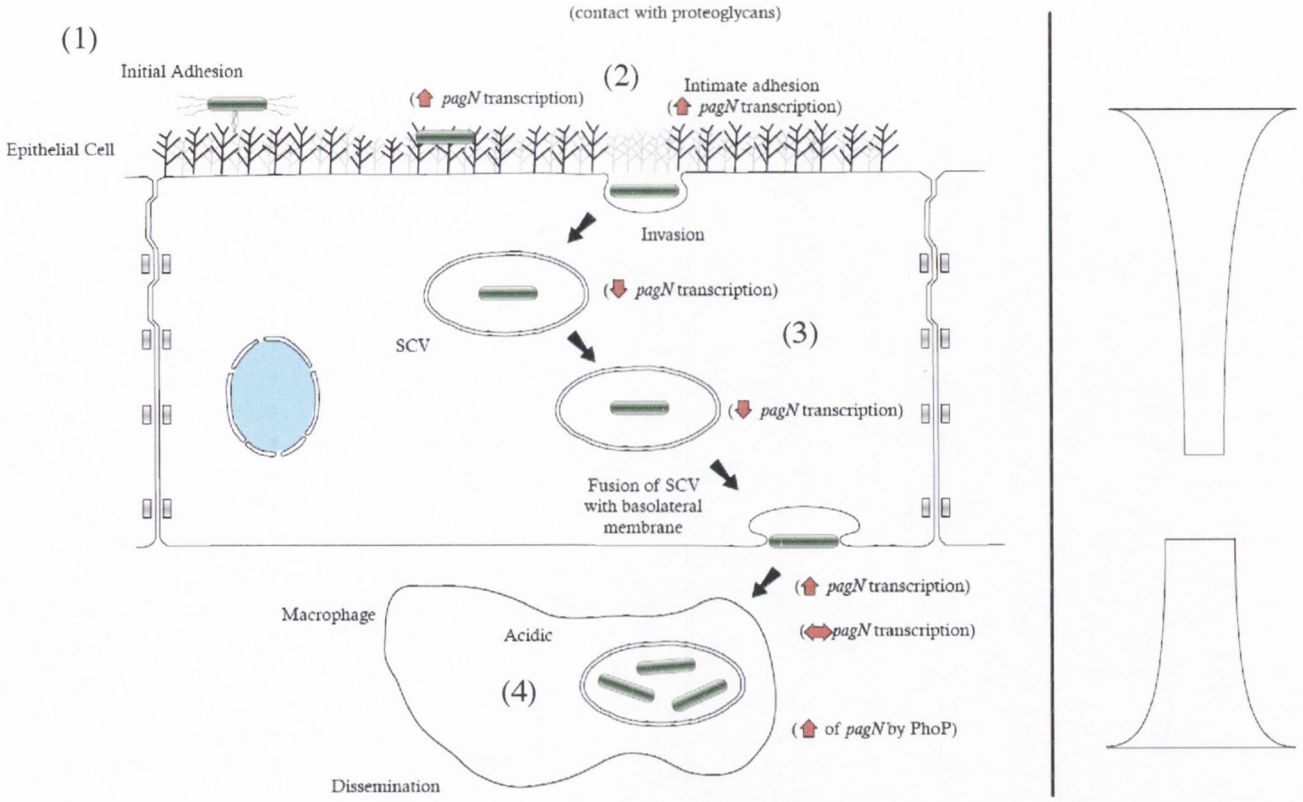

FIG 7.1. Schematic representation of the proposed role of PagN during *Salmonella* infection. The bars at the right side of the diagram represent the expression levels of the *pagN* gene. The location of the bacteria in the diagram on the left correlates with the expression profile on the right. **(1)** *Salmonella* establish an initial interaction with epithelial cells via fimbrial adhesins. **(2)** Upon binding, PagN expression is up-regulated and the transition from initial to intimate cell association is mediated by PagN/proteoglycan interactions. These interactions may give rise to signal transduction events promoting actin polymerisation and thus enhancing the effects of the TTSS effector proteins. **(3)** Upon bacterial internalisation, PagN expression is down-regulated. **(4)** Traversal of the basolateral membrane subsequently causes up-regulated of *pagN* transcription, and expression of the PagN protein enhances *Salmonella* survival within the SCV of macrophages.

fractions could then be analysed by SDS-PAGE and candidate proteins identified by mass spectrometry. In this manner PagN/cell interactions may be further defined.

Analysis of the predicted PagN structure revealed interesting subtleties in the manner in which the structure of the protein and its function as an adhesin relate. Unlike many β-barrel proteins, which show a preference for utilising specific loop domains during interactions with target receptors (107, 255), PagN shows no bias. All loops appear to be equally important. The deletion of any one loop reduced PagN-promoted invasion of CHO-K1 cells by over 90% in each case. The absolute requirement of all four loops may suggest that these regions interact to form a structural binding pocket for the PagN receptor. Such a structure has been identified in the *N. meningitidis* afimbrial adhesin OpcA (325). The loops of OpcA form a cleft (lined with basic residues) at the top of the barrel which has been proposed as a heparin-binding pocket. In a similar manner, the loops of PagN may be highly structured with all four interacting to form a complex binding domain. The abundance of positively charged amino acids present in the extracellular loops may form possible points of contact with the negatively charged GAG moieties of proteoglycan. The proposed conformation of the PagN loops is reminiscent of antibody-binding sites, which consist of loop regions built onto a β-structure framework. Three charged residues, namely D97, K99 and D103, located in the predicted second loop were established as contributing to PagN/receptor interactions. These amino acids may use their charged side chains to interact with the PagN receptor. Further identification of important residues will help elucidate the method by which PagN interacts with proteoglycans. Ultimately, solving the crystal structure of PagN would confirm these hypothesised structural predictions, and would clarify the apparent requirement of all four loops for functional PagN/receptor interactions.

In conclusion, this work has characterised the *Salmonella*-specific protein PagN. Transcription of the *pagN* gene was established as being activated directly by the PhoP response regulator, and is promoted at both early stages of epithelial cell invasion and from an intra-macrophage environment. The gene-product is predicted to adopt an 8-stranded β-barrel conformation located in the outer membrane of *Salmonella.* The PagN protein was established as an adhesin and invasin, promoting interactions with mammalian epithelial cells and subsequent bacterial internalisation. The host surface-expressed target of PagN was identified as proteoglycan. In particular the protein was shown to interact with the negatively charged GAG moieties of these proteoglycan target receptors. Interestingly, all

four of the predicted loops of PagN were required for cell interactions suggesting that a structural binding domain is formed through specific folding of the individual loops.

The function of PagN with regard to *Salmonella* pathogenesis may be to effect the transition from initial intestinal cell contact to a more intimate cell interaction. As *S.* Typhimurium possesses a large array of fimbrial and afimbrial adhesins, PagN is likely to act in concert with one or more of these bacterial appendages. Upon *Salmonella* internalisation, the expression of PagN subsides, only to be re-initiated in an intra-macrophage environment. PagN, although it promotes *Salmonella* survival, has an as yet undefined role within macrophages. An attractive hypothesis is that the protein is involved in anchorage of the bacteria to the SCV inner membrane, thus stabilising the cell for effector delivery via the SPI-2-encoded TTSS. Further studies are required to dissect the exact role of PagN during *Salmonella* survival within macrophages.

The findings of this study have identified PagN as a novel *Salmonella*-specific invasin and thus warrant the categorisation of this protein as a virulence determinant. This study has expanded our knowledge of the multi-factorial mechanisms by which *Salmonella* thrive within an animal host.

Bibliography

1. **Abromaitis, S., S. Faucher, M. Beland, R. Curtiss, 3rd, and F. Daigle.** 2005. The presence of the *tet* gene from cloning vectors impairs *Salmonella* survival in macrophages. FEMS Microbiol Lett **242:**305-12.
2. **Aguirre, A., M. L. Cabeza, S. V. Spinelli, M. McClelland, E. Garcia Vescovi, and F. C. Soncini.** 2006. PhoP-induced genes within *Salmonella* pathogenicity island 1. J Bacteriol **188:**6889-98.
3. **Aguirre, A., S. Lejona, E. G. Vescovi, and F. C. Soncini.** 2000. Phosphorylated PmrA interacts with the promoter region of *ugd* in *Salmonella enterica* serovar Typhimurium. J Bacteriol **182:**3874-6.
4. **Ahmer, B. M., J. van Reeuwijk, C. D. Timmers, P. J. Valentine, and F. Heffron.** 1998. *Salmonella typhimurium* encodes an SdiA homolog, a putative quorum sensor of the LuxR family, that regulates genes on the virulence plasmid. J Bacteriol **180:**1185-93.
5. **Akbar, S., L. M. Schechter, C. P. Lostroh, and C. A. Lee.** 2003. AraC/XylS family members, HilD and HilC, directly activate virulence gene expression independently of HilA in *Salmonella typhimurium*. Mol Microbiol **47:**715-28.
6. **Akeda, Y., and J. E. Galan.** 2005. Chaperone release and unfolding of substrates in type III secretion. Nature **437:**911-5.
7. **Almiron, M., A. J. Link, D. Furlong, and R. Kolter.** 1992. A novel DNA-binding protein with regulatory and protective roles in starved *Escherichia coli*. Genes Dev **6:**2646-54.
8. **Alpuche Aranda, C. M., J. A. Swanson, W. P. Loomis, and S. I. Miller.** 1992. *Salmonella typhimurium* activates virulence gene transcription within acidified macrophage phagosomes. Proc Natl Acad Sci U S A **89:**10079-83.
9. **Alvarez-Dominguez, C., J. A. Vazquez-Boland, E. Carrasco-Marin, P. Lopez-Mato, and F. Leyva-Cobian.** 1997. Host cell heparan sulfate proteoglycans mediate attachment and entry of *Listeria monocytogenes*, and the listerial surface protein ActA is involved in heparan sulfate receptor recognition. Infect Immun **65:**78-88.
10. **Amann, E. B., B. Ochs, and K.-J. Abel.** 1988. Tightly regulated *tac* promoter vectors useful for the expression of fused and unfused proteins in *Escherichia coli*. Gene **69:**301-315.
11. **Amavisit, P., D. Lightfoot, G. F. Browning, and P. F. Markham.** 2003. Variation between pathogenic serovars within *Salmonella* pathogenicity islands. J Bacteriol **185:**3624-35.
12. **Anderson, D. M., and O. Schneewind.** 1997. A mRNA signal for the type III secretion of Yop proteins by *Yersinia enterocolitica*. Science **278:**1140-3.
13. **Ausubel, F. M., R. Brent, R. R. Kingston, J. G. Moore, J. A. Seidman, and K. Struhl.** 1990. Current Protocols in Molecular Biology, vol. 1 Section 2.1A, New York.
14. **Bader, M. W., S. Sanowar, M. E. Daley, A. R. Schneider, U. Cho, W. Xu, R. E. Klevit, H. Le Moual, and S. I. Miller.** 2005. Recognition of antimicrobial peptides by a bacterial sensor kinase. Cell **122:**461-72.
15. **Bajaj, V., C. Hwang, and C. A. Lee.** 1995. *hilA* is a novel *ompR/toxR* family member that activates the expression of *Salmonella typhimurium* invasion genes. Mol Microbiol **18:**715-27.
16. **Bajaj, V., R. L. Lucas, C. Hwang, and C. A. Lee.** 1996. Co-ordinate regulation of *Salmonella typhimurium* invasion genes by environmental and regulatory factors is mediated by control of *hilA* expression. Mol Microbiol **22:**703-14.
17. **Bakshi, C. S., V. P. Singh, M. W. Wood, P. W. Jones, T. S. Wallis, and E. E. Galyov.** 2000. Identification of SopE2, a *Salmonella* secreted protein which is

highly homologous to SopE and involved in bacterial invasion of epithelial cells. J Bacteriol **182:**2341-4.

18. **Balbas, P., X. Soberon, F. Bolivar, and R. L. Rodriguez.** 1988. The plasmid, pBR322. Biotechnology **10:**5-41.
19. **Barondess, J. J., and J. Beckwith.** 1990. A bacterial virulence determinant encoded by lysogenic coliphage lambda. Nature **346:**871-4.
20. **Barrow, P. A., J. M. Simpson, M. A. Lovell, and M. M. Binns.** 1987. Contribution of *Salmonella gallinarum* large plasmid toward virulence in fowl typhoid. Infect Immun **55:**388-92.
21. **Basle, A., G. Rummel, P. Storici, J. P. Rosenbusch, and T. Schirmer.** 2006. Crystal structure of osmoporin OmpC from *E. coli* at 2.0 A. J Mol Biol **362:**933-42.
22. **Baumler, A. J., and F. Heffron.** 1995. Identification and sequence analysis of *lpfABCDE*, a putative fimbrial operon of Salmonella typhimurium. J Bacteriol **177:**2087-97.
23. **Baumler, A. J., R. M. Tsolis, F. A. Bowe, J. G. Kusters, S. Hoffmann, and F. Heffron.** 1996. The *pef* fimbrial operon of *Salmonella typhimurium* mediates adhesion to murine small intestine and is necessary for fluid accumulation in the infant mouse. Infect Immun **64:**61-8.
24. **Baumler, A. J., R. M. Tsolis, and F. Heffron.** 1996. Contribution of fimbrial operons to attachment to and invasion of epithelial cell lines by *Salmonella typhimurium*. Infect Immun **64:**1862-5.
25. **Baumler, A. J., R. M. Tsolis, and F. Heffron.** 1996. The *lpf* fimbrial operon mediates adhesion of *Salmonella typhimurium* to murine Peyer's patches. Proc Natl Acad Sci U S A **93:**279-83.
26. **Baumler, A. J., R. M. Tsolis, P. J. Valentine, T. A. Ficht, and F. Heffron.** 1997. Synergistic effect of mutations in *invA* and *lpfC* on the ability of *Salmonella typhimurium* to cause murine typhoid. Infect Immun **65:**2254-9.
27. **Bearson, S. M., W. H. Benjamin, Jr., W. E. Swords, and J. W. Foster.** 1996. Acid shock induction of RpoS is mediated by the mouse virulence gene *mviA* of *Salmonella typhimurium*. J Bacteriol **178:**2572-9.
28. **Belden, W. J., and S. I. Miller.** 1994. Further characterization of the PhoP regulon: identification of new PhoP-activated virulence loci. Infect Immun **62:**5095-101.
29. **Bendtsen, J. D., H. Nielsen, G. von Heijne, and S. Brunak.** 2004. Improved prediction of signal peptides: SignalP 3.0. J Mol Biol **340:**783-95.
30. **Benz, I., and M. A. Schmidt.** 1992. AIDA-I, the adhesin involved in diffuse adherence of the diarrhoeagenic *Escherichia coli* strain 2787 (O126:H27), is synthesized via a precursor molecule. Mol Microbiol **6:**1539-46.
31. **Bernfield, M., M. Gotte, P. W. Park, O. Reizes, M. L. Fitzgerald, J. Lincecum, and M. Zako.** 1999. Functions of cell surface heparan sulfate proteoglycans. Annu Rev Biochem **68:**729-77.
32. **Bernfield, M., R. Kokenyesi, M. Kato, M. T. Hinkes, J. Spring, R. L. Gallo, and E. J. Lose.** 1992. Biology of the syndecans: a family of transmembrane heparan sulfate proteoglycans. Annu Rev Cell Biol **8:**365-93.
33. **Beuzon, C. R., S. P. Salcedo, and D. W. Holden.** 2002. Growth and killing of a *Salmonella enterica* serovar Typhimurium *sifA* mutant strain in the cytosol of different host cell lines. Microbiology **148:**2705-15.
34. **Bhat, K. S., C. P. Gibbs, O. Barrera, S. G. Morrison, F. Jahnig, A. Stern, E. M. Kupsch, T. F. Meyer, and J. Swanson.** 1991. The opacity proteins of *Neisseria gonorrhoeae* strain MS11 are encoded by a family of 11 complete genes. Mol Microbiol **5:**1889-901.

35. **Bijlsma, J. J., and E. A. Groisman.** 2005. The PhoP/PhoQ system controls the intramacrophage type three secretion system of *Salmonella enterica*. Mol Microbiol **57:**85-96.
36. **Blanc-Potard, A. B., and E. A. Groisman.** 1997. The *Salmonella selC* locus contains a pathogenicity island mediating intramacrophage survival. Embo J **16:**5376-85.
37. **Blanc-Potard, A. B., F. Solomon, J. Kayser, and E. A. Groisman.** 1999. The SPI-3 pathogenicity island of *Salmonella enterica*. J Bacteriol **181:**998-1004.
38. **Boddicker, J. D., B. M. Knosp, and B. D. Jones.** 2003. Transcription of the *Salmonella* invasion gene activator, *hilA*, requires HilD activation in the absence of negative regulators. J Bacteriol **185:**525-33.
39. **Boddicker, J. D., N. A. Ledeboer, J. Jagnow, B. D. Jones, and S. Clegg.** 2002. Differential binding to and biofilm formation on, HEp-2 cells by *Salmonella enterica* serovar Typhimurium is dependent upon allelic variation in the *fimH* gene of the *fim* gene cluster. Mol Microbiol **45:**1255-65.
40. **Botelho, R. J., M. Teruel, R. Dierckman, R. Anderson, A. Wells, J. D. York, T. Meyer, and S. Grinstein.** 2000. Localized biphasic changes in phosphatidylinositol-4,5-bisphosphate at sites of phagocytosis. J Cell Biol **151:**1353-68.
41. **Bowe, F., C. J. Lipps, R. M. Tsolis, E. Groisman, F. Heffron, and J. G. Kusters.** 1998. At least four percent of the *Salmonella typhimurium* genome is required for fatal infection of mice. Infect Immun **66:**3372-7.
42. **Boyle, E. C., N. F. Brown, and B. B. Finlay.** 2006. *Salmonella enterica* serovar Typhimurium effectors SopB, SopE, SopE2 and SipA disrupt tight junction structure and function. Cell Microbiol **8:**1946-57.
43. **Brennan, M. A., and B. T. Cookson.** 2000. *Salmonella* induces macrophage death by caspase-1-dependent necrosis. Mol Microbiol **38:**31-40.
44. **Brown, N. F., B. A. Vallance, B. K. Coombes, Y. Valdez, B. A. Coburn, and B. B. Finlay.** 2005. *Salmonella* pathogenicity island 2 is expressed prior to penetrating the intestine. PLoS Pathog **1:**e32.
45. **Browne, S. H., M. L. Lesnick, and D. G. Guiney.** 2002. Genetic requirements for *Salmonella*-induced cytopathology in human monocyte-derived macrophages. Infect Immun **70:**7126-35.
46. **Brumell, J. H., D. L. Goosney, and B. B. Finlay.** 2002. SifA, a type III secreted effector of *Salmonella typhimurium*, directs *Salmonella*-induced filament (Sif) formation along microtubules. Traffic **3:**407-15.
47. **Brumell, J. H., and S. Grinstein.** 2004. *Salmonella* redirects phagosomal maturation. Curr Opin Microbiol **7:**78-84.
48. **Brumell, J. H., P. Tang, S. D. Mills, and B. B. Finlay.** 2001. Characterization of *Salmonella*-induced filaments (Sifs) reveals a delayed interaction between *Salmonella*-containing vacuoles and late endocytic compartments. Traffic **2:**643-53.
49. **Brumell, J. H., P. Tang, M. L. Zaharik, and B. B. Finlay.** 2002. Disruption of the *Salmonella*-containing vacuole leads to increased replication of *Salmonella enterica* serovar Typhimurium in the cytosol of epithelial cells. Infect Immun **70:**3264-70.
50. **Buchmeier, N. A., S. J. Libby, Y. Xu, P. C. Loewen, J. Switala, D. G. Guiney, and F. C. Fang.** 1995. DNA repair is more important than catalase for *Salmonella* virulence in mice. J Clin Invest **95:**1047-53.
51. **Buchmeier, N. A., C. J. Lipps, M. Y. So, and F. Heffron.** 1993. Recombination-deficient mutants of *Salmonella typhimurium* are avirulent and sensitive to the oxidative burst of macrophages. Mol Microbiol **7:**933-6.

52. **Buchwald, G., A. Friebel, J. E. Galan, W. D. Hardt, A. Wittinghofer, and K. Scheffzek.** 2002. Structural basis for the reversible activation of a Rho protein by the bacterial toxin SopE. Embo J **21:**3286-95.
53. **Burrows, W.** 1959. Textbook of Microbiology, 7th ed. ed, Philadelphia, Pa.
54. **Cano, D. A., M. Martinez-Moya, M. G. Pucciarelli, E. Groisman, J. Casadesus, and F. Garcia-del Portillo.** 2001. *Salmonella enterica* serovar Typhimurium response involved in attenuation of pathogen intracellular proliferation. Infect Immun **69:**6463-6474.
55. **Cantalupo, G., P. Alifano, V. Roberti, C. B. Bruni, and C. Bucci.** 2001. Rab-interacting lysosomal protein (RILP): the Rab7 effector required for transport to lysosomes. Embo J **20:**683-93.
56. **Castelli, M. E., E. Garcia Vescovi, and F. C. Soncini.** 2000. The phosphatase activity is the target for Mg2+ regulation of the sensor protein PhoQ in *Salmonella*. J Biol Chem **275:**22948-54.
57. **Chakravortty, D., I. Hansen-Wester, and M. Hensel.** 2002. *Salmonella* pathogenicity island 2 mediates protection of intracellular *Salmonella* from reactive nitrogen intermediates. J Exp Med **195:**1155-66.
58. **Chamnongpol, S., M. Cromie, and E. A. Groisman.** 2003. Mg2+ sensing by the Mg2+ sensor PhoQ of *Salmonella enterica*. J Mol Biol **325:**795-807.
59. **Chang, A. C., and S. N. Cohen.** 1978. Construction and characterization of amplifiable multicopy DNA cloning vehicles derived from the P15A cryptic miniplasmid. J Bacteriol **134:**1141-56.
60. **Chang, J., J. Chen, and D. Zhou.** 2005. Delineation and characterization of the actin nucleation and effector translocation activities of *Salmonella* SipC. Mol Microbiol **55:**1379-89.
61. **Chatfield, S. N., C. J. Dorman, C. Hayward, and G. Dougan.** 1991. Role of *ompR*-dependent genes in *Salmonella typhimurium* virulence: mutants deficient in both ompC and ompF are attenuated *in vivo*. Infect Immun **59:**449-52.
62. **Chaveroche, M. K., J. M. Ghigo, and C. d'Enfert.** 2000. A rapid method for efficient gene replacement in the filamentous fungus *Aspergillus nidulans*. Nucleic Acids Res **28:**E97.
63. **Chen, L. M., K. Kaniga, and J. E. Galan.** 1996. *Salmonella* spp. are cytotoxic for cultured macrophages. Mol Microbiol **21:**1101-15.
64. **Chopra, I., and S. W. Shales.** 1980. Comparison of the polypeptide composition of *Escherichia coli* outer membranes prepared by two methods. J Bacteriol **144:**425-7.
65. **Chu, C., S. F. Hong, C. Tsai, W. S. Lin, T. P. Liu, and J. T. Ou.** 1999. Comparative physical and genetic maps of the virulence plasmids of *Salmonella enterica* serovars Typhimurium, Enteritidis, Choleraesuis, and Dublin. Infect Immun **67:**2611-4.
66. **Cirillo, D. M., E. J. Heffernan, L. Wu, J. Harwood, J. Fierer, and D. G. Guiney.** 1996. Identification of a domain in Rck, a product of the *Salmonella typhimurium* virulence plasmid, required for both serum resistance and cell invasion. Infect Immun **64:**2019-23.
67. **Cirillo, D. M., R. H. Valdivia, D. M. Monack, and S. Falkow.** 1998. Macrophage-dependent induction of the *Salmonella* pathogenicity island 2 type III secretion system and its role in intracellular survival. Mol Microbiol **30:**175-88.
68. **Clegg, S., B. K. Purcell, and J. Pruckler.** 1987. Characterization of genes encoding type 1 fimbriae of *Klebsiella pneumoniae*, *Salmonella typhimurium*, and *Serratia marcescens*. Infect Immun **55:**281-7.

69. **Collazo, C. M., and J. E. Galan.** 1996. Requirement for exported proteins in secretion through the invasion-associated type III system of *Salmonella typhimurium*. Infect Immun **64:**3524-31.
70. **Collazo, C. M., and J. E. Galan.** 1997. The invasion-associated type-III protein secretion system in *Salmonella*--a review. Gene **192:**51-9.
71. **Collinson, S. K., S. C. Clouthier, J. L. Doran, P. A. Banser, and W. W. Kay.** 1996. *Salmonella enteritidis agfBAC* operon encoding thin, aggregative fimbriae. J Bacteriol **178:**662-7.
72. **Conner, C. P., D. M. Heithoff, S. M. Julio, R. L. Sinsheimer, and M. J. Mahan.** 1998. Differential patterns of acquired virulence genes distinguish *Salmonella* strains. Proc Natl Acad Sci U S A **95:**4641-5.
73. **Cossart, P., and P. J. Sansonetti.** 2004. Bacterial invasion: the paradigms of enteroinvasive pathogens. Science **304:**242-8.
74. **Couchman, J. R.** 2003. Syndecans: proteoglycan regulators of cell-surface microdomains? Nat Rev Mol Cell Biol **4:**926-37.
75. **Crago, A. M., and V. Koronakis.** 1999. Binding of extracellular matrix laminin to *Escherichia coli* expressing the *Salmonella* outer membrane proteins Rck and PagC. FEMS Microbiol Lett **176:**495-501.
76. **Crump, J. A., S. P. Luby, and E. D. Mintz.** 2004. The global burden of typhoid fever. Bull World Health Organ **82:**346-53.
77. **Cunliffe, R. N.** 2003. Alpha-defensins in the gastrointestinal tract. Mol Immunol **40:**463-7.
78. **Daefler, S.** 1999. Type III secretion by *Salmonella typhimurium* does not require contact with a eukaryotic host. Mol Microbiol **31:**45-51.
79. **Dai, S., P. D. Sarmiere, O. Wiggan, J. R. Bamburg, and D. Zhou.** 2004. Efficient *Salmonella* entry requires activity cycles of host ADF and cofilin. Cell Microbiol **6:**459-71.
80. **Danbara, H., R. Moriguchi, S. Suzuki, Y. Tamura, M. Kijima, K. Oishi, H. Matsui, A. Abe, and M. Nakamura.** 1992. Effect of 50 kilobase-plasmid, pKDSC50, of *Salmonella choleraesuis* RF-1 strain on pig septicemia. J Vet Med Sci **54:**1175-8.
81. **Darwin, K. H., and V. L. Miller.** 1999. Molecular basis of the interaction of *Salmonella* with the intestinal mucosa. Clin Microbiol Rev **12:**405-28.
82. **Darwin, K. H., and V. L. Miller.** 2001. Type III secretion chaperone-dependent regulation: activation of virulence genes by SicA and InvF in *Salmonella typhimurium*. Embo J **20:**1850-62.
83. **Datsenko, K. A., and B. L. Wanner.** 2000. One-step inactivation of chromosomal genes in *Escherichia coli* K-12 using PCR products. Proc Natl Acad Sci U S A **97:**6640-5.
84. **David, G., B. van der Schueren, P. Marynen, J. J. Cassiman, and H. van den Berghe.** 1992. Molecular cloning of amphiglycan, a novel integral membrane heparan sulfate proteoglycan expressed by epithelial and fibroblastic cells. J Cell Biol **118:**961-9.
85. **De Groote, M. A., D. Granger, Y. Xu, G. Campbell, R. Prince, and F. C. Fang.** 1995. Genetic and redox determinants of nitric oxide cytotoxicity in a *Salmonella typhimurium* model. Proc Natl Acad Sci U S A **92:**6399-403.
86. **De Groote, M. A., U. A. Ochsner, M. U. Shiloh, C. Nathan, J. M. McCord, M. C. Dinauer, S. J. Libby, A. Vazquez-Torres, Y. Xu, and F. C. Fang.** 1997. Periplasmic superoxide dismutase protects *Salmonella* from products of phagocyte NADPH-oxidase and nitric oxide synthase. Proc Natl Acad Sci U S A **94:**13997-4001.

87. **De Groote, M. A., T. Testerman, Y. Xu, G. Stauffer, and F. C. Fang.** 1996. Homocysteine antagonism of nitric oxide-related cytostasis in *Salmonella typhimurium*. Science **272:**414-7.
88. **Deighan, P., A. Free, and C. J. Dorman.** 2000. A role for the *Escherichia coli* H-NS-like protein StpA in OmpF porin expression through modulation of micF RNA stability. Mol Microbiol **38:**126-39.
89. **Dersch, P., H. Fsihi, and E. Bremer.** 1994. Low-copy-number T7 vectors for selective gene expression and efficient protein overproduction in *Escherichia coli*. FEMS Microbiol Lett **123:**19-26.
90. **DiGiuseppe, P. A., and T. J. Silhavy.** 2003. Signal detection and target gene induction by the CpxRA two-component system. J Bacteriol **185:**2432-40.
91. **Dinjus, U., I. Hanel, W. Rabsch, and R. Helmuth.** 1998. Studies of the presence of the virulence factors, adhesion, invasion, intracellular multiplication and toxin formation in salmonellas of different origin. Zentralbl Bakteriol **287:**387-98.
92. **Dorman, C. J., S. Chatfield, C. F. Higgins, C. Hayward, and G. Dougan.** 1989. Characterization of porin and *ompR* mutants of a virulent strain of *Salmonella typhimurium*: *ompR* mutants are attenuated *in vivo*. Infect Immun **57:**2136-40.
93. **Dorsey, C. W., M. C. Laarakker, A. D. Humphries, E. H. Weening, and A. J. Baumler.** 2005. *Salmonella enterica* serotype Typhimurium MisL is an intestinal colonization factor that binds fibronectin. Mol Microbiol **57:**196-211.
94. **Dower, W. J., J. F. Miller, and C. W. Ragsdale.** 1988. High efficiency transformation of *E. coli* by high voltage electroporation. Nucleic Acids Res **16:**6127-45.
95. **Dreher, D., M. Kok, L. Cochand, S. G. Kiama, P. Gehr, J. C. Pechere, and L. P. Nicod.** 2001. Genetic background of attenuated *Salmonella typhimurium* has profound influence on infection and cytokine patterns in human dendritic cells. J Leukoc Biol **69:**583-589.
96. **Duensing, T. D., and J. P. van Putten.** 1997. Vitronectin mediates internalization of *Neisseria gonorrhoeae* by Chinese hamster ovary cells. Infect Immun **65:**964-70.
97. **Duensing, T. D., J. S. Wing, and J. P. van Putten.** 1999. Sulfated polysaccharide-directed recruitment of mammalian host proteins: a novel strategy in microbial pathogenesis. Infect Immun **67:**4463-8.
98. **Duguid, J. P., E. S. Anderson, and I. Campbell.** 1966. Fimbriae and adhesive properties in *Salmonellae*. J Pathol Bacteriol **92:**107-38.
99. **Duguid, J. P., M. R. Darekar, and D. W. Wheater.** 1976. Fimbriae and infectivity in *Salmonella typhimurium*. J Med Microbiol **9:**459-73.
100. **Duguid, J. P., and R. R. Gillies.** 1958. Fimbriae and haemagglutinating activity in *Salmonella*, *Klebsiella*, *Proteus*, and *Chromobacterium*. J Pathol Bacteriol **75:**519-520.
101. **Ehrt, S., D. Schnappinger, S. Bekiranov, J. Drenkow, S. Shi, T. R. Gingeras, T. Gaasterland, G. Schoolnik, and C. Nathan.** 2001. Reprogramming of the macrophage transcriptome in response to interferon-gamma and *Mycobacterium tuberculosis*: signaling roles of nitric oxide synthase-2 and phagocyte oxidase. J Exp Med **194:**1123-40.
102. **Eichelberg, K., and J. E. Galan.** 1999. Differential regulation of *Salmonella typhimurium* type III secreted proteins by pathogenicity island 1 (SPI-1)-encoded transcriptional activators InvF and HilA. Infect Immun **67:**4099-105.
103. **Ellermeier, C. D., and J. M. Slauch.** 2003. RtsA and RtsB coordinately regulate expression of the invasion and flagellar genes in *Salmonella enterica* serovar Typhimurium. J Bacteriol **185:**5096-108.

104. **Emmerth, M., W. Goebel, S. I. Miller, and C. J. Hueck.** 1999. Genomic subtraction identifies *Salmonella typhimurium* prophages, F-related plasmid sequences, and a novel fimbrial operon, *stf*, which are absent in *Salmonella typhi*. J Bacteriol **181:**5652-61.
105. **Engler, M. J., and C. C. Richardson.** 1982. The Enzymes, vol. 5. Academic Press, San Diego.
106. **Eriksson, S., S. Lucchini, A. Thompson, M. Rhen, and J. C. Hinton.** 2003. Unravelling the biology of macrophage infection by gene expression profiling of intracellular *Salmonella enterica*. Mol Microbiol **47:**103-18.
107. **Fagan, R. P.** 2006. Adhesion and invasion by *Escherichia coli* K1. Trinity College, Dublin.
108. **Fagan, R. P., and S. G. Smith.** 2007. The Hek outer membrane protein of *Escherichia coli* is an auto-aggregating adhesin and invasin. FEMS Microbiol Lett.
109. **Fang, F. C., M. A. DeGroote, J. W. Foster, A. J. Baumler, U. Ochsner, T. Testerman, S. Bearson, J. C. Giard, Y. Xu, G. Campbell, and T. Laessig.** 1999. Virulent *Salmonella typhimurium* has two periplasmic Cu, Zn-superoxide dismutases. Proc Natl Acad Sci U S A **96:**7502-7.
110. **Farrant, J. L., A. Sansone, J. R. Canvin, M. J. Pallen, P. R. Langford, T. S. Wallis, G. Dougan, and J. S. Kroll.** 1997. Bacterial copper- and zinc-cofactored superoxide dismutase contributes to the pathogenesis of systemic salmonellosis. Mol Microbiol **25:**785-96.
111. **Feldman, M. F., and G. R. Cornelis.** 2003. The multitalented type III chaperones: all you can do with 15 kDa. FEMS Microbiol Lett **219:**151-8.
112. **Fields, P. I., R. V. Swanson, C. G. Haidaris, and F. Heffron.** 1986. Mutants of *Salmonella typhimurium* that cannot survive within the macrophage are avirulent. Proc Natl Acad Sci U S A **83:**5189-93.
113. **Filmus, J., and S. B. Selleck.** 2001. Glypicans: proteoglycans with a surprise. J Clin Invest **108:**497-501.
114. **Finlay, B. B., and S. Falkow.** 1988. Comparison of the invasion strategies used by *Salmonella cholerae-suis*, *Shigella flexneri* and *Yersinia enterocolitica* to enter cultured animal cells: endosome acidification is not required for bacterial invasion or intracellular replication. Biochimie **70:**1089-99.
115. **Fitts, R.** 1985. Food Technol (*Chicago*) **39:**95-102.
116. **Fleckenstein, J. M., J. T. Holland, and D. L. Hasty.** 2002. Interaction of an outer membrane protein of enterotoxigenic *Escherichia coli* with cell surface heparan sulfate proteoglycans. Infect Immun **70:**1530-7.
117. **Fleckenstein, J. M., D. J. Kopecko, R. L. Warren, and E. A. Elsinghorst.** 1996. Molecular characterization of the *tia* invasion locus from enterotoxigenic *Escherichia coli*. Infect Immun **64:**2256-65.
118. **Fogh, J., and G. Trempe.** 1975. New Human cell lines. Plenum Publishing Corp., New York.
119. **Folkesson, A., A. Advani, S. Sukupolvi, J. D. Pfeifer, S. Normark, and S. Lofdahl.** 1999. Multiple insertions of fimbrial operons correlate with the evolution of *Salmonella* serovars responsible for human disease. Mol Microbiol **33:**612-22.
120. **Folkesson, A., S. Lofdahl, and S. Normark.** 2002. The *Salmonella enterica* subspecies I specific centisome 7 genomic island encodes novel protein families present in bacteria living in close contact with eukaryotic cells. Res Microbiol **153:**537-45.
121. **Francis, C. L., M. N. Starnbach, and S. Falkow.** 1992. Morphological and cytoskeletal changes in epithelial cells occur immediately upon interaction with *Salmonella typhimurium* grown under low-oxygen conditions. Mol Microbiol **6:**3077-87.

122. **Fratti, R. A., J. M. Backer, J. Gruenberg, S. Corvera, and V. Deretic.** 2001. Role of phosphatidylinositol 3-kinase and Rab5 effectors in phagosomal biogenesis and mycobacterial phagosome maturation arrest. J Cell Biol **154:**631-44.
123. **Freissler, E., A. Meyer auf der Heyde, G. David, T. F. Meyer, and C. Dehio.** 2000. Syndecan-1 and syndecan-4 can mediate the invasion of OpaHSPG-expressing *Neisseria gonorrhoeae* into epithelial cells. Cell Microbiol **2:**69-82.
124. **Frevert, U., P. Sinnis, C. Cerami, W. Shreffler, B. Takacs, and V. Nussenzweig.** 1993. Malaria circumsporozoite protein binds to heparan sulfate proteoglycans associated with the surface membrane of hepatocytes. J Exp Med **177:**1287-98.
125. **Friebel, A., H. Ilchmann, M. Aepfelbacher, K. Ehrbar, W. Machleidt, and W. D. Hardt.** 2001. SopE and SopE2 from *Salmonella typhimurium* activate different sets of RhoGTPases of the host cell. J Biol Chem **276:**34035-40.
126. **Friedrich, M. J., N. E. Kinsey, J. Vila, and R. J. Kadner.** 1993. Nucleotide sequence of a 13.9 kb segment of the 90 kb virulence plasmid of *Salmonella typhimurium*: the presence of fimbrial biosynthetic genes. Mol Microbiol **8:**543-58.
127. **Froehlich, B. J., A. Karakashian, L. R. Melsen, J. C. Wakefield, and J. R. Scott.** 1994. CooC and CooD are required for assembly of CS1 pili. Mol Microbiol **12:**387-401.
128. **Fu, Y., and J. E. Galan.** 1999. A *salmonella* protein antagonizes Rac-1 and Cdc42 to mediate host-cell recovery after bacterial invasion. Nature **401:**293-7.
129. **Fu, Y., and J. E. Galan.** 1998. The *Salmonella typhimurium* tyrosine phosphatase SptP is translocated into host cells and disrupts the actin cytoskeleton. Mol Microbiol **27:**359-68.
130. **Galan, J. E.** 1996. Molecular and cellular bases of *Salmonella* entry into host cells. Curr Top Microbiol Immunol **209:**43-60.
131. **Galan, J. E.** 2001. *Salmonella* interactions with host cells: type III secretion at work. Annu Rev Cell Dev Biol **17:**53-86.
132. **Galan, J. E., and R. Curtiss, 3rd.** 1989. Cloning and molecular characterization of genes whose products allow *Salmonella typhimurium* to penetrate tissue culture cells. Proc Natl Acad Sci U S A **86:**6383-7.
133. **Galan, J. E., and R. Curtiss, 3rd.** 1990. Expression of *Salmonella typhimurium* genes required for invasion is regulated by changes in DNA supercoiling. Infect Immun **58:**1879-85.
134. **Galan, J. E., and R. Curtiss, 3rd.** 1989. Virulence and vaccine potential of *phoP* mutants of *Salmonella typhimurium*. Microb Pathog **6:**433-43.
135. **Galan, J. E., C. Ginocchio, and P. Costeas.** 1992. Molecular and functional characterization of the *Salmonella* invasion gene *invA*: homology of InvA to members of a new protein family. J Bacteriol **174:**4338-49.
136. **Galan, J. E., and H. Wolf-Watz.** 2006. Protein delivery into eukaryotic cells by type III secretion machines. Nature **444:**567-73.
137. **Galan, J. E., and D. Zhou.** 2000. Striking a balance: modulation of the actin cytoskeleton by *Salmonella*. Proc Natl Acad Sci U S A **97:**8754-61.
138. **Galyov, E. E., M. W. Wood, R. Rosqvist, P. B. Mullan, P. R. Watson, S. Hedges, and T. S. Wallis.** 1997. A secreted effector protein of Salmonella dublin is translocated into eukaryotic cells and mediates inflammation and fluid secretion in infected ileal mucosa. Mol Microbiol **25:**903-12.
139. **Garcia-del Portillo, F., M. B. Zwick, K. Y. Leung, and B. B. Finlay.** 1993. *Salmonella* induces the formation of filamentous structures containing lysosomal membrane glycoproteins in epithelial cells. Proc Natl Acad Sci U S A **90:**10544-8.

140. **Garvis, S. G., C. R. Beuzon, and D. W. Holden.** 2001. A role for the PhoP/Q regulon in inhibition of fusion between lysosomes and *Salmonella*-containing vacuoles in macrophages. Cell Microbiol **3:**731-44.
141. **Goddette, D. W., and C. Frieden.** 1986. Actin polymerization. The mechanism of action of cytochalasin D. J Biol Chem **261:**15974-80.
142. **Goodier, R. I., and B. M. Ahmer.** 2001. SirA orthologs affect both motility and virulence. J Bacteriol **183:**2249-58.
143. **Grkovic, S., M. H. Brown, and R. A. Skurray.** 2002. Regulation of bacterial drug export systems. Microbiol Mol Biol Rev **66:**671-701, table of contents.
144. **Groisman, E. A.** 1998. The ins and outs of virulence gene expression: Mg2+ as a regulatory signal. Bioessays **20:**96-101.
145. **Groisman, E. A.** 2001. The pleiotropic two-component regulatory system PhoP-PhoQ. J Bacteriol **183:**1835-42.
146. **Groisman, E. A., E. Chiao, C. J. Lipps, and F. Heffron.** 1989. *Salmonella typhimurium phoP* virulence gene is a transcriptional regulator. Proc Natl Acad Sci U S A **86:**7077-81.
147. **Groisman, E. A., and C. Mouslim.** 2006. Sensing by bacterial regulatory systems in host and non-host environments. Nat Rev Microbiol **4:**705-9.
148. **Groisman, E. A., and H. Ochman.** 1997. How *Salmonella* became a pathogen. Trends Microbiol **5:**343-9.
149. **Groisman, E. A., and H. Ochman.** 1996. Pathogenicity islands: bacterial evolution in quantum leaps. Cell **87:**791-4.
150. **Groisman, E. A., M. A. Sturmoski, F. R. Solomon, R. Lin, and H. Ochman.** 1993. Molecular, functional, and evolutionary analysis of sequences specific to *Salmonella*. Proc Natl Acad Sci U S A **90:**1033-7.
151. **Grund, S., and A. Weber.** 1988. A new type of fimbriae on *Salmonella typhimurium*. Zentralbl Veterinarmed B **35:**779-82.
152. **Guan, C., P. Li, P. D. Riggs, and H. Inouye.** 1987. Vectors that facilitate the expression and purification of foreign peptides in *Escherichia coli* by fusion to maltose-binding protein. Gene **67:**21-30.
153. **Guilloteau, L. A., T. S. Wallis, A. V. Gautier, S. MacIntyre, D. J. Platt, and A. J. Lax.** 1996. The *Salmonella* virulence plasmid enhances *Salmonella*-induced lysis of macrophages and influences inflammatory responses. Infect Immun **64:**3385-93.
154. **Guiney, D. G., F. C. Fang, M. Krause, S. Libby, N. A. Buchmeier, and J. Fierer.** 1995. Biology and clinical significance of virulence plasmids in *Salmonella* serovars. Clin Infect Dis **21 Suppl 2:**S146-51.
155. **Gulig, P. A.** 1990. Virulence plasmids of *Salmonella typhimurium* and other salmonellae. Microb Pathog **8:**3-11.
156. **Gulig, P. A., H. Danbara, D. G. Guiney, A. J. Lax, F. Norel, and M. Rhen.** 1993. Molecular analysis of *spv* virulence genes of the *Salmonella* virulence plasmids. Mol Microbiol **7:**825-30.
157. **Gulig, P. A., and T. J. Doyle.** 1993. The *Salmonella typhimurium* virulence plasmid increases the growth rate of salmonellae in mice. Infect Immun **61:**504-11.
158. **Gunn, J. S., W. J. Belden, and S. I. Miller.** 1998. Identification of PhoP-PhoQ activated genes within a duplicated region of the *Salmonella typhimurium* chromosome. Microb Pathog **25:**77-90.
159. **Guo, L., K. B. Lim, J. S. Gunn, B. Bainbridge, R. P. Darveau, M. Hackett, and S. I. Miller.** 1997. Regulation of lipid A modifications by *Salmonella typhimurium* virulence genes *phoP-phoQ*. Science **276:**250-3.
160. **Hakansson, S., K. Schesser, C. Persson, E. E. Galyov, R. Rosqvist, F. Homble, and H. Wolf-Watz.** 1996. The YopB protein of *Yersinia pseudotuberculosis* is

essential for the translocation of Yop effector proteins across the target cell plasma membrane and displays a contact-dependent membrane disrupting activity. Embo J **15:**5812-23.

161. **Hall, A.** 1998. Rho GTPases and the actin cytoskeleton. Science **279:**509-14.
162. **Hara-Kaonga, B., and T. G. Pistole.** 2004. OmpD but not OmpC is involved in adherence of *Salmonella enterica* serovar Typhimurium to human cells. Can J Microbiol **50:**719-27.
163. **Hardt, W. D., H. Urlaub, and J. E. Galan.** 1998. A substrate of the centisome 63 type III protein secretion system of *Salmonella typhimurium* is encoded by a cryptic bacteriophage. Proc Natl Acad Sci U S A **95:**2574-9.
164. **Harrison, R. E., J. H. Brumell, A. Khandani, C. Bucci, C. C. Scott, X. Jiang, B. B. Finlay, and S. Grinstein.** 2004. *Salmonella* impairs RILP recruitment to Rab7 during maturation of invasion vacuoles. Mol Biol Cell **15:**3146-54.
165. **Harrison, R. E., C. Bucci, O. V. Vieira, T. A. Schroer, and S. Grinstein.** 2003. Phagosomes fuse with late endosomes and/or lysosomes by extension of membrane protrusions along microtubules: role of Rab7 and RILP. Mol Cell Biol **23:**6494-506.
166. **Hautefort, I., M. J. Proenca, and J. C. Hinton.** 2003. Single-copy green fluorescent protein gene fusions allow accurate measurement of *Salmonella* gene expression *in vitro* and during infection of mammalian cells. Appl Environ Microbiol **69:**7480-91.
167. **Hayward, R. D., and V. Koronakis.** 1999. Direct nucleation and bundling of actin by the SipC protein of invasive *Salmonella*. Embo J **18:**4926-34.
168. **Hayward, R. D., E. J. McGhie, and V. Koronakis.** 2000. Membrane fusion activity of purified SipB, a *Salmonella* surface protein essential for mammalian cell invasion. Mol Microbiol **37:**727-39.
169. **Heffernan, E. J., J. Harwood, J. Fierer, and D. Guiney.** 1992. The *Salmonella typhimurium* virulence plasmid complement resistance gene *rck* is homologous to a family of virulence-related outer membrane protein genes, including *pagC* and *ail*. J Bacteriol **174:**84-91.
170. **Heffernan, E. J., S. Reed, J. Hackett, J. Fierer, C. Roudier, and D. Guiney.** 1992. Mechanism of resistance to complement-mediated killing of bacteria encoded by the *Salmonella typhimurium* virulence plasmid gene *rck*. J Clin Invest **90:**953-64.
171. **Heffernan, E. J., L. Wu, J. Louie, S. Okamoto, J. Fierer, and D. G. Guiney.** 1994. Specificity of the complement resistance and cell association phenotypes encoded by the outer membrane protein genes *rck* from *Salmonella typhimurium* and *ail* from *Yersinia enterocolitica*. Infect Immun **62:**5183-6.
172. **Heithoff, D. M., C. P. Conner, P. C. Hanna, S. M. Julio, U. Hentschel, and M. J. Mahan.** 1997. Bacterial infection as assessed by *in vivo* gene expression. Proc Natl Acad Sci U S A **94:**934-9.
173. **Heithoff, D. M., C. P. Conner, U. Hentschel, F. Govantes, P. C. Hanna, and M. J. Mahan.** 1999. Coordinate intracellular expression of *Salmonella* genes induced during infection. J Bacteriol **181:**799-807.
174. **Hengge-Aronis, R.** 2002. Signal transduction and regulatory mechanisms involved in control of the sigma(S) (RpoS) subunit of RNA polymerase. Microbiol Mol Biol Rev **66:**373-95, table of contents.
175. **Hengge-Aronis, R., R. Lange, N. Henneberg, and D. Fischer.** 1993. Osmotic regulation of *rpoS*-dependent genes in *Escherichia coli*. J Bacteriol **175:**259-65.
176. **Henry-Stanley, M. J., D. J. Hess, E. A. Erickson, R. M. Garni, and C. L. Wells.** 2003. Role of heparan sulfate in interactions of *Listeria monocytogenes* with enterocytes. Med Microbiol Immunol (Berl) **192:**107-15.

177. **Henry-Stanley, M. J., D. J. Hess, S. L. Erlandsen, and C. L. Wells.** 2005. Ability of the heparan sulfate proteoglycan syndecan-1 to participate in bacterial translocation across the intestinal epithelial barrier. Shock **24:**571-6.
178. **Henry-Stanley, M. J., B. Zhang, S. L. Erlandsen, and C. L. Wells.** 2006. Synergistic effect of tumor necrosis factor-alpha and interferon-gamma on enterocyte shedding of syndecan-1 and associated decreases in internalization of *Listeria monocytogenes* and *Staphylococcus aureus*. Cytokine **34:**252-9.
179. **Hensel, M.** 2000. *Salmonella* pathogenicity island 2. Mol Microbiol **36:**1015-23.
180. **Hensel, M., T. Nikolaus, and C. Egelseer.** 1999. Molecular and functional analysis indicates a mosaic structure of *Salmonella* pathogenicity island 2. Mol Microbiol **31:**489-98.
181. **Hensel, M., J. E. Shea, C. Gleeson, M. D. Jones, E. Dalton, and D. W. Holden.** 1995. Simultaneous identification of bacterial virulence genes by negative selection. Science **269:**400-3.
182. **Hensel, M., J. E. Shea, B. Raupach, D. Monack, S. Falkow, C. Gleeson, T. Kubo, and D. W. Holden.** 1997. Functional analysis of *ssaJ* and the *ssaK/U* operon, 13 genes encoding components of the type III secretion apparatus of *Salmonella* Pathogenicity Island 2. Mol Microbiol **24:**155-67.
183. **Hernandez, L. D., M. Pypaert, R. A. Flavell, and J. E. Galan.** 2003. A *Salmonella* protein causes macrophage cell death by inducing autophagy. J Cell Biol **163:**1123-31.
184. **Hersh, D., D. M. Monack, M. R. Smith, N. Ghori, S. Falkow, and A. Zychlinsky.** 1999. The *Salmonella* invasin SipB induces macrophage apoptosis by binding to caspase-1. Proc Natl Acad Sci U S A **96:**2396-401.
185. **Hess, D. J., M. J. Henry-Stanley, S. L. Erlandsen, and C. L. Wells.** 2006. Heparan sulfate proteoglycans mediate *Staphylococcus aureus* interactions with intestinal epithelium. Med Microbiol Immunol **195:**133-41.
186. **Higgins, C. F., and G. F. Ames.** 1981. Two periplasmic transport proteins which interact with a common membrane receptor show extensive homology: complete nucleotide sequences. Proc Natl Acad Sci U S A **78:**6038-42.
187. **Hohmann, A. W., G. Schmidt, and D. Rowley.** 1978. Intestinal colonization and virulence of *Salmonella* in mice. Infect Immun **22:**763-70.
188. **Hoiczyk, E., and G. Blobel.** 2001. Polymerization of a single protein of the pathogen *Yersinia enterocolitica* into needles punctures eukaryotic cells. Proc Natl Acad Sci U S A **98:**4669-74.
189. **Hong, K. H., and V. L. Miller.** 1998. Identification of a novel Salmonella invasion locus homologous to Shigella ipgDE. J Bacteriol **180:**1793-802.
190. **Hsu, L. C., J. M. Park, K. Zhang, J. L. Luo, S. Maeda, R. J. Kaufman, L. Eckmann, D. G. Guiney, and M. Karin.** 2004. The protein kinase PKR is required for macrophage apoptosis after activation of Toll-like receptor 4. Nature **428:**341-5.
191. **Hueck, C. J.** 1998. Type III protein secretion systems in bacterial pathogens of animals and plants. Microbiol Mol Biol Rev **62:**379-433.
192. **Hueffer, K., and J. E. Galan.** 2004. *Salmonella*-induced macrophage death: multiple mechanisms, different outcomes. Cell Microbiol **6:**1019-25.
193. **Humphries, A., S. Deridder, and A. J. Baumler.** 2005. *Salmonella enterica* serotype Typhimurium fimbrial proteins serve as antigens during infection of mice. Infect Immun **73:**5329-38.
194. **Humphries, A. D., M. Raffatellu, S. Winter, E. H. Weening, R. A. Kingsley, R. Droleskey, S. Zhang, J. Figueiredo, S. Khare, J. Nunes, L. G. Adams, R. M. Tsolis, and A. J. Baumler.** 2003. The use of flow cytometry to detect expression

of subunits encoded by 11 *Salmonella enterica* serotype Typhimurium fimbrial operons. Mol Microbiol **48:**1357-76.

195. **Humphries, A. D., S. M. Townsend, R. A. Kingsley, T. L. Nicholson, R. M. Tsolis, and A. J. Baumler.** 2001. Role of fimbriae as antigens and intestinal colonization factors of *Salmonella* serovars. FEMS Microbiol Lett **201:**121-5.
196. **Irie, F., and Y. Yamaguchi.** 2002. EphB receptors regulate dendritic spine development via intersectin, Cdc42 and N-WASP. Nat Neurosci **5:**1117-8.
197. **Isaac, D. D., J. S. Pinkner, S. J. Hultgren, and T. J. Silhavy.** 2005. The extracytoplasmic adaptor protein CpxP is degraded with substrate by DegP. Proc Natl Acad Sci U S A **102:**17775-9.
198. **Isberg, R. R., and S. Falkow.** 1985. A single genetic locus encoded by *Yersinia pseudotuberculosis* permits invasion of cultured animal cells by *Escherichia coli* K-12. Nature **317:**262-4.
199. **Isberg, R. R., and J. M. Leong.** 1990. Multiple beta 1 chain integrins are receptors for invasin, a protein that promotes bacterial penetration into mammalian cells. Cell **60:**861-71.
200. **Isberg, R. R., D. L. Voorhis, and S. Falkow.** 1987. Identification of invasin: a protein that allows enteric bacteria to penetrate cultured mammalian cells. Cell **50:**769-78.
201. **Jeanteur, D., T. Schirmer, D. Fourel, V. Simonet, G. Rummel, C. Widmer, J. P. Rosenbusch, F. Pattus, and J. M. Pages.** 1994. Structural and functional alterations of a colicin-resistant mutant of OmpF porin from *Escherichia coli*. Proc Natl Acad Sci U S A **91:**10675-9.
202. **Jesenberger, V., K. J. Procyk, J. Yuan, S. Reipert, and M. Baccarini.** 2000. *Salmonella*-induced caspase-2 activation in macrophages: a novel mechanism in pathogen-mediated apoptosis. J Exp Med **192:**1035-46.
203. **Jost, M., F. Simpson, J. M. Kavran, M. A. Lemmon, and S. L. Schmid.** 1998. Phosphatidylinositol-4,5-bisphosphate is required for endocytic coated vesicle formation. Curr Biol **8:**1399-402.
204. **Juncker, A. S., H. Willenbrock, G. Von Heijne, S. Brunak, H. Nielsen, and A. Krogh.** 2003. Prediction of lipoprotein signal peptides in Gram-negative bacteria. Protein Sci **12:**1652-62.
205. **Kamio, Y., and H. Nikaido.** 1977. Outer membrane of *Salmonella typhimurium*. Identification of proteins exposed on cell surface. Biochim Biophys Acta **464:**589-601.
206. **Kaniga, K., J. Uralil, J. B. Bliska, and J. E. Galan.** 1996. A secreted protein tyrosine phosphatase with modular effector domains in the bacterial pathogen *Salmonella typhimurium*. Mol Microbiol **21:**633-41.
207. **Kapust, R. B., and D. S. Waugh.** 1999. *Escherichia coli* maltose-binding protein is uncommonly effective at promoting the solubility of polypeptides to which it is fused. Protein Sci **8:**1668-74.
208. **Kato, A., H. Tanabe, and R. Utsumi.** 1999. Molecular characterization of the PhoP-PhoQ two-component system in *Escherichia coli* K-12: identification of extracellular Mg2+-responsive promoters. J Bacteriol **181:**5516-20.
209. **Kellerman, O. K., and T. Ferenci.** 1982. Methods in Enzymology, vol. 90. Academic Press, New York.
210. **Kier, L. D., R. M. Weppelman, and B. N. Ames.** 1979. Regulation of nonspecific acid phosphatase in *Salmonella*: *phoN* and *phoP* genes. J Bacteriol **138:**155-61.
211. **Kim, W., and M. G. Surette.** 2006. Coordinated regulation of two independent cell-cell signaling systems and swarmer differentiation in *Salmonella enterica* serovar Typhimurium. J Bacteriol **188:**431-40.

212. **Kingsley, R. A., D. Abi Ghanem, N. Puebla-Osorio, A. M. Keestra, L. Berghman, and A. J. Baumler.** 2004. Fibronectin binding to the *Salmonella enterica* serotype Typhimurium ShdA autotransporter protein is inhibited by a monoclonal antibody recognizing the A3 repeat. J Bacteriol **186:**4931-9.
213. **Kjellen, L., and U. Lindahl.** 1991. Proteoglycans: structures and interactions. Annu Rev Biochem **60:**443-75.
214. **Knodler, L. A., A. Bestor, C. Ma, I. Hansen-Wester, M. Hensel, B. A. Vallance, and O. Steele-Mortimer.** 2005. Cloning vectors and fluorescent proteins can significantly inhibit *Salmonella enterica* virulence in both epithelial cells and macrophages: implications for bacterial pathogenesis studies. Infect Immun **73:**7027-31.
215. **Knutton, S., I. Rosenshine, M. J. Pallen, I. Nisan, B. C. Neves, C. Bain, C. Wolff, G. Dougan, and G. Frankel.** 1998. A novel EspA-associated surface organelle of enteropathogenic *Escherichia coli* involved in protein translocation into epithelial cells. Embo J **17:**2166-76.
216. **Koebnik, R., and L. Kramer.** 1995. Membrane assembly of circularly permuted variants of the *E. coli* outer membrane protein OmpA. J Mol Biol **250:**617-26.
217. **Koebnik, R., K. P. Locher, and P. Van Gelder.** 2000. Structure and function of bacterial outer membrane proteins: barrels in a nutshell. Mol Microbiol **37:**239-53.
218. **Koski, P., H. Saarilahti, S. Sukupolvi, S. Taira, P. Riikonen, K. Osterlund, R. Hurme, and M. Rhen.** 1992. A new alpha-helical coiled coil protein encoded by the *Salmonella typhimurium* virulence plasmid. J Biol Chem **267:**12258-65.
219. **Kox, L. F., M. M. Wosten, and E. A. Groisman.** 2000. A small protein that mediates the activation of a two-component system by another two-component system. Embo J **19:**1861-72.
220. **Kramer, H., and M. Phistry.** 1999. Genetic analysis of hook, a gene required for endocytic trafficking in *Drosophila*. Genetics **151:**675-84.
221. **Kubori, T., and J. E. Galan.** 2003. Temporal regulation of *Salmonella* virulence effector function by proteasome-dependent protein degradation. Cell **115:**333-42.
222. **Kubori, T., Y. Matsushima, D. Nakamura, J. Uralil, M. Lara-Tejero, A. Sukhan, J. E. Galan, and S. I. Aizawa.** 1998. Supramolecular structure of the *Salmonella typhimurium* type III protein secretion system. Science **280:**602-5.
223. **Kubori, T., A. Sukhan, S. I. Aizawa, and J. E. Galan.** 2000. Molecular characterization and assembly of the needle complex of the *Salmonella typhimurium* type III protein secretion system. Proc Natl Acad Sci U S A **97:**10225-30.
224. **Kuhle, V., and M. Hensel.** 2002. SseF and SseG are translocated effectors of the type III secretion system of *Salmonella* pathogenicity island 2 that modulate aggregation of endosomal compartments. Cell Microbiol **4:**813-24.
225. **Kukkonen, M., M. Suomalainen, P. Kyllonen, K. Lahteenmaki, H. Lang, R. Virkola, I. M. Helander, O. Holst, and T. K. Korhonen.** 2004. Lack of O-antigen is essential for plasminogen activation by *Yersinia pestis* and *Salmonella enterica*. Mol Microbiol **51:**215-25.
226. **Laemmli, U. K.** 1970. Cleavage of structural proteins during the assembly of the head of bacteriophage T4. Nature **227:**680-5.
227. **Latasa, C., A. Roux, A. Toledo-Arana, J. M. Ghigo, C. Gamazo, J. R. Penades, and I. Lasa.** 2005. BapA, a large secreted protein required for biofilm formation and host colonization of *Salmonella enterica* serovar Enteritidis. Mol Microbiol **58:**1322-39.
228. **Law, C. J., C. N. Penfold, D. C. Walker, G. R. Moore, R. James, and C. Kleanthous.** 2003. OmpF enhances the ability of BtuB to protect susceptible *Escherichia coli* cells from colicin E9 cytotoxicity. FEBS Lett **545:**127-32.

229. **Lawhon, S. D., J. G. Frye, M. Suyemoto, S. Porwollik, M. McClelland, and C. Altier.** 2003. Global regulation by CsrA in *Salmonella typhimurium*. Mol Microbiol **48:**1633-45.
230. **Lawley, T. D., K. Chan, L. J. Thompson, C. C. Kim, G. R. Govoni, and D. M. Monack.** 2006. Genome-wide screen for *Salmonella* genes required for long-term systemic infection of the mouse. PLoS Pathog **2:**e11.
231. **Lee, A. H., M. P. Zareei, and S. Daefler.** 2002. Identification of a NIPSNAP homologue as host cell target for *Salmonella* virulence protein SpiC. Cell Microbiol **4:**739-50.
232. **Lee, I. S., J. Lin, H. K. Hall, B. Bearson, and J. W. Foster.** 1995. The stationary-phase sigma factor sigma S (RpoS) is required for a sustained acid tolerance response in virulent *Salmonella typhimurium*. Mol Microbiol **17:**155-67.
233. **Lejona, S., A. Aguirre, M. L. Cabeza, E. Garcia Vescovi, and F. C. Soncini.** 2003. Molecular characterization of the Mg2+-responsive PhoP-PhoQ regulon in *Salmonella enterica*. J Bacteriol **185:**6287-94.
234. **Lesnick, M. L., N. E. Reiner, J. Fierer, and D. G. Guiney.** 2001. The *Salmonella spvB* virulence gene encodes an enzyme that ADP-ribosylates actin and destabilizes the cytoskeleton of eukaryotic cells. Mol Microbiol **39:**1464-70.
235. **Li, M., B. Choo, Z. M. Wong, J. Filmus, and R. N. Buick.** 1997. Expression of OCI-5/glypican 3 during intestinal morphogenesis: regulation by cell shape in intestinal epithelial cells. Exp Cell Res **235:**3-12.
236. **Liang, O. D., F. Ascencio, L. A. Fransson, and T. Wadstrom.** 1992. Binding of heparan sulfate to *Staphylococcus aureus*. Infect Immun **60:**899-906.
237. **Liang, O. D., F. Ascencio, R. Vazquez-Juarez, and T. Wadstrom.** 1993. Binding of collagen, fibronectin, lactoferrin, laminin, vitronectin and heparan sulphate to *Staphylococcus aureus* strain V8 at various growth phases and under nutrient stress conditions. Zentralbl Bakteriol **279:**180-90.
238. **Libby, S. J., L. G. Adams, T. A. Ficht, C. Allen, H. A. Whitford, N. A. Buchmeier, S. Bossie, and D. G. Guiney.** 1997. The *spv* genes on the *Salmonella dublin* virulence plasmid are required for severe enteritis and systemic infection in the natural host. Infect Immun **65:**1786-92.
239. **Libeu, C. P., S. Lund-Katz, M. C. Phillips, S. Wehrli, M. J. Hernaiz, I. Capila, R. J. Linhardt, R. L. Raffai, Y. M. Newhouse, F. Zhou, and K. H. Weisgraber.** 2001. New insights into the heparan sulfate proteoglycan-binding activity of apolipoprotein E. J Biol Chem **276:**39138-44.
240. **Licht, T. R., K. A. Krogfelt, P. S. Cohen, L. K. Poulsen, J. Urbance, and S. Molin.** 1996. Role of lipopolysaccharide in colonization of the mouse intestine by *Salmonella typhimurium* studied by in situ hybridization. Infect Immun **64:**3811-7.
241. **Lietha, D., D. Y. Chirgadze, B. Mulloy, T. L. Blundell, and E. Gherardi.** 2001. Crystal structures of NK1-heparin complexes reveal the basis for NK1 activity and enable engineering of potent agonists of the MET receptor. Embo J **20:**5543-55.
242. **Lindgren, S. W., I. Stojiljkovic, and F. Heffron.** 1996. Macrophage killing is an essential virulence mechanism of *Salmonella typhimurium*. Proc Natl Acad Sci U S A **93:**4197-201.
243. **Linehan, S. A., and D. W. Holden.** 2003. The interplay between *Salmonella typhimurium* and its macrophage host--what can it teach us about innate immunity? Immunol Lett **85:**183-92.
244. **Litwack, E. D., J. K. Ivins, A. Kumbasar, S. Paine-Saunders, C. S. Stipp, and A. D. Lander.** 1998. Expression of the heparan sulfate proteoglycan glypican-1 in the developing rodent. Dev Dyn **211:**72-87.

245. **Lloyd, S. A., M. Sjostrom, S. Andersson, and H. Wolf-Watz.** 2002. Molecular characterization of type III secretion signals via analysis of synthetic N-terminal amino acid sequences. Mol Microbiol **43:**51-9.
246. **Lockman, H. A., and R. Curtiss, 3rd.** 1992. Virulence of non-type 1-fimbriated and nonfimbriated nonflagellated *Salmonella typhimurium* mutants in murine typhoid fever. Infect Immun **60:**491-6.
247. **Loewen, P. C., B. Hu, J. Strutinsky, and R. Sparling.** 1998. Regulation in the *rpoS* regulon of *Escherichia coli*. Can J Microbiol **44:**707-17.
248. **Lohse, D. L., and R. J. Linhardt.** 1992. Purification and characterization of heparin lyases from *Flavobacterium heparinum*. J Biol Chem **267:**24347-55.
249. **Lucas, R. L., and C. A. Lee.** 2000. Unravelling the mysteries of virulence gene regulation in *Salmonella typhimurium*. Mol Microbiol **36:**1024-33.
250. **Lucas, R. L., C. P. Lostroh, C. C. DiRusso, M. P. Spector, B. L. Wanner, and C. A. Lee.** 2000. Multiple factors independently regulate *hilA* and invasion gene expression in *Salmonella enterica* serovar Typhimurium. J Bacteriol **182:**1872-82.
251. **Lundberg, B. E., R. E. Wolf, Jr., M. C. Dinauer, Y. Xu, and F. C. Fang.** 1999. Glucose 6-phosphate dehydrogenase is required for *Salmonella typhimurium* virulence and resistance to reactive oxygen and nitrogen intermediates. Infect Immun **67:**436-8.
252. **Lupi, N., A. Bourgois, A. Bernadac, S. Laboucarie, and J. M. Pages.** 1989. Immunological analysis of porin polymorphism in *Escherichia coli* B and K-12. Mol Immunol **26:**1027-36.
253. **Lutwyche, P., R. Rupps, J. Cavanagh, R. A. Warren, and D. E. Brooks.** 1994. Cloning, sequencing, and viscometric adhesion analysis of heat-resistant agglutinin 1, an integral membrane hemagglutinin from *Escherichia coli* O9:H10:K99. Infect Immun **62:**5020-6.
254. **MacMicking, J., Q. W. Xie, and C. Nathan.** 1997. Nitric oxide and macrophage function. Annu Rev Immunol **15:**323-50.
255. **Mammarappallil, J. G., and E. A. Elsinghorst.** 2000. Epithelial cell adherence mediated by the enterotoxigenic *Escherichia coli* Tia protein. Infect Immun **68:**6595-601.
256. **Mandel, M., and A. Higa.** 1970. Calcium-dependent bacteriophage DNA infection. J Mol Biol **53:**159-62.
257. **Marcus, S. L., J. H. Brumell, C. G. Pfeifer, and B. B. Finlay.** 2000. *Salmonella* pathogenicity islands: big virulence in small packages. Microbes Infect **2:**145-56.
258. **Marlovits, T. C., T. Kubori, M. Lara-Tejero, D. Thomas, V. M. Unger, and J. E. Galan.** 2006. Assembly of the inner rod determines needle length in the type III secretion injectisome. Nature **441:**637-40.
259. **Marlovits, T. C., T. Kubori, A. Sukhan, D. R. Thomas, J. E. Galan, and V. M. Unger.** 2004. Structural insights into the assembly of the type III secretion needle complex. Science **306:**1040-2.
260. **Marshall, D. G., F. Bowe, C. Hale, G. Dougan, and C. J. Dorman.** 2000. DNA topology and adaptation of *Salmonella typhimurium* to an intracellular environment. Philos Trans R Soc Lond B Biol Sci **355:**565-74.
261. **Marshall, D. G., B. J. Sheehan, and C. J. Dorman.** 1999. A role for the leucine-responsive regulatory protein and integration host factor in the regulation of the *Salmonella* plasmid virulence (*spv*) locus in *Salmonella typhimurium*. Mol Microbiol **34:**134-45.
262. **Matsui, H., C. M. Bacot, W. A. Garlington, T. J. Doyle, S. Roberts, and P. A. Gulig.** 2001. Virulence plasmid-borne *spvB* and *spvC* genes can replace the 90-kilobase plasmid in conferring virulence to *Salmonella enterica* serovar Typhimurium in subcutaneously inoculated mice. J Bacteriol **183:**4652-8.

263. **McAleese, F. M., E. J. Walsh, M. Sieprawska, J. Potempa, and T. J. Foster.** 2001. Loss of clumping factor B fibrinogen binding activity by *Staphylococcus aureus* involves cessation of transcription, shedding and cleavage by metalloprotease. J Biol Chem **276:**29969-78.

264. **McClelland, M., K. E. Sanderson, J. Spieth, S. W. Clifton, P. Latreille, L. Courtney, S. Porwollik, J. Ali, M. Dante, F. Du, S. Hou, D. Layman, S. Leonard, C. Nguyen, K. Scott, A. Holmes, N. Grewal, E. Mulvaney, E. Ryan, H. Sun, L. Florea, W. Miller, T. Stoneking, M. Nhan, R. Waterston, and R. K. Wilson.** 2001. Complete genome sequence of *Salmonella enterica* serovar Typhimurium LT2. Nature **413:**852-6.

265. **McGhie, E. J., R. D. Hayward, and V. Koronakis.** 2004. Control of actin turnover by a *Salmonella* invasion protein. Mol Cell **13:**497-510.

266. **McGhie, E. J., R. D. Hayward, and V. Koronakis.** 2001. Cooperation between actin-binding proteins of invasive *Salmonella*: SipA potentiates SipC nucleation and bundling of actin. Embo J **20:**2131-9.

267. **Mecsas, J., R. Welch, J. W. Erickson, and C. A. Gross.** 1995. Identification and characterization of an outer membrane protein, OmpX, in *Escherichia coli* that is homologous to a family of outer membrane proteins including Ail of *Yersinia enterocolitica*. J Bacteriol **177:**799-804.

268. **Meresse, S., O. Steele-Mortimer, B. B. Finlay, and J. P. Gorvel.** 1999. The rab7 GTPase controls the maturation of *Salmonella typhimurium*-containing vacuoles in HeLa cells. Embo J **18:**4394-403.

269. **Merighi, M., C. D. Ellermeier, J. M. Slauch, and J. S. Gunn.** 2005. Resolvase-in vivo expression technology analysis of the *Salmonella enterica* serovar Typhimurium PhoP and PmrA regulons in BALB/c mice. J Bacteriol **187:**7407-16.

270. **Meyer, P. N., M. R. Wilmes-Riesenberg, C. Stathopoulos, and R. Curtiss, 3rd.** 1998. Virulence of a *Salmonella typhimurium* OmpD mutant. Infect Immun **66:**387-90.

271. **Miao, E. A., J. A. Freeman, and S. I. Miller.** 2002. Transcription of the SsrAB regulon is repressed by alkaline pH and is independent of PhoPQ and magnesium concentration. J Bacteriol **184:**1493-7.

272. **Miao, H. Q., T. A. Fritz, J. D. Esko, J. Zimmermann, A. Yayon, and I. Vlodavsky.** 1995. Heparan sulfate primed on beta-D-xylosides restores binding of basic fibroblast growth factor. J Cell Biochem **57:**173-84.

273. **Mikcha, J. M., M. G. Freire, M. L. Macedo, T. Yano, and A. J. Piantino Ferreira.** 2006. Characterization of a nonfimbrial mannose-sensitive hemagglutinin (MSH) produced by *Salmonella enterica* serovar Enteritidis. Comp Immunol Microbiol Infect Dis **29:**301-14.

274. **Miller, S. I., A. M. Kukral, and J. J. Mekalanos.** 1989. A two-component regulatory system (*phoP phoQ*) controls *Salmonella typhimurium* virulence. Proc Natl Acad Sci U S A **86:**5054-8.

275. **Miller, V. L., K. B. Beer, G. Heusipp, B. M. Young, and M. R. Wachtel.** 2001. Identification of regions of Ail required for the invasion and serum resistance phenotypes. Mol Microbiol **41:**1053-62.

276. **Miller, V. L., J. B. Bliska, and S. Falkow.** 1990. Nucleotide sequence of the *Yersinia enterocolitica ail* gene and characterization of the Ail protein product. J Bacteriol **172:**1062-9.

277. **Miller, V. L., and J. J. Mekalanos.** 1984. Synthesis of cholera toxin is positively regulated at the transcriptional level by *toxR*. Proc Natl Acad Sci U S A **81:**3471-5.

278. **Mills, D. M., V. Bajaj, and C. A. Lee.** 1995. A 40 kb chromosomal fragment encoding *Salmonella typhimurium* invasion genes is absent from the corresponding region of the *Escherichia coli* K-12 chromosome. Mol Microbiol **15:**749-59.

279. **Monack, D. M., C. S. Detweiler, and S. Falkow.** 2001. *Salmonella* pathogenicity island 2-dependent macrophage death is mediated in part by the host cysteine protease caspase-1. Cell Microbiol **3:**825-37.
280. **Monack, D. M., B. Raupach, A. E. Hromockyj, and S. Falkow.** 1996. *Salmonella typhimurium* invasion induces apoptosis in infected macrophages. Proc Natl Acad Sci U S A **93:**9833-8.
281. **Montagne, M., A. Martel, and H. Le Moual.** 2001. Characterization of the catalytic activities of the PhoQ histidine protein kinase of *Salmonella enterica* serovar Typhimurium. J Bacteriol **183:**1787-91.
282. **Morgan, E., A. J. Bowen, S. C. Carnell, T. S. Wallis, and M. P. Stevens.** 2007. SiiE Is Secreted by the *Salmonella enterica* Serovar Typhimurium Pathogenicity Island 4-Encoded Secretion System and Contributes to Intestinal Colonization in Cattle. Infect Immun **75:**1524-33.
283. **Morgan, E., J. D. Campbell, S. C. Rowe, J. Bispham, M. P. Stevens, A. J. Bowen, P. A. Barrow, D. J. Maskell, and T. S. Wallis.** 2004. Identification of host-specific colonization factors of *Salmonella enterica* serovar Typhimurium. Mol Microbiol **54:**994-1010.
284. **Mroczenski-Wildey, M. J., J. L. Di Fabio, and F. C. Cabello.** 1989. Invasion and lysis of HeLa cell monolayers by *Salmonella* typhi: the role of lipopolysaccharide. Microb Pathog **6:**143-52.
285. **Mueller, C. A., P. Broz, S. A. Muller, P. Ringler, F. Erne-Brand, I. Sorg, M. Kuhn, A. Engel, and G. R. Cornelis.** 2005. The V-antigen of *Yersinia* forms a distinct structure at the tip of injectisome needles. Science **310:**674-6.
286. **Mukherjee, K., S. Parashuraman, M. Raje, and A. Mukhopadhyay.** 2001. SopE acts as an Rab5-specific nucleotide exchange factor and recruits non-prenylated Rab5 on *Salmonella*-containing phagosomes to promote fusion with early endosomes. J Biol Chem **276:**23607-15.
287. **Muller, S. A., C. Pozidis, R. Stone, C. Meesters, M. Chami, A. Engel, A. Economou, and H. Stahlberg.** 2006. Double hexameric ring assembly of the type III protein translocase ATPase HrcN. Mol Microbiol **61:**119-25.
288. **Murray, R. A., and C. A. Lee.** 2000. Invasion genes are not required for *Salmonella enterica* serovar Typhimurium to breach the intestinal epithelium: evidence that *Salmonella* pathogenicity island 1 has alternative functions during infection. Infect Immun **68:**5050-5.
289. **Nagy, G., V. Danino, U. Dobrindt, M. Pallen, R. Chaudhuri, L. Emody, J. C. Hinton, and J. Hacker.** 2006. Down-regulation of key virulence factors makes the *Salmonella enterica* serovar Typhimurium *rfaH* mutant a promising live-attenuated vaccine candidate. Infect Immun **74:**5914-25.
290. **Navarre, W. W., T. A. Halsey, D. Walthers, J. Frye, M. McClelland, J. L. Potter, L. J. Kenney, J. S. Gunn, F. C. Fang, and S. J. Libby.** 2005. Co-regulation of *Salmonella enterica* genes required for virulence and resistance to antimicrobial peptides by SlyA and PhoP/PhoQ. Mol Microbiol **56:**492-508.
291. **Neidhardt, F. C., P. L. Bloch, and D. F. Smith.** 1974. Culture medium for enterobacteria. J Bacteriol **119:**736-47.
292. **Nicholson, B., and D. Low.** 2000. DNA methylation-dependent regulation of *pef* expression in *Salmonella typhimurium*. Mol Microbiol **35:**728-42.
293. **Niedergang, F., J. C. Sirard, C. T. Blanc, and J. P. Kraehehbuhl.** 2000. Entry and survival of *Salmonella typhimurium* in dendritic cells and presentation of recombinant antigens do not require macrophage-specific virulence factors. Proc Natl Acad Sci U S A **97:**14650-14655.
294. **Nikaido, H.** 1994. Isolation of outer membranes. Methods Enzymol **235:**225-34.
295. **Nikaido, H.** 1996. Outer Membrane. ASM Press, Washington, D. C.

296. **Nikaido, H.** 1994. Porins and specific diffusion channels in bacterial outer membranes. J Biol Chem **269:**3905-8.
297. **Nilsson, I. M., O. Hartford, T. Foster, and A. Tarkowski.** 1999. Alpha-toxin and gamma-toxin jointly promote *Staphylococcus aureus* virulence in murine septic arthritis. Infect Immun **67:**1045-9.
298. **Norioka, S., G. Ramakrishnan, K. Ikenaka, and M. Inouye.** 1986. Interaction of a transcriptional activator, OmpR, with reciprocally osmoregulated genes, *ompF* and *ompC*, of *Escherichia coli*. J Biol Chem **261:**17113-9.
299. **Norris, F. A., M. P. Wilson, T. S. Wallis, E. E. Galyov, and P. W. Majerus.** 1998. SopB, a protein required for virulence of *Salmonella dublin*, is an inositol phosphate phosphatase. Proc Natl Acad Sci U S A **95:**14057-9.
300. **Norris, T. L., R. A. Kingsley, and A. J. Bumler.** 1998. Expression and transcriptional control of the *Salmonella typhimurium Ipf* fimbrial operon by phase variation. Mol Microbiol **29:**311-20.
301. **Norte, V. A., M. R. Stapleton, and J. Green.** 2003. PhoP-responsive expression of the *Salmonella enterica* serovar Typhimurium *slyA* gene. J Bacteriol **185:**3508-14.
302. **Novick, R.** 1967. Properties of a cryptic high-frequency transducing phage in *Staphylococcus aureus*. Virology **33:**155-66.
303. **O'Byrne, C. P., and C. J. Dorman.** 1994. The *spv* virulence operon of *Salmonella typhimurium* LT2 is regulated negatively by the cyclic AMP (cAMP)-cAMP receptor protein system. J Bacteriol **176:**905-12.
304. **O'Byrne, C. P., and C. J. Dorman.** 1994. Transcription of the *Salmonella typhimurium* spv virulence locus is regulated negatively by the nucleoid-associated protein H-NS. FEMS Microbiol Lett **121:**99-105.
305. **O'Reilly, M., J. C. de Azavedo, S. Kennedy, and T. J. Foster.** 1986. Inactivation of the alpha-haemolysin gene of *Staphylococcus aureus* 8325-4 by site-directed mutagenesis and studies on the expression of its haemolysins. Microb Pathog **1:**125-38.
306. **Ochman, H., and E. A. Groisman.** 1996. Distribution of pathogenicity islands in *Salmonella* spp. Infect Immun **64:**5410-2.
307. **Ochman, H., F. C. Soncini, F. Solomon, and E. A. Groisman.** 1996. Identification of a pathogenicity island required for *Salmonella* survival in host cells. Proc Natl Acad Sci U S A **93:**7800-4.
308. **Ohl, M. E., and S. I. Miller.** 2001. *Salmonella*: a model for bacterial pathogenesis. Annu Rev Med **52:**259-74.
309. **Okada, N., Y. Oi, M. Takeda-Shitaka, K. Kanou, H. Umeyama, T. Haneda, T. Miki, S. Hosoya, and H. Danbara.** 2007. Identification of amino acid residues of *Salmonella* SlyA that are critical for transcriptional regulation. Microbiology **153:**548-60.
310. **Ostermeier, C., and H. Michel.** 1997. Crystallization of membrane proteins. Curr Opin Struct Biol **7:**697-701.
311. **Otto, K., J. Norbeck, T. Larsson, K. A. Karlsson, and M. Hermansson.** 2001. Adhesion of type 1-fimbriated *Escherichia coli* to abiotic surfaces leads to altered composition of outer membrane proteins. J Bacteriol **183:**2445-53.
312. **Otto, K., and T. J. Silhavy.** 2002. Surface sensing and adhesion of *Escherichia coli* controlled by the Cpx-signaling pathway. Proc Natl Acad Sci U S A **99:**2287-92.
313. **Park, P. W., T. J. Foster, E. Nishi, S. J. Duncan, M. Klagsbrun, and Y. Chen.** 2004. Activation of syndecan-1 ectodomain shedding by *Staphylococcus aureus* alpha-toxin and beta-toxin. J Biol Chem **279:**251-8.

314. **Park, P. W., G. B. Pier, M. J. Preston, O. Goldberger, M. L. Fitzgerald, and M. Bernfield.** 2000. Syndecan-1 shedding is enhanced by LasA, a secreted virulence factor of *Pseudomonas aeruginosa*. J Biol Chem **275:**3057-64.

315. **Parkhill, J., G. Dougan, K. D. James, N. R. Thomson, D. Pickard, J. Wain, C. Churcher, K. L. Mungall, S. D. Bentley, M. T. Holden, M. Sebaihia, S. Baker, D. Basham, K. Brooks, T. Chillingworth, P. Connerton, A. Cronin, P. Davis, R. M. Davies, L. Dowd, N. White, J. Farrar, T. Feltwell, N. Hamlin, A. Haque, T. T. Hien, S. Holroyd, K. Jagels, A. Krogh, T. S. Larsen, S. Leather, S. Moule, P. O'Gaora, C. Parry, M. Quail, K. Rutherford, M. Simmonds, J. Skelton, K. Stevens, S. Whitehead, and B. G. Barrell.** 2001. Complete genome sequence of a multiple drug resistant *Salmonella* enterica serovar Typhi CT18. Nature **413:**848-52.

316. **Patel, A. H., P. Nowlan, E. D. Weavers, and T. Foster.** 1987. Virulence of protein A-deficient and alpha-toxin-deficient mutants of *Staphylococcus aureus* isolated by allele replacement. Infect Immun **55:**3103-10.

317. **Patel, M., M. Yanagishita, G. Roderiquez, D. C. Bou-Habib, T. Oravecz, V. C. Hascall, and M. A. Norcross.** 1993. Cell-surface heparan sulfate proteoglycan mediates HIV-1 infection of T-cell lines. AIDS Res Hum Retroviruses **9:**167-74.

318. **Pattni, K., M. Jepson, H. Stenmark, and G. Banting.** 2001. A PtdIns(3)P-specific probe cycles on and off host cell membranes during *Salmonella* invasion of mammalian cells. Curr Biol **11:**1636-42.

319. **Pellegrini, L., D. F. Burke, F. von Delft, B. Mulloy, and T. L. Blundell.** 2000. Crystal structure of fibroblast growth factor receptor ectodomain bound to ligand and heparin. Nature **407:**1029-34.

320. **Perez-Casal, J., J. S. Swartley, and J. R. Scott.** 1990. Gene encoding the major subunit of CS1 pili of human enterotoxigenic *Escherichia coli*. Infect Immun **58:**3594-600.

321. **Pettersson, J., R. Nordfelth, E. Dubinina, T. Bergman, M. Gustafsson, K. E. Magnusson, and H. Wolf-Watz.** 1996. Modulation of virulence factor expression by pathogen target cell contact. Science **273:**1231-3.

322. **Plotkowski, M. C., A. O. Costa, V. Morandi, H. S. Barbosa, H. B. Nader, S. de Bentzmann, and E. Puchelle.** 2001. Role of heparan sulphate proteoglycans as potential receptors for non-piliated *Pseudomonas aeruginosa* adherence to non-polarised airway epithelial cells. J Med Microbiol **50:**183-90.

323. **Pojasek, K., Z. Shriver, Y. Hu, and R. Sasisekharan.** 2000. Histidine 295 and histidine 510 are crucial for the enzymatic degradation of heparan sulfate by heparinase III. Biochemistry **39:**4012-9.

324. **Prentki, P., and H. M. Krisch.** 1984. *In vitro* insertional mutagenesis with a selectable DNA fragment. Gene **29:**303-13.

325. **Prince, S. M., M. Achtman, and J. P. Derrick.** 2002. Crystal structure of the OpcA integral membrane adhesin from *Neisseria meningitidis*. Proc Natl Acad Sci U S A **99:**3417-21.

326. **Pugsley, A. P.** 1989. Protein targeting, p. 45-48. Academic Press, San Diego, Calif.

327. **Pulkkinen, W. S., and S. I. Miller.** 1991. A *Salmonella typhimurium* virulence protein is similar to a *Yersinia enterocolitica* invasion protein and a bacteriophage lambda outer membrane protein. J Bacteriol **173:**86-93.

328. **Raffatellu, M., R. P. Wilson, D. Chessa, H. Andrews-Polymenis, Q. T. Tran, S. Lawhon, S. Khare, L. G. Adams, and A. J. Baumler.** 2005. SipA, SopA, SopB, SopD, and SopE2 contribute to *Salmonella enterica* serotype Typhimurium invasion of epithelial cells. Infect Immun **73:**146-54.

329. **Raiborg, C., K. G. Bache, D. J. Gillooly, I. H. Madshus, E. Stang, and H. Stenmark.** 2002. Hrs sorts ubiquitinated proteins into clathrin-coated microdomains of early endosomes. Nat Cell Biol **4:**394-8.
330. **Raiborg, C., and H. Stenmark.** 2002. Hrs and endocytic sorting of ubiquitinated membrane proteins. Cell Struct Funct **27:**403-8.
331. **Rapraeger, A. C.** 2001. Molecular interactions of syndecans during development. Semin Cell Dev Biol **12:**107-16.
332. **Reece, K. S., and G. J. Phillips.** 1995. New plasmids carrying antibiotic-resistance cassettes. Gene **165:**141-2.
333. **Rhen, M., P. Riikonen, and S. Taira.** 1993. Transcriptional regulation of *Salmonella enterica* virulence plasmid genes in cultured macrophages. Mol Microbiol **10:**45-56.
334. **Roberts, R. L., M. A. Barbieri, J. Ullrich, and P. D. Stahl.** 2000. Dynamics of rab5 activation in endocytosis and phagocytosis. J Leukoc Biol **68:**627-32.
335. **Rostand, K. S., and J. D. Esko.** 1997. Microbial adherence to and invasion through proteoglycans. Infect Immun **65:**1-8.
336. **Rotger, R., and J. Casadesus.** 1999. The virulence plasmids of *Salmonella*. Int Microbiol **2:**177-84.
337. **Ruiz, N., D. Kahne, and T. J. Silhavy.** 2006. Advances in understanding bacterial outer-membrane biogenesis. Nat Rev Microbiol **4:**57-66.
338. **Ruiz-Albert, J., R. Mundy, X. J. Yu, C. R. Beuzon, and D. W. Holden.** 2003. SseA is a chaperone for the SseB and SseD translocon components of the *Salmonella* pathogenicity-island-2-encoded type III secretion system. Microbiology **149:**1103-11.
339. **Ruiz-Albert, J., X. J. Yu, C. R. Beuzon, A. N. Blakey, E. E. Galyov, and D. W. Holden.** 2002. Complementary activities of SseJ and SifA regulate dynamics of the *Salmonella typhimurium* vacuolar membrane. Mol Microbiol **44:**645-61.
340. **Ruoslahti, E.** 1988. Structure and biology of proteoglycans. Annu Rev Cell Biol **4:**229-55.
341. **Russmann, H., T. Kubori, J. Sauer, and J. E. Galan.** 2002. Molecular and functional analysis of the type III secretion signal of the *Salmonella enterica* InvJ protein. Mol Microbiol **46:**769-79.
342. **Saaf, A., M. Hermansson, and G. von Heijne.** 2000. Formation of cytoplasmic turns between two closely spaced transmembrane helices during membrane protein integration into the ER membrane. J Mol Biol **301:**191-7.
343. **Saiki, R. K., D. H. Gelfand, S. Stoffel, S. J. Scharf, R. Higuchi, G. T. Horn, K. B. Mullis, and H. A. Erlich.** 1988. Primer-directed enzymatic amplification of DNA with a thermostable DNA polymerase. Science **239:**487-91.
344. **Salzman, N. H., D. Ghosh, K. M. Huttner, Y. Paterson, and C. L. Bevins.** 2003. Protection against enteric *salmonellosis* in transgenic mice expressing a human intestinal defensin. Nature **422:**522-6.
345. **Santiviago, C. A., C. S. Toro, A. A. Hidalgo, P. Youderian, and G. C. Mora.** 2003. Global regulation of the *Salmonella enterica* serovar Typhimurium major porin, OmpD. J Bacteriol **185:**5901-5.
346. **Saunders, S., S. Paine-Saunders, and A. D. Lander.** 1997. Expression of the cell surface proteoglycan glypican-5 is developmentally regulated in kidney, limb, and brain. Dev Biol **190:**78-93.
347. **Schechter, L. M., S. M. Damrauer, and C. A. Lee.** 1999. Two AraC/XylS family members can independently counteract the effect of repressing sequences upstream of the *hilA* promoter. Mol Microbiol **32:**629-42.

348. **Schechter, L. M., S. Jain, S. Akbar, and C. A. Lee.** 2003. The small nucleoid-binding proteins H-NS, HU, and Fis affect *hilA* expression in *Salmonella enterica* serovar Typhimurium. Infect Immun **71:**5432-5.
349. **Schechter, L. M., and C. A. Lee.** 2001. AraC/XylS family members, HilC and HilD, directly bind and derepress the *Salmonella typhimurium hilA* promoter. Mol Microbiol **40:**1289-99.
350. **Scherer, C. A., E. Cooper, and S. I. Miller.** 2000. The *Salmonella* type III secretion translocon protein SspC is inserted into the epithelial cell plasma membrane upon infection. Mol Microbiol **37:**1133-45.
351. **Schesser, K., E. Frithz-Lindsten, and H. Wolf-Watz.** 1996. Delineation and mutational analysis of the *Yersinia pseudotuberculosis* YopE domains which mediate translocation across bacterial and eukaryotic cellular membranes. J Bacteriol **178:**7227-33.
352. **Schwan, W. R., M. T. Beck, S. J. Hultgren, J. Pinkner, N. L. Woolever, and T. Larson.** 2005. Down-regulation of the *kps* region 1 capsular assembly operon following attachment of *Escherichia coli* type 1 fimbriae to D-mannose receptors. Infect Immun **73:**1226-31.
353. **Schweder, T., K. H. Lee, O. Lomovskaya, and A. Matin.** 1996. Regulation of *Escherichia coli* starvation sigma factor (sigma s) by ClpXP protease. J Bacteriol **178:**470-6.
354. **Scott, C. C., P. Cuellar-Mata, T. Matsuo, H. W. Davidson, and S. Grinstein.** 2002. Role of 3-phosphoinositides in the maturation of *Salmonella*-containing vacuoles within host cells. J Biol Chem **277:**12770-6.
355. **Scott, J. R., J. C. Wakefield, P. W. Russell, P. E. Orndorff, and B. J. Froehlich.** 1992. CooB is required for assembly but not transport of CS1 pilin. Mol Microbiol **6:**293-300.
356. **Seaman, G. V. F.** 1974. Electrokinetic behaviour of red cells, p. 1135-1229, 2nd ed, vol. 2. Academic Press Inc., New York.
357. **Shafer, W. M.** 1988. Lipopolysaccharide masking of gonococcal outer-membrane proteins modulates binding of bacterial cathepsin G to gonococci. J Gen Microbiol **134:**539-45.
358. **Shea, J. E., M. Hensel, C. Gleeson, and D. W. Holden.** 1996. Identification of a virulence locus encoding a second type III secretion system in *Salmonella typhimurium*. Proc Natl Acad Sci U S A **93:**2593-7.
359. **Sheppard, M., C. Webb, F. Heath, V. Mallows, R. Emilianus, D. Maskell, and P. Mastroeni.** 2003. Dynamics of bacterial growth and distribution within the liver during *Salmonella* infection. Cell Microbiol **5:**593-600.
360. **Sherlock, O., M. A. Schembri, A. Reisner, and P. Klemm.** 2004. Novel roles for the AIDA adhesin from diarrheagenic *Escherichia coli*: cell aggregation and biofilm formation. J Bacteriol **186:**8058-65.
361. **Shi, Y., T. Latifi, M. J. Cromie, and E. A. Groisman.** 2004. Transcriptional control of the antimicrobial peptide resistance *ugtL* gene by the *Salmonella* PhoP and SlyA regulatory proteins. J Biol Chem **279:**38618-25.
362. **Shieh, M. T., D. WuDunn, R. I. Montgomery, J. D. Esko, and P. G. Spear.** 1992. Cell surface receptors for herpes simplex virus are heparan sulfate proteoglycans. J Cell Biol **116:**1273-81.
363. **Shin, D., E. J. Lee, H. Huang, and E. A. Groisman.** 2006. A positive feedback loop promotes transcription surge that jump-starts *Salmonella* virulence circuit. Science **314:**1607-9.
364. **Shotland, Y., H. Kramer, and E. A. Groisman.** 2003. The *Salmonella* SpiC protein targets the mammalian Hook3 protein function to alter cellular trafficking. Mol Microbiol **49:**1565-76.

365. **Simonet, M., and S. Falkow.** 1992. Invasin expression in *Yersinia pseudotuberculosis*. Infect Immun **60:**4414-7.
366. **Singh SP, Miller S, Williams YU, Rudd KE, and N. H.** 1996. Immunochemical structure of the OmpD porin from *Salmonella typhimurium*. Microbiology **142:**3201-3210.
367. **Singh, S. P., Y. Upshaw, T. Abdullah, S. R. Singh, and P. E. Klebba.** 1992. Structural relatedness of enteric bacterial porins assessed with monoclonal antibodies to *Salmonella typhimurium* OmpD and OmpC. J Bacteriol **174:**1965-73.
368. **Snavely, M. D., S. A. Gravina, T. T. Cheung, C. G. Miller, and M. E. Maguire.** 1991. Magnesium transport in *Salmonella typhimurium*. Regulation of *mgtA* and *mgtB* expression. J Biol Chem **266:**824-9.
369. **Snavely, M. D., C. G. Miller, and M. E. Maguire.** 1991. The *mgtB* Mg2+ transport locus of *Salmonella typhimurium* encodes a P-type ATPase. J Biol Chem **266:**815-23.
370. **Sohel, I., J. L. Puente, W. J. Murray, J. Vuopio-Varkila, and G. K. Schoolnik.** 1993. Cloning and characterization of the bundle-forming pilin gene of enteropathogenic *Escherichia coli* and its distribution in *Salmonella* serotypes. Mol Microbiol **7:**563-75.
371. **Soncini, F. C., E. G. Vescovi, and E. A. Groisman.** 1995. Transcriptional autoregulation of the *Salmonella typhimurium* phoPQ operon. J Bacteriol **177:**4364-71.
372. **Sorg, J. A., N. C. Miller, and O. Schneewind.** 2005. Substrate recognition of type III secretion machines--testing the RNA signal hypothesis. Cell Microbiol **7:**1217-25.
373. **Sory, M. P., A. Boland, I. Lambermont, and G. R. Cornelis.** 1995. Identification of the YopE and YopH domains required for secretion and internalization into the cytosol of macrophages, using the *cyaA* gene fusion approach. Proc Natl Acad Sci U S A **92:**11998-2002.
374. **Stanier, R. Y., J. L. Ingraham, M. L. Wheelis, and P. R. Painter.** 1987. The enteric group and related eubacteria, Fifth ed, vol. 19. Macmillan Education.
375. **Stebbins, C. E., and J. E. Galan.** 2003. Priming virulence factors for delivery into the host. Nat Rev Mol Cell Biol **4:**738-43.
376. **Stebbins, C. E., and J. E. Galan.** 2001. Structural mimicry in bacterial virulence. Nature **412:**701-5.
377. **Steele-Mortimer, O., M. St-Louis, M. Olivier, and B. B. Finlay.** 2000. Vacuole acidification is not required for survival of *Salmonella enterica* serovar Typhimurium within cultured macrophages and epithelial cells. Infect Immun **68:**5401-4.
378. **Stephens, R. S., K. Koshiyama, E. Lewis, and A. Kubo.** 2001. Heparin-binding outer membrane protein of *chlamydiae*. Mol Microbiol **40:**691-9.
379. **Stone, B. J., C. M. Garcia, J. L. Badger, T. Hassett, R. I. Smith, and V. L. Miller.** 1992. Identification of novel loci affecting entry of *Salmonella enteritidis* into eukaryotic cells. J Bacteriol **174:**3945-52.
380. **Strindelius, L., A. Folkesson, S. Normark, and I. Sjoholm.** 2004. Immunogenic properties of the *Salmonella* atypical fimbriae in BALB/c mice. Vaccine **22:**1448-56.
381. **Studier, F. W.** 2005. Protein production by auto-induction in high density shaking cultures. Protein Expr Purif **41:**207-34.
382. **Sukupolvi, S., R. Vuorio, S. Y. Qi, D. O'Connor, and M. Rhen.** 1990. Characterization of the traT gene and mutants that increase outer membrane permeability from the *Salmonella typhimurium* virulence plasmid. Mol Microbiol **4:**49-57.

383. **Swenson, D. L., and S. Clegg.** 1992. Identification of ancillary *fim* genes affecting FimA expression in *Salmonella typhimurium*. J Bacteriol **174:**7697-704.
384. **Tamm, L. K., H. Hong, and B. Liang.** 2004. Folding and assembly of beta-barrel membrane proteins. Biochim Biophys Acta **1666:**250-63.
385. **Tardy, F., F. Homble, C. Neyt, R. Wattiez, G. R. Cornelis, J. M. Ruysschaert, and V. Cabiaux.** 1999. *Yersinia enterocolitica* type III secretion-translocation system: channel formation by secreted Yops. Embo J **18:**6793-9.
386. **Tauxe, R. V., and A. T. Pavia.** 1998. Salmonellosis: nontyphoidal, 3rd ed ed. Plenum Medical Book Co, New York, N.Y.
387. **Terebiznik, M. R., O. V. Vieira, S. L. Marcus, A. Slade, C. M. Yip, W. S. Trimble, T. Meyer, B. B. Finlay, and S. Grinstein.** 2002. Elimination of host cell PtdIns(4,5)P(2) by bacterial SigD promotes membrane fission during invasion by *Salmonella*. Nat Cell Biol **4:**766-73.
388. **Tezcan-Merdol, D., T. Nyman, U. Lindberg, F. Haag, F. Koch-Nolte, and M. Rhen.** 2001. Actin is ADP-ribosylated by the *Salmonella enterica* virulence-associated protein SpvB. Mol Microbiol **39:**606-19.
389. **Tierrez, A., and F. Garcia-del Portillo.** 2005. New concepts in *Salmonella* virulence: the importance of reducing the intracellular growth rate in the host. Cell Microbiol **7:**901-909.
390. **Tsolis, R. M., S. M. Townsend, E. A. Miao, S. I. Miller, T. A. Ficht, L. G. Adams, and A. J. Baumler.** 1999. Identification of a putative *Salmonella enterica* serotype Typhimurium host range factor with homology to IpaH and YopM by signature-tagged mutagenesis. Infect Immun **67:**6385-93.
391. **Tu, X., T. Latifi, A. Bougdour, S. Gottesman, and E. A. Groisman.** 2006. The PhoP/PhoQ two-component system stabilizes the alternative sigma factor RpoS in *Salmonella enterica*. Proc Natl Acad Sci U S A **103:**13503-8.
392. **Turnbull, P. C. B.** 1979. Food poisoning with special reference to *Salmonella*-its epidemiology, pathogenesis and control. Clin. Gastroenterol **8:**663-714.
393. **Uchiya, K., M. A. Barbieri, K. Funato, A. H. Shah, P. D. Stahl, and E. A. Groisman.** 1999. A *Salmonella* virulence protein that inhibits cellular trafficking. Embo J **18:**3924-33.
394. **Uchiya, K., and T. Nikai.** 2004. *Salmonella enterica* serovar Typhimurium infection induces cyclooxygenase 2 expression in macrophages: involvement of Salmonella pathogenicity island 2. Infect Immun **72:**6860-9.
395. **Unsworth, K. E., M. Way, M. McNiven, L. Machesky, and D. W. Holden.** 2004. Analysis of the mechanisms of *Salmonella*-induced actin assembly during invasion of host cells and intracellular replication. Cell Microbiol **6:**1041-55.
396. **Valle, E., and D. G. Guiney.** 2005. Characterization of *Salmonella*-induced cell death in human macrophage-like THP-1 cells. Infect Immun **73:**2835-40.
397. **van der Straaten, T., A. van Diepen, K. Kwappenberg, S. van Voorden, K. Franken, R. Janssen, J. G. Kusters, D. L. Granger, and J. T. van Dissel.** 2001. Novel *Salmonella enterica* serovar Typhimurium protein that is indispensable for virulence and intracellular replication. Infect Immun **69:**7413-8.
398. **van der Velden, A. W., A. J. Baumler, R. M. Tsolis, and F. Heffron.** 1998. Multiple fimbrial adhesins are required for full virulence of *Salmonella typhimurium* in mice. Infect Immun **66:**2803-8.
399. **van der Velden, A. W., S. W. Lindgren, M. J. Worley, and F. Heffron.** 2000. *Salmonella* pathogenicity island 1-independent induction of apoptosis in infected macrophages by *Salmonella enterica* serotype Typhimurium. Infect Immun **68:**5702-9.

400. **van Putten, J. P., T. D. Duensing, and R. L. Cole.** 1998. Entry of OpaA+ gonococci into HEp-2 cells requires concerted action of glycosaminoglycans, fibronectin and integrin receptors. Mol Microbiol **29:**369-79.

401. **van Putten, J. P., and S. M. Paul.** 1995. Binding of syndecan-like cell surface proteoglycan receptors is required for *Neisseria gonorrhoeae* entry into human mucosal cells. Embo J **14:**2144-54.

402. **Vandenbosch, J. L., D. R. Kurlandsky, R. Urdangaray, and G. W. Jones.** 1989. Evidence of coordinate regulation of virulence in *Salmonella typhimurium* involving the *rsk* element of the 95-kilobase plasmid. Infect Immun **57:**2566-8.

403. **Vazquez-Torres, A., J. Jones-Carson, A. J. Baumler, S. Falkow, R. Valdivia, W. Brown, M. Le, R. Berggren, W. T. Parks, and F. C. Fang.** 1999. Extraintestinal dissemination of Salmonella by CD18-expressing phagocytes. Nature **401:**804-8.

404. **Vazquez-Torres, A., Y. Xu, J. Jones-Carson, D. W. Holden, S. M. Lucia, M. C. Dinauer, P. Mastroeni, and F. C. Fang.** 2000. *Salmonella* pathogenicity island 2-dependent evasion of the phagocyte NADPH oxidase. Science **287:**1655-8.

405. **Vieira, O. V., C. Bucci, R. E. Harrison, W. S. Trimble, L. Lanzetti, J. Gruenberg, A. D. Schreiber, P. D. Stahl, and S. Grinstein.** 2003. Modulation of Rab5 and Rab7 recruitment to phagosomes by phosphatidylinositol 3-kinase. Mol Cell Biol **23:**2501-14.

406. **Waldispuhl, J., B. Berger, P. Clote, and J. M. Steyaert.** 2006. Predicting transmembrane beta-barrels and interstrand residue interactions from sequence. Proteins **65:**61-74.

407. **Waterman, S. R., and D. W. Holden.** 2003. Functions and effectors of the *Salmonella* pathogenicity island 2 type III secretion system. Cell Microbiol **5:**501-11.

408. **Watson, P. R., A. V. Gautier, S. M. Paulin, A. P. Bland, P. W. Jones, and T. S. Wallis.** 2000. *Salmonella enterica* serovars Typhimurium and Dublin can lyse macrophages by a mechanism distinct from apoptosis. Infect Immun **68:**3744-7.

409. **Weiss, M. S., U. Abele, J. Weckesser, W. Welte, E. Schiltz, and G. E. Schulz.** 1991. Molecular architecture and electrostatic properties of a bacterial porin. Science **254:**1627-30.

410. **Wells, C. L., R. P. Jechorek, K. M. Kinneberg, S. M. Debol, and S. L. Erlandsen.** 1999. The isoflavone genistein inhibits internalization of enteric bacteria by cultured Caco-2 and HT-29 enterocytes. J Nutr **129:**634-40.

411. **Wilmes-Riesenberg, M. R., J. W. Foster, and R. Curtiss, 3rd.** 1997. An altered *rpoS* allele contributes to the avirulence of *Salmonella typhimurium* LT2. Infect Immun **65:**203-10.

412. **Wimley, W. C.** 2003. The versatile beta-barrel membrane protein. Curr Opin Struct Biol **13:**404-11.

413. **Wong, K. K., M. McClelland, L. C. Stillwell, E. C. Sisk, S. J. Thurston, and J. D. Saffer.** 1998. Identification and sequence analysis of a 27-kilobase chromosomal fragment containing a *Salmonella* pathogenicity island located at 92 minutes on the chromosome map of *Salmonella enterica* serovar Typhimurium LT2. Infect Immun **66:**3365-71.

414. **Wood, M. W., M. A. Jones, P. R. Watson, S. Hedges, T. S. Wallis, and E. E. Galyov.** 1998. Identification of a pathogenicity island required for *Salmonella* enteropathogenicity. Mol Microbiol **29:**883-91.

415. **Wood, M. W., R. Rosqvist, P. B. Mullan, M. H. Edwards, and E. E. Galyov.** 1996. SopE, a secreted protein of *Salmonella* dublin, is translocated into the target eukaryotic cell via a sip-dependent mechanism and promotes bacterial entry. Mol Microbiol **22:**327-38.

416. **Wosten, M. M., L. F. Kox, S. Chamnongpol, F. C. Soncini, and E. A. Groisman.** 2000. A signal transduction system that responds to extracellular iron. Cell **103:**113-25.
417. **Wulff-Strobel, C. R., A. W. Williams, and S. C. Straley.** 2002. LcrQ and SycH function together at the Ysc type III secretion system in *Yersinia pestis* to impose a hierarchy of secretion. Mol Microbiol **43:**411-23.
418. **Yamagata, T., H. Saito, O. Habuchi, and S. Suzuki.** 1968. Purification and properties of bacterial chondroitinases and chondrosulfatases. J Biol Chem **243:**1523-35.
419. **Yamamoto, K., H. Ogasawara, N. Fujita, R. Utsumi, and A. Ishihama.** 2002. Novel mode of transcription regulation of divergently overlapping promoters by PhoP, the regulator of two-component system sensing external magnesium availability. Mol Microbiol **45:**423-38.
420. **Yanisch-Perron, C., J. Vieira, and J. Messing.** 1985. Improved M13 phage cloning vectors and host strains: nucleotide sequences of the M13mp18 and pUC19 vectors. Gene **33:**103-19.
421. **Zhou, D., M. S. Mooseker, and J. E. Galan.** 1999. An invasion-associated *Salmonella* protein modulates the actin-bundling activity of plastin. Proc Natl Acad Sci U S A **96:**10176-81.
422. **Zhou, D., M. S. Mooseker, and J. E. Galan.** 1999. Role of the *Salmonella typhimurium* actin-binding protein SipA in bacterial internalization. Science **283:**2092-5.
423. **Zurawski, D. V., and M. A. Stein.** 2003. SseA acts as the chaperone for the SseB component of the *Salmonella* Pathogenicity Island 2 translocon. Mol Microbiol **47:**1341-51.
424. **Zwir, I., D. Shin, A. Kato, K. Nishino, T. Latifi, F. Solomon, J. M. Hare, H. Huang, and E. A. Groisman.** 2005. Dissecting the PhoP regulatory network of *Escherichia coli* and *Salmonella enterica*. Proc Natl Acad Sci U S A **102:**2862-7.

Appendix I

Mascot Search Results

```
          : Mascot Daemon
          :
 title    : Submitted from Matthew 2 3 4 rpt bacteria by Mascot Daemon on BMSQSPROC2 (Matthew 4 rpt)
a file    : E:\PE Sciex Data\Projects\data from Q-Star\Matthew 4 rpt.wiff
se        : MSDB 20060518 (2344227 sequences; 779380795 residues)
my        : Bacteria (Eubacteria) (857805 sequences)
amp       : 16 Mar 2007 at 10:10:34 GMT
icant hits: RPECL          lactose operon repressor - Escherichia coli (strain K-12)
            E85566         probable ATP-binding protein in pho regulon ybeZ [imported] - Escherichia coli (strain O157:H7, sub
            JGECM          periplasmic maltose-binding protein precursor - Escherichia coli (strain K-12)
            Q5QYC4_IDILO   Phosphate starvation-inducible protein PhoH.- Idiomarina loihiensis.
            PNECP          beta-lactamase (EC 3.5.2.6) precursor - Escherichia coli plasmids
            DNAJ_ECO57     Chaperone protein dnaJ.- Escherichia coli O157:H7.
```

ıbility Based Mowse Score

ore is -10*Log(P), where P is the probability that the observed match is a random event.
lual ions scores > 43 indicate identity or extensive homology (p<0.05).
ı scores are derived from ions scores as a non-probabilistic basis for ranking protein hits.

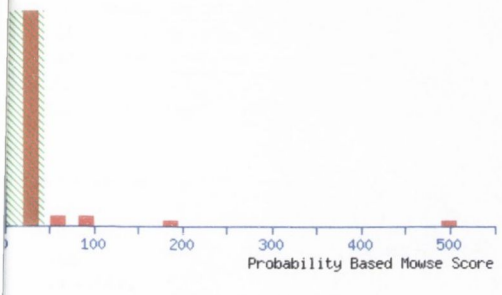

ide Summary Report

nat As | Peptide Summary | Help

Significance threshold p< 0.05 Max. number of hits AUTO

Standard scoring ◉ MudPIT scoring ○ Ions score cut-off 0 Show sub-sets ☐

Show pop-ups ◉ Suppress pop-ups ○ Sort unassigned Decreasing Score Require bold red ☐

ct All | Select None | Search Selected | ☐ Error tolerant | Archive Report

RPECL **Mass:** 38737 **Score:** 499 **Queries matched:** 23
lactose operon repressor - Escherichia coli (strain K-12)
☐ Check to include this hit in error tolerant search or archive report

	Query	Observed	Mr(expt)	Mr(calc)	Delta	Miss	Score	Expect	Rank	Peptide
☑	542	494.77	987.53	987.53	-0.00	0	48	0.023	1	R.LLGQTSVDR.L
☑	544	494.77	987.53	987.53	-0.00	0	(22)	9.9	1	R.LLGQTSVDR.L
	645	364.88	1091.62	1091.62	0.00	0	(9)	1.6e+002	4	K.AAVHNLLAQR.V
☑	646	364.88	1091.62	1091.62	0.00	0	(11)	91	1	K.AAVHNLLAQR.V
☑	647	364.89	1091.65	1091.62	0.03	0	34	0.49	1	K.AAVHNLLAQR.V
☑	695	584.36	1166.71	1166.70	0.01	0	33	0.48	1	K.GNQLLPVSLVK.R
☑	703	592.84	1183.66	1183.69	-0.03	0	62	0.0008	1	R.LLQLSQGQAVK.G
☑	704	592.84	1183.66	1183.69	-0.03	0	(43)	0.065	1	R.LLQLSQGQAVK.G
	705	592.86	1183.71	1183.69	0.02	0	(13)	61	2	R.LLQLSQGQAVK.G
☑	711	602.81	1203.61	1203.63	-0.02	0	(32)	0.84	1	R.ALADSLMQLAR.Q + Oxidation (M)
☑	712	602.82	1203.63	1203.63	0.00	0	84	5e-006	1	R.ALADSLMQLAR.Q + Oxidation (M)
☑	755	441.95	1322.82	1322.80	0.02	1	21	6.8	1	K.GNQLLPVSLVKR.K
☑	769	679.35	1356.69	1356.70	-0.01	0	(62)	0.00077	1	K.TTLAPNTQTASPR.A
☑	771	679.38	1356.74	1356.70	0.04	0	82	7.5e-006	1	K.TTLAPNTQTASPR.A
☑	772	679.38	1356.74	1356.70	0.04	0	(71)	9.7e-005	1	K.TTLAPNTQTASPR.A
☑	832	788.88	1575.75	1575.79	-0.04	0	35	0.34	1	R.ADQLGASVVVSMVER.S + Oxidation (M)
☑	833	526.28	1575.82	1575.79	0.03	0	(32)	0.65	1	R.ADQLGASVVVSMVER.S + Oxidation (M)
☑	840	536.29	1605.84	1605.78	0.06	0	22	6.2	1	K.VEAAMAELNYIPNR.V + Oxidation (M)
☑	889	607.32	1818.95	1818.93	0.02	1	19	11	1	K.SRADQLGASVVVSMVER.S + Oxidation (M)
☑	890	607.32	1818.95	1818.93	0.02	1	(18)	15	1	K.SRADQLGASVVVSMVER.S + Oxidation (M)
☑	900	621.98	1862.93	1862.92	0.01	1	(22)	6	1	R.EKVEAAMAELNYIPNR.V + Oxidation (M)
☑	901	621.98	1862.93	1862.92	0.01	1	31	0.68	1	R.EKVEAAMAELNYIPNR.V + Oxidation (M)
☑	912	718.74	2153.21	2153.22	-0.01	1	28	1	1	R.LLGQTSVDRLLQLSQGQAVK.G

Proteins matching the same set of peptides:

CAC39977 **Mass:** 39023 **Score:** 499 **Queries matched:** 23
Sequence 2 from Patent EP1106695.- synthetic construct.
AAC83652 **Mass:** 38711 **Score:** 499 **Queries matched:** 23
REPRESSOR PROTEIN LACI.- Integrational vector pMUTIN2.

E85566 **Mass:** 40743 **Score:** 182 **Queries matched:** 5
probable ATP-binding protein in pho regulon ybeZ [imported] - Escherichia coli (strain O157:H7, sub
Check to include this hit in error tolerant search or archive report

Query	Observed	Mr(expt)	Mr(calc)	Delta	Miss	Score	Expect	Rank	Peptide
696	584.78	1167.55	1167.56	-0.01	0	6	3e+002	7	R.SLYVDTAPMR.G + Oxidation (M)
724	614.83	1227.64	1227.61	0.03	0	26	3.2	1	R.EITLEPADNAR.L
785	696.37	1390.72	1390.73	-0.00	0	35	0.39	1	R.NVIEVAPLAYMR.G + Oxidation (M)
807	749.42	1496.82	1496.82	0.00	0	77	1.8e-005	1	K.AVITGDVTQIDLPR.N
815	768.37	1534.73	1534.75	-0.02	0	39	0.13	1	R.VLEQSAESVPEYGK.A

JGECM **Mass:** 43360 **Score:** 79 **Queries matched:** 4
periplasmic maltose-binding protein precursor - Escherichia coli (strain K-12)
Check to include this hit in error tolerant search or archive report

Query	Observed	Mr(expt)	Mr(calc)	Delta	Miss	Score	Expect	Rank	Peptide
421	447.26	892.52	892.50	0.01	0	13	62	1	K.DLLPNPPK.T
759	446.23	1335.66	1335.63	0.03	1	7	2.2e+002	7	K.SYEEELAKDPR.I
761	669.37	1336.73	1336.74	-0.00	0	49	0.013	1	K.VNYGVTVLPTFK.G
911	713.73	2138.16	2138.15	0.01	0	9	87	2	K.GQPSKPFVGVLSAGINAASPNK.E

Proteins matching the same set of peptides:
1A7LA **Mass:** 41707 **Score:** 79 **Queries matched:** 4
male-b363, chain A - Escherichia coli k12
1A7LB **Mass:** 40889 **Score:** 79 **Queries matched:** 4
male-b363, chain B - Escherichia coli k12
1A7LC **Mass:** 39657 **Score:** 79 **Queries matched:** 4
male-b363, chain C - Escherichia coli k12
1IUD **Mass:** 40555 **Score:** 79 **Queries matched:** 4
maltodextrin-binding protein male-b133 mutant INSERTED B-CELL EPITOPE FROM THE PRES2 REGION OF hepa
1MDPA **Mass:** 39897 **Score:** 79 **Queries matched:** 4
maltose-binding protein mutant (ins(D134, P135), del(136-142)) (with maltose), chain A - Escherichi
1MDQ **Mass:** 40755 **Score:** 79 **Queries matched:** 4
maltose-binding protein mutant (A301GS) (with maltose) - Escherichia coli
1MPB **Mass:** 40652 **Score:** 79 **Queries matched:** 4
maltodextrin-binding protein mutant W230R - Escherichia coli
4MBP **Mass:** 40682 **Score:** 79 **Queries matched:** 4
maltodextrin binding protein - Escherichia coli
E961510 **Mass:** 43366 **Score:** 79 **Queries matched:** 4
E.COLI MALE PROTEIN.- Escherichia coli.

Q5QYC4_IDILO **Mass:** 37040 **Score:** 78 **Queries matched:** 2
Phosphate starvation-inducible protein PhoH.- Idiomarina loihiensis.
Check to include this hit in error tolerant search or archive report

Query	Observed	Mr(expt)	Mr(calc)	Delta	Miss	Score	Expect	Rank	Peptide
785	696.37	1390.72	1390.73	-0.00	0	35	0.39	1	R.NVIEVAPLAYMR.G + Oxidation (M)
807	749.42	1496.82	1496.82	0.00	0	44	0.045	2	R.AVITGDITQVDLPR.G

PNECP **Mass:** 31666 **Score:** 65 **Queries matched:** 3
beta-lactamase (EC 3.5.2.6) precursor - Escherichia coli plasmids
Check to include this hit in error tolerant search or archive report

Query	Observed	Mr(expt)	Mr(calc)	Delta	Miss	Score	Expect	Rank	Peptide
643	544.32	1086.62	1086.62	-0.00	0	14	55	4	K.VLLCGAVLSR.V
751	654.35	1306.68	1306.68	0.00	0	35	0.35	1	R.VGYIELDLNSGK.I
766	451.27	1350.78	1350.76	0.01	0	16	25	3	R.GIIAALGPDGKPSR.I

Proteins matching the same set of peptides:
1AXB **Mass:** 29045 **Score:** 65 **Queries matched:** 3
tem-1 beta lactamase (EC 3.5.2.6) mutant VARIANT V84I, A184V - Escherichia coli
1XPB **Mass:** 29003 **Score:** 65 **Queries matched:** 3
beta-lactamase (EC 3.5.2.6) - Escherichia coli
Q4GX46_SALDE **Mass:** 31669 **Score:** 65 **Queries matched:** 3
TEM-derived extended spectrum beta-lactamase.- Salmonella derby.
Q4GY26_ECOLI **Mass:** 29664 **Score:** 65 **Queries matched:** 3

Mascot Search Results

```
          : Mascot Daemon
          :
 title    : Submitted from Matthew 2 3 4 rpt bacteria by Mascot Daemon on BMSQSPROC2 (Matthew 3 rpt)
 file     : E:\PE Sciex Data\Projects\data from Q-Star\Matthew 3 rpt.wiff
se        : MSDB 20060518 (2344227 sequences; 779380795 residues)
ny        : Bacteria (Eubacteria) (857805 sequences)
mp        : 16 Mar 2007 at 10:04:47 GMT
icant hits: E86053        heat shock protein [imported] - Escherichia coli (strain O157:H7, substrain EDL933)
            AD0496        heat shock protein [imported] - Yersinia pestis (strain CO92)
            AAA24425      ECOPROTS NID:  - Escherichia coli W3110
            R5EC14        ribosomal protein L14 [validated] - Escherichia coli (strain K-12)
            O605C2_METCA  50S ribosomal protein L14.- Methylococcus capsulatus.
            S55903        phosphotransferase system enzyme II, galactitol specific, protein A - Escherichia coli (strain EC31
```

bility Based Mowse Score

ore is -10*Log(P), where P is the probability that the observed match is a random event.
ual ions scores > 42 indicate identity or extensive homology (p<0.05).
scores are derived from ions scores as a non-probabilistic basis for ranking protein hits.

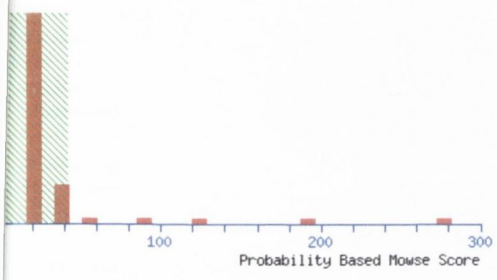

de Summary Report

at As Peptide Summary Help

Significance threshold p< 0.05 Max. number of hits AUTO

Standard scoring ◉ MudPIT scoring ○ Ions score cut-off 0 Show sub-sets ☐

Show pop-ups ◉ Suppress pop-ups ○ Sort unassigned Decreasing Score Require bold red ☐

t All Select None Search Selected ☐ Error tolerant Archive Report

E86053 **Mass:** 15764 **Score:** 277 **Queries matched:** 8
heat shock protein [imported] - Escherichia coli (strain O157:H7, substrain EDL933)
☐ Check to include this hit in error tolerant search or archive report

Query	Observed	Mr(expt)	Mr(calc)	Delta	Miss	Score	Expect	Rank	Peptide
335	562.81	1123.60	1123.57	0.03	0	15	33	4	R.NFDLSPLYR.S
☑ 368	607.32	1212.63	1212.61	0.02	0	62	0.00082	1	R.TYLYQGIAER.N
☑ 369	607.34	1212.66	1212.61	0.04	0	(13)	63	1	R.TYLYQGIAER.N
☑ 374	409.57	1225.69	1225.66	0.03	0	31	0.96	1	K.FQLAENIHVR.G
☑ 406	452.27	1353.79	1353.75	0.04	1	32	0.64	1	R.KFQLAENIHVR.G
☑ 426	476.59	1426.75	1426.70	0.05	1	27	2	1	-.MRNFDLSPLYR.S + Oxidation (M)
☑ 475	830.47	1658.92	1658.90	0.02	0	90	8.5e-007	1	R.GANLVNGLLYIDLER.V
☑ 488	587.32	1758.94	1758.87	0.08	1	20	9	1	R.TYLYQGIAERNFER.K

AD0496 **Mass:** 15638 **Score:** 185 **Queries matched:** 5
heat shock protein [imported] - Yersinia pestis (strain CO92)
☐ Check to include this hit in error tolerant search or archive report

Query	Observed	Mr(expt)	Mr(calc)	Delta	Miss	Score	Expect	Rank	Peptide
368	607.32	1212.63	1212.61	0.02	0	62	0.00082	1	R.TYLYQGIAER.N
369	607.34	1212.66	1212.61	0.04	0	(13)	63	1	R.TYLYQGIAER.N
374	409.57	1225.69	1225.72	-0.03	1	13	59	8	K.FQLAEHIKIK.G
475	830.47	1658.92	1658.90	0.02	0	90	8.5e-007	1	K.GANLVNGLLYIDLER.L
488	587.32	1758.94	1758.87	0.08	1	20	9	1	R.TYLYQGIAERNFER.K

AAA24425 **Mass:** 16083 **Score:** 124 **Queries matched:** 5
ECOPROTS NID: - Escherichia coli W3110
☐ Check to include this hit in error tolerant search or archive report

Query	Observed	Mr(expt)	Mr(calc)	Delta	Miss	Score	Expect	Rank	Peptide

245	481.31	960.60	960.58	0.03	0	48	0.022	1	R.ITLALAGFR.Q
323	554.79	1107.56	1107.54	0.03	0	7	2.2e+002	4	R.NFDLSPLMR.Q + Oxidation (M)
356	585.84	1169.67	1169.64	0.03	0	24	5	1	R.IAISERPALNS.-
428	715.89	1429.76	1429.70	0.06	0	32	0.73	1	R.QEDLEIQLEGTR.L
515	764.40	2290.16	2290.12	0.04	0	12	38	1	K.LANALQNAGESQSFPPYNIEK.S

Proteins matching the same set of peptides:
B91207 **Mass:** 16315 **Score:** 124 **Queries matched:** 5
heat shock protein IbpB [imported] - Escherichia coli (strain O157:H7, substrain RIMD 0509952)

R5EC14 **Mass:** 13646 **Score:** 88 **Queries matched:** 4
ribosomal protein L14 [validated] - Escherichia coli (strain K-12)
Check to include this hit in error tolerant search or archive report

Query	Observed	Mr(expt)	Mr(calc)	Delta	Miss	Score	Expect	Rank	Peptide
145	395.25	788.48	788.45	0.02	0	21	14	2	R.IFGPVTR.E
225	468.27	934.52	934.51	0.01	0	21	11	1	R.YAGVGDIIK.I
240	477.80	953.58	953.58	0.01	0	14	43	1	K.IISLAPEVL.-
501	637.31	1908.92	1908.87	0.05	0	32	0.48	1	-.MIQEQTMLNVADNSGAR.R + 2 Oxidation (M)

Proteins matching the same set of peptides:
AC1007 **Mass:** 13674 **Score:** 88 **Queries matched:** 4
50S ribosomal chain protein L14 [imported] - Salmonella enterica subsp. enterica serovar Typhi (str
JC2276 **Mass:** 13687 **Score:** 88 **Queries matched:** 4
ribosomal protein L14 - pea aphid symbiont bacterium

O605C2_METCA **Mass:** 13639 **Score:** 53 **Queries matched:** 3
50S ribosomal protein L14.- Methylococcus capsulatus.
Check to include this hit in error tolerant search or archive report

Query	Observed	Mr(expt)	Mr(calc)	Delta	Miss	Score	Expect	Rank	Peptide
145	395.25	788.48	788.45	0.02	0	21	14	2	R.IFGPVTR.E
240	477.80	953.58	953.58	0.01	0	14	43	1	K.IISLAPEVL.-
501	637.31	1908.92	1908.85	0.07	0	18	12	4	-.MIQMQTCLDVADNSGAR.Q

S55903 **Mass:** 17025 **Score:** 45 **Queries matched:** 3
phosphotransferase system enzyme II, galactitol specific, protein A - Escherichia coli (strain EC31
Check to include this hit in error tolerant search or archive report

Query	Observed	Mr(expt)	Mr(calc)	Delta	Miss	Score	Expect	Rank	Peptide
128	375.23	748.44	748.42	0.01	0	18	28	1	M.TNLFVR.S
408	454.94	1361.80	1361.77	0.04	0	17	23	2	K.SSAIYLLRPTNK.V
453	519.96	1556.87	1556.79	0.08	0	11	86	3	R.SEVLTHIGNEMLAK.G + Oxidation (M)

Proteins matching the same set of peptides:
A90991 **Mass:** 17011 **Score:** 45 **Queries matched:** 3
pts system, galactitol-specific IIA component - Escherichia coli (strain O157:H7, substrain RIMD 05

---

ide matches not assigned to protein hits: (no details means no match)

Query	Observed	Mr(expt)	Mr(calc)	Delta	Miss	Score	Expect	Rank	Peptide
381	624.33	1246.65	1246.63	0.02	0	38	0.19	1	STPFAAQVAAER
382	625.30	1248.59	1248.54	0.05	0	33	0.67	1	YADVGSFDYGR
148	400.27	798.52	798.53	-0.01	1	32	0.83	1	IVAIAKGK
105	368.71	735.41	735.36	0.05	0	29	1.7	1	DSVPYR
375	615.32	1228.63	1228.67	-0.03	1	27	2.6	1	AELGAKLEAEAK
136	387.21	772.40	772.43	-0.03	1	26	4.5	1	QSVAGRR
169	421.76	841.51	841.50	0.01	0	23	6.3	1	VAAELAIR
347	576.32	1150.63	1150.59	0.04	0	23	5.8	1	YSGEGDLAIVK
170	421.77	841.53	841.45	0.07	0	22	8.1	1	VAAEIDPK
115	371.32	740.63	740.45	0.17	0	22	2.4	1	KPEIVR
238	476.28	950.54	950.44	0.10	1	21	9.6	1	LAECRMR + Oxidation (M)
145	395.25	788.48	788.33	0.15	0	21	13	1	LMMNHQ + Oxidation (M)
335	562.81	1123.60	1123.50	0.10	0	21	9.9	1	SDSSLSENASK
84	348.73	695.45	695.26	0.19	0	19	11	1	MGYYF + Oxidation (M)
173	428.77	855.53	855.50	0.03	0	19	14	1	LAVGMPIR
135	387.20	772.38	772.44	-0.06	1	19	22	1	MTPLRR
376	411.90	1232.69	1232.71	-0.02	1	19	18	1	VPSLGARAAHVR
208	456.27	910.52	910.46	0.06	1	18	14	1	CPHRSVR
390	425.90	1274.69	1274.65	0.04	0	18	18	1	LLNDAPFETQK
97	360.23	718.44	718.38	0.06	0	18	27	1	IACSLR
199	450.26	898.51	898.45	0.06	0	18	20	1	HTTLNGEK
113	371.30	740.59	740.44	0.14	0	18	9.4	1	GVILPDK
273	505.80	1009.59	1009.49	0.11	0	18	16	1	MSSSGSSVIR
101	364.23	726.44	726.41	0.03	0	18	15	1	IYYIR

Mascot Search Results

```
          : Mascot Daemon
          :
 title    : Submitted from Matthew 2 3 4 rpt bacteria by Mascot Daemon on BMSQSPROC2 (Matthew 2 rpt)
 file     : E:\PE Sciex Data\Projects\data from Q-Star\Matthew 2 rpt.wiff
se        : MSDB 20060518 (2344227 sequences; 779380795 residues)
ny        : Bacteria (Eubacteria) (857805 sequences)
amp       : 16 Mar 2007 at 10:01:02 GMT
icant hits: DPS_ECOLI     DNA protection during starvation protein.- Escherichia coli, Escherichia coli O157:H7, and Shigella
            AD0601        DNA protection during starvation protein [imported] - Salmonella enterica subsp. enterica serovar T
            R5EC15        ribosomal protein L15 [validated] - Escherichia coli (strain K-12)
            Q5PF85_SALPA  Possible outer membrane adhesin.- Salmonella paratyphi-a.
            Q6HH36_BACHK  Transcriptional regulator, AraC family.- Bacillus thuringiensis subsp. konkukian.
```

bility Based Mowse Score

ore is -10*Log(P), where P is the probability that the observed match is a random event.
ual ions scores > 42 indicate identity or extensive homology (p<0.05).
scores are derived from ions scores as a non-probabilistic basis for ranking protein hits.

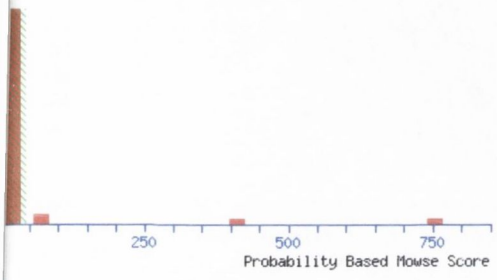

de Summary Report

at As | Peptide Summary | Help

Significance threshold p< 0.05 | Max. number of hits AUTO

Standard scoring ◉ MudPIT scoring ○ | Ions score cut-off 0 | Show sub-sets ☐

Show pop-ups ◉ Suppress pop-ups ○ | Sort unassigned Decreasing Score | Require bold red ☐

t All | Select None | Search Selected | ☐ Error tolerant | Archive Report

DPS_ECOLI **Mass:** 18553 **Score:** 752 **Queries matched:** 25
DNA protection during starvation protein.- Escherichia coli, Escherichia coli O157:H7, and Shigella
☐ Check to include this hit in error tolerant search or archive report

	Query	Observed	Mr(expt)	Mr(calc)	Delta	Miss	Score	Expect	Rank	Peptide
☑	147	458.28	914.54	914.52	0.03	0	48	0.029	1	K.ATVELLNR.Q
☑	162	476.28	950.54	950.52	0.03	0	56	0.0034	1	K.ATNLLYTR.N
☑	218	348.56	1042.65	1042.61	0.04	1	(24)	5.9	1	K.KATVELLNR.Q
	219	348.57	1042.67	1042.61	0.06	1	26	3	3	K.KATVELLNR.Q
	270	383.56	1147.66	1147.63	0.03	1	(11)	90	9	R.YAIVANDVRK.A
☑	271	383.57	1147.69	1147.63	0.05	1	34	0.45	1	R.YAIVANDVRK.A
	273	383.57	1147.69	1147.63	0.05	1	(15)	41	9	R.YAIVANDVRK.A
	275	383.57	1147.69	1147.63	0.05	1	(27)	2.4	3	R.YAIVANDVRK.A
	276	383.57	1147.69	1147.63	0.05	1	(12)	72	7	R.YAIVANDVRK.A
	277	383.57	1147.69	1147.63	0.05	1	(16)	29	9	R.YAIVANDVRK.A
	290	389.57	1165.69	1165.65	0.05	1	(14)	43	3	K.SKATNLLYTR.N
☑	291	389.57	1165.69	1165.65	0.05	1	24	3.7	1	K.SKATNLLYTR.N
	292	389.57	1165.69	1165.65	0.05	1	(23)	5.4	2	K.SKATNLLYTR.N
	293	389.57	1165.69	1165.65	0.05	1	(20)	11	2	K.SKATNLLYTR.N
	294	389.57	1165.69	1165.65	0.05	1	(14)	38	2	K.SKATNLLYTR.N
☑	343	682.34	1362.67	1362.63	0.05	0	82	6.3e-006	1	K.DDDTADILTAASR.D
☑	375	501.27	1500.78	1500.72	0.06	0	43	0.058	1	R.TALIDHLDTMAER.A + Oxidation (M)
☑	382	759.47	1516.92	1516.89	0.04	0	68	0.00015	1	R.QVIQFIDLSLITK.Q
☑	390	535.64	1603.89	1603.83	0.06	1	42	0.066	1	K.ELADRYAIVANDVR.K
☑	394	560.31	1677.91	1677.85	0.06	0	29	1.3	1	K.SYPLDIHNVQDHLK.E
☑	396	564.96	1691.85	1691.81	0.04	0	43	0.049	1	R.GANFIAVHEMLDGFR.T + Oxidation (M)
☑	402	586.02	1755.05	1754.99	0.06	0	78	9.3e-006	1	R.AVQLGGVALGTTQVINSK.T
☑	407	609.33	1824.96	1824.89	0.07	1	38	0.13	1	K.ATNLLYTRNDVSDSEK.K
☑	419	645.01	1932.00	1931.94	0.06	1	68	0.00013	1	K.AIGEAKDDDTADILTAASR.D
☑	427	732.45	2194.32	2194.27	0.05	1	73	1.3e-005	1	R.AVQLGGVALGTTQVINSKTPLK.S

Proteins matching the same set of peptides:
LDPSA **Mass:** 17898 **Score:** 752 **Queries matched:** 25
dps mutant S164C, chain A - Escherichia coli
Q6Y1R6_PROVU **Mass:** 18711 **Score:** 752 **Queries matched:** 25
Dps.- Proteus vulgaris.
B90740 **Mass:** 18684 **Score:** 752 **Queries matched:** 25
global regulator protein Dps [imported] - Escherichia coli (strain O157:H7, substrain RIMD 0509952)

AD0601 **Mass:** 18706 **Score:** 389 **Queries matched:** 13
DNA protection during starvation protein [imported] - Salmonella enterica subsp. enterica serovar T
Check to include this hit in error tolerant search or archive report

Query	Observed	Mr(expt)	Mr(calc)	Delta	Miss	Score	Expect	Rank	Peptide
147	458.28	914.54	914.52	0.03	0	48	0.029	1	K.ATVELLNR.Q
218	348.56	1042.65	1042.61	0.04	1	(24)	5.9	1	K.KATVELLNR.Q
219	348.57	1042.67	1042.61	0.06	1	26	3	3	K.KATVELLNR.Q
290	389.57	1165.69	1165.65	0.05	1	(14)	43	3	K.TKASNLLYTR.N
291	389.57	1165.69	1165.65	0.05	1	24	3.7	1	K.TKASNLLYTR.N
292	389.57	1165.69	1165.65	0.05	1	(23)	5.4	2	K.TKASNLLYTR.N
293	389.57	1165.69	1165.65	0.05	1	(20)	11	2	K.TKASNLLYTR.N
294	389.57	1165.69	1165.65	0.05	1	(14)	38	2	K.TKASNLLYTR.N
382	759.47	1516.92	1516.89	0.04	0	68	0.00015	1	R.QVIQFIDLSLITK.Q
394	560.31	1677.91	1677.85	0.06	0	29	1.3	1	K.SYPLDIHNVQDHLK.E
396	564.96	1691.85	1691.81	0.04	0	43	0.049	1	R.GANFIAVHEMLDGFR.T + Oxidation (M)
402	586.02	1755.05	1754.99	0.06	0	78	9.3e-006	1	R.AVQLGGVALGTTQVINSK.T
427	732.45	2194.32	2194.27	0.05	1	73	1.3e-005	1	R.AVQLGGVALGTTQVINSKTPLK.S

R5EC15 **Mass:** 14971 **Score:** 82 **Queries matched:** 2
ribosomal protein L15 [validated] - Escherichia coli (strain K-12)
Check to include this hit in error tolerant search or archive report

Query	Observed	Mr(expt)	Mr(calc)	Delta	Miss	Score	Expect	Rank	Peptide
284	579.83	1157.64	1157.59	0.05	1	5	4.7e+002	2	R.AAIEAAGGKIEE.-
367	727.95	1453.89	1453.85	0.04	0	77	1.6e-005	1	K.VILAGEVTTPVTVR.G

Proteins matching the same set of peptides:
AD1008 **Mass:** 14957 **Score:** 82 **Queries matched:** 2
50S ribosomal chain protein L15 [imported] - Salmonella enterica subsp. enterica serovar Typhi (str
AAA58098 **Mass:** 15025 **Score:** 81 **Queries matched:** 2
ECOUW67 NID: - Escherichia coli

Q5PF85_SALPA **Mass:** 25762 **Score:** 52 **Queries matched:** 2
Possible outer membrane adhesin.- Salmonella paratyphi-a.
Check to include this hit in error tolerant search or archive report

Query	Observed	Mr(expt)	Mr(calc)	Delta	Miss	Score	Expect	Rank	Peptide
186	497.78	993.54	993.51	0.03	0	27	2.5	1	R.LELDTTFR.G
301	603.33	1204.64	1204.60	0.04	0	25	3.7	1	K.NNFAWGAGIGAK.Y

Proteins matching the same set of peptides:
Q8VM53_SALDZ **Mass:** 25767 **Score:** 52 **Queries matched:** 2
Putative invasin.- Salmonella enterica IIIb 50:k:z.
Q8ZRJ9_SALTY **Mass:** 25749 **Score:** 52 **Queries matched:** 2
Homolog of sapA.- Salmonella typhimurium.
Q57SU8_SALCH **Mass:** 25791 **Score:** 52 **Queries matched:** 2
SapA-like protein.- Salmonella choleraesuis.
AH0541 **Mass:** 25788 **Score:** 52 **Queries matched:** 2
probable outer membrane adhesin STY0351 [imported] - Salmonella enterica subsp. enterica serovar Ty

---

Q6HH36_BACHK **Mass:** 35210 **Score:** 42 **Queries matched:** 2
Transcriptional regulator, AraC family.- Bacillus thuringiensis subsp. konkukian.
Check to include this hit in error tolerant search or archive report

Query	Observed	Mr(expt)	Mr(calc)	Delta	Miss	Score	Expect	Rank	Peptide
162	476.28	950.54	950.52	0.03	0	42	0.08	2	R.ATNLLTYR.S
163	476.30	950.58	950.52	0.06	0	(5)	3.9e+002	2	R.ATNLLTYR.S

Proteins matching the same set of peptides:
Q81NW5_BACAN **Score:** 42 **Queries matched:** 2
Q639O4_BACCZ **Score:** 42 **Queries matched:** 2

---

ide matches not assigned to protein hits: (no details means no match)

Mascot Search Results

```
          : Mascot Daemon
          :
 title    : Submitted from Matthew 1 rpt bacteria by Mascot Daemon on BMSQSPROC2 (Matthew 1 rpt)
ta file   : E:\PE Sciex Data\Projects\data from Q-Star\Matthew 1 rpt.wiff
ase       : MSDB 20060518 (2344227 sequences; 779380795 residues)
omy       : Bacteria (Eubacteria) (857805 sequences)
tamp      : 15 Mar 2007 at 15:34:03 GMT
ficant hits: MMECF          outer membrane porin ompF precursor - Escherichia coli (strain K-12)
             O8FFZ0_ECOL6   Galactitol-1-phosphate 5-dehydrogenase (EC 1.1.1.251).- Escherichia coli O6.
             RPECL          lactose operon repressor - Escherichia coli (strain K-12)
             O62070_BACLD   Hypothetical protein.- Bacillus licheniformis (strain DSM 13 / ATCC 14580).
             O93SG6_CLOBI   Tetrachloroethylene dehalogenase precursor.- Clostridium bifermentans.
```

ability Based Mowse Score

core is -10*Log(P), where P is the probability that the observed match is a random event.
dual ions scores > 42 indicate identity or extensive homology (p<0.05).
n scores are derived from ions scores as a non-probabilistic basis for ranking protein hits.

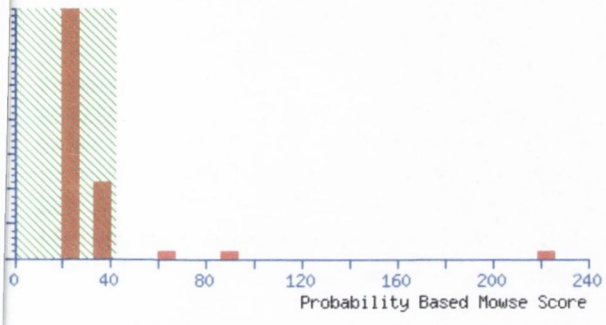

tide Summary Report

mat As | Peptide Summary | Help

Significance threshold p< 0.05 | Max. number of hits AUTO

Standard scoring ◉ MudPIT scoring ○ | Ions score cut-off 0 | Show sub-sets ☐

Show pop-ups ◉ Suppress pop-ups ○ | Sort unassigned Decreasing Score | Require bold red ☐

ct All | Select None | Search Selected | ☐ Error tolerant | Archive Report

MMECF **Mass:** 39309 **Score:** 223 **Queries matched:** 11
outer membrane porin ompF precursor - Escherichia coli (strain K-12)
☐ Check to include this hit in error tolerant search or archive report

	Query	Observed	Mr(expt)	Mr(calc)	Delta	Miss	Score	Expect	Rank	Peptide
☑	201	360.23	718.45	718.44	0.02	0	42	0.1	1	R.LAFAGLK.Y
☑	672	625.28	1248.55	1248.54	0.01	0	(18)	19	1	K.YADVGSFDYGR.N
☑	673	625.29	1248.57	1248.54	0.03	0	(60)	0.0011	1	K.YADVGSFDYGR.N
☑	674	625.29	1248.57	1248.54	0.03	0	69	0.00015	1	K.YADVGSFDYGR.N
☑	709	685.37	1368.72	1368.70	0.02	0	(23)	5.9	1	R.TNLQEAQPLGNGK.K
☑	711	685.38	1368.74	1368.70	0.04	0	64	0.00042	1	R.TNLQEAQPLGNGK.K
	713	685.38	1368.74	1368.70	0.04	0	(13)	60	4	R.TNLQEAQPLGNGK.K
	714	685.39	1368.77	1368.70	0.07	0	(9)	1.5e+002	3	R.TNLQEAQPLGNGK.K
	825	924.44	1846.87	1846.85	0.03	0	(16)	22	2	K.YDANNIYLAANYGETR.N
☑	826	616.66	1846.97	1846.85	0.12	0	29	1	1	K.YDANNIYLAANYGETR.N
☑	845	642.69	1925.04	1924.96	0.07	1	18	14	1	R.NATPITNKFTNTSGFANK.T

Proteins matching the same set of peptides:
1BT9A **Mass:** 37018 **Score:** 223 **Queries matched:** 11
matrix porin outer membrane protein f mutant YES - Escherichia coli

1GFM **Mass:** 37004 **Score:** 223 **Queries matched:** 11
matrix porin outer membrane protein f mutant D113G - Escherichia coli
1GFO **Mass:** 37003 **Score:** 223 **Queries matched:** 11
matrix porin outer membrane protein f mutant R132P - Escherichia coli
1GFP **Mass:** 37066 **Score:** 223 **Queries matched:** 11
matrix porin outer membrane protein f mutant R42C - Escherichia coli
1MPF **Mass:** 37120 **Score:** 223 **Queries matched:** 11
Matrix porin (ompf) mutant with gly 119 replaced by asp (g119d) - Escherichia coli
1OMF **Mass:** 37062 **Score:** 223 **Queries matched:** 11
Porin (matrix) (ompf) - Escherichia coli
Q83RY4_SHIFL **Mass:** 39339 **Score:** 223 **Queries matched:** 11
Outer membrane protein 1a (Ia;b;F).- Shigella flexneri.

Q8FFZ0_ECOL6 **Mass:** 37785 **Score:** 92 **Queries matched:** 3
Galactitol-1-phosphate 5-dehydrogenase (EC 1.1.1.251).- Escherichia coli O6.
☐ Check to include this hit in error tolerant search or archive report

Query	Observed	Mr(expt)	Mr(calc)	Delta	Miss	Score	Expect	Rank	Peptide
595	542.83	1083.64	1083.62	0.03	0	14	43	6	R.VAESVIPEIK.H
☑ 637	575.33	1148.64	1148.59	0.04	0	38	0.18	1	K.SVTAIDISSEK.L
☑ 661	599.84	1197.66	1197.58	0.08	0	39	0.13	1	R.GSFESFAQAVR.D

Proteins matching the same set of peptides:
B64976 **Mass:** 37822 **Score:** 92 **Queries matched:** 3
galactitol-1-phosphate dehydrogenase (EC 1.1.1.-) - Escherichia coli (strain K-12)

RPECL **Mass:** 38737 **Score:** 70 **Queries matched:** 3
lactose operon repressor - Escherichia coli (strain K-12)
☐ Check to include this hit in error tolerant search or archive report

Query	Observed	Mr(expt)	Mr(calc)	Delta	Miss	Score	Expect	Rank	Peptide
☑ 648	584.37	1166.73	1166.70	0.03	0	18	17	1	K.GNQLLPVSLVK.R
658	592.87	1183.73	1183.69	0.04	0	16	28	2	R.LLQLSQGQAVK.G
☑ 662	602.85	1203.68	1203.63	0.05	0	36	0.31	1	R.ALADSLMQLAR.Q + Oxidation (M)

Proteins matching the same set of peptides:
1LBGA **Mass:** 38495 **Score:** 70 **Queries matched:** 3
lactose operon repressor, chain A - Escherichia coli
1LBHA **Mass:** 31820 **Score:** 70 **Queries matched:** 3
intact lactose operon repressor with gratuitous inducer iptg, chain A - Escherichia coli
1TLFA **Mass:** 31748 **Score:** 70 **Queries matched:** 3
tryptic core fragment of the lactose repressor of escherichia coli, chain A - Escherichia coli
Q8FKG5_ECOL6 **Mass:** 9884 **Score:** 70 **Queries matched:** 3
LacI protein.- Escherichia coli O6.
CAC39977 **Mass:** 39023 **Score:** 70 **Queries matched:** 3
Sequence 2 from Patent EP1106695.- synthetic construct.
CAA41383 **Mass:** 38687 **Score:** 70 **Queries matched:** 3
ECLACT41 NID: - Escherichia coli
AAC83652 **Mass:** 38711 **Score:** 70 **Queries matched:** 3
REPRESSOR PROTEIN LACI.- Integrational vector pMUTIN2.
F90678 **Mass:** 38721 **Score:** 70 **Queries matched:** 3
lac operon transcription repressor [imported] - Escherichia coli (strain O157:H7, substrain RIMD 05

Q62Q70_BACLD **Mass:** 21473 **Score:** 42 **Queries matched:** 2
Hypothetical protein.- Bacillus licheniformis (strain DSM 13 / ATCC 14580).
☐ Check to include this hit in error tolerant search or archive report

Query	Observed	Mr(expt)	Mr(calc)	Delta	Miss	Score	Expect	Rank	Peptide
201	360.23	718.45	718.44	0.02	0	42	0.1	1	K.IAFAGIK.M
204	360.24	718.47	718.44	0.03	0	(26)	4.9	3	K.IAFAGIK.M

Proteins matching the same set of peptides:
Q65EQ6_BACLD **Mass:** 23031 **Score:** 42 **Queries matched:** 2
Hypothetical protein.- Bacillus licheniformis (strain DSM 13 / ATCC 14580).

Q93SG6_CLOBI **Score:** 42 **Queries matched:** 1
Tetrachloroethylene dehalogenase precursor.- Clostridium bifermentans.
Check to include this hit in error tolerant search or archive report

Query	Observed	Mr(expt)	Mr(calc)	Delta	Miss	Score	Expect	Rank	Peptide
201	360.23	718.45	718.44	0.02	0	42	0.1	1	R.LAFAGIK.V

Proteins matching the same set of peptides:
Q87754_KLEPN **Score:** 42 **Queries matched:** 1

---

ide matches not assigned to protein hits: (no details means no match)

Query	Observed	Mr(expt)	Mr(calc)	Delta	Miss	Score	Expect	Rank	Peptide
558	522.83	1043.64	1043.61	0.02	0	40	0.15	1	VGPALTFALR
685	646.89	1291.77	1291.75	0.01	0	29	1.4	1	LPPLATLWLTPA
341	421.77	841.53	841.49	0.03	0	28	2.1	1	VATLPVDK
531	341.21	1020.60	1020.63	-0.04	1	27	2.4	1	AVVVPPKSPK
540	515.32	1028.63	1028.56	0.07	1	26	3.2	1	VIDEELRR
344	421.77	841.53	841.49	0.03	0	26	3.4	1	VATLPVDK
204	360.24	718.47	718.38	0.09	0	26	4.9	1	IACSLR
233	371.30	740.59	740.47	0.12	1	25	1.9	1	RIISPR
199	360.23	718.45	718.38	0.07	0	24	6.4	1	IACSLR
526	339.21	1014.60	1014.56	0.03	0	24	5.3	1	GVGLGLAICR
360	428.78	855.55	855.49	0.06	1	24	4.5	1	LATRGNPK
205	360.24	718.47	718.35	0.12	0	23	8.4	1	IAGDSEK
247	371.30	740.59	740.40	0.19	0	23	2.9	1	CLLAHK
200	360.23	718.45	718.42	0.03	1	23	8.9	1	IARGFR
361	428.78	855.55	855.52	0.03	0	23	6.2	1	IAEALALR
207	360.24	718.47	718.42	0.05	1	23	9.6	1	IARGFR
342	421.77	841.53	841.45	0.07	0	22	7.6	1	VAAEIDPK
340	421.77	841.53	841.45	0.07	0	22	7.7	1	VAAEIDPK
604	371.30	1110.88	1110.71	0.17	1	22	0.32	1	RILSTIPAIK
713	685.38	1368.74	1368.69	0.05	0	22	6.5	1	IDINEAEPEALR
352	421.78	841.54	841.45	0.09	0	22	7.8	1	VAAEIDPK
169	347.22	692.42	692.30	0.12	1	22	7.4	1	DSQKTD
347	421.77	841.53	841.45	0.07	0	22	8.6	1	VAAEIDPK
396	447.27	892.53	892.56	-0.03	0	22	9.4	1	LDLIIPPI
351	421.78	841.54	841.49	0.05	0	22	9.2	1	GLTVDLPK
720	685.88	1369.75	1369.77	-0.02	1	21	8	1	SQLQKEVGVLNR
721	685.88	1369.75	1369.78	-0.03	1	21	8.8	1	SQLRQLSQAALR
271	381.21	760.41	760.38	0.03	0	21	15	1	QLGSGGSR
345	421.77	841.53	841.49	0.03	0	21	11	1	GLTVDLPK
454	473.26	944.52	944.46	0.05	0	20	16	1	LELMAGGPAS
717	685.86	1369.70	1369.73	-0.03	0	20	12	1	LPFVEMPTVPPK + Oxidation (M)
359	428.76	855.51	855.52	-0.00	0	19	14	1	ITAVLSPR
825	924.44	1846.87	1846.83	0.04	0	19	10	1	EVNDVFGHPVGDMLMR + 2 Oxidation (M)
585	536.30	1070.59	1070.60	-0.01	0	19	16	1	ALGIVDINEK
256	371.34	740.66	740.52	0.14	0	19	2.2	1	GVLLVIK
775	538.30	1611.88	1611.85	0.03	0	19	12	1	SNPQLLISDIEDLR
616	371.30	1110.88	1110.71	0.17	1	19	0.7	1	QLIAGAGKILK
384	442.33	882.65	882.47	0.18	0	19	7.8	1	LTQTHQR
544	516.32	1030.62	1030.55	0.06	1	19	18	1	VLDSVIEKE
285	387.30	772.59	772.42	0.17	1	19	22	1	AIEERR
387	443.28	884.55	884.50	0.05	1	19	20	1	MVRGAVPR
615	371.30	1110.88	1110.71	0.17	1	19	0.76	1	QLIAGAGKILK
244	371.30	740.59	740.45	0.13	1	19	8.5	1	KEPLVR
618	371.30	1110.88	1110.71	0.17	1	18	0.81	1	QLIAGAGKILK
348	421.77	841.53	841.50	0.02	0	18	20	1	SLISAVPR
114	329.20	656.39	656.41	-0.02	1	18	20	1	RVGGIR
612	371.30	1110.88	1110.71	0.17	1	18	0.84	1	QLIAGAGKILK
533	341.25	1020.72	1020.56	0.16	1	18	11	1	QTLSRSTTK